Modelling Default Correlations in a Two-Firm Model with Dynamic Leverage Ratios

A Thesis Submitted for the Degree of

Doctor of Philosophy

by

Ming Xi Huang

B.Sc. (The Chinese University of Hong Kong, Hong Kong)

M.Sc. (The Chinese University of Hong Kong, Hong Kong)

MingXi.Huang@student.uts.edu.au

in

The School of Finance and Economics

University of Technology, Sydney

PO Box 123 Broadway

NSW 2007, Australia

August 11, 2009

CERTIFICATE OF AUTHORSHIP/ORIGINALITY

I certify that the work in this thesis has not previously been submitted for a degree nor has it been submitted as part of requirement for a degree except as fully acknowledged within the text.

I also certify that the thesis has been written by me. Any help that I have received in my research work and the preparation of the thesis itself has been acknowledged. In addition, I certify that all information sources and literature used are indicated in the thesis.

Signature of Candidate . . . . . .

Date . . . . . .

Acknowledgments

I would like to thank my supervisor, Professor Carl Chiarella for his guidance, advice and assistance throughout my PhD studies, and for his encouragement and support to me to participate in international conferences, seminars and workshops that have been an important part of the building up of my research experience. I would also like to thank my co-supervisor, Associate Professor Xue-Zhong (Tony) He and my alternate supervisor, Associate Professor Erik Schlogl, for their additional supervision and their insightful comments and suggestions.

I would especially thank Professor Chi-Fai Lo (Institute of Theoretical Physics and Department of Physics, The Chinese University of Hong Kong), for raising the initial motivation of this research topic and providing much useful advice on several technical aspects of this thesis. Special thanks are also due to Dr. Hing Hung (formerly of the School of Finance and Economics, UTS and now at the Commonwealth Bank of Australia), who shared with me a great deal of useful knowledge in implementation methodologies. I would also like to thank all staff and academic colleagues of the School of Finance and Economics at UTS, for their friendship and assistance over the last four years.

Additionally, the financial assistance from various scholarships and conference grants from the University of Technology, Sydney, the Faculty of Business, the Quantitative Finance Research Centre and the School of Finance and Economics are all greatly appreciated.

Last but not least, I would like to thank my parents, sisters and my husband for their endless love, support and encouragement over the years of my studies.

Contents

Abstract

Default correlations have been an important research area in credit risk analysis. This thesis aims to extend the one-firm structural model of default to the two-firm situation for valuing default correlations. In the structural approach, default happens when the firm value falls below a default threshold. In the fundamental model of Merton (1974), the default threshold is simply the face value of the bond. Collin-Dufresne & Goldstein (2001) related the default threshold to the firm's debts and modelled it as mean-reverting to a constant long-term target. Hui et al. (2006) generalized the Collin-Dufresne & Goldstein (2001) model to consider the default threshold as stochastic and the long-term target as time-dependent. In these models, the corporate bond price is a function of the leverage ratio - a ratio of the firm's debt to its asset value. For this combined measure of the firm's default risk, Hui et al. (2007) proposed a dynamic leverage ratio model, where default happens when the leverage ratio falls below a certain level.

The aim of this thesis is to extend the one-firm dynamic leverage ratio model of Hui et al. (2007) to incorporate the default risk of two firms and interest rate risk. The model will be based on the consideration of a financial instrument (a credit linked note) that is exposed to the default risk of the two firms. Initially, the dynamic leverage ratios will be assumed to follow geometric Brownian motions and the stochastic interest rate assumed to follow a Vasicek (1977) process. The pricing problem will then be reduced to that of solving the first-passage-time problem that plays an important part in the valuation of default correlations.

In order to study the impact of the capital structures of firms on default correlations, the two-firm model is extended by allowing the dynamic leverage ratios to follow mean-reverting processes, so as to capture the behavior of firms when they adjust their capital structures to a long-term target. Then in order to capture the effect of external shocks on default correlations, the model is further extended to consider the situation in which the dynamic leverage ratios follow jump-diffusion processes. Finally, the numerical results of default correlations based on the two-firm model are studied and compared when the firm's leverage ratios follow these three types of processes.

The thesis concludes by pointing to some future research directions. These includes further development of the method of images approach for the solution of the first passage time problem to the time varying coefficients case by use of the multi-stage approximation. Development of approximate analytical methods to extend the range of applicability of the method of images approach. Extension of Fortet's integral equation approach for the solution of first passage time problem to

the two-dimensional situation. The estimation and calibration of leverage ratio models, including estimation of market prices of risk.

The main contributions of the thesis are:

- The setting up the two firm leverage ratio framework for evaluation of default correlations.
- The extension of the method of images approach to the two-dimensional situation for solving the first passage time problem with constant coefficients and the time varying barrier approach for time-dependent coefficients.
- Extension of the leverage ratio framework to incorporate jumps in both the one and two firm cases.
- A comparative study of the impact on default correlations and joint survival probabilities of the different types of processes for the leverage ratio dynamics.

CHAPTER 1

Introduction

The recent financial crisis that initiated in the United States and rapidly spread elsewhere was related to the large amount of correlated defaults indicating clearly the topicality and importance of this research topic. This thesis provides a generalized two-firm model of default correlation, based on the structural approach incorporating the stochastic interest rate model of Vasicek (1977). It sets up a two-firm framework with dynamic leverage ratios allowed to follow different types of stochastic processes that represent the different features of firms' capital structure. The thesis investigates analytical and numerical tools to solve the underlying first passage time problem and studies the impact on default correlations of various assumptions about the stochastic processes followed by the leverage ratio.

This thesis is organized as follows:

Chapter 2 reviews the key features of some major structural models in credit risk modelling, from the fundamental model of Merton (1974) to the stationary-leverage-ratio models of Collin-Dufresne & Goldstein (2001) and Hui et al. (2006), and then to a dynamic leverage ratio model of Hui et al. (2007).

Chapter 3 reviews the details of the one-firm dynamic leverage ratio model of Hui et al. (2007) for corporate bond pricing. This chapter also discusses the method of images applied by Hui et al. (2007) to obtain an analytical solution to the associated first passage time problem. An approach used to deal with time-dependent parameters is also discussed. The second part of this chapter extends the dynamic leverage ratio model to the two-firm situation for pricing financial derivatives involving default risks among two firms. The model will be based on the consideration of a credit linked note that is exposed to the default risk of the two firms. The dynamic leverage ratios will be assumed to follow geometric Brownian motions and the stochastic interest rate assumed to follow a Vasicek (1977) process. The pricing problem will be then reduced to that of solving the first-passage-time problem that plays an important part in the evaluation of default correlations. The first original contribution of the thesis is the setting up of the two-firm model dynamic leverage ratio framework.

Chapter 4 seeks the analytical solution for the pricing function of the credit linked note by using the method of images. The exact solution will be derived in terms of the bivariate cumulative normal

function. When the coefficients are time-dependent, the time varying barrier approach is used to obtain an approximate solution. However, the method of images only gives an exact analytical solution for particular values of the correlation coefficient between the dynamics of the leverage ratios of the two firms. Its use in subsequent chapters is to serve as a benchmark solution against which various approximate methods will be tested. The second original contribution of the thesis is the extension of the method of images to the two-dimensional case for solving the first passage problem with constant coefficients and then extending the time varying barrier approach to deal with time-dependent coefficients.

Chapter 5 considers numerical methods to efficiently solve the problem for all values of the correlation coefficient. The first part of this chapter sets up an alternating direction implicit scheme that was introduced in Douglas & Rachford (1956). The second part develops a Monte Carlo scheme to serve as a benchmark. At the end of this Chapter, the accuracy of the numerical results based on the method of images, the alternating direction implicit scheme and Monte Carlo methods are compared.

Chapter 6 presents some numerical results for joint survival probabilities and default correlations based on the two-firm model developed in the previous chapters. The chapter also discusses the choice of parameters, and goes on to study the impact on joint survival probabilities and default correlations of various parameters. The third original contribution of the thesis is the study of the properties of default correlations and joint survival probabilities when the leverage ratios follow geometric Brownian motions.

Chapter 7 extends the two-firm model in Chapter 3 by allowing the dynamic leverage ratios to follow mean-reverting processes, so capturing the behavior of firms when they alter their capital structures to long-term targets. An approximate analytical solution via the method of images that was developed in Chapter 4 is extended (for certain values of the correlation coefficient) and the Monte Carlo scheme of Chapter 5 is also extended to this situation to cater for general values of the correlation coefficient. This Chapter concludes by comparing the two numerical methods and studying the impact of mean-reverting capital structures on joint survival probabilities and default correlations. The fourth original contribution of the thesis is the extension of the method of images and time varying barrier approaches to the two-firm model when the leverage ratios follow mean-reverting processes and their impact on default correlations and joint survival probabilities.

Chapter 8 considers the case in which dynamic leverage ratios follow jump-diffusion processes, thereby capturing the surprise due to unexpected external shocks. This chapter focuses on the one-firm case. The problem is reduced to that of finding the single firm default probability and the

Monte Carlo simulation method is extended to cover this case. The impact of the jump components: the average jump size, the jump size volatility and the jump intensity on single firm default probabilities for different credit rated firms are studied. Then, we search for the optimal values of average jump sizes by calibrating to Standard & Poor's (2001) historical default data for different credit ratings. The fifth original contribution of the thesis is the setting up of the one-firm leverage ratio model with jump risks, the calibration of the model to market data, and the study of the impact of jump risks on default probabilities.

Chapter 9 extends the one-firm model developed in Chapter 8 to the two-firm situation, thereby capturing the surprise risk of default in a group of firms. The Monte Carlo simulation method is extended to study the impact of jump components on joint survival probabilities and default correlations. The impact of the sign of the average jump sizes on joint survival probabilities and default correlations are also studied. The sixth original contribution of the thesis is the setting up of the two-firm leverage ratio model with jump risks and study of their impact on default correlations and joint survival probabilities.

Chapter 10 brings together the results of earlier chapters and compares the individual default probabilities, joint survival probabilities and default correlations when the firms' leverage ratios follow the three different processes discussed in the thesis. The final original contribution of the thesis is the study of the relative differences for credit risk analysis of the various types of stochastic processes for the leverage ratio dynamics.

Chapter 11 summarizes the main findings of the thesis, draws some conclusions and raises suggestions for future research topics arising out of the issues considered here.

CHAPTER 2

Literature Review

One of the main challenges in credit risk analysis is the estimation of correlation among defaults of firms. A number of approaches have been developed to tackle this problem. The Gaussian copula method has become a kind of market standard to estimate default correlations. It is easy to implement, but has the drawback that there is no easy way of knowing which copula to use. Another approach is the reduced-form approach, in which default is driven by surprises captured by some jump process. The probability of surprise depends on an intensity parameter which is estimated by calibration. Another common approach, the structural approach, relates the advent of default to the dynamics of the underlying structure of firm. This approach developed out of the work of Merton (1974) who developed a corporate bond pricing model depending on the firm asset value and the face value of debt. In order to study how default correlations are effected by firms' capital structure, this thesis will develop a two-firm model of default correlation based on the structural approach.

This chapter reviews the key features of certain major structural models in credit risk modelling. From the fundamental model of Merton (1974) to that of Black & Cox (1976) allowing early default before the maturity date of risky debt. Then the later developments include Longstaff & Schwartz (1995) who combine many distinctive features in a one-firm model, Briys & de Varenne (1997) who propose a stochastic default threshold. Finally the stationary-leverage-ratio models of Collin-Dufresne & Goldstein (2001) and Hui et al. (2006).

The structural models were initiated by Merton (1974), who was the pioneer in using the contingent claim analysis approach to corporate bond pricing. In the structural approach, the default event is driven by the firm value and occurs when it falls below some default threshold. In Merton (1974), the default threshold is simply the face value of the bond, however, the main limitation of the approach is that bondholders cannot force the firm to default before the maturity date. In order to consider a safety covenant for the protection of bondholders, a default-triggering level for the firm's asset value is proposed in the model of Black & Cox (1976), who extend Merton (1974) by allowing default to occur at any time when the firm's asset value is less than the default threshold. However, both models are limited by the setting of a deterministic short-term risk-free interest rate.

The later development of Longstaff & Schwartz (1995) combines the early default mechanism in Black & Cox (1976) and the stochastic interest rate model of Vasicek (1977). The Longstaff & Schwartz (1995) approach captures the idea of the Merton model in a more flexible way, in particular it accommodates complicated liability structures and payoffs by deriving the solution as a function of a ratio of the firm value to the payoff. Instead of using a constant default threshold, Briys & de Varenne (1997) consider a time-dependent default threshold and assume that it depends on the risk-free interest rate.

Collin-Dufresne & Goldstein (2001) point out that most structural models preclude the possibility that firms may alter their capital structure. They stress the fact that in practice, firms could adjust their outstanding debt levels in response to the change in firm value, and hence generate mean-reverting leverage ratios. To model this feature, Collin-Dufresne & Goldstein (2001) assume that the default threshold changes dynamically over time, in particular, that the dynamics of the log-default threshold is mean-reverting. This setting captures the fact that firms tend to issue debt when their leverage ratio falls below some target, and replace maturing debt when their leverage ratio is above this target. Collin-Dufresne & Goldstein (2001) mention that in general, the default threshold is not necessarily the outstanding book value of debt, but it seems reasonable to assume that they are related. For example, they are identical in the Merton (1974) model. Collin-Dufresne & Goldstein (2001) interpret their model with a more general definition of leverage, which is the ratio of a default threshold that reflects the market value of total liabilities of the firm to its firm value.

The two main features introduced in the Collin-Dufresne & Goldstein (2001) model, are the use of the leverage ratio and the fact that it is mean-reverting. These features capture the tendency of firms to issue debt when their leverage ratio falls below some target, and replace maturing debt when their leverage ratio is above this target. Hui et al. (2006) generalize the Collin-Dufresne & Goldstein (2001) model to consider the situation in which the target leverage ratio is time-dependent and the default threshold follows a mean-reverting process. Hui et al. (2006) argue that the time-dependent target leverage ratio reflects the movements of a firm's initial target ratio towards a long-run target ratio over time. In the Hui et al. (2006) model, the dynamic equation of the default threshold has its own source of randomness. The solutions of both models are derived as a function of leverage ratios. For this combined measure of default risk of the firm, Hui et al. (2007) proposed a dynamic leverage ratio model, where default is driven by the firm's leverage ratio when it is above a certain level. Empirical support for the use of the leverage ratio model can be found in Hui et al. (2005), who present an empirical study of the estimation of default probabilities using the leverage ratio model for benchmarking listed companies. The empirical results show that the

benchmarking ratings can broadly track the S&P ratings of U.S. sample companies. A recent study of Huang & Zhou (2008) conducts a specification analysis of five structural models by using the term structure of credit default swap spreads and equity volatility from high-frequency return data. Their empirical tests show that the stationary leverage ratio model of Collin-Dufresne & Goldstein (2001) is the best performing structural model compared to the other four, which are those of Merton (1974), Black & Cox (1976), Longstaff & Schwartz (1995) and Huang & Huang (2003).

The principal aim of this thesis is to extend the dynamic leverage ratio model of Hui et al. (2007) to the two-firm case so as to study the implications for default correlations. The idea of the two-firm model is proposed by Zhou (2001*a*), who extends the one-firm model of Black & Cox (1976) to the two-firm situation. In Zhou's model the default possibilities of the two firms are driven by their asset values and the short-term risk-free interest rate is deterministic.

In order to study the impact on default correlations of firms altering their capital structure , the framework of the two-firm model is here extended to consider the case in which the dynamic leverage ratios are mean-reverting to constant target ratios (the case considered in Collin-Dufresne & Goldstein (2001)) and time-dependent target ratios (the case considered in Hui et al. (2006)).

Another extension draws on the discussion of Zhou (1997), who argues that in reality, a firm can default either by a gradual diffusion process, or by surprise due to unexpected external shocks. Zhou (2001*b*) combines these measures of risk by assuming the firm value follows a jump-diffusion process. In order to capture the effect of external shocks on default correlations, the two-firm model is extended to consider the situation in which the dynamic leverage ratios follow jump-diffusion processes.

The main features of the structural models discussed are summarized in Table 2.1. Structural models based on the work of Merton (1974) are more refined as one moves down the table. In particular, the modelling of the default threshold D from the initial assumption of being identical to the debt face value in Merton (1974), to being a constant ratio of debt face value in Longstaff & Schwartz (1995), to being time-dependent in Briys & de Varenne (1997), then to being mean-reverting in Collin-Dufresne & Goldstein (2001) and finally to being allowed to follow a stochastic process in Hui et al. (2006). The nature of the leverage ratio models, for example, Collin-Dufresne & Goldstein (2001), Hui et al. (2006) and Hui et al. (2007) provides a combined measure of default risk of the firm. Moreover, this class of models is able to avoid a direct parametrization in terms of the firm value V and the default threshold D by directly examining the leverage ratio L. Given these advantages, it seems natural to extend the one-firm leverage ratio models to the two-firm situation. Our approach considers the evaluation of default correlations when the dynamic

leverage ratios follow geometric Brownian motions, mean-reverting processes and jump-diffusion processes. The shaded boxes in last row of Table 2.1 indicates the models to be studied in this thesis.

Structural Models	*Firm Value V*	*Default Threshold D*	*Risk-Free Interest Rate*
Merton (1974)	$dV/V = \mu dt + \sigma dZ$	Bond face value D=F	Deterministic
Longstaff & Schwartz (1995)	$dV/V = \mu dt + \sigma dZ$	A constant D=K	Vasicek (1977)
Zhou (2001a)	$dV_i/V_i = \mu_i dt + \sigma_i dZ_i$,($i$ =1,2)	A time-dependent case D=$e^{\bar{\mu}_i t} K_i$	Deterministic
Zhou (2001b)	$dV/V = (\mu - \lambda_q k_q)dt + \sigma dZ + (Y-1)dq$	D=$e^{\bar{\mu} t} K$	Vasicek (1977)
Briys & de Varenne (1997)	$dV/V = rdt + \sigma(\sqrt{1-\rho^2} dZ_{\mathbb{B}V} + \rho dZ_r)$	Depends on the dynamics of risk free interest rate D=$\xi F B(r,t)$	Hull & White (1990)
Collin-Dufresne & Goldstein (2001)	$dV/V = (r-\delta)dt + \sigma dZ$	k=ln D, k is mean-reverting $dk = \lambda(\ln V - \nu - k)\, dt$	Vasicek (1977)
Hui et al. (2006)	$dV/V = \mu_V(t)dt + \sigma_V(t)dZ_V$	k follows the mean-reverting process $dk = [\mu(t) + \lambda(t)(\ln V - k) - \sigma^2/2]dt + \sigma(t) dZ_{\mathbb{B}}$	Hull & White (1990)
Hui et al. (2007)	$dL/L = \mu_L(t)dt + \sigma_L(t)dZ_L$, where $L \equiv D/V$		Hull & White (1990)
Two-firm model	$dL_i/L_i = \mu_i dt + \sigma_i dZ_i$, (i=1,2)		Vasicek (1977)
Ex. I: mean-reverting	$dL_i/L_i = \kappa_i[\ln \theta_i(t) - \ln L_i]dt + \sigma_i dZ_i$		
Ex. II: with jumps	$dL_i/L_i = (\mu_i - \lambda_{qi} k_{qi})dt + \sigma_i dZ_i + (Y_i - 1)dq$		

TABLE 2.1. Taxonomy of earlier structural models and the two-firm model of this thesis. The shaded boxes indicate the new models considered in this thesis.

The relationship among the various structural models is also illustrated in Table 2.2. The shaded boxes indicate the new developments to be undertaken in this thesis. The main differences between the two-firm model studied in this thesis and that to the Zhou (2001*a*) is that the model of Zhou was based on deterministic interest rates, while interest rate risk is taken into account in this thesis. The other key difference is that default probabilities are driven by the dynamic leverage ratios of firms in our two-firm model, while it is driven by the firm values in Zhou (2001*a*) (see Table 2.1). Moreover, Zhou (2001*a*) does not consider the situation where firms alter their capital structure, whereas the two-firm model in this thesis is extended to consider the situation in which dynamic

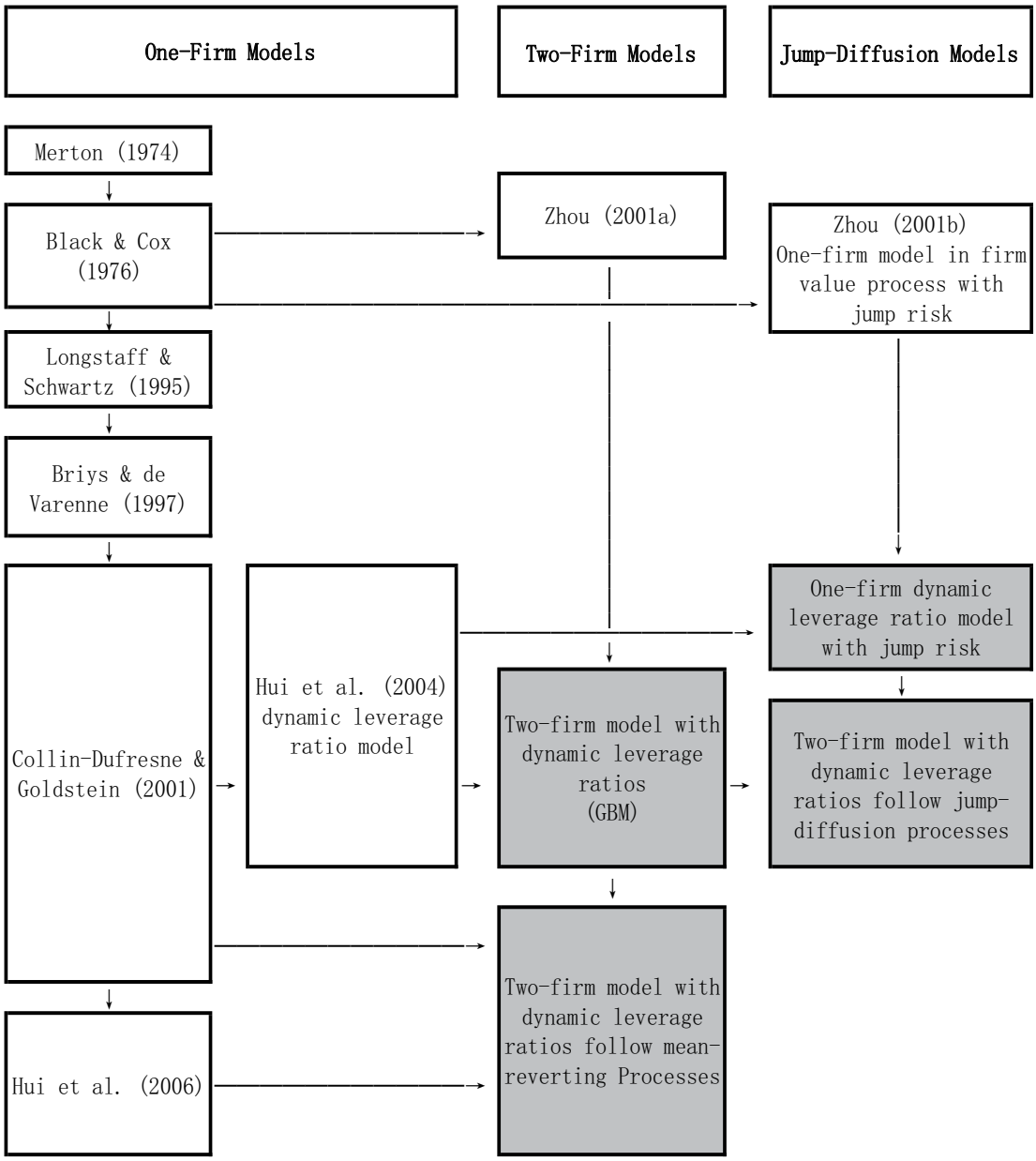

TABLE 2.2. The development of structural models and the relationship among these models to the two-firm model in this thesis. The shaded boxes indicate the new developments undertaken in this thesis.

leverage ratios are mean-reverting. More generally, the thesis extends the approaches of Collin-Dufresne & Goldstein (2001) and Hui et al. (2006) to the two-firm situation. The one-firm dynamic leverage ratio model is also extended to include the jump risk, and compared to Zhou (2001*b*), the difference being that here default is driven by the firm's leverage ratio with jumps, whereas in Zhou (2001*b*) it is the firm value that contains a jump component, respectively. The one-firm

leverage ratio with jumps is then generalized to the two-firm case, such that the two-firm model in this thesis provides a more comprehensive insight into default correlations for firms having the different features represented by these processes.

CHAPTER 3

Framework of the Two-Firm Model

The first part of this chapter presents the one-firm dynamic leverage ratio model of Hui et al. (2007) for corporate bond pricing. In their model, the corporate bond price is interpreted as the product of a risk-free bond price and a discounting factor by the separation of variables method. Since the risk-free bond price solution is known, therefore the main focus is on solving for this discounting factor. Hui et al. (2007) apply the method of images approach to obtain the closed-form solution in terms of the cumulative normal distribution function. However, when the parameters are time-dependent, the analytical solution is not so readily obtained. Lo et al. (2003) suggested an approach to deal with this problem using a time varying barrier method to obtain an approximate analytical solution.

The second part of the chapter extends the dynamic leverage ratio model to the two-firm situation for pricing financial derivatives involving default risks among two firms, with the credit linked note being the example here, and describes its application to evaluating default correlations.

Section 3.1 reviews the one-firm dynamic leverage ratio model framework. It illustrates the method of images approach for solving the one-dimensional first-passage-time problem. Section 3.2 outlines the time varying barrier approach to obtain an approximate analytical solution for the case in which parameters are time-dependent. The method of images and time varying barrier approaches will then be extended to the two-dimensional situation in Chapter 4 to obtain a solution for the two-firm model. Section 3.3 develops the two-firm dynamic leverage ratio model framework and Section 3.4 describes its application to the evaluation of default correlations.

3.1. The One-Firm Model

Hui et al. (2007) proposed that the corporate bond price depends on the firm's leverage ratio and risk-free interest rate, the leverage ratio L being defined as the total debt to the market-value capitalization of the firm (a similar definition can be found in Collin-Dufresne & Goldstein (2001)). The leverage ratio is assumed to follow the stochastic differential equation

$$dL = \mu_L(t)Ldt + \sigma_L(t)LdZ_L, \tag{3.1}$$

where $\mu_L(t)$ and $\sigma_L(t)$ are the time dependent drift rate and the volatility of the proportional change in the leverage ratio (that is dL/L) respectively, and Z_L is a Wiener process capturing the uncertainty in the leverage ratio dynamics under the historical measure $\mathbb{P}$.

The dynamics of the instantaneous spot rate of interest r is assumed to be given by the Hull & White (1990) generalization of the Vasicek (1977) model, so that

$$dr = \kappa_r(t)\left[\theta_r(t) - r\right]dt + \sigma_r(t)dZ_r, \tag{3.2}$$

where the instantaneous spot rate of interest r is mean-reverting to the long-run mean $\theta_r(t)$ at speed $\kappa_r(t)$, $\sigma_r(t)$ is the instantaneous volatility of interest rate changes and Z_r is a Wiener process capturing the uncertainty in the interest rate market under the historical measure $\mathbb{P}$.

The Wiener increments dZ_L and dZ_r are assumed to be correlated with

$$\mathbb{E}[dZ_L dZ_r] \;=\; \rho_{Lr}(t)dt. \tag{3.3}$$

Let $P(L, r, t)$ be the corporate bond price, dependent on the leverage ratio and interest rate dynamics in (3.1) and (3.2). Applying the standard bond pricing argument, we find that the pricing function satisfies the partial differential equation

$$\begin{aligned} -\frac{\partial P}{\partial t} \;=\; & \frac{1}{2}\sigma_L^2(t)L^2\frac{\partial^2 P}{\partial L^2} + \widetilde{\mu}_L(t)L\frac{\partial P}{\partial L} + \rho_{Lr}(t)\sigma_L(t)\sigma_r(t)L\frac{\partial^2 P}{\partial L \partial r} \\ & + \frac{1}{2}\sigma_r^2(t)\frac{\partial^2 P}{\partial r^2} + \kappa_r(t)[\widetilde{\theta}_r(t) - r]\frac{\partial P}{\partial r} - rP, \end{aligned} \tag{3.4}$$

for $t \in (0, T)$, $L \in (0, \widehat{L})$ and subject to the boundary conditions

$$P(L, r, T) = 1, \tag{3.5}$$

$$P(\widehat{L}, r, t) = 0. \tag{3.6}$$

Here

$$\widetilde{\mu}_L(t) \;=\; \mu_L(t) - \lambda_L\sigma_L(t), \tag{3.7}$$

$$\widetilde{\theta}_r(t) \;=\; \theta_r(t) - \frac{\lambda_r\sigma_r(t)}{\kappa_r(t)}, \tag{3.8}$$

where λ_L and λ_r are the market prices of risk (assumed constant) associated with the uncertainty impinging on the leverage ratio and interest rate processes, respectively. Moreover, since the growth rates of the firm's asset value and the firm's debt value equal the risk-free interest rate

under the risk-neutral measure, then the drift of the leverage ratio under risk-neutral measure $\widetilde{\mu}_L(t)$ is independent of the risk-free interest rate[1].

The boundary condition (3.6) describes the early default mechanism. In the Hui et al. (2007) model, default occurs when the firm's leverage ratio rises above a predefined level $\widehat{L}$ anytime during the life of the bond, and the bondholders receive nothing upon default. Otherwise, no default happens, and bondholders receive the par value of the bond at the maturity T which is the boundary condition (3.5). It is the boundary condition (3.6) that gives defaultable bond pricing problems their particular structure and difficulty. This is essentially a barrier type condition and in one form or another requires the solution of the first passage time problem associated with the partial differential equation (3.4).

In order to obtain an analytical solution to (3.4), Hui et al. (2007) employed the separation of variables method, where the solution for the corporate bond price turns out to be the product of two separate functions, one depending only on the leverage ratio and the other function depending only on the interest rate, so that

$$P(L,r,t) = B(r,t)\widehat{P}(L,t), \tag{3.9}$$

where Hui et al. (2007) point out that $B(r,t)$ is simply the risk-free bond price.

We note that the function $\widehat{P}(L,t)$ can be expressed as

$$\widehat{P}(L,t) = \frac{P(L,r,t)}{B(r,t)}, \tag{3.10}$$

which is a ratio of the corporate bond price to the risk-free bond price. We interpret $\widehat{P}$ as a risk ratio function that is inversely related to the degree of risk of a bond. If the ratio in (3.10) is close to 1, this means that the corporate bond is less likely to default, which would be the case for example with a AAA rated bond; while if it is very small, the corporate bond is very risky compared to the risk-free bond price, which would be the case for example with a CCC rated bond. That is the lower value of the ratio, the higher risk of the corporate bond defaulting.

By substituting (3.9) into (3.4) we find that the risk ratio function $\widehat{P}(L,t)$ satisfies the partial differential equation[2]

$$-\frac{\partial \widehat{P}}{\partial t} = \frac{1}{2}\sigma_L^2(t)L^2\frac{\partial^2 \widehat{P}}{\partial L^2} + \left[\widetilde{\mu}_L(t) + \rho_{Lr}(t)\sigma_L(t)\sigma_r(t)b(t)\right] L\frac{\partial \widehat{P}}{\partial L}, \tag{3.11}$$

[1]For a derivation of the corporate bond price as a function of the leverage ratio based on the firm's asset value and the firm's debt, see Hui et al. (2006) (Appendix A).

[2]A derivation of (3.11) by application of the separation of variables approach can be found in Appendix A.

subject to the boundary conditions

$$\widehat{P}(L,T) = 1, \tag{3.12}$$

$$\widehat{P}(\widehat{L},t) = 0. \tag{3.13}$$

In (3.11) $b(t)$ is a time-dependent parameter and depends on the speed of mean reversion of the risk-free interest rate and is given by

$$b(t) = -\int_t^T e^{\mathcal{K}(t)-\mathcal{K}(v)}dv, \tag{3.14}$$

for $\mathcal{K}(t) = \int_0^t \kappa_r(u)du$.

Denote by $x = \ln(L/\widehat{L})$ the normalized log-leverage ratio, and $\tau = T - t$ the time-to-maturity. Set $\widehat{P}(\widehat{L}e^x, t)$ equal to $\bar{P}(x,\tau)$, then $\bar{P}(x,\tau)$ satisfies the partial differential equation

$$\frac{\partial \bar{P}}{\partial \tau} = \frac{1}{2}\sigma_L^2(\tau)\frac{\partial^2 \bar{P}}{\partial x^2} + \gamma(\tau)\frac{\partial \bar{P}}{\partial x}, \tag{3.15}$$

for $\tau \in (0,T)$, $x \in (\infty, 0)$ and subject to the boundary conditions

$$\bar{P}(x,0) = 1, \tag{3.16}$$

$$\bar{P}(0,\tau) = 0, \tag{3.17}$$

where the drift coefficient $\gamma(\tau)$ is given by

$$\gamma(\tau) = \widetilde{\mu}_L(T-\tau) + \rho_{Lr}(T-\tau)\sigma_L(T-\tau)\sigma_r(T-\tau)b(T-\tau) - \frac{1}{2}\sigma_L^2(T-\tau), \tag{3.18}$$

we use $\sigma_L^2(\tau)$ for $\sigma_L^2(T-\tau)$ for expressions convenience.

The solution to the partial differential equation (3.15) for the risk ratio function $\bar{P}(x,\tau)$ can be written as

$$\bar{P}(x,\tau) = \int_{-\infty}^0 f(x,y;\tau)\bar{P}(y)dy, \tag{3.19}$$

where $f(x,y;\tau)$ is the transition probability density function for x starting at the value $x(0) = y$ at time-to-maturity $\tau = 0$ and ending at the value x at time-to-maturity τ. The initial condition function $\bar{P}(x,0) \equiv \bar{P}(y)$ is given in (3.16).

We notice that the transition probability density function $f(x, y; \tau)$ is subject to the zero boundary condition in (3.17). A general approach to obtaining the solution is to apply the method of images, see for example, Albanese & Campolieti (2006), Chapter 3.2 or Wilmott et al. (1995), Chapter 12.2.

3.1.1. The Method of Images for the One-Firm case.

To illustrate the method of images, we consider the heat equation

$$\frac{\partial u}{\partial \tau} = \frac{1}{2}\frac{\partial^2 u}{\partial x^2}, \tag{3.20}$$

where x is unrestricted in the region $x \in (-\infty, \infty)$. The solution to (3.20) is known[3] to be of the form

$$u(x, \tau) = \int_{-\infty}^{\infty} g(x, y; \tau) u(y) dy, \tag{3.21}$$

where $u(y)$ is the initial condition function, g is the transition probability density function that has the form

$$g(x, y; \tau) = \frac{e^{-(x-y)^2/2\tau}}{\sqrt{2\pi\tau}}. \tag{3.22}$$

If a zero boundary condition is imposed along x-axis at $x = 0$, then

$$u(0, \tau) = 0, \tag{3.23}$$

and the region of interest for the solution becomes $x \in (-\infty, 0)$. Applying the method of images approach, the exact solution to the heat equation (3.20) subject to the zero boundary condition (3.23) is

$$u(x, \tau) = \int_{-\infty}^{0} \widetilde{g}(x, y; \tau) u(y) dy, \tag{3.24}$$

where $\widetilde{g}$ is the transition probability density function for the restricted process. It is obtained by subtracting from the original density for the (for the unrestricted process) g centered at y within the ("physical") region $y \in (-\infty, 0)$ the same density centered at $-y$ within the ("nonphysical") region $y \in (0, \infty)$, that is

$$\widetilde{g}(x, y; \tau) = g(x, y; \tau) - g(x, -y; \tau), \tag{3.25}$$

[3]The solution of the heat equation can be found in many reference. For example, Wilmott et al. (1995) (Chpaters 4 and 5) give a good discussion and derivation of the solution of the heat equation.

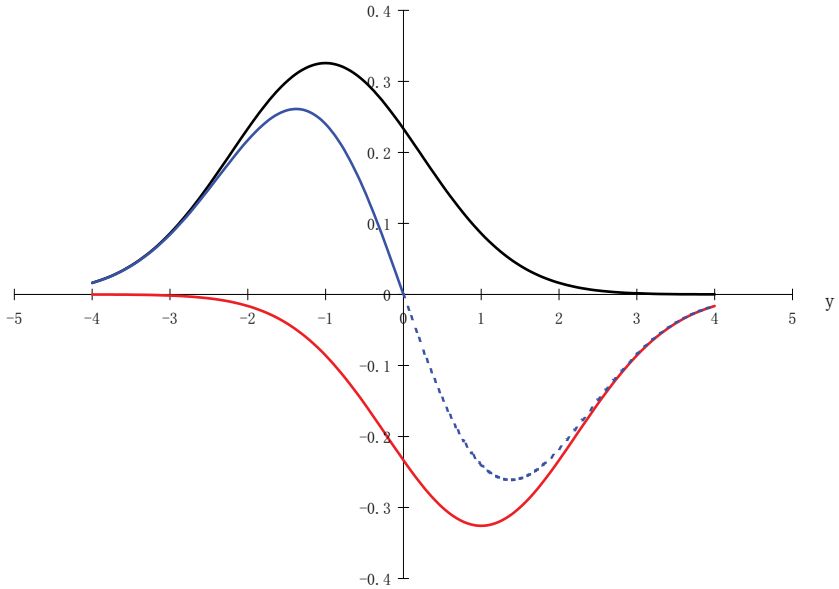

FIGURE 3.1. A sample plot of the density function $\widetilde{g}$ (blue curve) for absorption at the barrier $y = 0$ with parameter choices $x = -1$, $\tau = 1.5$ and $\tau_0 = 0$. The solid line gives $\widetilde{g}$ in the physical solution region, while the dashed line extends it into the nonphysical region. The plot of $\widetilde{g}$ is obtained by subtracting two density functions g for unrestricted processes, one centered at y (black curve) and the other at $-y$ (red curve).

so that the the boundary condition (3.23) is satisfied, as is easily verified.

Figure 3.1 illustrates the density function $\widetilde{g}$ (blue curve) for absorption at the barrier $y = 0$ with the parameter choices $x = -1$, $\tau = 1.5$ and $\tau_0 = 0$. The solid line gives $\widetilde{g}$ in the physical solution region, while the dashed line extends it into the nonphysical region. The plot of $\widetilde{g}$ is obtained by subtracting two density functions g for unrestricted processes, one centered at y (black curve) and the other at $-y$ (red curve) which is in fact $-g(x, -y; \tau)$, respectively.

3.1.2. Using the Reflection Principle to Obtain the Transition Probability Density Function.

Albanese & Campolieti (2006) give an alternative argument based on purely probabilistic arguments and basic properties of Brownian paths to show that equation (3.25) is indeed the transition

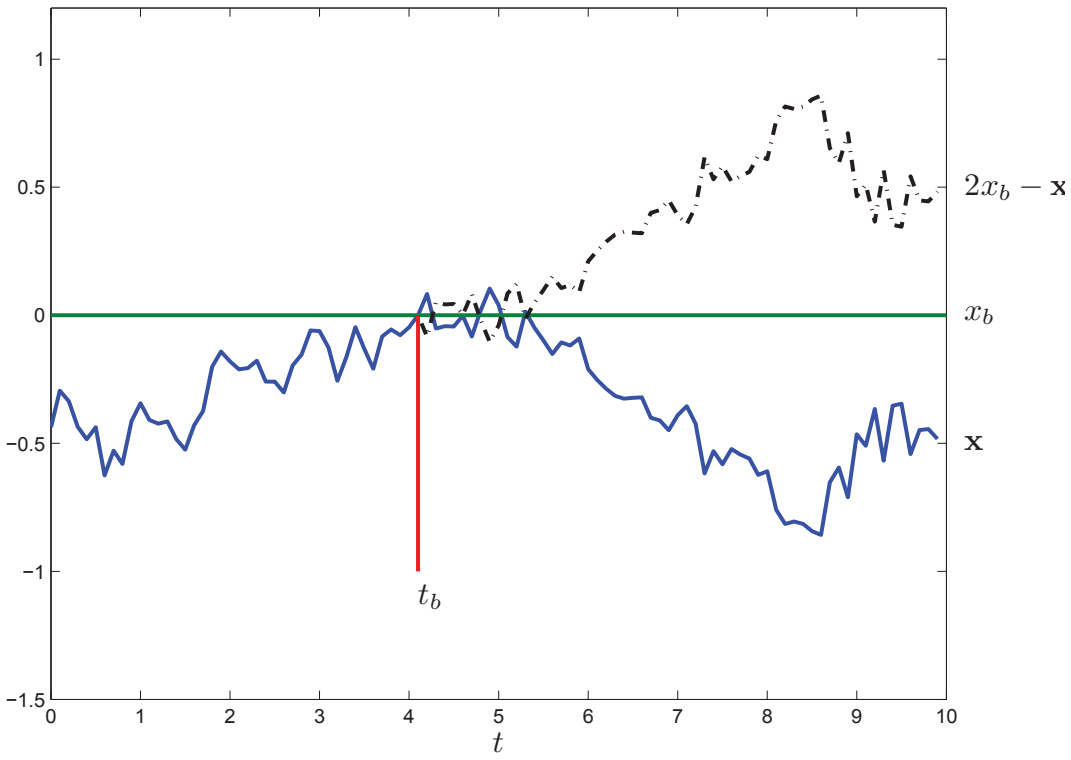

FIGURE 3.2. A Brownian motion and its reflection at the barrier $x_b = 0$.

probability density for Brownian motion x on the interval $x \in (-\infty, 0]$ with an the absorbing barrier at $x = 0$.

The idea briefly is as follows. Let x_t denote a Brownian motion starting at $x_0 < x_b$ at initial time t_0 with an upper absorbing barrier at $x = x_b$. Let $\tilde{x}_t$ denote the same Brownian process but without a barrier, that is the standard Wiener process that has the transition probability density $g(x_0, \tilde{x}_t; t - t_0)$ as given in (3.22). Then the probability of a path x_t having a value of $\mathbf{x}$ below the barrier, that is $\mathbf{x} < x_b$ for $t \geq t_0$, is equal to the probability of a barrier-free path $\tilde{x}_t$ having the value of $\mathbf{x}$, minus the probability of a barrier-free path $\tilde{x}_t$ at the barrier x_b at the first time t_b attaining the value $\mathbf{x}$ at terminal time t, which is the same as that for a reflected path starting at x_b at time t_b and attaining a value $2x_b - \mathbf{x}$ at time t (see Figure 3.2):

$$\mathbf{P}(x_t \leq \mathbf{x}) = \mathbf{P}(\tilde{x}_t \leq \mathbf{x}) - \mathbf{P}(\tilde{x}_t \geq 2x_b - \mathbf{x}) \tag{3.26}$$

for all $\mathbf{x} < x_b$.

By placing the expression for the density function and g, (3.22) into (3.26), then the cumulative probability of any path starting below the barrier $x_0 < x_b$ and attaining any value $y = x_t \leq \mathbf{x}$ (where $\mathbf{x} < x_b$) within the time interval $\tau = t - t_0$, conditional on paths being absorbed if the

barrier x_b is crossed, is

$$\mathbf{P}(y \leq \mathbf{x}) = \int_{-\infty}^{\mathbf{x}} g(x_0, y; \tau)dy - \int_{2x_b - \mathbf{x}}^{\infty} g(x_0, y; \tau)dy. \tag{3.27}$$

If the barrier is $x_b = 0$, and we are interested on the probability of a path starting at $x < 0$ and ending in the region $(-\infty, \mathbf{x} = 0)$ for the time interval $\tau = t - t_0$, then (3.27) can be expressed as

$$\mathbf{P}(x, \tau) \;\; = \;\; \int_{-\infty}^{0} g(x, y; \tau)dy - \int_{0}^{\infty} g(x, y; \tau)dy. \tag{3.28}$$

Making a change of variable in the second integral, we have

$$\mathbf{P}(x, \tau) \;\; = \;\; \int_{-\infty}^{0} [g(x, y; \tau) - g(x, -y; \tau)]dy. \tag{3.29}$$

If we differentiate the cumulative probability function with respect to y, then the transition probability density obtained is the same as (3.25), the density derived by the method of images.

3.1.3. Exact Solutions for the Case of Constant Parameters.

Next, we solve the partial differential equation (3.15). Consider the case in which the coefficients in (3.15) are constant, that is $\sigma_L(\tau) = \sigma_L$ and $\gamma(\tau) = \gamma$, and the partial differential equation (3.15) becomes

$$\frac{\partial \bar{P}}{\partial \tau} = \frac{1}{2}\sigma_L^2 \frac{\partial^2 \bar{P}}{\partial x^2} + \gamma \frac{\partial \bar{P}}{\partial x}. \tag{3.30}$$

We note that the partial differential equation (3.30) can be reduced to the heat equation (3.20) by the transformation[4]

$$\bar{P}(x, \tau) \;\; = \;\; e^{\eta x + \xi \tau} u(x, \zeta), \tag{3.31}$$

where we set parameters η and ξ as

$$\eta = -\frac{\gamma}{\sigma_L^2}, \; \xi = -\frac{\gamma^2}{2\sigma_L^2}, \text{ and } \zeta = \sigma_L^2 \tau.$$

At the initial conditions time-to-maturity $\tau_0 = 0$, the risk ratio function $\bar{P}$ and the solution to the heat equation u are related by $\big($setting $\bar{P}(y, 0) = \bar{P}(y)$ and $u(y, 0) = u(y)\big)$

$$\bar{P}(y) = 1 = e^{\eta y} u(y), \tag{3.32}$$

[4]The details of the transformation can be found in Appendix B.

so that

$$u(y) = e^{-\eta y}, \tag{3.33}$$

where we set x at $\tau_0 = 0$ equal to y.

Substituting the relations (3.31) and (3.33) into (3.24), yields

$$e^{-\eta x - \xi \tau} \bar{P}(x, \tau) = \int_{-\infty}^{0} \widetilde{g}(x, y; \zeta) e^{-\eta y} \bar{P}(y) dy. \tag{3.34}$$

Rearranging equation (3.34), we have

$$\bar{P}(x, \tau) = \int_{-\infty}^{0} e^{\eta(x-y)+\xi\tau}\, \widetilde{g}(x, y; \zeta) \bar{P}(y) dy. \tag{3.35}$$

Comparing equations (3.35) and (3.19), the transition probability density function f with constant coefficients, is thus identified as

$$f(x, y; \tau) = e^{\eta(x-y)+\xi\tau}\, \widetilde{g}(x, y; \zeta). \tag{3.36}$$

As discussed in Subsection 3.1.2, the cumulative probability for x follows a Brownian motion with an upper absorbing barrier at $x = 0$, starting below the barrier $x < 0$ at initial time t_0 (assume $t_0 = 0$) , then the probability of this path terminating within a period of time $\tau = t - t_0$ in the interval $x \in (-\infty, 0]$ conditional on absorption at $x = 0$ is

$$F(x, \tau) = \int_{-\infty}^{0} f(x, y; \zeta) dy, \tag{3.37}$$

for $\zeta = \sigma_L \tau$.

The probability $F(x, \tau)$ can be also interpreted as the survival probability for the absorption not yet having occurred during the period of time $\tau = t - t_0$. On the other hand, $1 - F(x, \tau)$ gives the probability of absorption having occurred, which can be interpreted as the default probability.

3.2. The One-Firm Model with Time-Dependent Parameters

If the coefficients in the partial differential equation (3.15) are time-dependent, the transformation of (3.15) to the heat equation will not be as straight forward as in the constant coefficients case. Lo

& Hui (2001) present a Lie-algebraic approach for the valuation of financial derivatives with time-dependent parameters. The Lie-algebraic approach to deal with this problem provides a way to obtain the propagator (the transition probability density function) of the partial differential equation with time-dependent parameters[5]. The Lie-algebraic makes use of the evolution operator $e^{c(\tau)\frac{\partial}{\partial x}}$ for $c(\tau)$ as defined below. This operator operates on an arbitrary, infinitely differentiable, function $f(x)$ according to

$$e^{c(\tau)\frac{\partial}{\partial x}} f(x) \quad = \quad \sum_{n=0}^{\infty} \frac{1}{n!} (c(\tau))^n \frac{\partial^n f(x)}{\partial x^n}. \tag{3.38}$$

A calculus for this operator has been developed in quantum mechanics for solving Fokker-Planck equations and Schrödinger equations, and is expounded for example in Suzuki (1989). We shall merely cite the results that we use as our arguments develop and give proofs in Appendix C. Many of the results obtained using this operator calculus can be obtained by other approaches, however this calculus provides a convenient unified approach, which is why we use it in this thesis.

Using the operator (3.38), we transform the partial differential equation (3.15) with time-dependent coefficients to the heat equation (3.20) by setting (see Appendix C)

$$\bar{P}(x,\tau)) \quad = \quad e^{\int_0^\tau \gamma(v)dv \frac{\partial}{\partial x}} \widetilde{u}(x,\zeta), \tag{3.39}$$

in which we transform time-to-maturity according to $\zeta = \int_0^\tau \sigma_L^2(v)dv$. Substituting (3.39) into (3.15), we find that the heat equation $\widetilde{u}(x,\zeta)$ satisfies the partial differential equation

$$\frac{\partial \widetilde{u}}{\partial \zeta} \quad = \quad \frac{1}{2} \frac{\partial^2 \widetilde{u}}{\partial x^2}. \tag{3.40}$$

We note that the transformation on the right hand side of equation (3.39) can be expressed as[6]

$$e^{\int_0^\tau \gamma(v)dv \frac{\partial}{\partial x}} \widetilde{u}(x,\zeta) = \widetilde{u}(x + \int_0^\tau \gamma(v)dv, \zeta), \tag{3.41}$$

[5]The Lie-algebraic approach has been successfully applied in physics to solve time-dependent Schrödinger equations associated with generalized quantum time-dependent oscillators and Fokker-Planck equation. For example, Lo (1997) applied the Lie-algebraic approach to obtain the exact form of the propagator of the Fokker-Planck equations with time-dependent parameters

$$\frac{\partial P}{\partial t} = \Big\{ B(t) \frac{\partial^2}{\partial x^2} - [C(t)x + D(t)] \frac{\partial}{\partial x} - C(t) \Big\} P(x,t).$$

On the other hand, an identical result is obtained by Demo et al. (2000) using the Green's function technique on the space of generalized functions.

[6]See Proposition C.6 in Appendix C.

so that

$$\bar{P}(x,\tau) = \widetilde{u}(x + \int_0^\tau \gamma(v)dv, \zeta). \tag{3.42}$$

The boundary condition of $\bar{P}$ implies the boundary condition of $\widetilde{u}$, which is (by substituting (3.42) into (3.17))

$$\bar{P}(0,\tau) = 0 = \widetilde{u}(\int_0^\tau \gamma(v)dv, \zeta). \tag{3.43}$$

We notice that the partial differential equation (3.40) for $\widetilde{u}$ is same as the heat equation (3.20). To apply the solution (3.24) to $\widetilde{u}$, we require that $\widetilde{u}$ satisfy the zero boundary condition equivalent to (3.23), that is

$$\widetilde{u}(0,\zeta) = 0. \tag{3.44}$$

However, from (3.43), the zero boundary condition (3.44) is not fulfilled. In order to satisfy the condition (3.44), we impose an additional structure on the function $\bar{P}$. We assume that the zero boundary condition for $\bar{P}$ is no longer at $x = 0$, but at a time varying barrier, denoted by $x^*(\tau)$, having the dynamic form[7]

$$x^*(\tau) = -\int_0^\tau \gamma(v)dv - \beta \int_0^\tau \sigma_L^2(v)dv, \tag{3.45}$$

where β is a real parameter, which is free to be chosen in some optimal way (as we will show later) so as to minimize the deviation between the time varying barrier $x^*(\tau)$ and the exact barrier at $x = 0$.

Since the zero boundary condition is not at $x = 0$, but at $x^*(\tau)$, therefore, the solution based on this new zero boundary condition at $x^*(\tau)$, is an approximate solution, and since it will depend on the value of β chosen we denote it as $\bar{P}_\beta$, hence we can write

$$\bar{P}_\beta(x,\tau) = \int_{-\infty}^0 f_\beta(x,y;\tau)\bar{P}_\beta(y)dy, \tag{3.46}$$

where $f_\beta(x,y;\tau)$ is the transition probability density function for the process restricted to the region $x \in (-\infty, x^*(\tau))$.

The quantity $\bar{P}_\beta$ also satisfies the partial differential equation (3.15), that is

$$\frac{\partial \bar{P}_\beta}{\partial \tau} = \frac{1}{2}\sigma_L^2(\tau)\frac{\partial^2 \bar{P}_\beta}{\partial x^2} + \gamma(\tau)\frac{\partial \bar{P}_\beta}{\partial x}, \tag{3.47}$$

[7]The time varying barrier technique was proposed by Lo et al. (2003) to facilitate the solution of such problems with time-dependent parameters.

with the zero boundary condition at an artificial time varying barrier $x^*(\tau)$ so that

$$\bar{P}_\beta(x^*(\tau), \tau) = 0, \tag{3.48}$$

for $x \in (-\infty, x^*(\tau))$ and $\tau \in (0, T)$. The initial condition of the approximate solution $\bar{P}_\beta$ is the same as the exact function $\bar{P}$, namely

$$\bar{P}_\beta(x, 0) = 1. \tag{3.49}$$

Next, we apply the transformation of the partial differential equation (3.47) by setting

$$\begin{aligned} \bar{P}_\beta(x, \tau) &= e^{-x^*(\tau)\frac{\partial}{\partial x}} \left[e^{\beta x/2 - \beta^2 \zeta/4} \widetilde{u}(x, \zeta) \right], & (3.50) \\ &= e^{\beta(x - x^*(\tau))/2 - \beta^2 \zeta/4} \widetilde{u}(x - x^*(\tau), \zeta), & (3.51) \end{aligned}$$

where $\widetilde{u}$ satisfies the partial differential equation (3.40).

The motivation of the transformation (3.50) is to reduce the partial differential equation (3.47) to (3.40), which has the same form as the heat equation (3.20), so that the solution of the heat equation can be applied to solve the partial differential equation (3.50).

It is convenient to carry out the transformation (3.50) in two steps. First we consider

$$\bar{P}_\beta(x, \tau) = e^{-x^*(\tau)\frac{\partial}{\partial x}} \widetilde{P}(x, \zeta). \tag{3.52}$$

The partial differential equation for $\widetilde{P}$ can be obtained by following the same technique as illustrated in Appendix C, so that

$$\frac{\partial \widetilde{P}}{\partial \zeta} = \frac{1}{2} \frac{\partial^2 \widetilde{P}}{\partial x^2} - \beta \frac{\partial \widetilde{P}}{\partial x}, \tag{3.53}$$

which has constant coefficients. In the second step, we apply the transformation described in Appendix B, then this last partial differential equation can be reduced to the partial differential equation (3.40) by setting

$$\widetilde{P}(x, \zeta) = e^{\beta x - \beta^2 \zeta/2} u(x, \zeta).$$

Next, we substitute (3.48) into (3.51) and so obtain the zero boundary condition for $\widetilde{u}$ as[8]

$$\widetilde{u}(0, \zeta) = 0. \tag{3.54}$$

[8]We note that

$$\bar{P}_\beta(x^*(\tau), \tau) = 0 = e^{\beta \cdot 0 - \beta^2 \zeta/2} \widetilde{u}(0, \zeta).$$

As mentioned previously, to apply the solution (3.24) for the heat equation u to $\widetilde{u}$, we require that the zero boundary condition of $\widetilde{u}$ satisfies (3.44). From (3.54), we note that this condition is fulfilled, hence, we can apply the solution for the heat equation (3.24) to obtain the solution for $\bar{P}_\beta$ via the relation (3.51). We first obtain the initial condition for u by substituting (3.51) into (3.48) with $x(0) = y$, namely

$$\bar{P}_\beta(y) = 1 = e^{\beta y}\widetilde{u}(y). \tag{3.55}$$

Then, we substitute (3.55) and (3.51) into the solution for the heat equation (3.24), to obtain

$$e^{-\beta(x-x^*(\tau))+\beta^2\zeta/2}\bar{P}_\beta(x,\tau) = \int_{-\infty}^{0} \widetilde{g}(x - x^*(\tau), y; \zeta)e^{-\beta y}\bar{P}_\beta(y)dy. \tag{3.56}$$

Then rearranging (3.56), we obtain the solution for the risk ratio function for the case in which the parameters are time-dependent, namely

$$\bar{P}_\beta(x,\tau) = \int_{-\infty}^{0} e^{\beta[x-y-x^*(\tau)]-\beta^2\zeta/2}\widetilde{g}(x - x^*(\tau), y; \zeta)\bar{P}_\beta(y)dy. \tag{3.57}$$

Comparing equations (3.46) and (3.57), we see that

$$f_\beta(x, y, \tau) = e^{\beta[x-y-x^*(\tau)]-\beta^2\zeta/2}\widetilde{g}(x - x^*(\tau), y; \zeta). \tag{3.58}$$

Similar to the constant coefficient case in the previous Subsection 3.1.3, we denote by $F_\beta(x,t)$ the survival probability (dependant on β) of a path initiating below the barrier at x at time $t_0 = 0$ and ending up in the region $(-\infty, 0)$ at the later time t, over the period of time $\tau = t - t_0$, is

$$F_\beta(x,\tau) = \int_{-\infty}^{0} f_\beta(x, y; \tau)dy. \tag{3.59}$$

Note that (3.57) and (3.59) are approximate solutions to the exact solution which has the zero boundary condition at $x = 0$. These approximate solutions depend on the parameter β. By choosing certain forms of β, we are able to form a lower bound or an upper bound to the exact solution[9]. For example, if the time interval of interest is $0 \le \tau \le T$, a lower bound barrier (that is $x^*(\tau) < 0$)

[9]A proof can be found in Lo et al. (2003) Appendix A.2. They showed that if $x^*(\tau) \le 0$ on the time interval of interest (for example, $0 \le \tau \le T$), then by the maximum principle (John (1978)), it can be concluded that the approximate solution $\bar{P}_\beta$ is less than the solution $\bar{P}$ for the exact barrier, therefore $\bar{P}_\beta$ forms a lower bound to the exact solution. On the other hand, if $x^*(\tau) \ge 0$ on the time interval of interest, then by the maximum principle the approximate solution $\bar{P}_\beta$ is larger than $\bar{P}$, therefore $\bar{P}_\beta$ forms an upper bound to the exact solution.

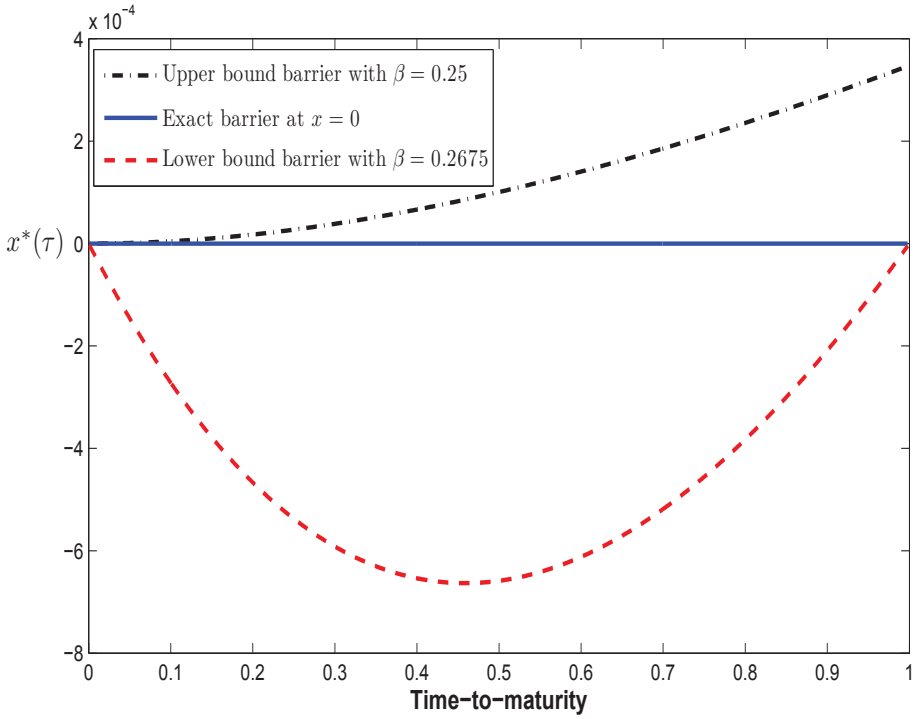

FIGURE 3.3. Lower and upper bounds for the time varying barrier. The exact barrier is at $x = 0$ (solid line). The lower bound barrier (dashed red line) with $\beta = 0.2675$ is estimated based on equation (3.60). The upper bound barrier (dashed-dotted blue line) with $\beta = 0.25$ is estimated based on equation (3.61). Parameters used are $\widetilde{\mu}_L = 0$, $\sigma_L = 0.299$, $\rho_{Lr} = 0.9$, $\kappa_r = 1.0$, $\sigma_r = 0.03162$ and $T = 1$.

can be formed by choosing a value of β such that $x^*(0) = x^*(T) = 0$, which from (3.45) determines β according to

$$\beta = -\frac{\int_0^T \gamma(v)dv}{\int_0^T \sigma_L^2(v)dv}. \tag{3.60}$$

An upper bound barrier (that is $x^*(\tau) > 0$) can be formed by choosing a value of β such that the instantaneous rate of change of the time varying barrier $x^*(\tau)$ is zero at time-to-maturity $\tau = 0$, that is

$$\frac{d[x^*(\tau)]}{d\tau}\Big|_{\tau=0} = -\frac{d[\int_0^\tau \gamma(v)dv]}{d\tau}\Big|_{\tau=0} - \beta\frac{d[\int_0^\tau \sigma_L^2(v)dv]}{d\tau}\Big|_{\tau=0} = 0.$$

from which

$$\beta = -\gamma(0)/\sigma_L^2(0). \tag{3.61}$$

To illustrate this idea, Figure 3.3 plots the lower and upper bounds curves for the time varying barrier. We stress that the values on the vertical axis are multiples of 10^{-4}, so very small values. Since the time varying barrier is closer to the exact barrier, then the approximate solutions are

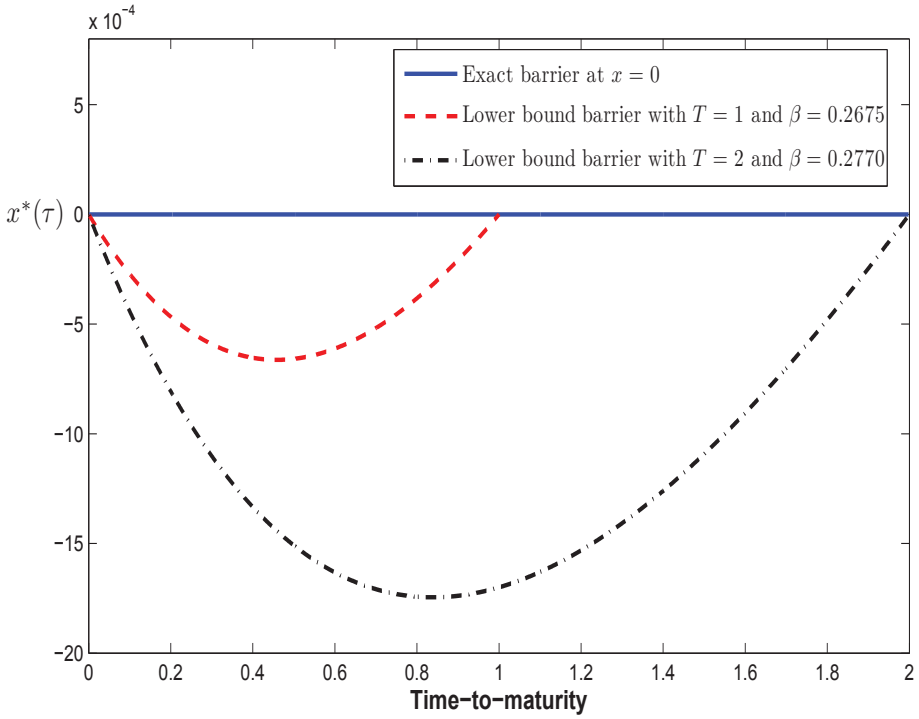

FIGURE 3.4. Lower bound for the time varying barrier with maturity $T = 1$ and $T = 2$. The lower bound barrier for $T = 1$ (dashed red line) with $\beta = 0.2675$, and barrier for $T = 2$ (dashed-dotted blue line) with $\beta = 0.2770$. Other parameters used are $\widetilde{\mu}_L = 0$, $\sigma_L = 0.299$, $\rho_{Lr} = 0.9$, $\kappa_r = 1.0$ and $\sigma_r = 0.03162$.

more accurate. The other factor that will effect the accuracy of the approximate solution is the maturity date. The larger is T, the less accurate will be the approximation. Figure 3.4 shows that when T increases, for example to $T = 2$, the deviation of a lower bound time varying barrier (dashed-dotted line) from the exact barrier at $x = 0$ is larger than that of the $T = 1$ case (dashed line). This is a result that indicates that the accuracy of the approximate solutions will decrease as the maturity T increases.

Lo et al. (2003) propose a multi-stage approximation method to deal with the problem of decreasing accuracy with increasing maturity. For example if the maturity is $T = 2$, in the first-stage, estimate the value of β, say β_{01} for the period time-to-maturity from $\tau = 0$ to $\tau = \tau_1 = 1$ and obtain the solution $\bar{P}_{\beta_{01}}(x, \tau_1)$ using equation (3.46) with the initial condition $\bar{P}_{\beta_{01}}(y) = 1$. In this case equation (3.46) can be expressed in terms of the normal distribution function $N(.)$ which has the computational advantage that is can be computed very efficiently. Next, in the second-stage consider the period of time-to-maturity from τ_1 to $\tau = \tau_2 = 2$, estimate another value of β, denoted β_{12} and then compute the solution $\bar{P}_{\beta_{12}}(x, \tau_2)$ using equation (3.46) again, however, the

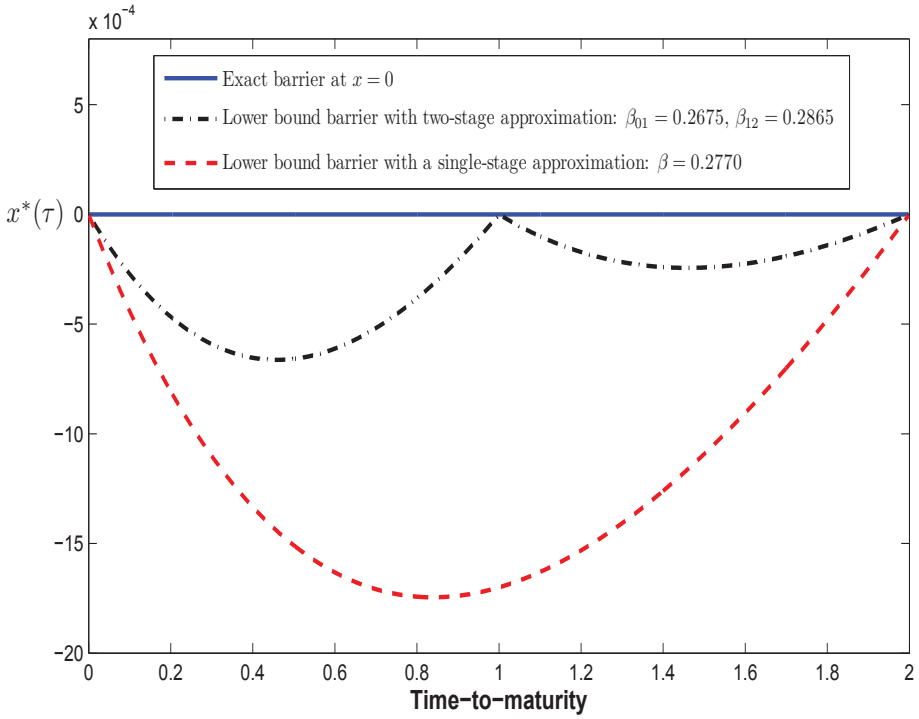

FIGURE 3.5. Lower bound for the time varying barrier for a single-stage and a two-stage approximations. The lower bound for the single-stage approximation (dashed red line) with $\beta = 0.2770$. The lower bound for the two-stage approximation (dashed-dotted blue line): first-stage $\beta_{01} = 0.2675$ and second-stage $\beta_{12} = 0.2865$. Other parameters used are $\widetilde{\mu}_L = 0$, $\sigma_L = 0.299$, $\rho_{Lr} = 0.9$, $\kappa_r = 1.0$, $\sigma_r = 0.03162$ and $T = 2$.

initial condition now is $\bar{P}_{\beta_{01}}(x, \tau_1)$, and the equation (3.46) becomes

$$\bar{P}_{\beta}(x, \tau_2) = \int_{-\infty}^{0} f_{\beta_{12}}(x, x'; \tau_2) \bar{P}_{\beta_{01}}(x', \tau_1) dx', \tag{3.62}$$

$$= \int_{-\infty}^{0} f_{\beta_{12}}(x, x'; \tau_2) \left[\int_{-\infty}^{0} f_{\beta_{01}}(x', y; \tau_1) \bar{P}(y) dy \right] dx', \tag{3.63}$$

which can expressed in terms of the bivariate normal distribution.

Figure 3.5 illustrates the plot for a single-stage and a two-stage time varying barrier of the maturity $T = 2$. We note that the vertical axis for the two-stage time varying barrier attains its minimum at 6×10^{-4} which is closer to the exact barrier compared to the single-stage approximation (minimum at about 17×10^{-4}). However, if there is a third-stage or fourth-stage... etc up to the nth-stage solution, (3.46) would involve multiple integration since the n-fold normal distribution would be involved, and numerical methods, such as the Gaussian quadrature method would need to be used.

3.3. Framework of the Two-Firm Model

In this section, we extend the dynamic leverage ratio model of Hui et al. (2007) to incorporate two firms. The credit derivative, in particular, a credit linked note is modelled since it refers to a single obligation and gives exposure to the default risk of the two firms. Many other derivatives share similar features to those of credit linked notes.

A credit linked note (CLN) is a form of funded credit derivative that allows the issuer to transfer a specific credit risk to credit investors. For example, as illustrated in Figure 3.6, a bank, B lends money to a company, C, (for example buys its bond), and at the time issues credit linked notes bought by investors. If company C (the"reference obligor") is solvent, the bank (the "issuer") is obligated to pay the notes to the investors in full at maturity. If company B goes bankrupt, the note-holders (investors) receive a recovery rate.

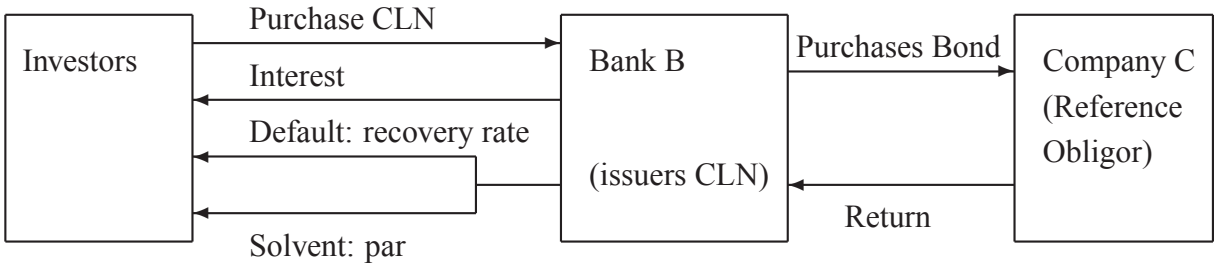

FIGURE 3.6. Mechanics of a credit linked note (CLN).

Under this structure, the price of the note is linked to the performance of a reference asset and the default risk of the note issuer. To model this credit derivative, we extend the Hui et al. (2007) dynamic leverage ratio model to incorporate two firms and a stochastic risk-free interest rate.

The main assumptions of the two-firm model with dynamic leverage ratios that we develop are:

Assumption 1. *Let L_1 and L_2 denote respectively the leverage ratios of the note issuer and the reference obligor. The leverage ratio is defined as the ratio of a firm's liability to its market-value capitalization. The dynamics of L_1 and L_2 are described by*

$$dL_i \;=\; \mu_i L_i dt + \sigma_i L_i dZ_i,\ (i = 1, 2), \tag{3.64}$$

where μ_i and σ_i denote the constant drift rate and volatility of the proportional change in leverage ratios respectively, and Z_1 and Z_2 are Wiener processes capturing the uncertainty in the leverage ratio dynamics under the historical measure $\mathbb{P}$. The Wiener increments dZ_1 and dZ_2 are correlated

with

$$\mathbb{E}[dZ_1 dZ_2] = \rho_{12} dt, \tag{3.65}$$

where ρ_{12} denotes the correlation coefficient of the proportional leverage ratio level of the two firms.

Assumption 2. *Let the dynamics of the instantaneous spot rate of interest follow the Vasicek (1977) process*

$$dr = \kappa_r \left(\theta_r - r\right) dt + \sigma_r dZ_r, \tag{3.66}$$

where the instantaneous spot rate of interest r is mean-reverting to the constant long-term mean θ_r at constant speed κ, and Z_r is a Wiener process capturing the uncertainty in the interest rate market under the historical measure $\mathbb{P}$. The Wiener processes Z_i and Z_r are correlated with

$$\mathbb{E}[dZ_i dZ_r] = \rho_{ir} dt, \ (i = 1, 2), \tag{3.67}$$

where ρ_{ir} denotes the correlation coefficient of the proportional changes of the leverage ratio level of firm i and the instantaneous spot rate of interest.

Assumption 3. *We assume default(s) occur anytime during the life of the credit linked note when either firm's leverage ratio rises above a predefined default threshold $\widehat{L}_i$, that is $L_i \geq \widehat{L}_i$. If the firms' leverage ratios never reach $\widehat{L}_i$, the note holder receives the face value, which is equal to unity. If default occurs the firm defaults on all of its obligations immediately, and the note holder receives nothing (that is there is no recovery) upon default of either firm.*

There could be a recovery payment if the default event happens. However, the assumption of zero recovery captures the worst situation in which investors lose all their investment on credit linked notes. The framework is easily adjusted to handle the case of some residual recovery rate.

Assumption 4. *We assume perfect and frictionless markets where the securities trade in continuous time.*

To obtain the partial differential equation for the credit linked note price $P(L_1, L_2, r, t)$ the standard arbitrage pricing argument is applied. Of course the leverage ratios L_1, L_2 are not themselves traded quantities so we employ the "trick" of setting up a portfolio containing four credit linked notes with different maturities in order to hedge away the risks of non-traded assets L_1, L_2 and r, see Wilmott et al. (1995) (Chapter 17.5) for the basic idea of this approach and Chiarella (2009)

(Chapter 10.4) for a more general discussion. The details in the present situation are set out in Appendix D and the price of credit linked note is found to satisfy the partial differential equation

$$\begin{aligned}
-\frac{\partial P(L_1,L_2,r,t)}{\partial t} &= \frac{1}{2}\sigma_1^2 L_1^2\frac{\partial^2 P}{\partial L_1^2}+\frac{1}{2}\sigma_2^2 L_2^2\frac{\partial^2 P}{\partial L_2^2}+\frac{1}{2}\sigma_r^2\frac{\partial^2 P}{\partial r^2}+\rho_{12}\sigma_1\sigma_2 L_1 L_2\frac{\partial^2 P}{\partial L_1\partial L_2}\\
&\quad+\rho_{1r}\sigma_1\sigma_r L_1\frac{\partial^2 P}{\partial L_1\partial r}+\rho_{2r}\sigma_2\sigma_r L_2\frac{\partial^2 P}{\partial L_2\partial r}\\
&\quad+[\mu_1-\lambda_1\sigma_1]L_1\frac{\partial P}{\partial L_1}+[\mu_2-\lambda_2\sigma_2]L_2\frac{\partial P}{\partial L_2}\\
&\quad+[\kappa_r(\theta_r-r)-\lambda_r\sigma_r]\frac{\partial P}{\partial r}-rP, \qquad (3.68)
\end{aligned}$$

in the interval of $t\in(0,T)$, $L_1\in(0,\widehat{L}_1)$, $L_2\in(0,\widehat{L}_2)$ and subject to the boundary conditions

$$P(L_1,L_2,r,T) = 1, \qquad (3.69)$$

$$P(\widehat{L}_1,L_2,r,t) = 0, \qquad (3.70)$$

$$P(L_1,\widehat{L}_2,r,t) = 0. \qquad (3.71)$$

The parameters $\widetilde{\mu}_i$ and $\widetilde{\theta}_r$ incorporate the market prices of risk, λ_1,λ_2 and λ_r (all assumed to be constant in this thesis), associated with leverage ratios and interest rate processes respectively and are defined as

$$\widetilde{\mu}_i = \mu_i-\lambda_i\sigma_i,\ (i=1,2), \qquad (3.72)$$

$$\widetilde{\theta}_r = \theta_r-\frac{\lambda_r\sigma_r}{\kappa_r}. \qquad (3.73)$$

in terms of which (3.74), becomes

$$\begin{aligned}
-\frac{\partial P(L_1,L_2,r,t)}{\partial t} &= \frac{1}{2}\sigma_1^2 L_1^2\frac{\partial^2 P}{\partial L_1^2}+\frac{1}{2}\sigma_2^2 L_2^2\frac{\partial^2 P}{\partial L_2^2}+\frac{1}{2}\sigma_r^2\frac{\partial^2 P}{\partial r^2}+\rho_{12}\sigma_1\sigma_2 L_1 L_2\frac{\partial^2 P}{\partial L_1\partial L_2}\\
&\quad+\rho_{1r}\sigma_1\sigma_r L_1\frac{\partial^2 P}{\partial L_1\partial r}+\rho_{2r}\sigma_2\sigma_r L_2\frac{\partial^2 P}{\partial L_2\partial r}\\
&\quad+\widetilde{\mu}_1 L_1\frac{\partial P}{\partial L_1}+\widetilde{\mu}_2 L_2\frac{\partial P}{\partial L_2}\\
&\quad+\kappa_r[\widetilde{\theta}_r-r]\frac{\partial P}{\partial r}-rP. \qquad (3.74)
\end{aligned}$$

Extending the separation of variables method used in Hui et al. (2007) to the two-firm case, we seek to express the credit linked note price in the separable form

$$P(L_1,L_2,r,t) = B(r,t)\widehat{P}(L_1,L_2,t), \qquad (3.75)$$

where $B(r,t)$ is the risk-free bond price. Equation (3.75) can be also expressed as

$$\widehat{P}(L_1, L_2, t) = \frac{P(L_1, L_2, r, t)}{B(r,t)}, \tag{3.76}$$

where $\widehat{P}(L_1, L_2, t)$ is the ratio of the risky credit linked note price to the risk-free bond price. In a similar way to the one-firm case (3.10), $\widehat{P}(L_1, L_2, t)$ can be also interpreted as a risk ratio function and it satisfies[10]

$$\begin{aligned} -\frac{\partial \widehat{P}}{\partial t} &= \frac{1}{2}\sigma_1^2 L_1^2 \frac{\partial^2 \widehat{P}}{\partial L_1^2} + \rho_{12}\sigma_1\sigma_2 L_1 L_2 \frac{\partial^2 \widehat{P}}{\partial L_1 \partial L_2} + \frac{1}{2}\sigma_2^2 L_2^2 \frac{\partial^2 \widehat{P}}{\partial L_2^2} \\ &\quad + \left[\widetilde{\mu}_1 + \rho_{1r}\sigma_1\sigma_r b(t)\right] L_1 \frac{\partial \widehat{P}}{\partial L_1} + \left[\widetilde{\mu}_2 + \rho_{2r}\sigma_2\sigma_r b(t)\right] L_2 \frac{\partial \widehat{P}}{\partial L_2}, \end{aligned} \tag{3.77}$$

subject to the boundary conditions

$$\widehat{P}(L_1, L_2, T) = 1, \tag{3.78}$$

$$\widehat{P}(\widehat{L}_1, L_2, t) = 0, \tag{3.79}$$

$$\widehat{P}(L_1, \widehat{L}_2, t) = 0. \tag{3.80}$$

In (3.77) $b(t)$ is a time-dependent parameter depending on the speed of mean reversion of the spot rate of interest given by

$$b(t) = \frac{e^{-\kappa_r(T-t)} - 1}{\kappa_r}. \tag{3.81}$$

Define the normalized log-leverage ratios

$$x_i = \ln(L_i/\widehat{L}_i), \tag{3.82}$$

and the volatility adjusted log-leverage ratios

$$X_i = x_i/\sigma_i. \tag{3.83}$$

Then denote $\widehat{P}(\widehat{L}_1 e^{\sigma_1 X_1}, \widehat{L}_2 e^{\sigma_2 X_2}, t)$ by $\bar{P}(X_1, X_2, \tau)$, so that in terms of time-to-maturity variable $\tau = T - t$, the partial differential equation (3.77) becomes

$$\begin{aligned} \frac{\partial \bar{P}}{\partial \tau} &= \frac{1}{2}\frac{\partial^2 \bar{P}}{\partial X_1^2} + \rho_{12}\frac{\partial^2 \bar{P}}{\partial X_1 \partial X_2} + \frac{1}{2}\frac{\partial^2 \bar{P}}{\partial X_2^2} \\ &\quad + \gamma_1(\tau)\frac{\partial \bar{P}}{\partial X_1} + \gamma_2(\tau)\frac{\partial \bar{P}}{\partial X_2}, \end{aligned} \tag{3.84}$$

[10] A derivation of (3.77) by application of the separation of variables approach can be found in Appendix E.

in the region bounded by the intervals $X_i \in (-\infty, 0)$, $\tau \in (0, T)$ and subject to the boundary conditions

$$\bar{P}(X_1, X_2, 0) = 1, \tag{3.85}$$

$$\bar{P}(0, X_2, \tau) = 0, \tag{3.86}$$

$$\bar{P}(X_1, 0, \tau) = 0. \tag{3.87}$$

The drift coefficients $\gamma_i(\tau)$ in (3.84) are defined as

$$\gamma_i(\tau) = [\widetilde{\mu}_i + \rho_{ir}\sigma_i\sigma_r b(T-\tau) - \sigma_i^2/2]/\sigma_i, \ (i = 1, 2). \tag{3.88}$$

The solution to the partial differential equation (3.84) for an initial distribution condition $\bar{P}(Y_1, Y_2, \tau_0)$ and subject to zero boundary conditions (3.86)-(3.87) is given by the integral

$$\bar{P}(X_1, X_2, \tau) = \int_{-\infty}^{0}\int_{-\infty}^{0} f(X_1, X_2, Y_1, Y_2; \tau)\bar{P}(Y_1, Y_2)dY_1dY_2, \tag{3.89}$$

where $f(X_1, X_2, Y_1, Y_2; \tau)$ is the transition probability density function for X_1 and X_2 for transition from the values $X_1(0) = Y_1$ and $X_1(0) = Y_2$ at time-to-maturity $\tau = 0$ below the barriers to the value X_1 and X_2 at time-to-maturity τ within the region $X_1 \in (-\infty, 0)$ and $X_2 \in (-\infty, 0)$. The initial condition function $\bar{P}(X_1, X_2, 0) \equiv \bar{P}(Y_1, Y_2)$ is given in (3.85).

Note that the transition probability density function f is subject to the zero boundary conditions in (3.86) and (3.87). Using a similar argument to Subsection 3.1.2, the probability of any paths with barriers at zero, initiating below the barriers $X_1 < 0$ and $X_2 < 0$ at time $t_0 = 0$ and ending up in the region $X_1 \in (-\infty, 0)$ and $X_2 \in (-\infty, 0)$ at later time t in the period of time $\tau = t - t_0$, is

$$F(X_1, X_2, \tau) = \int_{-\infty}^{0}\int_{-\infty}^{0} f(X_1, X_2, Y_1, Y_2; \tau)dY_1dY_2, \tag{3.90}$$

The cumulative probability $F(X_1, X_2, \tau)$ can be interpreted as the joint survival probability that the absorption at $X_1 = 0$ and $X_2 = 0$ has not yet occurred during the period of time τ.

3.4. Default Correlations

Estimation of probabilities of multiple defaults is important in credit risk analysis and risk management. Given a firm default, default correlation measures the likelihood of the default of the second firm. The joint survival probability can be used to evaluate the default correlations of two firms. For example, Zhou (2001*a*) uses the basic laws of probability to show that the default correlation

ρ_D of two firms is related to their joint survival probability by

$$\rho_D = \frac{\text{PD}(1 \cap 2) - \text{PD}_1\text{PD}_2}{\sqrt{\text{PD}_1(1-\text{PD}_1)}\sqrt{\text{PD}_1(1-\text{PD}_2)}}, \tag{3.91}$$

where PD_i is the probability of default of firm i and $\text{PD}(1 \cap 2)$ is the joint default probability of the two-firms. We note the identities

$$\text{PD}(1 \cap 2) \;=\; \text{PD}_1 + \text{PD}_2 - \text{PD}(1 \cup 2), \tag{3.92}$$

and

$$\text{PD}(1 \cup 2) \;=\; 1 - \text{PS}(1 \cap 2), \tag{3.93}$$

where $\text{PD}(1 \cup 2)$ is the probability of at least one firm defaulting and $\text{PS}(1 \cap 2)$ is the probability of both firms surviving during the time interval, that is the joint survival probability. Using the relations (3.91)-(3.93), the default correlation over a period of time t can be replaced in terms of the joint survival probability as

$$\rho_D = \frac{F(X_1, X_2, \tau) - 1 + \text{PD}_1 + \text{PD}_2 - \text{PD}_1\text{PD}_2}{\sqrt{\text{PD}_1(1-\text{PD}_1)}\sqrt{\text{PD}_2(1-\text{PD}_2)}}, \tag{3.94}$$

where the individual default probabilities can be calculated using the identity PD_i=1-PS_i, where PS_i is the survival probability of firm i based on equations (3.37) for constant parameters or (3.59) for time-dependent parameters.

The other type of default correlation model is the reduced-form approach, where defaults of different firms are driven by default intensities that follow stochastic processes. The default correlation between two firms is based on a mechanism by which the default intensity process of one firm affects the intensity process of another. For example, if one firm's default intensity is high this is a signal for the default intensity of the second firm to be high.

In comparing the structural approach and the reduced-form approach, we note that reduced-form models rely on input information from markets and calibrate the model to market data, while the structural approach is based on the underlying capital structure of firms. In this thesis, default is assumed to occur when either firm's leverage ratio is above a predefined default barrier. The default correlation between two firms is based on the assumption that the stochastic processes for the leverage ratios of the two firms are correlated.

On the other hand, the popular practical approach, the Gaussian copula model assumes that all firms will default eventually and the correlation between the probability distributions of default

dates are associated with a Gaussian copula, see Li (2000). The Gaussian copula model can be characterized as a simplified structural model. In a comparative study, Hull et al. (2006) show that when a simplifying assumption[11] is made to the structural model approach, the Gaussian copula and structural approaches give the same joint default probabilities. Compared to the Gaussian copula model, the two-firm model of this thesis allows for the feature that firms can adjust their capital structures over time to long-term targets, or experience external shocks, which are modelled by mean-reverting processes (Chapter 7) and jump-diffusion processes (Chapters 9).

3.5. Overview

This chapter has presented the one-firm dynamic leverage ratio model framework, reviewed the method of images approach to obtaining the survival probability, and demonstrated the time varying barrier approach to obtain an approximate analytical solution when the parameters are time-dependent in the one-firm situation. The second part of this chapter has presented the two-firm dynamic leverage ratio model framework and its application to the evaluation of default correlations. In the next chapter, we will solve the partial differential equation of the risk ratio function $\bar{P}$ in the two-firm case and obtain the solution by applying the method of images and the time varying barrier approaches that have been discussed in Section 3.1 and Section 3.2 .

[11] Namely that once a firm's asset value falls below the barrier it remains below the barrier thereafter.

CHAPTER 4

The Method of Images: Methodology and Implementation

This chapter extends the method of images approach as discussed in Section 3.1 to obtain the solution for the two-dimensional heat equation subject to the zero boundary conditions. The result is then used to solve the partial differential equation (3.84) for the risk ratio $\bar{P}$ with constant coefficients. If the coefficients are time-dependent, it is not so straight forward to obtain the solution as in the constant coefficients case. To deal with this problem, in Section 4.3 we thus apply the time varying barrier approach discussed in Section 3.2 to the two-dimensional case to obtain an approximate solution. In Section 4.4, the solutions are simplified and expressed in terms of the cumulative bivariate normal distribution functions in order to facilitate the implementation. However, as we will see even though the method of images approach applied to the two-dimensional case works very well, it can only give exact analytical solutions at certain values of the correlation coefficient ρ_{12}. Hence there is a need to develop robust numerical procedures as well, and this will be the topic of Chapter 5.

4.1. The Method of Images in the 2-D Situation

To extend the method of images illustrated in Section 3.1 to the two-dimensional case, we consider the two-dimensional heat equation

$$\frac{\partial u}{\partial \tau} = \frac{1}{2}\frac{\partial^2 u}{\partial x_1^2} + \rho_{12}\frac{\partial^2 u}{\partial x_1 \partial x_2} + \frac{1}{2}\frac{\partial^2 u}{\partial x_2^2}, \tag{4.1}$$

where x_1 and x_2 are unrestricted in the region $x_1, x_2 \in (-\infty, \infty)$. Its solution is known to be of the form

$$u(x_1, x_2, \tau) = \int_{-\infty}^{\infty}\int_{-\infty}^{\infty} g(x_1, x_2, y_1, y_2; \tau) u(y_1, y_2) dy_1 dy_2. \tag{4.2}$$

where $u(y_1, y_2)$ is the initial condition function and g is the bivariate transition probability density function for transition from y_1, y_2 to x_1, x_2 in time period τ, and has the form[1]

[1] A discussion of multivariate continuous distributions can be found in Albanese & Campolieti (2006) Chapter 1.3.

$$g(x_1, x_2, y_1, y_2; \tau)$$
$$= \frac{1}{2\pi\tau\sqrt{1-\rho_{12}^2}} \exp\left\{-\frac{(x_1-y_1)^2 - 2\rho_{12}(x_1-y_1)(x_2-y_2) + (x_2-y_2)^2}{2\tau(1-\rho_{12}^2)}\right\}. \quad (4.3)$$

The zero boundary conditions are imposed at $x_1 = 0$ and $x_2 = 0$, and require that

$$u(0, x_2, \tau) = 0, \quad (4.4)$$

$$u(x_1, 0, \tau) = 0, \quad (4.5)$$

and the region of interest for the solution is given by $x_1, x_2 \in (\infty, 0)$. The solution of the partial differential equation (4.1) subject to the boundary conditions (4.4) and (4.5) may be expressed as

$$u(x_1, x_2, \tau) = \int_{-\infty}^{0}\int_{-\infty}^{0} \widetilde{g}(x_1, x_2, y_1, y_2; \tau) u(y_1, y_2) dy_1 dy_2, \quad (4.6)$$

where $\widetilde{g}$ is the bivariate transition probability density function for the restricted process.

Applying the method of images approach, the solution for the density function $\widetilde{g}$ is a linear combinations of density functions g (for the unrestricted process) in such a way that their net effect cancels out at the barriers $x_1 = 0$ and $x_2 = 0$, then as a result the boundary conditions (4.4)-(4.5) are satisfied. To illustrate this concept, imagine there is a "source" density function (say g^0) located in the physical region[2] at the position (y_1^0, y_2^0) in the lower left hand quadrant (that is $g^0 = g^0(x_1, x_2, y_1^0, y_2^0; \tau)$), then we introduce an "image" density function (say g^1) in the nonphysical region at the position (y_1^1, y_2^1) in the lower right hand quadrant (that is $g^1 = g^1(x_1, x_2, y_1^1, y_2^1; \tau)$), such that the net effect of the two g functions cancel at the barrier $x_1 = 0$ as shown in Figure 4.1.

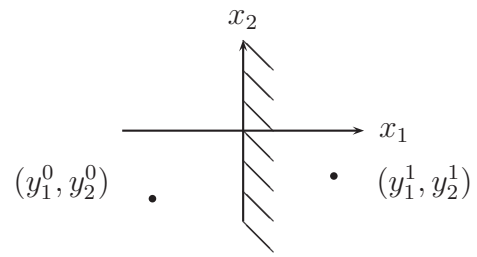

FIGURE 4.1. The 1st image reflected in $x_1 = 0$.

[2]By the physical region we mean the region $-\infty < x_1 < 0$, $-\infty < x_2 < 0$.

To determine (y_1^1, y_2^1), we consider the linear combination which in this case is given by

$$g^0(x_1, x_2 y_1^0, y_2^0; \tau) - g^1(x_1, x_2 y_1^1, y_2^1; \tau). \tag{4.7}$$

We require the combination in (4.7) to be zero at $x_1 = 0$, that is

$$g^0(0, x_2, y_1^0, y_2^0; \tau) - g^1(0, x_2, y_1^1, y_2^1; \tau) = 0. \tag{4.8}$$

Substituting equation (4.3) into (4.8), we see that the zero boundary condition at $x_1 = 0$ is satisfied provided that

$$\begin{aligned} &(0 - y_1^0)^2 - 2\rho_{12}(0 - y_1^0)(x_2 - y_2^0) + (x_2 - y_2^0)^2 \\ &= (0 - y_1^1)^2 - 2\rho_{12}(0 - y_1^1)(x_2 - y_2^1) + (x_2 - y_2^1)^2. \end{aligned} \tag{4.9}$$

Rearranging this expression, we obtain

$$x_2\phi + \alpha = 0, \tag{4.10}$$

where

$$\phi = 2(\rho_{12} y_1^0 - \rho_{12} y_1^1 - y_2^0 + y_2^1), \tag{4.11}$$

$$\alpha = (y_1^0)^2 - (y_1^1)^2 - 2\rho_{12} y_1^0 y_2^0 + 2\rho_{12} y_1^1 y_2^1 + (y_2^0)^2 - (y_2^1)^2. \tag{4.12}$$

In order that (4.10) hold for all x_2, it must be the case that $\phi = 0$ and $\alpha = 0$ hold simultaneously, in other words if

$$2(\rho_{12} y_1^0 - \rho_{12} y_1^1 - y_2^0 + y_2^1) = 0, \tag{4.13}$$

$$(y_1^0)^2 - (y_1^1)^2 - 2\rho_{12} y_1^0 y_2^0 + 2\rho_{12} y_1^1 y_2^1 + (y_2^0)^2 - (y_2^1)^2 = 0. \tag{4.14}$$

Solving (4.13) and (4.14) for y_1^1 and y_2^1, we obtain

$$y_1^1 = -y_1^0, \tag{4.15}$$

$$y_2^1 = y_2^0 - 2\rho_{12} y_1^0. \tag{4.16}$$

In the two-dimensional situation, there is also a barrier at $x_2 = 0$ and it is easy to verify that

$$g^0(x_1, 0, y_1^0, y_2^0; \tau) - g^1(x_1, 0, y_1^1, y_2^1; \tau) \neq 0. \tag{4.17}$$

Thus, we need to introduce another density function in the nonphysical region (say g^2) at the position (y_1^2, y_2^2) in the upper right hand quadrant (that is $g^2 = g^2(x_1, x_2, y_1^2, y_2^2; \tau)$, see Figure 4.2), such that it cancels out the effect of the image g^1 at $x_2 = 0$, that is, we require

$$g^1(x_1, 0, y_1^1, y_2^1; \tau) - g^2(x_1, 0, y_1^2, y_2^2; \tau) = 0. \tag{4.18}$$

To determine the vales of (y_1^2, y_2^2), we solve (4.18) similar to the way (4.9) was solved to obtain

$$y_2^2 = -y_2^1, \tag{4.19}$$

$$y_1^2 = y_1^1 - 2\rho_{12} y_2^1. \tag{4.20}$$

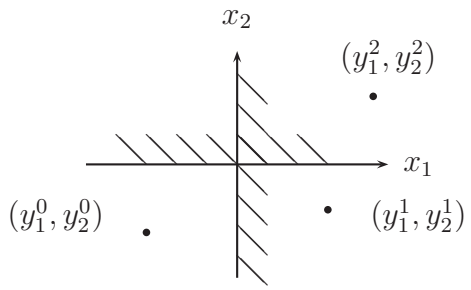

FIGURE 4.2. The 2nd image reflected in $x_2 = 0$.

However the introduction of the image density function g^2 will perturb the boundary condition at $x_1 = 0$[3]. So in order to cancel out this impact we need to introduce a third density function g^3 at (y_1^3, y_2^3) in the upper left hand quadrant as shown in Figure 4.3. In order to satisfy the boundary condition at $x_1 = 0$ we require

$$g^2(0, x_2, y_1^2, y_2^2; \tau) - g^3(0, x_2, y_1^3, y_2^3; \tau) = 0. \tag{4.21}$$

Solving equation (4.21) similarly to the way equation (4.9) was solved to obtain

$$y_1^3 = -y_1^2, \tag{4.22}$$

$$y_2^3 = y_2^2 - 2\rho_{12} y_1^2. \tag{4.23}$$

[3]It is readily confirmed that

$$g^1(0, x_2, y_1^1, y_2^1; \tau) - g^2(0, x_2, y_1^2, y_2^2; \tau) \neq 0$$

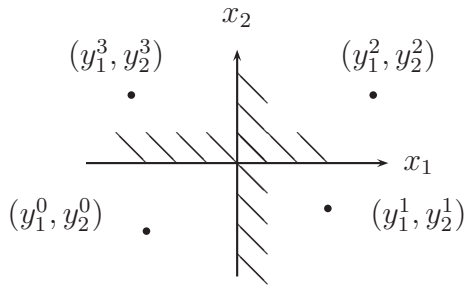

FIGURE 4.3. The 3rd image reflected in $x_1 = 0$.

Of course the introduction of density function g^3 could potentially perturb the boundary condition at $x_2 = 0$. However in the case $\rho_{12} = 0$ it turns out that the primary source at (y_1^0, y_2^0) and the image density functions g^1, g^2 and g^3 all balance each other such that the desired boundary conditions at $x_1 = 0$ and $x_2 = 0$ are preserved. One can view this as the fact that if one were to obtain a fourth image g^4, the reflection of g^3 in $x_2 = 0$, it would be precisely the primary source (that is it turns out that $y_1^4 = y_1^0$, $y_2^4 = y_2^0$). Of course, in the method of images approach, an image cannot in fact be located in the region of interest (or the physical region), where the source is located. Thus for the case in which $\rho_{12} = 0$, the solution for $\widetilde{g}$ is the linear combination of the density functions g^0, g^1, g^2 and g^3, namely

$$\begin{aligned}\widetilde{g}(x_1, x_2, y_1^0, y_2^0; \tau) &= g^0(x_1, x_2, y_1^0, y_2^0; \tau) - g^1(x_1, x_2, y_1^1, y_2^1; \tau) \\ &\quad + g^2(x_1, x_2, y_1^2, y_2^2; \tau) - g^3(x_1, x_2, y_1^3, y_2^3; \tau), \end{aligned} \tag{4.24}$$

which satisfies $\widetilde{g}(0, x_2, y_1^0, y_2^0; \tau) = \widetilde{g}(x_1, 0, y_1^0, y_2^0; \tau) = 0$.

For general values of $\rho_{12} \in (-1, 1)$, we need to reflect successively more than three times in a set of mirrors located at lines from the origin in the image region in such a way that the "loop closes" and so we would obtain after m reflections a set of m images such that the $(m+1)^{\text{st}}$ image would be the original source term. These m image terms just balance each other in such a way that the desired boundary conditions at $x_1 = 0$ and $x_2 = 0$ are preserved. In fact it turns out that only for specific values of ρ_{12} will the "loop close" after a finite number of reflections as shown in Appendix F, which also shows how to locate the set of reflecting mirrors. The values of ρ_{12} (rounded to 3 decimal places) that result in a "closed-loop" are shown in Table 4.1.

Dropping the superscripts in g^0 and (y_1^0, y_2^0), the solution for the density function $\widetilde{g}$ appearing in equation (4.6) may be written

$$\widetilde{g}(x_1, x_2, y_1, y_2; \tau) = g(x_1, x_2, y_1, y_2; \tau) + \sum_{k=1}^{m} (-1)^k g^k(x_1, x_2, y_1^k, y_2^k; \tau), \tag{4.25}$$

total no. of images m	ρ_{12}	values of ρ_{12}
3	$-\cos\frac{\pi}{2}$	0
5	$-\cos\frac{\pi}{3}$	-0.5
7	$-\cos\frac{\pi}{4}$	-0.707
9	$-\cos\frac{\pi}{5}$	-0.809
:	:	:
13	$-\cos\frac{\pi}{7}$	-0.901
:	:	:
m	$\cos\frac{2\pi}{(m+1)}$	:

TABLE 4.1. The relation between the number of images m required to form the "closed-loop" and the corresponding value of ρ_{12}.

where m is the total number of images used to form the closed-loop. Here y_1^k and y_2^k are obtained recursively from the relations between successive images[4]

$$y_1^k = \begin{cases} -y_1^{k-1} & \text{for odd } k, \\ y_1^{k-1} - 2\rho_{12} y_2^{k-1} & \text{for even } k, \end{cases} \tag{4.26}$$

$$y_2^k = \begin{cases} y_2^{k-1} - 2\rho_{12} y_1^{k-1} & \text{for odd } k\ , \\ -y_2^{k-1} & \text{for even } k\ , \end{cases} \tag{4.27}$$

where

$$y_1^1 = -y_1, \tag{4.28}$$

$$y_2^1 = y_2 - 2\rho_{12} y_1. \tag{4.29}$$

4.2. Method of Images for Constant Coefficients at Certain Non-Zero Values of ρ_{12}

Next, we consider the partial differential equation for the risk ratio function $\bar{P}(X_1, X_2, \tau)$, given by (3.84) in Section 3.3. If we set to zero the correlation between the interest rate and leverage ratio dynamics, so that $\rho_{ir} = 0$, then drift terms are no longer time-dependent and equation (3.84) becomes

$$\begin{aligned} \frac{\partial \bar{P}}{\partial \tau} = & \frac{1}{2}\frac{\partial^2 \bar{P}}{\partial X_1^2} + \rho_{12}\frac{\partial^2 \bar{P}}{\partial X_1 \partial X_2} + \frac{1}{2}\frac{\partial^2 \bar{P}}{\partial X_2^2} \\ & + \gamma_1 \frac{\partial \bar{P}}{\partial X_1} + \gamma_2 \frac{\partial \bar{P}}{\partial X_2}, \end{aligned} \tag{4.30}$$

[4]Equations (4.26), (4.28) and (4.29) are derived in the same way as equations (4.15-4.16), (4.19-4.20) and (4.22-4.23) were derived.

where the drift coefficients γ_1 and γ_2 are given in (3.88) with $\rho_{1r} = \rho_{2r} = 0$, that is

$$\gamma_i = \frac{\widetilde{\mu}_i - \sigma_i^2/2}{\sigma_i}, \ (i = 1, 2). \tag{4.31}$$

We note that the partial differential equation (4.30) can be transformed to the two-dimensional heat equation (4.1) by setting[5]

$$\bar{P}(X_1, X_2, \tau) \ = \ e^{\eta_1 X_1 + \eta_2 X_2 + \xi\tau} u(X_1, X_2, \tau), \tag{4.32}$$

where η_1, η_2 and ξ are constants derived in Appendix G and given by

$$\eta_1 = \frac{\gamma_2\rho_{12} - \gamma_1}{1 - \rho_{12}^2}, \tag{4.33}$$

$$\eta_2 = \frac{\gamma_1\rho_{12} - \gamma_2}{1 - \rho_{12}^2}, \tag{4.34}$$

$$\xi = -\frac{\left(\frac{1}{2}\gamma_1^2 - \rho_{12}\gamma_1\gamma_2 + \frac{1}{2}\gamma_2^2\right)}{1 - \rho_{12}^2}. \tag{4.35}$$

The initial and boundary conditions (3.86)-(3.87) determine the initial and boundary conditions of u with $X_1(0) = Y_1$ and $X_2(0) = Y_2$, thus

$$\bar{P}(Y_1, Y_2) = 1 = e^{\eta_1 Y_1 + \eta_2 Y_2} u(Y_1, Y_2), \tag{4.36}$$

$$\bar{P}(0, X_2, \tau) = 0 = u(0, X_2, \tau), \tag{4.37}$$

$$\bar{P}(X_1, 0, \tau) = 0 = u(X_1, 0, \tau). \tag{4.38}$$

Now substituting relations (4.32) and (4.36) into the solution for heat equation (4.6), we obtain

$$e^{-\eta_1 X_1 - \eta_2 X_2 - \xi\tau} \bar{P}(X_1, X_2, \tau) = \int_{-\infty}^{0}\int_{-\infty}^{0} \widetilde{g}(X_1, X_2, Y_1, Y_2; \tau) e^{-\eta_1 Y_1 - \eta_2 Y_2} \bar{P}(Y_1, Y_2) dY_1 dY_2, \tag{4.39}$$

which simplifies to

$$\bar{P}(X_1, X_2, \tau) = \int_{-\infty}^{0}\int_{-\infty}^{0} e^{+\eta_1(X_1 - Y_1) + \eta_2(X_2 - Y_2) + \xi\tau} \widetilde{g}(X_1, X_2, Y_1, Y_2; \tau) \bar{P}(Y_1, Y_2) dY_1 dY_2, \tag{4.40}$$

[5]A derivation can be found in Appendix G.

Substituting (4.25) for $\widetilde{g}$ into (4.40), we obtain the solution for the risk ratio function with constant coefficients, namely

$$\begin{aligned}\bar{P}(X_1, X_2, \tau) &= \int_{-\infty}^{0}\int_{-\infty}^{0} e^{+\eta_1(X_1-Y_1)+\eta_2(X_2-Y_2)+\xi\tau}\Big[g(X_1, X_2, Y_1, Y_2; \tau) \\ &\quad + \sum_{k=1}^{m}(-1)^k g^k(X_1, X_2, Y_1^k, Y_2^k; \tau)\Big]\bar{P}(Y_1, Y_2)dY_1dY_2, \end{aligned} \tag{4.41}$$

If we compare equations (4.41) and (3.89), we get the result that the joint transition probability density function f for the processes restricted to the region $X_1 \in (-\infty, 0)$ and $X_2 \in (-\infty, 0)$, is given by

$$\begin{aligned}f(X_1, X_2, Y_1, Y_2; \tau) &= e^{+\eta_1(X_1-Y_1)+\eta_2(X_2-Y_2)+\xi\tau}\Big[g(X_1, X_2, Y_1, Y_2; \tau) \\ &\quad + \sum_{k=1}^{m}(-1)^k g^k(X_1, X_2, Y_1^k, Y_2^k; \tau)\Big]. \end{aligned} \tag{4.42}$$

Then the solution for the joint survival probability (3.90) over the period $\tau = t - t_0$ is

$$\begin{aligned}F(X_1, X_2, \tau) &= \int_{-\infty}^{0}\int_{-\infty}^{0} e^{+\eta_1(X_1-Y_1)+\eta_2(X_2-Y_2)+\xi\tau}\Big[g(X_1, X_2, Y_1, Y_2; \tau) \\ &\quad + \sum_{k=1}^{m}(-1)^k g^k(X_1, X_2, Y_1^k, Y_2^k; \tau)\Big]dY_1dY_2. \end{aligned} \tag{4.43}$$

We stress that the solution for the risk ratio function (4.41) and the joint survival probability (4.43) are only valid for the values of ρ_{12} given in Table 4.1.

4.3. Method of Images for Time Varying Coefficients at Certain Non-Zero Values of ρ_{12}

This section will extend to the two-firm case the time varying barrier approach in Section 3.2. As discussed in Section 3.2 for the one-firm situation, the solution for the heat equation obtained by the method of images approach for solving the zero boundary condition cannot be applied directly to the case in which the drift terms are time-dependent. This is due to the fact that the zero boundary condition of the function in which we are interested, after being transformed to the heat equation, is no longer at zero, see for example (3.43). The time varying barrier approach solves this problem by setting the zero boundary condition at a time varying barrier, which depends on a parameter β. The parameter β is free to be chosen in an optimal way so as to minimize the deviation between the time varying barrier and the exact barrier. Therefore, the solution depends on β and is an approximation to the exact solution. In this section, we extend the approach outlined

in Section 3.2 to the two-firm situation to obtain an approximate solution for the partial differential equation for (3.84) when the drift terms are time-dependent.

Denote by $\bar{P}_{\boldsymbol{\beta}}$ the approximate solution to the exact solution $\bar{P}$ of the partial differential equation (3.84). It is assumed that $\bar{P}_{\boldsymbol{\beta}}$ satisfies the same partial differential equation, that is

$$\frac{\partial \bar{P}_{\boldsymbol{\beta}}}{\partial \tau} = \frac{1}{2}\frac{\partial^2 \bar{P}_{\boldsymbol{\beta}}}{\partial X_1^2} + \rho_{12}\frac{\partial^2 \bar{P}_{\boldsymbol{\beta}}}{\partial X_1 \partial X_2} + \frac{1}{2}\frac{\partial^2 \bar{P}_{\boldsymbol{\beta}}}{\partial X_2^2} + \gamma_1(\tau)\frac{\partial \bar{P}_{\boldsymbol{\beta}}}{\partial X_1} + \gamma_2(\tau)\frac{\partial \bar{P}_{\boldsymbol{\beta}}}{\partial X_2}. \tag{4.44}$$

We assume that the zero boundary conditions for the approximate solution $\bar{P}_{\boldsymbol{\beta}}$ are not the same as those the exact solution $\bar{P}$ at $X_1 = 0$ and $X_2 = 0$ (shown in (3.86) and (3.87)), but become

$$\bar{P}_{\boldsymbol{\beta}}(X_1^*(\tau), X_2, \tau) = 0, \tag{4.45}$$

$$\bar{P}_{\boldsymbol{\beta}}(X_1, X_2^*(\tau), \tau) = 0, \tag{4.46}$$

where $X_1^*(\tau)$ and $X_2^*(\tau)$ are time varying barriers along the X_1-axis and X_2-axis respectively. Now, X_1 and X_2 are restricted to the region $X_1 \in (-\infty, X_1^*(\tau))$ and $X_2 \in (-\infty, X_2^*(\tau))$. Using an argument similar to the one in Section 3.2, the time varying barriers are given by

$$X_i^*(\tau) = -\int_0^\tau \gamma_i(v)dv - \beta_i \tau, \ (i = 1, 2). \tag{4.47}$$

The drift coefficients $\gamma_i(\tau)$ are given in (3.88), β_1 and β_2 are two real adjustable constants that control the shape of the time varying barriers $X_1^*(\tau)$ and $X_2^*(\tau)$ and would be chosen so that they remains as close as possible to the exact barrier $X_1 = 0$ and $X_2 = 0$ respectively, just as in the one firm case. Note that the initial condition of the approximate solution $\bar{P}_{\boldsymbol{\beta}}$ is the same as for the exact solution $\bar{P}$ in (3.85), that is

$$\bar{P}_{\boldsymbol{\beta}}(X_1, X_2, 0) = 1. \tag{4.48}$$

The approximate solution $\bar{P}_{\boldsymbol{\beta}}$ can thus be written as

$$\bar{P}_{\boldsymbol{\beta}}(X_1, X_1, \tau) = \int_{-\infty}^{0}\int_{-\infty}^{0} f_\beta(X_1, X_2, Y_1, Y_2; \tau)\bar{P}_{\boldsymbol{\beta}}(Y_1, Y_2)dY_1 dY_2. \tag{4.49}$$

To obtain the form of the joint transition probability density function f_β for the processes restricted to the region $X_1 \in (-\infty, X^*(\tau))$ and $X_2 \in (-\infty, X^*(\tau))$ in terms to the bivariate density functions g in (4.25), we extend the approach as discussed in Section 3.2 and transform the partial

differential equation (4.44) for $\bar{P}_{\boldsymbol{\beta}}$ to the heat equation by setting[6]

$$\bar{P}_{\boldsymbol{\beta}}(X_1, X_2, \tau) = e^{-X_1^*(\tau)\frac{\partial}{\partial X_1} - X_2^*(\tau)\frac{\partial}{\partial X_2}} \left[e^{\eta_1 X_1 + \eta_2 X_2 + \xi\tau} \widetilde{u}(X_1, X_2, \tau) \right], \tag{4.50}$$

$$= e^{\eta_1[X_1 - X_1^*(\tau)] + \eta_2[X_2 - X_2^*(\tau)] + \xi\tau} \widetilde{u}(X_1 - X_1^*(\tau), X_2 - X_2^*(\tau), \tau), \tag{4.51}$$

where $\widetilde{u}$ satisfies the heat equation (4.1) (with τ replaced by ζ and x_1, x_2 by X_1, X_2), and η_1, η_2 and ξ are constants derived in Appendix H and given by

$$\eta_1 = \frac{-\beta_2\rho_{12} + \beta_1}{1 - \rho_{12}^2}, \tag{4.52}$$

$$\eta_2 = \frac{-\beta_1\rho_{12} + \beta_2}{1 - \rho_{12}^2}, \tag{4.53}$$

$$\xi = -\frac{\left(\frac{1}{2}\beta_1^2 - \rho_{12}\beta_1\beta_2 + \frac{1}{2}\beta_2^2\right)}{1 - \rho_{12}^2}. \tag{4.54}$$

Substitution of the zero boundary conditions (4.45) and (4.46) into (4.51) yields the boundary conditions for $\widetilde{u}$ as[7]

$$\widetilde{u}(0, X_2 - X_2^*(\tau), \tau) = 0, \tag{4.55}$$

$$\widetilde{u}(X_1 - X_1^*(\tau), 0, \tau) = 0. \tag{4.56}$$

The zero boundary conditions (4.55) - (4.56) for $\widetilde{u}$ occur when the value of the barriers are equal to zero. These are similar to the zero boundary conditions in (4.4)-(4.5) for u, simply replacing the space variables x_i with $X_i - X_i^*(\tau)$. Hence, the solution $\widetilde{g}$ in (4.25) can be applied to obtain the solution for $\bar{P}_{\boldsymbol{\beta}}$. Substitution of the initial condition (4.48) with $X_1(0) = Y_1$ and $X_2(0) = Y_2$ into (4.51) determines the initial condition of $\widetilde{u}$, which is

$$\bar{P}_{\boldsymbol{\beta}}(Y_1, Y_2) = 1 = e^{\eta_1 Y_1 + \eta_2 Y_2} \widetilde{u}(Y_1, Y_2). \tag{4.57}$$

[6] A derivation of equations (4.50) and (4.51) can be found in Appendix H.

[7] We note that

$$\bar{P}_{\boldsymbol{\beta}}(X_1^*(\tau), X_2, \tau) = 0 = e^{\eta_1 \cdot 0 + \eta_2[X_2 - X_2^*(\tau)] + \xi\tau} \widetilde{u}(0, X_2 - X_2^*(\tau), \tau),$$
$$\bar{P}_{\boldsymbol{\beta}}(X_1, X_2^*(\tau), \tau) = 0 = e^{\eta_1[X_1 - X_1^*(\tau)] + \eta_2 \cdot 0) + \xi\tau} \widetilde{u}(X_1 - X_1^*(\tau), 0, \tau).$$

Substitution of the initial condition (4.57) and the relation (4.51) into the relation (4.6), yields

$$\begin{aligned} & e^{-\eta_1[X_1-X_1^*(\tau)]-\eta_2[X_2-X_2^*(\tau)]-\xi\tau}\bar{P}_{\boldsymbol{\beta}}(X_1,X_2,\tau) \\ & = \int_{-\infty}^{0}\int_{-\infty}^{0}\widetilde{g}(X_1-X_1^*(\tau),X_2-X_2^*(\tau),Y_1,Y_2;\tau)e^{-\eta_1 Y_1-\eta_2 Y_2}\bar{P}_{\boldsymbol{\beta}}(Y_1,Y_2)dY_1dY_2, \end{aligned} \tag{4.58}$$

which simplifies to

$$\begin{aligned} \bar{P}_{\boldsymbol{\beta}}(X_1,X_2,\tau) \;=\; & \int_{-\infty}^{0}\int_{-\infty}^{0} e^{\eta_1[X_1-X_1^*(\tau)-Y_1]+\eta_2[X_2-X_2^*(\tau)-Y_2]+\xi\tau} \\ & \widetilde{g}(X_1-X_1^*(\tau),X_2-X_2^*(\tau),Y_1,Y_2;\tau)\bar{P}_{\boldsymbol{\beta}}(Y_1,Y_2)dY_1dY_2. \end{aligned} \tag{4.59}$$

Substituting (4.25) into (4.59), we obtain

$$\begin{aligned} & \bar{P}_{\boldsymbol{\beta}}(X_1,X_2,\tau) = \\ & \int_{-\infty}^{0}\int_{-\infty}^{0} e^{\eta_1[X_1-X_1^*(\tau)-Y_1]+\eta_2[X_2-X_2^*(\tau)-Y_2]+\xi\tau}\Big[g(X_1-X_1^*(\tau),X_2-X_2^*(\tau),Y_1,Y_2;\tau) \\ & +\sum_{k=1}^{m}(-1)^k g^k(X_1-X_1^*(\tau),X_2-X_2^*(\tau),Y_1^k,Y_2^k;\tau)\Big]\bar{P}_{\boldsymbol{\beta}}(Y_1,Y_2)dY_1dY_2. \end{aligned} \tag{4.60}$$

Comparing (4.60) and (4.49), yields the joint transition probability density function

$$\begin{aligned} & f_\beta(X_1,X_2,Y_1,Y_2;\tau) = \\ & e^{\eta_1[X_1-X_1^*(\tau)-Y_1]+\eta_2[X_2-X_2^*(\tau)-Y_2]+\xi\tau}\Big[g(X_1-X_1^*(\tau),X_2-X_2^*(\tau),Y_1,Y_2;\tau) \\ & +\sum_{k=1}^{m}(-1)^k g^k(X_1-X_1^*(\tau),X_2-X_2^*(\tau),Y_1^k,Y_2^k;\tau)\Big]. \end{aligned} \tag{4.61}$$

Then the approximate solution to the joint survival probability (3.90) over the period $\tau = t - t_0$, is

$$\begin{aligned} & F_\beta(X_1,X_2,\tau) = \\ & \int_{-\infty}^{0}\int_{-\infty}^{0} e^{\eta_1[X_1-X_1^*(\tau)-Y_1]+\eta_2[X_2-X_2^*(\tau)-Y_2]+\xi\tau}\Big[g(X_1-X_1^*(\tau),X_2-X_2^*(\tau),Y_1,Y_2;\tau) \\ & +\sum_{k=1}^{m}(-1)^k g^k(X_1-X_1^*(\tau),X_2-X_2^*(\tau),Y_1^k,Y_2^k;\tau)\Big]dY_1dY_2. \end{aligned} \tag{4.62}$$

We also note that the approximate solutions (4.60) and (4.62) are only valid for the values of ρ_{12} given in Table 4.1.

4.4. Numerical Implementation

To implement the solutions for the risk ratio function in (4.41) and (4.60) or the joint survival probability functions in (4.43) and (4.62), a convenient way is to simplify those expressions and express them in terms of the cumulative bivariate normal distribution function $N_2(.)$, which has the form

$$\text{Prob}(U \leq a, V \leq b; \rho) = N_2(a, b, \rho) = \int_{-\infty}^{a} \int_{-\infty}^{b} n_2(u, v, \rho) dv du, \tag{4.63}$$

where the bivariate normal density function is given by

$$n_2(a, b, \rho) \quad = \quad \frac{1}{2\pi\sqrt{1-\rho^2}} \exp\left(-\frac{u^2 - 2\rho uv + v^2}{2(1-\rho^2)}\right). \tag{4.64}$$

A range of different analytical approximate methods have been proposed for the evaluation of (4.63). In this thesis, we apply the widely cited Drezner (1978) method, which is based on direct computation of the double integral by the Gauss quadrature method[8].

4.4.1. Numerical Implementation in the Constant Coefficients Case.

In the following subsections, we use the solutions of the joint survival probability in (4.43) for the constant coefficients case and (4.62) for the time varying coefficients case to illustrate the numerical implementation of these expressions.

Consider the solution for the joint survival probability (4.43) for the constant coefficients case, and rearrange it as

$$\begin{aligned} & F(X_1, X_2, \tau) \\ & = \int_{-\infty}^{0} \int_{-\infty}^{0} e^{\eta_1(X_1 - Y_1) + \eta_2(X_2 - Y_2) + \xi\tau} g(X_1, X_2, Y_1, Y_2; \tau) dY_1 dY_2 \\ & \quad + \sum_{k=1}^{m} (-1)^k \int_{-\infty}^{0} \int_{-\infty}^{0} e^{\eta_1(X_1 - Y_1) + \eta_2(X_2 - Y_2) + \xi\tau} g^k(X_1, X_2, Y_1^k, Y_2^k; \tau) dY_1 dY_2. \end{aligned} \tag{4.65}$$

Substituting the expression of the density function (4.3) into (4.65), the first integral in equation (4.65) can be written as[9]

$$e^{\eta_1 X_1 + \eta_2 X_2 + \xi\tau} \int_{-\infty}^{0} \int_{-\infty}^{0} \frac{1}{2\pi\tau\sqrt{1-\rho_{12}^2}} \exp\left(-\frac{\phi(Y_1, Y_2)}{2\tau(1-\rho_{12}^2)}\right) dY_1 dY_2. \tag{4.66}$$

[8]For a comparison of speed and accuracy between different approximate methods for computing the N_2 function, see Agca & Chance (2003).

[9]See Appendix I for the details.

where

$$\phi(Y_1, Y_2) = AY_1^2 + BY_2^2 + CY_1 + DY_2 + EY_1Y_2 + H, \tag{4.67}$$

and

$$\begin{aligned} A &= 1,\ B = 1, \\ C &= 2[\eta_1\tau(1-\rho_{12}^2) - X_1 + \rho_{12}X_2], \\ D &= 2[\eta_2\tau(1-\rho_{12}^2) - X_2 + \rho_{12}X_1], \\ E &= -2\rho_{12}, \\ H &= X_1^2 + X_2^2 - 2\rho_{12}X_1X_2. \end{aligned} \tag{4.68}$$

Then, equation (4.66) can be written in terms of the cumulative bivariate normal distribution function $N_2(.)$ by the change of variables illustrated in Appendix I, hence (4.66) becomes

$$e^{\eta_1 X_1 + \eta_2 X_2 + \xi\tau} \sqrt{\frac{(1-\rho_{12}^2)}{AB(1-\widetilde{\rho}^2)}}\ \exp\left(-\frac{\widetilde{h}}{2\tau(1-\rho_{12}^2)}\right) \times N_2(\widetilde{a}, \widetilde{b}, \widetilde{\rho}), \tag{4.69}$$

where

$$\widetilde{\rho} = -\frac{E}{2\sqrt{AB}}, \tag{4.70}$$

$$\widetilde{a} = \sqrt{2(1-\widetilde{\rho}^2)}\,\widetilde{u}_1 = \sqrt{\frac{A}{\tau}}\left(\frac{C}{2A} - \frac{Eh_2}{4Ah_1}\right)\sqrt{\frac{1-\widetilde{\rho}^2}{1-\rho_{12}^2}}, \tag{4.71}$$

$$\widetilde{b} = \sqrt{2(1-\widetilde{\rho}^2)}\,\widetilde{v}_1 = \frac{1}{\sqrt{\tau}}\sqrt{1 + \frac{E^2}{4Ah_1}}\,\frac{h_2}{2\sqrt{h_1}}\sqrt{\frac{1-\widetilde{\rho}^2}{1-\rho_{12}^2}}, \tag{4.72}$$

and

$$h_1 = B - \frac{E^2}{4A},\ h_2 = D - \frac{CE}{2A},\ \widetilde{h} = H - \frac{C^2}{4A} - \frac{h_2^2}{4h_1}. \tag{4.73}$$

Next we consider the second integral in equation (4.65). We note that it is convenient to rewrite Y_1^k and Y_2^k in terms of Y_1 and Y_2 by setting

$$Y_1^k = a_1^k Y_1 + b_1^k Y_2, \tag{4.74}$$

$$Y_2^k = a_2^k Y_1 + b_2^k Y_2. \tag{4.75}$$

Substituting equations (4.74) and (4.75) into (4.26)-(4.29), we find that for $k > 1$

$$\begin{aligned} a_1^k &= \begin{cases} -a_1^{k-1} & \text{for } k \text{ is odd,} \\ a_1^{k-1} - 2\rho_{12} a_2^{k-1} & \text{for } k \text{ is even,} \end{cases} \\ a_2^k &= \begin{cases} a_2^{k-1} - 2\rho_{12} a_1^{k-1} & \text{for } k \text{ is odd,} \\ -a_2^{k-1} & \text{for } k \text{ is even,} \end{cases} \\ b_1^k &= a_2^{k-1}, \\ b_2^k &= a_1^{k-1}, \end{aligned} \tag{4.76}$$

whilst for $k = 1$

$$\begin{aligned} a_1^1 &= -1 \ , \ b_1^1 = 0, \\ a_2^1 &= -2\rho_{12} \ , \ b_2^1 = 1. \end{aligned} \tag{4.77}$$

Then, the second integral in equation (4.65) can be expressed as

$$\begin{aligned} &\sum_{k=1}^{m} (-1)^k \int_{-\infty}^{0} \int_{-\infty}^{0} e^{\eta_1 (X_1 - Y_1) + \eta_2 (X_2 - Y_2) + \xi\tau} \\ &\times g^k \Big(X_1, X_2, (a_1^k Y_1 + b_1^k Y_2), (a_2^k Y_1 + b_2^k Y_2); \tau \Big) dY_1 dY_2. \end{aligned} \tag{4.78}$$

Following steps analogous to those shown in Appendix I, this can be written in terms of $N_2(.)$ as

$$e^{\eta_1 X_1 + \eta_2 X_2 + \xi\tau} \sum_{k=1}^{m} (-1)^k \sqrt{\frac{(1-\rho_{12}^2)}{A_k B_k (1 - \widetilde{\rho}_k^2)}} \ \exp\left(- \frac{\widetilde{h}_k}{2\tau(1-\rho_{12}^2)} \right) \times N_2\big(\widetilde{a}_k, \widetilde{b}_k, \widetilde{\rho}_k\big). \tag{4.79}$$

The expressions for $\widetilde{\rho}_k$, $\widetilde{a}_k$, $\widetilde{b}_k$ and $\widetilde{h}_k$ are the same as in (4.70)-(4.73) but obtained by replacing A, B, C, D and E by

$$\begin{aligned} A_k &= (a_1^k)^2 + (a_2^k)^2 - 2\rho_{12} a_1^k a_2^k, \\ B_k &= (b_1^k)^2 + (b_2^k)^2 - 2\rho_{12} b_1^k b_2^k, \\ C_k &= X_1(2\rho_{12} a_2^k - 2a_1^k) + X_2(2\rho_{12} a_1^k - 2a_2^k) + 2\eta_1 \tau (1 - \rho_{12}^2), \\ D_k &= X_1(2\rho_{12} b_2^k - 2b_1^k) + X_2(2\rho_{12} b_1^k - 2b_2^k) + 2\eta_2 \tau (1 - \rho_{12}^2), \\ E_k &= 2(a_1^k b_1^k + a_2^k b_2^k - \rho_{12} b_1^k a_2^k - \rho_{12} a_1^k b_2^k). \end{aligned} \tag{4.80}$$

4.4.2. Numerical Implementation in the Time Varying Coefficients Case.

In the case that the coefficients are time-dependent, the approximate solution for the joint survival probability in (4.62) after some algebraic manipulations, can be simplified to

$$\begin{aligned} F_\beta(X_1, X_2, \tau) = & \\ & \int_{-\infty}^{0}\int_{-\infty}^{0} g(X_1 + d_1(\tau), X_2 + d_2(\tau), Y_1, Y_2; \tau) dY_1 dY_2 \\ & + \sum_{k=1}^{m} (-1)^k \int_{-\infty}^{0}\int_{-\infty}^{0} g^k(X_1 + d_1(\tau), X_2 + d_2(\tau), Y_1^k, Y_2^k; \tau) e^{\beta_a^k Y_1 + \beta_b^k Y_2} dY_1 dY_2, \end{aligned} \tag{4.81}$$

where

$$d_i(\tau) = \int_0^t \gamma_i(v)dv, \ (i = 1, 2), \tag{4.82}$$

and

$$\beta_a^k = \eta_1(a_1^k - 1) + \eta_2 a_2^k, \tag{4.83}$$

$$\beta_b^k = \eta_1 b_1^k + \eta_2(b_2^k - 1), \tag{4.84}$$

and the a^k's and b^k's are given in (4.76)-(4.77).

Applying the same procedures as in Appendix I, the first integral in (4.81) can be rewritten in terms of $N_2(.)$ as

$$\begin{aligned} & \int_{-\infty}^{0}\int_{-\infty}^{0} g(X_1 + d_1(\tau), X_2 + d_2(\tau), Y_1, Y_2; \tau) dY_1 dY_2 \\ & = \sqrt{\frac{(1 - \rho_{12}^2)}{AB(1 - \widetilde{\rho}^2)}} \exp\left(-\frac{\widetilde{h}}{2\tau(1 - \rho_{12}^2)}\right) \times N_2(\widetilde{a}, \widetilde{b}, \widetilde{\rho}). \end{aligned} \tag{4.85}$$

The expressions for $\widetilde{\rho}$, $\widetilde{a}$, $\widetilde{b}$, h_1, h_2 and $\widetilde{h}$ are the same as in (4.70)-(4.73) after replacing C, D and H with

$$\begin{aligned} C &= 2(-\mathbb{X}_1 + \rho_{12}\mathbb{X}_2), \\ D &= 2(-\mathbb{X}_2 + \rho_{12}\mathbb{X}_1), \\ H &= \mathbb{X}_1^2 + \mathbb{X}_2^2 - 2\rho_{12}\mathbb{X}_1\mathbb{X}_2, \end{aligned} \tag{4.86}$$

and $\mathbb{X}_i = X_i + d_i(\tau)$ for $i = 1, 2$.

In a similar way to the calculation in Subsection 4.4.1, we simplify the second integral in (4.81) by rewriting Y_1^k and Y_2^k in terms of Y_1 and Y_2 using the expressions in (4.74)-(4.75), and applying the same procedures used in Appendix I, we obtain

$$\sum_{k=1}^{m}(-1)^k \int_{-\infty}^{0}\int_{-\infty}^{0} g^k(X_1+d_1(\tau), X_2+d_2(\tau), (a_1^kY_1+b_1^kY_2), (a_2^kY_1+b_2^kY_2);\tau)e^{\beta_a^kY_1+\beta_b^kY_2}dY_1dY_2$$

$$= \sum_{k=1}^{m}(-1)^k \sqrt{\frac{(1-\rho_{12}^2)}{A_kB_k(1-\widetilde{\rho}_k^2)}}\ \exp\left(-\frac{\widetilde{h}_k}{2\tau(1-\rho_{12}^2)}\right) N_2\big(\widetilde{a}_k, \widetilde{b}_k, \widetilde{\rho}_k\big). \tag{4.87}$$

The expressions for $\widetilde{\rho}_k$, $\widetilde{a}_k$, $\widetilde{b}_k$ and $\widetilde{h}_k$ are the same as in (4.70)-(4.73) but obtained by replacing A, B, C, D, E and H with

$$\begin{aligned}
A_k &= (a_1^k)^2 + (a_2^k)^2 - 2\rho_{12}a_1^ka_2^k,\\
B_k &= (b_1^k)^2 + (b_2^k)^2 - 2\rho_{12}b_1^kb_2^k,\\
C_k &= 2\mathbb{X}_1(\rho_{12}a_2^k - a_1^k) + 2\mathbb{X}_2(\rho_{12}a_1^k - a_2^k) - 2\tau(1-\rho_{12}^2)\beta_a^k,\\
D_k &= 2\mathbb{X}_1(\rho_{12}b_2^k - b_1^k) + 2\mathbb{X}_2(\rho_{12}b_1^k - b_2^k) - 2\tau(1-\rho_{12}^2)\beta_b^k,\\
E_k &= 2(a_1^kb_1^k + a_2^kb_2^k - \rho_{12}b_1^ka_2^k - \rho_{12}a_1^kb_2^k),\\
H &= \mathbb{X}_1^2 + \mathbb{X}_2^2 - 2\rho_{12}\mathbb{X}_1\mathbb{X}_2,
\end{aligned} \tag{4.88}$$

and $\mathbb{X}_i = X_i + d_i(\tau)$ for $i = 1, 2$.

4.5. Overview

This chapter has extended the method of images approach to the two-dimensional case and obtained the combination of density functions subject to the zero boundary conditions. The result is then used to solve the partial differential equation for the risk ratio $\bar{P}$ with constant coefficients. When the coefficients are time-dependent, the time varying barrier approach is extended to the two firm situation to obtain an approximate solution. In order to implement these solutions, we also simplify and express them in terms of the cumulative bivariate normal distribution functions. However, the solutions we obtained by the method of images approach can only give analytical solutions at the particular values of the correlation ρ_{12} given it in Table 4.1. Therefore, in the next chapter we will develop appropriate numerical methods to efficiently solve the problem for all values of the correlation coefficient ρ_{12}.

CHAPTER 5

Numerical Approaches

We remind the reader that the solutions obtained by the method of images in the previous chapter are only valid for the particular values of the correlation coefficient ρ_{12} shown in Table 4.1. In this chapter, we seek to develop appropriate numerical methods to solve the problem for all values of ρ_{12}. A very powerful method, in particular for solving multi-dimensional parabolic equations, is the alternating direction implicit method which has been described quite well in Strikwerda (1989).

The partial differential equation of the risk ratio function (3.84) is a two-dimensional convection-diffusion equation with a cross-derivative term and time-dependent drift terms[1]. In order to develop an efficient numerical solution, we consider alternating direction implicit schemes that are unconditionally stable, that is the stability without any restriction on the time step. However, there is very little literature concerning the stability relevant to general convection-diffusion problems with mixed derivative terms. It has only been recently in the study conducted by in't Hout & Welfert (2007) for three alternating direction implicit schemes that stability has been established for the situation with cross-derivative terms. The study of in't Hout & Welfert (2007) show that the finite difference schemes introduced by Douglas & Rachford (1956) (Douglas-Rachford scheme) is unconditionally stable in applications to two-dimensional convection-diffusion equations. Therefore, we will apply the Douglas-Rachford scheme to solve the partial differential equation (3.84).

In Section 5.1, we outline the Douglas-Rachford scheme. We develop a Monte Carlo scheme to serve as a benchmark in Section 5.2. Section 5.3 discusses the accuracy and convergence of both methods and compare them to the exact solution developed by using the method of images in Section 4.2 at specific values of the correlation coefficient ρ_{12}, for the constant coefficients case. When the coefficients are time-dependent, we use the Monte Carlo results as a benchmark, and discuss the accuracy of the alternating direction implicit method and the approximate solution that was developed in Section 4.3 by comparing them to the benchmark results.

[1]The term convection-diffusion refers to the fact that the partial differential equations has both the first derivative (convection) and second derivative (diffusion) terms.

5.1. Alternating Direction Implicit Method

In this section, we outline the Douglas-Rachford scheme for the two-dimensional convection-diffusion equation with a cross-derivative term and time-dependent drift terms, in particular, we consider the partial differential equation of the risk ratio function (3.84). For the sake of notation, we define $u(x, y, \tau) \equiv \bar{P}(X_1, X_2, \tau)$, so that

$$\frac{\partial u}{\partial \tau} = \frac{1}{2}\frac{\partial^2 u}{\partial x_1^2} + \rho_{12}\frac{\partial^2 u}{\partial x_1 \partial x_2} + \frac{1}{2}\frac{\partial^2 u}{\partial x_2^2} + \gamma_1(\tau)\frac{\partial u}{\partial x_1} + \gamma_2(\tau)\frac{\partial u}{\partial x_2}, \tag{5.1}$$

for $\tau \in (0, T)$, $x \in (-\infty, 0)$, $y \in (-\infty, 0)$ and the operators

$$J_x = \frac{1}{2}\frac{\partial^2}{\partial x^2} + \gamma_1(\tau)\frac{\partial}{\partial x}, \tag{5.2}$$

$$J_y = \frac{1}{2}\frac{\partial^2}{\partial y^2} + \gamma_2(\tau)\frac{\partial}{\partial y}, \tag{5.3}$$

$$J_{xy} = \rho_{12}\frac{\partial^2}{\partial x \partial y}, \tag{5.4}$$

where the drift terms are defined in (3.88).

Hence, we can write the partial differential equation (5.1) as

$$u_\tau = J_x u + J_y u + J_{xy} u. \tag{5.5}$$

In order to define a numerical solution to solve equation (5.5), we need to truncate the spatial domain to a bounded area given by $\{(x, y); x_{min} \leq x \leq 0, y_{min} \leq y \leq 0\}$. We also introduce a grid consisting of points in the time interval and in the truncated spatial domain:

$$\tau_j = j\frac{T}{N_\tau} = 0, 1, \ldots, N_\tau, \tag{5.6}$$

$$x_i = i\frac{x_{min}}{N_x} = 0, 1, \ldots, N_x, \tag{5.7}$$

$$y_k = k\frac{y_{min}}{N_y} = 0, 1, \ldots, N_y. \tag{5.8}$$

The time step size is $\Delta\tau = T/N_\tau$, and spatial step sizes are $\Delta x = x_{min}/N_x$ and $\Delta y = y_{min}/N_y$. The value of u at a point of the grid is denoted as $u_{i,k}^j = u(x_i, y_k, \tau_j)$.

We use the Douglas-Rachford scheme to obtain $u_{i,k}^{j+1}$ from $u_{i,k}^j$, where $j = 0, 1, 2, ..., N_\tau$. The Douglas-Rachford scheme is

$$\left(1 - \Delta\tau \bar{J}_x\right) u_{i,k}^{j+1/2} = \left(1 + \Delta\tau \bar{J}_y\right) u_{i,k}^j + \Delta\tau \bar{J}_{xy} u_{i,k}^j, \tag{5.9}$$

$$\left(1 - \Delta\tau \bar{J}_y\right) u_{i,k}^{j+1} = u_{i,k}^{j+1/2} - \Delta\tau \bar{J}_y u_{i,k}^j, \tag{5.10}$$

where $u_{i,k}^{j+1/2}$ is an intermediate value that links equations (5.9) and (5.10). A derivation of the Douglas-Rachford method can be found in Strikwerda (1989) (Chapter 7.3).

Here, $\bar{J}_x$, $\bar{J}_y$ and $\bar{J}_{xy}$ denote the second-order approximations to the operators J_x, J_y and J_{xy}, that is

$$\begin{aligned} \bar{J}_x &= \frac{1}{2}\delta_x^2 + \gamma_1(\tau_{j+1/2})\delta_x, && (5.11)\\ \bar{J}_y &= \frac{1}{2}\delta_y^2 + \gamma_2(\tau_{j+1/2})\delta_y, && (5.12)\\ \bar{J}_{xy} &= \rho_{12}\delta_{xy}^2, && (5.13) \end{aligned}$$

where

$$\begin{aligned} \delta_x u_{i,k}^j &= \frac{u_{i+1,k}^j - u_{i-1,k}^j}{2\Delta x},\ \delta_x^2 u_{i,k}^j = \frac{u_{i+1,k}^j - 2u_{i,k}^j + u_{i-1,k}^j}{\Delta x^2},\\ \delta_y u_{i,k}^j &= \frac{u_{i,k+1}^j - u_{i,k-1}^j}{2\Delta y},\ \delta_y^2 u_{i,k}^j = \frac{u_{i,k+1}^j - 2u_{i,k}^j + u_{i,k-1}^j}{\Delta y^2},\\ \delta_{xy}^2 u_{i,k}^j &= \frac{u_{i+1,k+1}^j + u_{i-1,k-1}^j - u_{i-1,k+1}^j - u_{i+1,k-1}^j}{4\Delta x\Delta y}. \end{aligned} \quad (5.14)$$

According to Douglas (1961) (page 40), if time τ appears in the coefficients, the evaluation should be at time $\tau_{j+1/2}$ in order to preserve second order precision in time. Therefore, $\gamma_1(\tau)$ and $\gamma_2(\tau)$ are evaluated at time $\tau_{j+1/2}$ as $\gamma_1(\tau_{j+1/2})$ and $\gamma_2(\tau_{j+1/2})$ in (5.9) and (5.10).

Next, we describe the implementation of the alternating direction method.

First Stage

The difference equation (5.9) for the step from time j to time $j+1/2$ can be written

$$p_1 u_{i+1,k}^{j+1/2} + p_2 u_{i,k}^{j+1/2} + p_{1d} u_{i-1,k}^{j+1/2} = p_3 u_{i,k+1}^j + p_4 u_{i,k}^j + p_{3d} u_{i,k-1}^j + \rho_{12} U_{ik}^j, \quad (5.15)$$

where

$$\begin{aligned} U_{i,k}^j &= \Delta\tau\delta_{xy}^2 u_{i,k}^j, && (5.16)\\ &= \frac{\Delta\tau}{4\Delta x\Delta y}(u_{i+1,k+1}^j + u_{i-1,k-1}^j - u_{i-1,k+1}^j - u_{i+1,k-1}^j), && (5.17) \end{aligned}$$

for $i = 1, \ldots, N_x - 1$, $k = 1, \ldots, N_y - 1$ and

$$p_1 = -\frac{\Delta\tau}{2\Delta x^2}[1 + \gamma_1(\tau_{j+1/2})\Delta x],\ p_2 = 1 + \frac{\Delta\tau}{\Delta x^2},\ p_{1d} = -\frac{\Delta\tau}{2\Delta x^2}[1 - \gamma_1(\tau_{j+1/2})\Delta x], \quad (5.18)$$

$$p_3 = \frac{\Delta\tau}{2\Delta y^2}[1 + \gamma_2(\tau_{j+1/2})\Delta y],\ p_4 = 1 - \frac{\Delta\tau}{\Delta y^2},\ p_{3d} = \frac{\Delta\tau}{2\Delta y^2}[1 - \gamma_2(\tau_{j+1/2})\Delta y]. \quad (5.19)$$

Denote by $\psi_{i,k}^{j}$ the right-hand side of equation (5.15), then we can express (5.15) as the matrix system

$$\begin{bmatrix} 1 & 0 & \cdots & & & & 0 \\ p_1 & p_2 & p_{1d} & . & . & . & 0 \\ 0 & p_1 & p_2 & p_{1d} & . & . & 0 \\ . & & & & & & . \\ . & & & & & & . \\ 0 & . & . & 0 & p_1 & p_2 & p_{1d} \\ 0 & . & . & . & . & 0 & 1 \end{bmatrix} \begin{bmatrix} u_{N_x,k}^{j+1/2} \\ u_{N_x-1,k}^{j+1/2} \\ . \\ . \\ . \\ u_{1,k}^{j+1/2} \\ u_{0,k}^{j+1/2} \end{bmatrix} = \begin{bmatrix} \psi_{N_x,k}^{j} \\ \psi_{N_x-1,k}^{j} \\ . \\ . \\ . \\ \psi_{1,k}^{j} \\ \psi_{0,k}^{j} \end{bmatrix}, \tag{5.20}$$

which because of the tridiagonal structure can be readily solved by Gaussian elimination. The values of $u_{i,k}^{j+1/2}$ turn out to be given by

$$u_{i,k}^{j+1/2} = \frac{\mathfrak{r}_i - p_1 u_{i+1,k}^{j+1/2}}{\mathfrak{c}_i} \tag{5.21}$$

for $i = 1, \ldots, N_x - 1$, where $\mathfrak{c}_i$ and $\mathfrak{r}_i$ are defined by the recurrence relations

$$\mathfrak{c}_i = p_2 - \frac{p_1 p_{1d}}{\mathfrak{c}_{i-1}},\ \mathfrak{r}_i = \psi_{i,k}^{j} - p_{1d}\frac{\mathfrak{r}_{i-1}}{\mathfrak{c}_{i-1}}. \tag{5.22}$$

for $i \geq 2$ with initial values

$$\mathfrak{c}_1 = p_2,\ \mathfrak{r}_1 = \psi_{1,k}^{j} - p_{1d}\psi_{0,k}^{j}. \tag{5.23}$$

The initial values of $\psi_{i,k}^{0}$ are obtained from the solution for $u_{i,k}^{0}$ at time τ_0, which is determined by the initial condition (3.85), that is

$$u_{i,k}^{0} = 1. \tag{5.24}$$

Since, the first stage is implicit in the x direction, so we need to specify the boundary conditions at $x = 0$ and $x = x_{min}$. Values at $x = 0$ can be obtained by the boundary condition (3.86) as

$$u_{0,k}^{j+1/2} = 0, \tag{5.25}$$

for $k = 0, \ldots, N_y$.

If $x \to -\infty$, which means the leverage ratio tends to zero, and y is small compared to x. We assume in this case the risk ratio function $\bar{P}(-\infty, y, \tau) = 1$. Therefore, the choice of x_{min} should

be sufficiently large so as the values of $u(x_{min}, y(\tau)$ is approximately equal to 1. Therefore,

$$u_{N_x,k}^{j+1/2} = 1, \tag{5.26}$$

for $k = 1, \ldots, N_y$.

Second Stage

In the second stage, we use $u_{i,k}^{j+1/2}$ to calculate $u_{i,k}^{j+1}$. The difference equation (5.10) for the step from time $j + 1/2$ to time $j + 1$ is

$$p_5 u_{i,k+1}^{j+1} + p_6 u_{i,k}^{j+1} + p_{5d} u_{i,k-1}^{j+1} = u_{i,k}^{j+1/2} + p_7 u_{i,k+1}^{j} + p_8 u_{i,k}^{j} + p_{7d} u_{i,k-1}^{j}, \tag{5.27}$$

for $i = 1, \ldots, N_x - 1$, $k = 1, \ldots, N_y - 1$ and

$$p_5 = -\frac{\Delta\tau}{2\Delta y^2}[1 + \gamma_2(\tau_{j+1/2})\Delta y],\ p_6 = 1 + \frac{\Delta\tau}{\Delta y^2},\ p_{5d} = -\frac{\Delta\tau}{2\Delta y^2}[1 - \gamma_2(\tau_{j+1/2})\Delta y], \tag{5.28}$$

$$p_7 = -\frac{\Delta\tau}{2\Delta y^2}[1 + \gamma_2(\tau_{j+1/2})\Delta y],\ p_8 = \frac{\Delta\tau}{\Delta y^2},\ p_{7d} = -\frac{\Delta\tau}{2\Delta y^2}[1 - \gamma_2(\tau_{j+1/2})\Delta y]. \tag{5.29}$$

Then the system (5.27) can be expressed in matrix form as

$$\begin{bmatrix} 1 & 0 & \cdots & & & & 0 \\ p_5 & p_6 & p_{5d} & . & . & . & 0 \\ 0 & p_5 & p_6 & p_{5d} & . & . & 0 \\ . & & & & & & . \\ . & & & & & & . \\ 0 & . & . & 0 & p_5 & p_6 & p_{5d} \\ 0 & . & . & . & . & 0 & 1 \end{bmatrix} \begin{bmatrix} u_{i,N_y}^{j+1} \\ u_{i,N_y-1}^{j+1} \\ . \\ . \\ . \\ u_{i,1}^{j+1} \\ u_{i,0}^{j+1} \end{bmatrix} = \begin{bmatrix} \tilde{\psi}_{i,N_y} \\ \tilde{\psi}_{i,N_y-1} \\ . \\ . \\ . \\ \tilde{\psi}_{i,1} \\ \tilde{\psi}_{i,0} \end{bmatrix}, \tag{5.30}$$

where we use $\tilde{\psi}_{i,k}$ to denote the right-hand side of equation (5.27). Therefore, the values of $u_{i,k}^{j+1}$ can be obtained by solving the matrix using Gaussian elimination and the solution is

$$u_{i,k}^{j+1} = \frac{\mathfrak{r}_k - p_5 u_{i,k+1}^{j+1}}{\mathfrak{c}_k} \tag{5.31}$$

for $k = 1, \ldots, N_y - 1$, where $\mathfrak{c}_k$ and $\mathfrak{r}_k$ are given by the recurrence relations

$$\begin{aligned} \mathfrak{c}_k &= p_6 - p_{5d}\frac{p_5}{\mathfrak{c}_{k-1}}, \\ \mathfrak{r}_k &= \tilde{\psi}_{i,k} - p_{5d}\frac{\mathfrak{r}_{k-1}}{\mathfrak{c}_{k-1}}. \end{aligned} \tag{5.32}$$

with the initial value

$$\begin{aligned}\mathfrak{c}_1 &= p_6,\\ \mathfrak{r}_1 &= \tilde{\psi}_{i,1} - p_{5d}\tilde{\psi}_{i,0}.\end{aligned} \tag{5.33}$$

This step is implicit in the y direction. Thus, we need to approximate the boundary conditions for $y = 0$ and $y = y_{min}$. Similar to the first stage, values at $y = 0$ can be obtained by the boundary condition (3.87), so that

$$u_{i,0}^{j+1} = 0, \tag{5.34}$$

for $i = 0, \ldots, N_x$.

If $y \to -\infty$, then x is small compare to y. We assume in this case that the risk ratio function $\bar{P}(x, -\infty, \tau) = 1$. Therefore, the choice of y_{min} must be sufficiently large so that the values of $u(x, y_{min}(\tau)$ are approximately equal to 1, thus,

$$u_{i,N_y}^{j+1} = 1, \tag{5.35}$$

for $i = 1, \ldots, N_x$.

In this section, we have developed a numerical scheme for the evaluation of the risk ratio function $\bar{P}(X_1, X_2, \tau)$ for all values of the correlation ρ_{12}. Exactly the same numerical algorithm and procedures can be applied to evaluate the joint survival probability function by defining $u(x, y(\tau) \equiv F(X_1, X_2, \tau)$ with boundary and initial conditions same as that shown in (5.25)-(5.26) and (5.34)-(5.35).

The accuracy of the Douglas-Rachford scheme (5.9) and (5.10), is first-order in time and second-order in space (see Strikwerda (1989) Chapter 7.3). The stability of this scheme was analyzed by in't Hout & Welfert (2007), who proved that it is unconditionally stable when the mixed derivative and convective terms are included. The convergence and the accuracy of this method as it applies to our problem, is based on numerical experiments that will be discussed in Section 5.3.

5.2. A Monte Carlo Simulation Scheme

In this section we will develop a Monte Carlo scheme to simulate the joint survival probability as a benchmark for the results obtained from the alternating direction implicit method scheme. The stochastic differential equations corresponding to the partial differential equation of the risk ratio

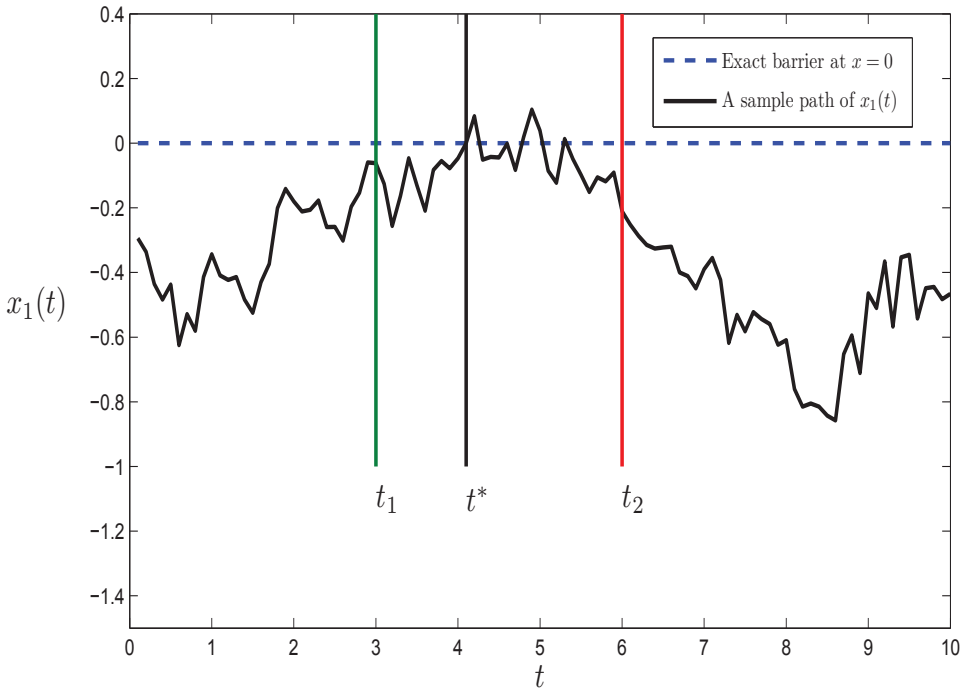

FIGURE 5.1. A path of $x_1(t)$ across a typical subintervals.

function (3.77), are

$$dL_1 = [\widetilde{\mu}_1 + \rho_{1r}\sigma_1\sigma_r b(t)]\, L_1 dt + \sigma_1 L_1 d\widetilde{Z}_1, \tag{5.36}$$

$$dL_2 = [\widetilde{\mu}_2 + \rho_{2r}\sigma_2\sigma_r b(t)]\, L_2 dt + \sigma_2 L_2 d\widetilde{Z}_2, \tag{5.37}$$

where $\widetilde{Z}_1$ and $\widetilde{Z}_2$ are Wiener processes under the risk-neutral measure $\widetilde{\mathbb{P}}$, and the Wiener increments $d\widetilde{Z}_1$ and $d\widetilde{Z}_2$ are correlated with $\mathbb{E}[d\widetilde{Z}_1 d\widetilde{Z}_2] = \rho_{12}dt$[2].

We rewrite (5.36) and (5.37) in terms of uncorrelated Wiener processes W_1, W_2, and change variables to the normalized log-leverage ratios x_1, x_2 as defined in (3.82), then (5.36) and (5.37) become

$$dx_1 = \left[\widetilde{\mu}_1 + \rho_{1r}\sigma_1\sigma_r b(t) - \frac{1}{2}\sigma_1^2\right] dt + \sigma_1 dW_1, \tag{5.38}$$

$$dx_2 = \left[\widetilde{\mu}_2 + \rho_{2r}\sigma_2\sigma_r b(t) - \frac{1}{2}\sigma_2^2\right] dt + \sigma_2\big(\rho_{12}dW_1 + \sqrt{1-\rho_{12}^2}dW_2\big). \tag{5.39}$$

If at any time in the time interval $t \in (0, T)$ either firm's leverage ratio L_i is on or above the default threshold $\widehat{L}_i$ (that is $x_1 \geq 0$ or $x_2 \geq 0$), then default occurs. Therefore, to ensure that default events are captured, the simulation time step Δt should be as small as possible. For example, Figure 5.1

[2]These stochastic differential equations may be obtained by an application of the Feynman-Kac formula, see for example Albanese & Campolieti (2006) page 36.

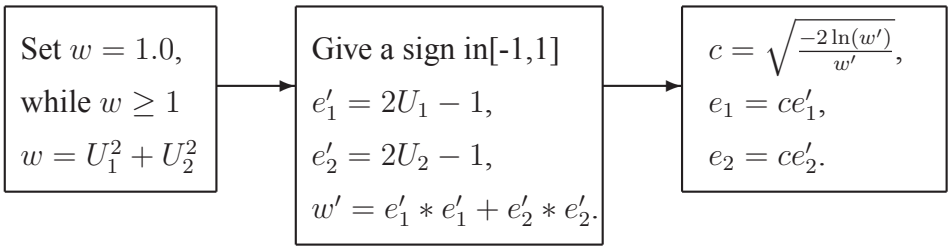

FIGURE 5.2. An algorithm of the polar rejection method.

shows that, if $\Delta t = t_2 - t_1$, and the barrier is breached at $t^*(t_1 < t^* < t_2)$ the default event will not be captured, and, a smaller $\Delta t = t^* - t_1$ would be required.

The following is the Monte Carlo scheme we have used to value the the joint survival probability (JSP).

Step 1. Divide the time interval [0,T] into $\mathfrak{n}$ equal sub-periods per year. Set $t_j = j\Delta t$ for $j = 1, 2, ..., \mathfrak{n}\Delta t$.

Step 2. Do the Monte Carlo simulations $M(m = 1, 2, ..., M)$ times.

2.1. For the m^{th} simulation, at the j^{th} time step, generate independent normal random numbers e_1 and e_2 from the distribution of $N(0, 1)$.

2.2. Let $x_i = \ln(L_i/L_{i0})$, then (5.38) and (5.39) in discretized form become

$$x_1(t_j) = x_1(t_{j-1}) + \left[\widetilde{\mu}_1 + \rho_{1r}\sigma_1\sigma_r b(t_{j-1}) - \frac{1}{2}\sigma_1^2\right]\Delta t + \sigma_1\sqrt{\Delta t}e_1, \tag{5.40}$$

$$x_2(t_j) = x_2(t_{j-1}) + \left[\widetilde{\mu}_2 + \rho_{2r}\sigma_2\sigma_r b(t_{j-1}) - \frac{1}{2}\sigma_2^2\right]\Delta t + \sigma_2\sqrt{\Delta t}\hat{e}_2, \tag{5.41}$$

where $\hat{e}_2 = \rho_{12}e_1 + \sqrt{1 - \rho_{12}^2}e_2$.

Step 3. Check the boundary conditions: if $x_i(t_j) \geq 0$ for either firm i, then joint survival probability for m^{th} path at time t_j is JSP$_m(t_j)$=0, and go to the next simulation m+1. Otherwise JSP$_m(t_j)$=1, and go to next time step j+1.

Set JSP$(t_j) = \sum_{m=1}^{M}$JSP$_m(t_j)/M$, which is an approximate value for the joint survival probability.

Here e_1 and e_2 are normal random numbers that are calculated by the polar rejection method suggested in Clewlow & Strickland (1998), and which is illustrated in Figure 5.2. The random

numbers U_1 and U_2 are generated by the Mersenne Twister[3], it is a pseudo random number generating algorithm developed by Makoto Matsumoto and Takuji Nishimura in 1997, and is a very fast random number generator of period $2^{19937} - 1$.

5.3. Accuracy

In this section, we discuss the accuracy and convergence of both methods and compare them to the exact solution developed by using the method of images in Section 4.2 at specific values of the correlation coefficient ρ_{12}, for the constant coefficients case. When coefficients are time-dependent, we use the Monte Carlo results as a benchmark, and discuss the accuracy of the alternating direction implicit method and the approximate solution that developed in Section 4.3 by comparing them to the benchmark results.

Douglas-Rachford ADI results compared to exact solutions			
N_t	N_x, N_y	$\rho_{12} = -0.9$	Relative % error
100	1018	0.74884	0.15403%
100	3830	0.74867	0.13148%
1000	3830	0.74779	0.01321%
1000	7705	0.74774	0.00755%
MOI exact results		0.74769	-

TABLE 5.1. Convergence of the alternating direction implicit based on the Douglas-Rachford method outlined in Section 5.1 for the joint survival probabilities. The exact solution is based on the method of images developed in Section 4.2. The time period is one year and other parameters used are $L_1 = 73.2\%$, $L_2 = 31.5\%$, $\sigma_1 = 0.299$, $\sigma_2 = 0.213$, $\widetilde{\mu}_1 = \widetilde{\mu}_2 = 0$, $\rho_{1r} = \rho_{2r} = 0$, $\rho_{12} = -0.9$. These data are for a CCC-BBB rated pair of firms.

To show the convergence of the alternating direction implicit method for the joint survival probabilities, we use a CCC-BBB rated pair of firms as an example. The exact analytical solution by the method of images (MOI) is based on Section 4.2 which is only valid for specific values of the correlation coefficient ρ_{12} (see Table 4.1), and we use $\rho_{12} = -0.9$ (corresponding to $\rho_{12} - \cos\frac{\pi}{7}$

[3]The Mersenne Twister Home Page: http://www.math.sci.hiroshima-u.ac.jp/ m-mat/MT/emt.html

in Table 4.1) as a demonstration here, we have found that other choices of ρ_{12} such as $\rho_{12} = 0$ and $\rho_{12} = -0.5$ give similar convergence results.

Table 5.1 shows the convergence of the alternating direction implicit results for the joint survival probabilities of a CCC-BBB rated pair of firms as compared to the exact analytical solution by the method of images (MOI) developed in Section 4.2. The time period chosen is one year. The relative percentage error is generally smaller than one percent. When the spatial grid increases from 1018 to 3830 steps, the relative percentage errors are similar and close to 0.1% with the number of time steps being 100 (per year). The relative percentage errors decrease to around 0.01% when the number of time steps increases to 1000 per year. With the same number of time steps and increase in spatial points from 3830 to 7705, the relative percentage errors decrease further to around 0.007%.

Monte Carlo results compared to exact solutions			
n	M	$\rho_{12} = -0.9$	Relative % error
3,650	500,000	0.2835	1.1670%
3,650	1,000,000	0.2830	0.9590%
36,500	500,000	0.2812	0.3243%
36,500	1,000,000	0.2804	0.0549%
MOI exact results		0.2803	-

TABLE 5.2. Accuracy of the Monte Carlo method developed in Section 5.2 for the joint survival probabilities. The approximate analytical solution is based on the method of images developed in Section 4.3. The exact solution is based on the method of images developed in Section 4.2. The time period is fifteen years and other parameters used are $L_1 = 73.2\%$, $L_2 = 31.5\%$, $\sigma_1 = 0.299$, $\sigma_2 = 0.213$, $\widetilde{\mu}_1 = \widetilde{\mu}_2 = 0$, $\rho_{1r} = \rho_{2r} = 0$, $\rho_{12} = -0.9$. These data are for a CCC-BBB rated pair of firms.

Next, we discuss the accuracy of the Monte Carlo method. Table 5.2 shows the accuracy of the Monte Carlo results for joint survival probability of a CCC-BBB rated pair of firms compared to the approximate analytical solution developed in Section 4.3. We note the relative percentage errors with $3,650$ time steps per year (that is 10 times a day) is slightly larger than 1% (exact value is 1.1670%) for $M = 500,000$ paths and very close to 1% (exact value is 0.9590%) for

Time	Monte Carlo results n=36500 M=1x10^6	2-D MOI single-stage approx.	Relative % error of MOI	Douglas-Rachford ADI Nt=1500, Nx=Ny=3830	Relative % error of ADI
1	0.7421	0.74091	-0.15873	0.74192	-0.02296
2	0.5997	0.59877	-0.15624	0.59936	-0.05667
3	0.5249	0.52404	-0.16117	0.52441	-0.09066
4	0.4766	0.47569	-0.18608	0.47595	-0.13301
5	0.4408	0.44051	-0.06517	0.44070	-0.02241
6	0.4134	0.41307	-0.07618	0.41322	-0.03986
7	0.3912	0.39070	-0.11673	0.39082	-0.08458
8	0.3725	0.37194	-0.15549	0.37205	-0.12600
9	0.3563	0.35588	-0.13182	0.35598	-0.10336
10	0.3424	0.34193	-0.13189	0.34203	-0.10156
11	0.3301	0.32968	-0.14110	0.32981	-0.10168
12	0.3193	0.31884	-0.13763	0.31906	-0.06962
13	0.3096	0.30924	-0.11026	0.30971	0.04030
14	0.3009	0.30084	-0.01313	0.30200	0.36983
15	0.2930	0.29390	0.30629	0.29692	1.33873

TABLE 5.3. Accuracy of the approximate solution based on method of images for time-dependent coefficients developed in Section 4.3, and the accuracy of the alternating direction implicit based on the Douglas-Rachford method outlined in Section 5.1 for the joint survival probabilities compared to the Monte Carlo results. The time period is fifteen years and other parameters used are $L_1 = 73.2\%$, $L_2 = 31.5\%$, $\sigma_1 = 0.299$, $\sigma_2 = 0.213$, $\widetilde{\mu}_1 = \widetilde{\mu}_2 = 0$, $\rho_{12} = -0.9$ and $\rho_{1r} = \rho_{2r} = -0.75$.

$M = 1,000,000$ paths. However, the relative percentage errors are reduced further to less than 0.4% if the number of time steps used is increased to $36,500$ per year (that is 100 times a day).

We note that when coefficients are time-dependent, the solution obtained by the method of images approach is not exact, since an approximate solution using the time varying barrier is involved (see Section 4.3). Therefore, we use the Monte Carlo results as a benchmark for comparing the accuracy of the approximate solution based on method of images for time-dependent coefficients developed in Section 4.3, and the accuracy of the alternating direction implicit method based on the Douglas-Rachford method outlined in Section 5.1 for the joint survival probabilities. Table 5.3 shows the relative percentage error of the approximate results by the method of images over the

time period is less than 1%. The relative percentage error of the results based on the alternating direction implicit scheme is less than 1% except at fifteen years where error is around 1.3%.

5.4. Overview

In this chapter, we have outlined the Douglas-Rachford scheme for solving the first passage time problem of the two-firm model for general values of the correlation coefficient between firms' leverage ratios. We also developed a Monte Carlo scheme to serve as a benchmark. We discussed the accuracy and convergence of both methods and compared them to the exact solution developed by using the method of images in Section 4.2 at specific values of the correlation coefficient ρ_{12}, for the constant coefficients case, and we found that the relative percentage error is generally less than 1% for the alternating direction implicit results based on 100 time steps per year and 3830 spatial points, and for the Monte Carlo results based on $36,500$ time steps per year with the number of paths between $500,000$ and $1,000,000$.

When the coefficients are time-dependent, we used the Monte Carlo results as a benchmark, and compared the accuracy of the alternating direction implicit method and the approximate solution based on the method of images. The relative percentage error for the approximate method is generally less than 1%. The relative percentage error for the alternating direction implicit method is less than 1% except at fifteen years where error is around 1.3%.

We have thus established reliable computational tools to calculate default correlations. We devote the rest of the thesis to the implications for the default correlations and joint survival probabilities in the two firm model of using different kinds of underlying processes to model the leverage ratio dynamics.

CHAPTER 6

The Two-Firm Model under Geometric Brownian Motions

In this chapter, we study the impact on joint survival probabilities and default correlations based on the two-firm model under geometric Brownian motion for the firms' leverage ratios, developed in the previous chapters. Section 6.1 discusses the choice of parameters. Section 6.2 gives the numerical results for joint survival probabilities and default correlations with different credit quality firms, under a range of different scenarios for correlations, drift levels, volatilities, initial leverage ratios and signs of companies' drift levels.

6.1. Choice of Parameters

We choose the set of parameters to be consistent with Hui et al. (2007), so allowing us to compare the effect of going from a one-firm model to a two-firm model. It is quite natural to set the default threshold at $\widehat{L}_1 = \widehat{L}_2 = 1$, to reflect the fact that the firm's debt level is equal to its asset level. This is equivalent to what is done by Collin-Dufresne & Goldstein (2001) where default occurs when the log-leverage ratio hits the barrier at zero. A firm can be also forced to default when its debt level is close to its asset level, for example 90% ($\widehat{L}_i = 0.9$), or higher than its asset level at 110% ($\widehat{L}_i = 1.1$). However the framework of the two-firm model can handle these more general situations, because the model is formulated in terms of the normalized log-leverage ratios (see equation (3.82)).

The leverage ratios used for different individual ratings are the typical values of industry medians in Standard & Poor's (2001). Following the same setting in Hui et al. (2007), the values of the volatility of leverage ratios are assumed to be similar to asset volatilities[1], the values of which are close to the estimates of Delianedis & Geske (1999), who observed that the volatility value is 0.17 for AA and A-rated firms and 0.27 for B-rated firms. Taking these values as reference points, volatilities for other rating categories can be tabulated for each successive rated category. The values of leverage ratios and volatilities used for different individual ratings are shown in Table 6.1.

[1]This follows from the assumption that volatilities of firms' liabilities are not significant, as can be seen from the mathematical relationship between volatilities of leverage ratio, firm's asset value and liability in Hui et al. (2006) Appendix A. Under this assumption the volatility of the leverage ratio is then close to the volatility of the firm asset value.

	AAA	AA	A	BBB	BB	B	CCC
Leverage ratios L_i (%)	3.1	9.5	17.2	31.5	49.5	53.8	73.2
Volatilities σ_i	0.127	0.156	0.184	0.213	0.241	0.270	0.299

TABLE 6.1. Parameters used for individual ratings

The time horizon is fifteen years which is the same as in Hui et al. (2007), who compared the individual default probabilities to S&P historical cumulative default rates for which the available data is up to fifteen years.

6.2. The Impact of Geometric Brownian Motions

We evaluate the joint survival probabilities based on the alternating direction implicit scheme outlined in Section 5.1. The total number of grid points used are $N_x = N_y = 3830$ and the number of time steps per year is $N_t = 100$. The values of x_{min} and y_{min} are selected such that the corresponding leverage ratios $L_i = 0.001$ $(i = 1, 2)$ are very close to zero. The accuracy of this setting is discussed in Section 5.3 and it is seen to result in a reasonable level of accuracy. The default correlations are evaluated based on the equation given in (3.94). The individual default probabilities are computed by using equation (3.37) for the case of constant coefficients and equation (3.59) for the case of time-varying coefficients. Note that in this thesis, the evaluation of the joint survival probabilities and default correlations (or default probabilities in later chapters) are based on the credit linked note price (or corporate bond price for default probabilities) which are derivative instruments and hence are calculated under the risk-neutral measure. Variances and correlations remain the same under both the physical and risk-neutral measures, however the drift coefficients differ in the two measures by amounts related to the market prices of risk λ_1 and λ_2. So in the comparative studies of the impact of drift coefficients that we undertake later we should really work in the physical measure. However, we are here only interested in qualitative questions, such as how does default correlation change if a drift coefficients increases or decreases. The answer to such qualitative questions will be the same in both measures (if one assume constant market prices

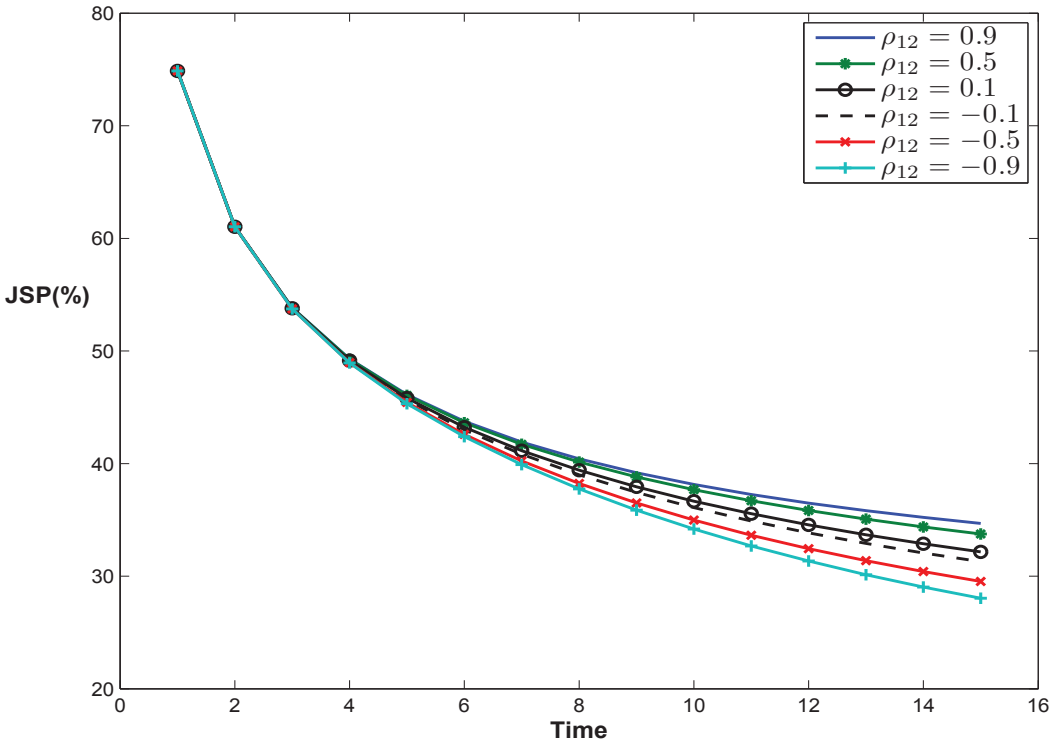

FIGURE 6.1. The impact of correlation ρ_{12} between BBB-CCC paired firms on joint survival probabilities. Initial leverage for the CCC-rated firm is L_1=73.2%, for the BBB-rated firm is L_2=31.5% and the volatilities are σ_1=0.299, σ_2 =0.213. Other parameters used are $\widetilde{\mu}_1 = \widetilde{\mu}_2 = 0$, $\rho_{1r} = \rho_{2r} = 0$ and $\rho_{12} = -0.9, -0.5, -0.1, 0.5$ and 0.9.

of risk[2] as we have), of course the actual quantitative values of such changes will be different under the two measures and to determine their values would require the development of econometric methodologies for the framework developed here.

The following subsections show the impact on joint survival probabilities and default correlations of a range of different scenarios, for example, paired firms having different credit quality, different values for correlations, drift levels, volatilities and initial leverage ratios.

6.2.1. The Impact of Correlation Between Two Firms.

This subsection explores the impact on joint survival probabilities and default correlations of the correlations between the two firms' leverage ratios. We use the BBB and CCC paired firms to

[2]We have assumed constant market prices of risk in order to be able to derive the explicit solution in Chapter 4. Of course the two-firm model could be extended to consider time dependent parameters, which would allow the incorporation the time varying market prices of risk. Such an extension would require the use of appropriate econometric tools to estimate these models. We leave this work to future research.

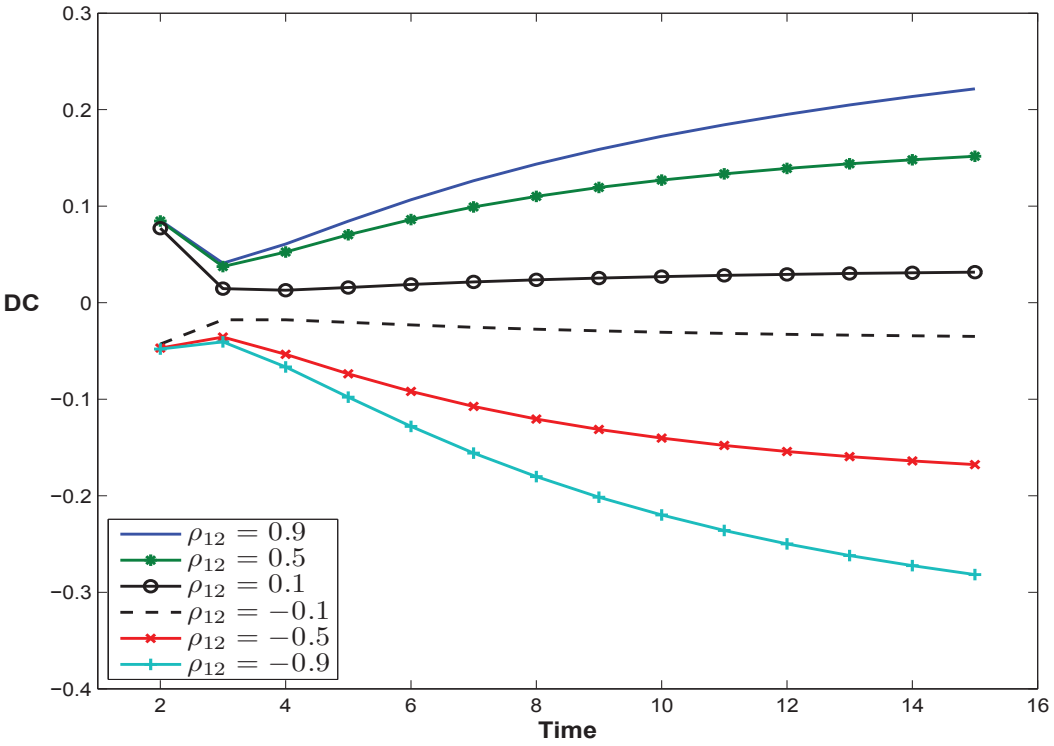

FIGURE 6.2. The impact of correlation ρ_{12} between BBB-CCC paired firms on default correlations. Initial leverage for the CCC-rated firm is L_1=73.2%, for the BBB-rated firm is L_2=31.5% and the volatilities are σ_1=0.299, σ_2 =0.213. Other parameters used are $\widetilde{\mu}_1 = \widetilde{\mu}_2 = 0$, $\rho_{1r} = \rho_{2r} = 0$ and $\rho_{12} = -0.9, -0.5, -0.1, 0.5$ and 0.9.

demonstrate the correlation effect. We consider the correlation levels of $\rho_{12} = -0.9, -0.5, -0.1, 0.5$ and 0.9.

In order to isolate the effects of the drift terms of the leverage ratio processes and correlation of the interest rate process, we set $\widetilde{\mu}_i$=0 and ρ_{ir}=0 (i=1,2). However, we will study later in this Chapter, the impact of these two factors on joint survival probabilities and default correlations.

The numerical results presented in this Chapter are computed based on the alternating direction implicit method that was developed in Section 5.1. The total number of grid points used are $N_x = N_y = 3830$ and the number of time steps per year is 100. The values of x_{N_x} and y_{N_y} are selected such that the corresponding leverage ratios $L_i = 0.001$ ($i = 1, 2$) are very close to zero. The accuracy of the numerical results are discussed in Section 5.3 where the relative percentage errors are less than 1% except at fifteen years where error rises to around 1.3%.

Figure 6.1 plots the joint survival probability of firm 1 and firm 2 from the beginning to the end of the investment period of fifteen years. This figure shows the impact on joint survival probabilities of the correlation coefficient ρ_{12} between BBB-CCC paired firms over the time horizon.

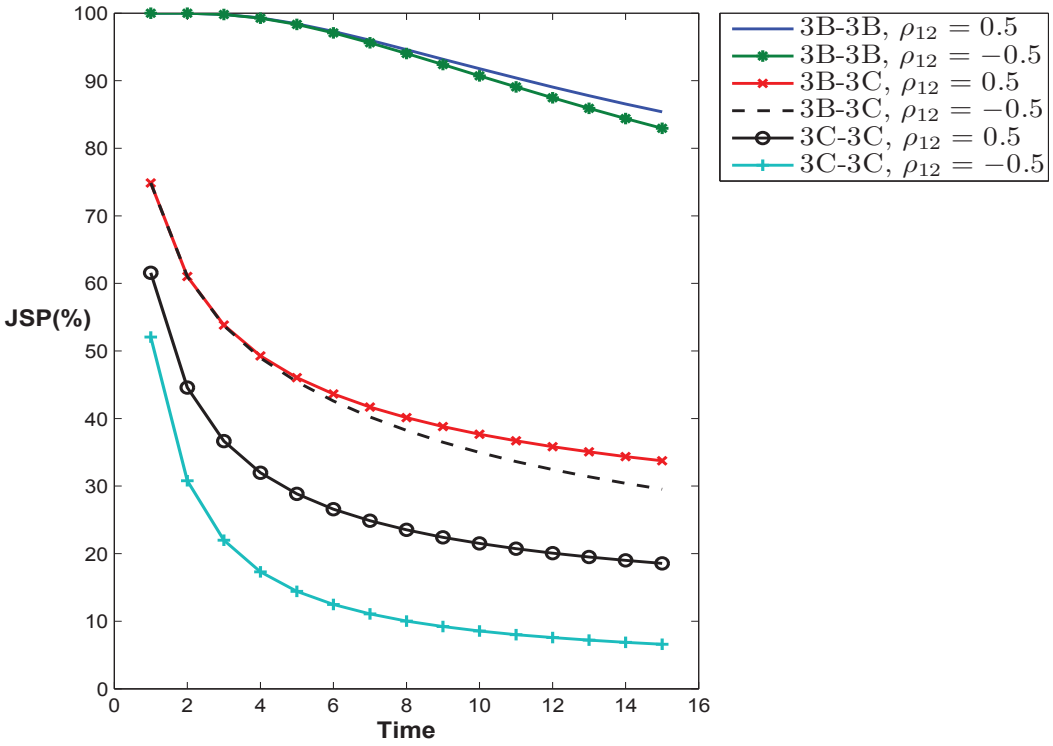

FIGURE 6.3. The impact of different credit rated pairing of firms on joint survival probabilities. Initial leverage for the CCC-rated firm is L_1=73.2%, for the BBB-rated firm is L_2=31.5% and volatilities σ_1=0.299, σ_2 =0.213. Other parameters used are $\widetilde{\mu}_1 = \widetilde{\mu}_2 = 0$, $\rho_{1r} = \rho_{2r} = 0$ and $\rho_{12} = -0.5, 0.5$.

We observe that the joint survival probability declines over time as the correlation coefficient ρ_{12} decreases. It reflects the fact that when firms' leverage ratios move in the same direction there is a higher joint survival probability than when the move is in the opposite direction. When firms' leverage ratios move in opposite directions, as one firm's leverage ratio moves closer to the default barrier (and so is more unlikely to survive), the second firm moves away from the default barrier (and more likely to survive), so the chance of both firms surviving is small, because the two firms are always in opposite situations.

We also observe that the variation of ρ_{12} makes little difference to the value of the joint survival probabilities with there being no discernable difference up to six years and a difference of 6.71% at fifteen years for $\rho_{12} = 0.9$ and -0.9.

Figure 6.2 plots the default correlation of firm 1 and firm 2 from the beginning to the end of the investment period of fifteen years. Figure 6.2 displays the impact on default correlations of the correlation coefficient ρ_{12} between BBB-CCC paired firms. We note that the sign of default correlations are the same as the correlation between two firms' leverage ratios ρ_{12}, which agrees with what was found by Zhou (2001*a*) and Cathcart & El-Jahel (2002). As one would expect that

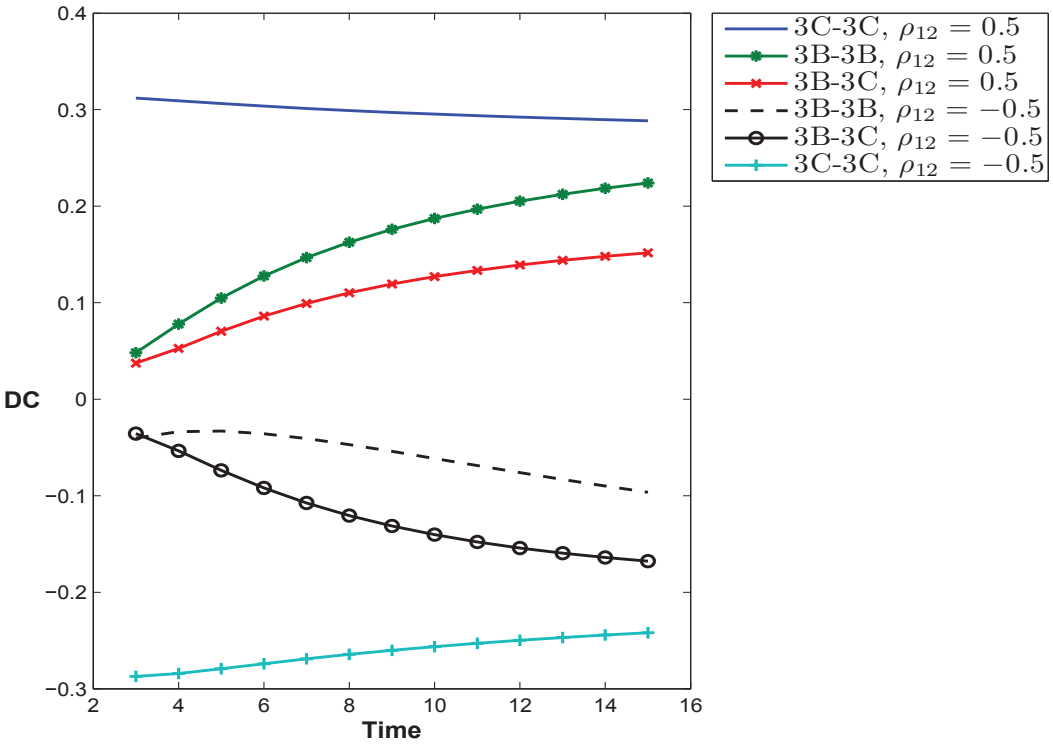

FIGURE 6.4. The impact of different credit rated pairing of firms on default correlations. Initial leverage for the CCC-rated firm is L_1=73.2%, for the BBB-rated firm is L_2=31.5% and volatilities σ_1=0.299, σ_2 =0.213. Other parameters used are $\widetilde{\mu}_1 = \widetilde{\mu}_2 = 0$, $\rho_{1r} = \rho_{2r} = 0$ and $\rho_{12} = -0.5, 0.5$.

firms in the same industry have higher default correlations than do the firms in different industries. This is quite intuitive, since firms' leverage ratios move in the same direction as they are positively correlated, so if one firm defaults, the second firm will more likely experience an increase in its leverage ratio and move closer to the default barrier. Firms' leverage ratios move in the opposite direction as they are negatively correlated, thus if one firm defaults, the second firm's leverage ratio will move away from the default barrier, and the firm will be less likely to default.

If the correlation coefficient ρ_{12} is close to zero, when a firm defaults, the likelihood of another firm defaulting is also close to zero. This can be seen from equation (3.91), the default correlation is zero when $\rho_{12} = 0$, because the joint default probability equals the product of the two firms' individual default probabilities.

We also note that the default correlation values at the very beginning of the time horizon are rising, this is due to division by the very small values of individual default probability for BBB-rated firm (for example, PD(BBB)$= 6.97838 \times 10^{-5}$). In order to avoid division by the extreme small values of default rates, in the remaining figures, the plot of default correlations will start at time equal to three years.

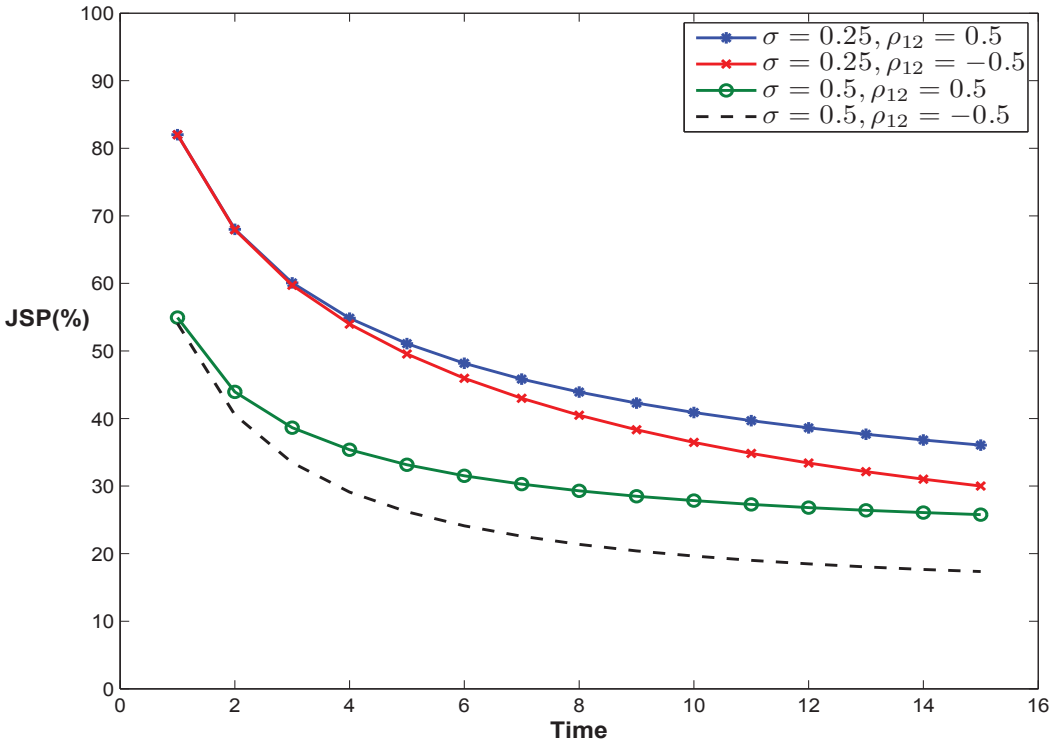

FIGURE 6.5. The impact of volatility levels σ_i of BBB-CCC paired firms on joint survival probabilities. Initial leverage for the CCC-rated firm is $L_1 = 73.2\%$, for the BBB-rated firm is $L_2 = 31.5\%$ and the volatilities are $\sigma_1 = \sigma_2 = \sigma = 0.25$ and 0.5. Other parameters used are $\widetilde{\mu}_1 = \widetilde{\mu}_2 = 0$, $\rho_{1r} = \rho_{2r} = 0$ and $\rho_{12} = -0.5, 0.5$.

6.2.2. The Impact of Different Credit Quality Paired Firms.

In this subsection, we discuss the impact of the difference of the credit pairing of firms on joint survival probabilities and default correlations. We demonstrate this effect by using BBB-BBB, BBB-CCC and CCC-CCC pairing of firms. To illustrate the effect of positive and negative correlation between two firms, we use the correlation values of $\rho_{12} = -0.5, 0.5$ here as well as in the rest of the thesis. We use these values of ρ_{12} because they are not extremes values.

Since the analytical solutions developed by the method of images in Chapter 4 are only valid for the values of ρ_{12} given in Table 4.1, we use one of the values of ρ_{12} (for example $\rho_{12} = -0.5$) that has the analytical solutions as a benchmark for the numerical results. On the other hand, in order to see effect of the positive correlation effect, we use a similar (in absolute value) positive value of $\rho_{12} = 0.5$. As in the previous Subsection, we also isolate the effects of drift terms of the leverage ratio processes and correlation of the interest rate process by setting $\widetilde{\mu}_i$=0 and ρ_{ir}=0 (i=1,2).

Figure 6.3 shows the impact on joint survival probabilities for BBB-BBB, BBB-CCC and CCC-CCC pairing of firms. The joint survival probabilities of the CCC-CCC paired-firms is lower than that of the BBB-CCC and BBB-BBB paired-firms. The joint survival probability curves decrease

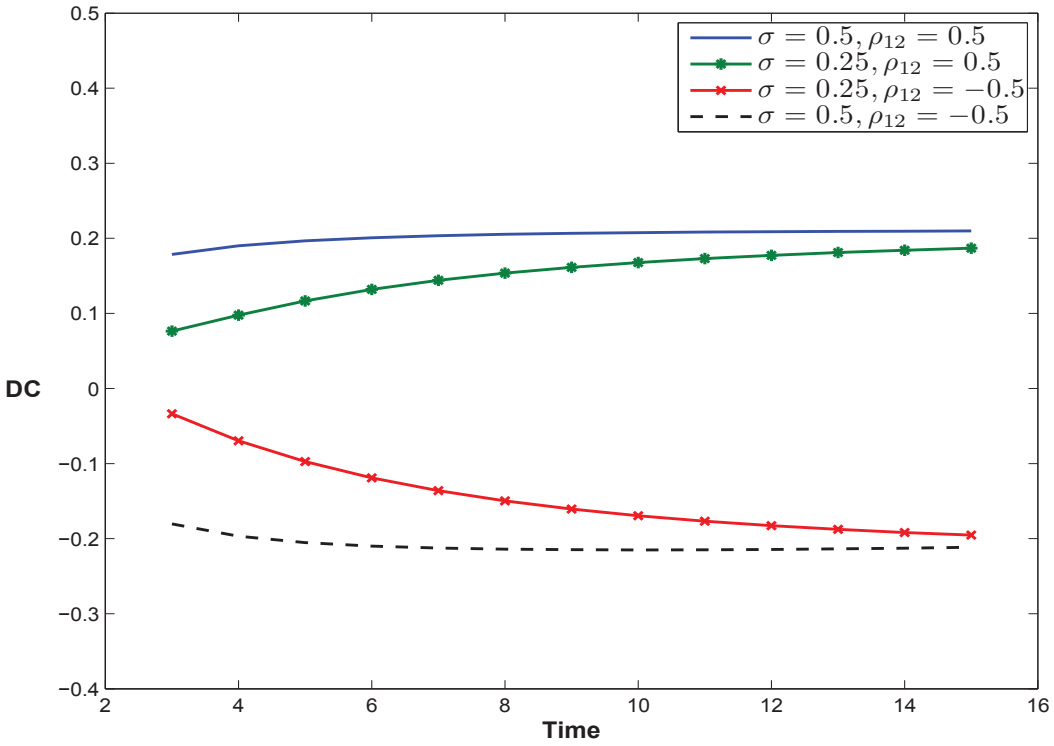

FIGURE 6.6. The impact of volatility levels σ_i of BBB-CCC paired firms on default correlations. Initial leverage for the CCC-rated firm is $L_1 = 73.2\%$, for the BBB-rated firm is $L_2 = 31.5\%$ and the volatilities are $\sigma_1 = \sigma_2 = \sigma = 0.25$ and 0.5. Other parameters used are $\widetilde{\mu}_1 = \widetilde{\mu}_2 = 0$, $\rho_{1r} = \rho_{2r} = 0$ and $\rho_{12} = -0.5, 0.5$.

slowly over time horizon for the BBB-BBB paired-firms, while for the BBB-CCC and CCC-CCC pairing of firms, joint survival probability curves decrease quickly at the beginning of the time horizon but flatten out towards the end of the time horizon. It makes sense that higher credit quality firms imply higher joint survival probabilities.

We also see from Figure 6.3 the effect of the correlation coefficient ρ_{12} between the two firms' leverage ratios becomes more significant as the quality of the firms' decreases. It is not significant at short time horizons for the BBB-BBB paired-firms, but its effect appears from around the middle of time horizon to the end. However, as we go from BBB-CCC to the CCC-CCC paired-firms, the correlation effect becomes progressively more significant from the beginning of the time horizon.

Since for firms of good credit quality, the initial leverage ratios are lower and distant from the default barrier, therefore, the joint survival probability is higher than for lower credit quality firms. If a firm has defaulted, the second firm will experience a rise (decline) in its leverage ratio because of the positive (negative) correlation, however, because of the low initial leverage ratio of the second firm, so this rise or decline in the leverage ratio for the second firm does not effect significantly its default probability. However, if the second firm is of low credit quality, its initial leverage ratio

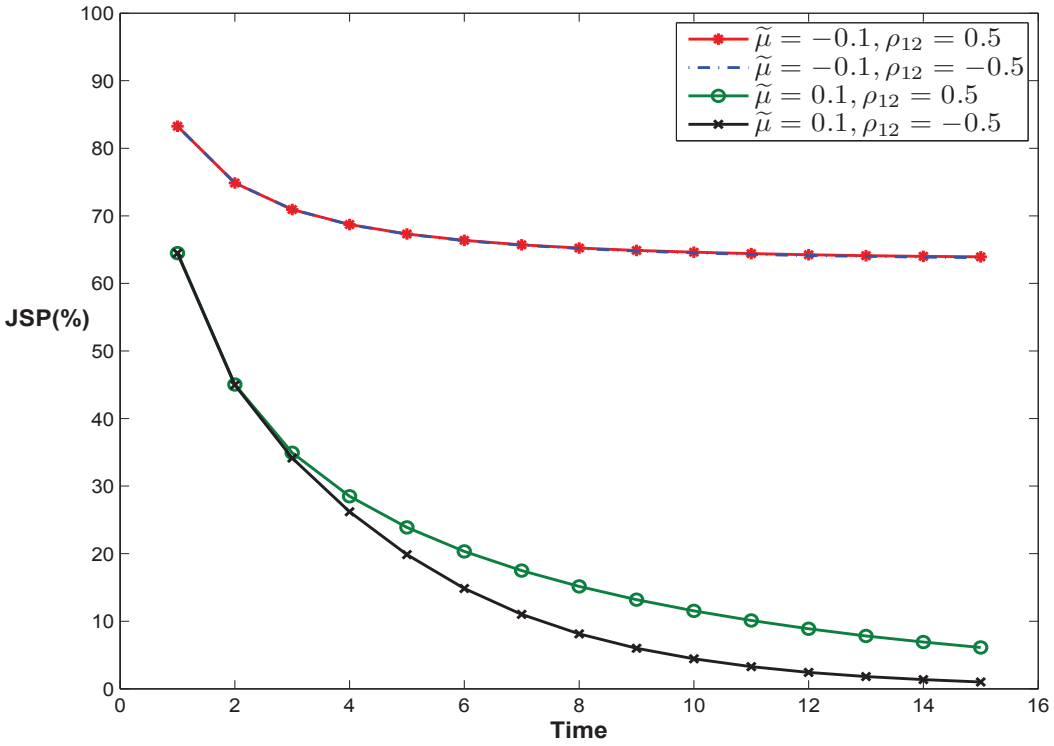

FIGURE 6.7. The impact of the means $\widetilde{\mu}_i$ of BBB-CCC paired firms on joint survival probabilities. Initial leverage for the CCC-rated firm is L_1=73.2%, for the BBB-rated firm is L_2=31.5% and the volatilities are σ_1=0.299, σ_2 =0.213. Other parameters used are $\widetilde{\mu}_1 = \widetilde{\mu}_2 = \widetilde{\mu} = -0.1$ and 0.1, $\rho_{1r} = \rho_{2r} = 0$ and $\rho_{12} = -0.5, 0.5$.

is high and closer to the default barrier, so that this rise or decline in leverage ratios will be more likely to bring the second firm into default, so that the correlation effect is more significant for lower credit quality firms than good credit quality firms. In other words, for a given a value of the correlation coefficient, the most important effect on the joint survival probability arises from the difference in credit ratings.

Figure 6.4 illustrates the impact on default correlations for BBB-BBB, BBB-CCC and CCC-CCC paired-firms. We also observe from Figure 6.4 that the lower credit quality paired firms (for example CCC-CCC) generally have higher values (in absolute terms) of default correlation for the cases of both positive and negative correlation. However, an interesting result is that for a good quality pair of firms, if they are positively correlated, the default correlation is higher than that of a good quality and low quality pairing of firms. But this situation is reversed (as far as the comparison of the absolute values of default correlation is concerned) if they are negatively correlated. Since it is difficult to relate this finding to any empirical evidence, though clearly it points to the need for more empirical research in this area.

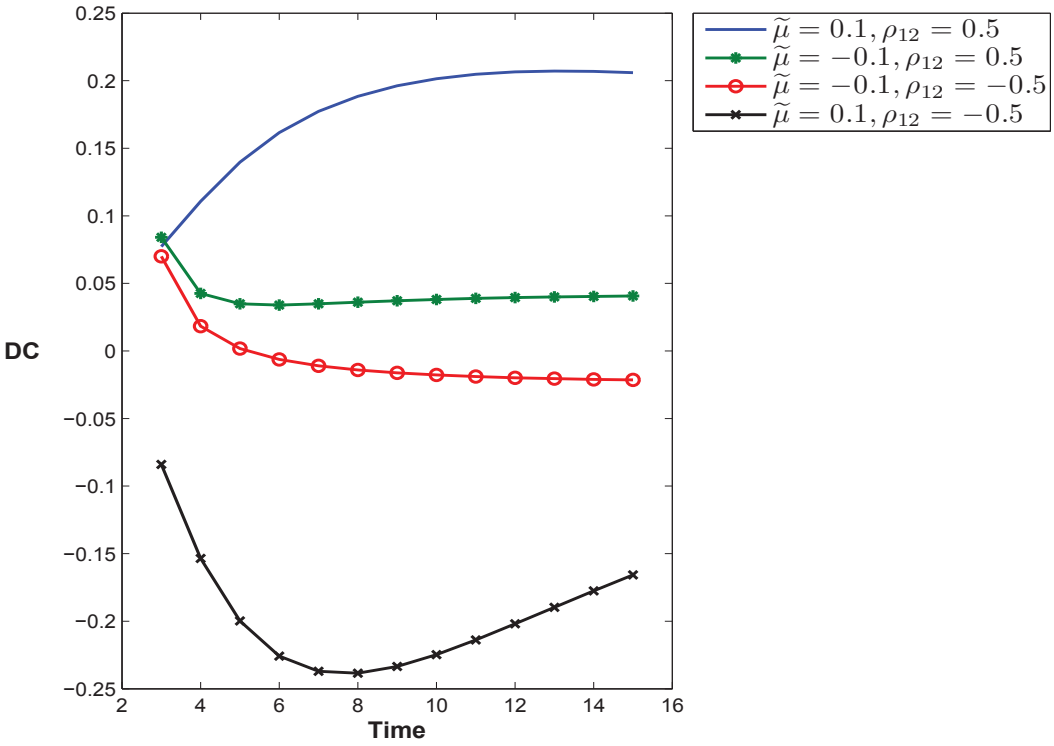

FIGURE 6.8. The impact of the means $\widetilde{\mu}_i$ of BBB-CCC paired firms on default correlations. Initial leverage for the CCC-rated firm is L_1=73.2%, for the BBB-rated firm is L_2=31.5% and the volatilities are σ_1=0.299, σ_2 =0.213. Other parameters used are $\widetilde{\mu}_1 = \widetilde{\mu}_2 = \widetilde{\mu} = -0.1$ and 0.1, $\rho_{1r} = \rho_{2r} = 0$ and $\rho_{12} = -0.5, 0.5$.

6.2.3. The impact of Volatilities.

This subsection illustrates the impact of volatility levels on joint survival probabilities and default correlations. We use the typical leverage ratio levels for BBB and CCC firms from Table 6.1. Consider the volatility levels ranging between $\sigma_i = 0.25$ and 0.5. The correlation between two firms are taken as $\rho_{12} = -0.5$ and $\rho_{12} = 0.5$. The drift terms and interest rates effects are again isolated by setting $\widetilde{\mu}_i = 0$ and $\rho_{ir} = 0$ $(i = 1, 2)$.

Figure 6.5 exhibits the effect of changes in the volatility levels σ_i on the joint survival probability for BBB-CCC paired firms. The joint survival probability drops as the volatility levels increases when firms are both positively ($\rho_{12} > 0$) as well as negatively ($\rho_{12} < 0$) correlated. This result seems natural, because when a market is volatile, the probability of default for a firm is higher, so the joint survival probability decreases.

Figure 6.6 shows the impact of volatility levels σ_i on the default correlation. As expected, the default correlation (in absolute value) rises as the volatilities increase. This indicates that when the market is less volatile, the probability of single firm default is low, which leads to the decline of the conditional default. We also observe that the difference in volatilities is more significant for

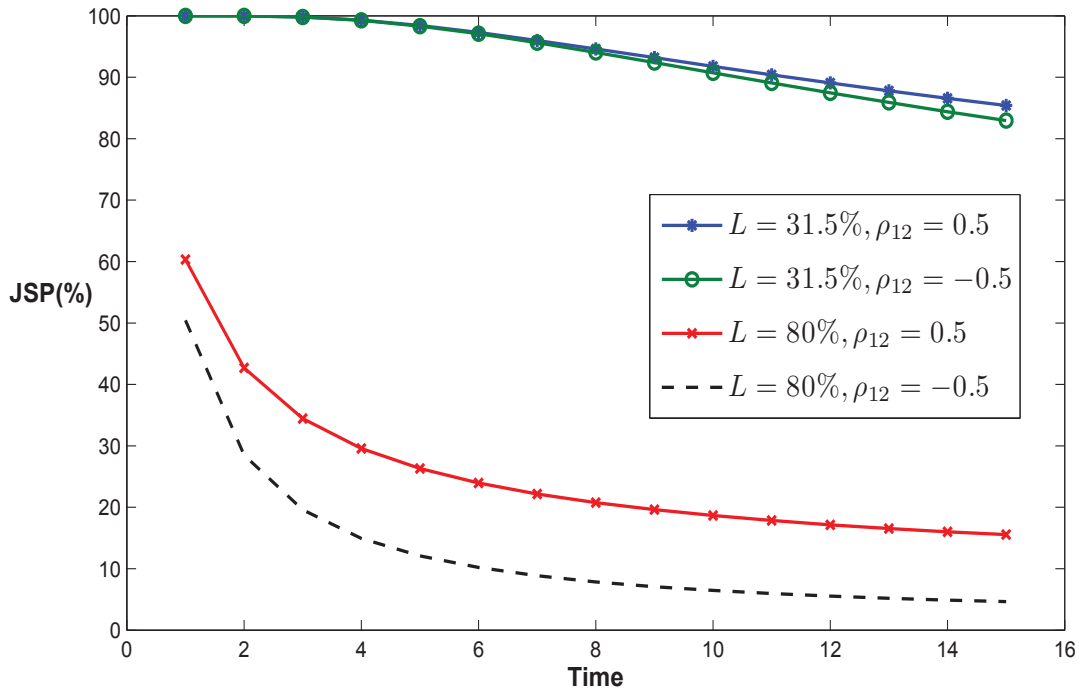

FIGURE 6.9. The impact of leverage ratio levels L_i on joint survival probabilities. Initial leverages used are (i) $L_1 = L_2 = L = 31.5\%$ and (ii) $L_1 = L_2 = L = 80\%$. The volatilities for both cases (i) and (ii) are $\sigma_1 = \sigma_2 = 0.213$. Other parameters used are $\widetilde{\mu}_1 = \widetilde{\mu}_2 = 0$, $\rho_{1r} = \rho_{2r} = 0$ and $\rho_{12} = -0.5, 0.5$.

short time horizons. This result seems to reflect the fact that the volatility effects on the default correlation are more significant in the short term.

6.2.4. The impact of Drift Levels.

In the previous subsections we isolated the impact of the drifts of the leverage ratio processes by setting $\widetilde{\mu}_i = 0$ $(i = 1, 2)$. Now, in this subsection, we illustrate the impact on joint survival probabilities and default correlations of the drifts levels. We use the BBB and CCC paired firms in order to illustrate this effect. We take the drift levels $\widetilde{\mu}_1 = \widetilde{\mu}_2 = -0.1, 0, 0.1$. Note that $\widetilde{\mu}_i$ is under the risk-neutral measure. We take as the correlation coefficient between the two firms the values $\rho_{12} = -0.5, 0.5$. We continue to isolate the effect of the interest rate process by setting $\rho_{ir} = 0$ $(i = 1, 2)$.

Figure 6.7 displays the impact on joint survival probabilities of different drift levels $\widetilde{\mu}_i$ of BBB-CCC paired firms. The joint survival probability is sensitive to changes in the drift levels, for example it decreases by 57.8% from $\widetilde{\mu}_i = -0.1$ to $\widetilde{\mu}_i = 0.1$ (for the case of $\rho_{12} = 0.5$). The joint survival probability declines as the drift levels increase, which reflects the fact that for lower $\widetilde{\mu}_i$,

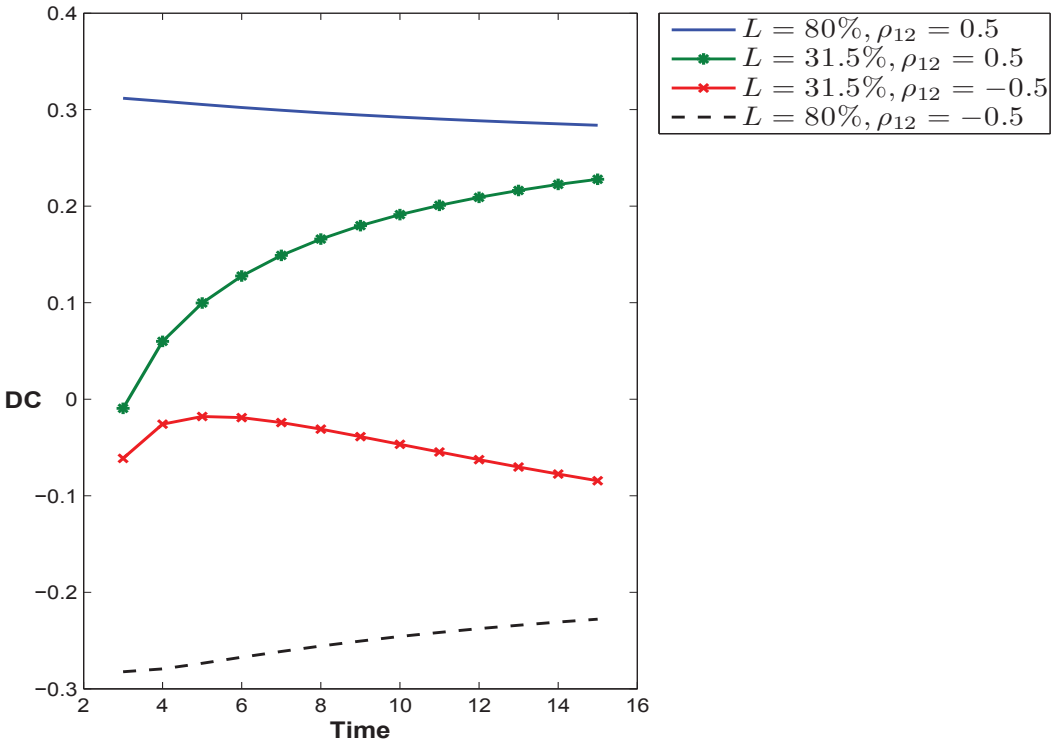

FIGURE 6.10. The impact of leverage ratio levels L_i on default correlations. Initial leverages used are (i) $L_1 = L_2 = L = 31.5\%$ and (ii) $L_1 = L_2 = L = 80\%$. The volatilities for both cases (i) and (ii) are $\sigma_1 = \sigma_2 = 0.213$. Other parameters used are $\widetilde{\mu}_1 = \widetilde{\mu}_2 = 0$, $\rho_{1r} = \rho_{2r} = 0$ and $\rho_{12} = -0.5, 0.5$.

the leverage ratios drift to smaller values on average, in the sense that firms' leverage ratio levels decrease over time, hence firms remain on average at a better credit quality status, and their joint survival probability is higher.

We observe that the effect of the correlation coefficient ρ_{12} is more pronounced for larger values of drift levels. There is no effect on joint survival probabilities in the case of negative drift, but a noticeable impact when the value of the drift is positive. The argument is similar to the effect on the low credit quality paired firms as indicated in Figure 6.3. Since the firms' leverage ratios drift to smaller values on average when the drift is negative, in the sense that firms' leverage ratios decrease and move away from the default barrier over time. Therefore, if a firm has defaulted, the second firm will experience a rise or decline in its leverage ratio because of the positive or negative correlation. However, because of the low leverage ratio of the second firm, this rise or decline in the leverage ratio for the second firm does not effect significantly its probability of default. While, if the drift is positive, the firms' leverage ratios increase and move closer to the default barrier over time, then if a firm has defaulted, the second firm will experience a rise or decline in its leverage ratio with positive or negative correlation. However, because of the high leverage ratio of the

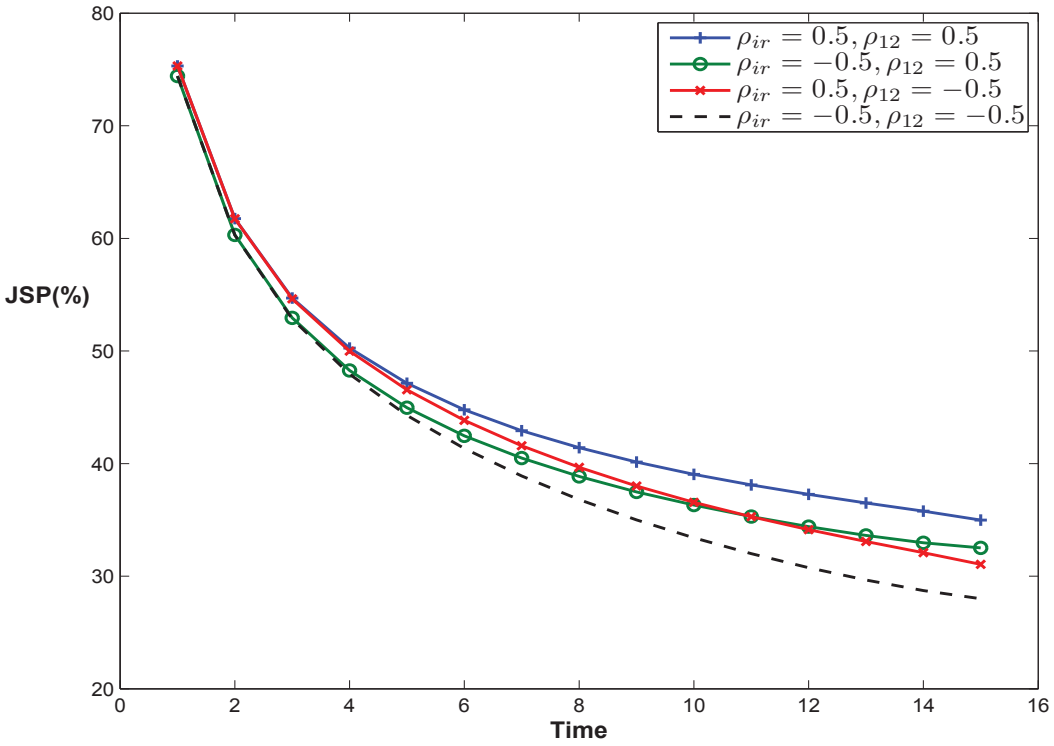

FIGURE 6.11. The impact of correlation ρ_{ir} between firms & interest rate for BBB-CCC paired firms on joint survival probabilities. Initial leverage for the CCC-rated firm is $L_1 = 73.2\%$, for the BBB-rated firm is $L_2 = 31.5\%$ and the volatilities are $\sigma_1 = 0.299$, $\sigma_2 = 0.213$. Other parameters used are $\widetilde{\mu}_1 = \widetilde{\mu}_2 = 0$, $\rho_{12} = -0.5, 0.5$, $\rho_{1r} = \rho_{2r} = -0.75, -0.1$ and 0.75, the maturity of risk-free bond price is $T = 15$, $\kappa_r = 1.0$ and $\sigma_r = 0.03162$.

second firm, this rise or decline in the leverage ratio will be more or less likely to bring the second firm into default, therefore, the effect of correlation is more significant for larger values of the drift.

Figure 6.8 graphs the default correlation of BBB-CCC paired firms for different drift levels $\widetilde{\mu}_i$. The default correlation is sensitive to the change in the drift levels, similar to what is indicated in Figure 6.7. The default correlation (in absolute value) declines as the average mean levels decrease. Consider the positively correlated case, when firms' leverage ratios drift to larger values on average, so that leverage ratios are close to the default barrier, when one firm defaults, the other firm will experience a rise of its leverage ratio (because of the positive correlation), and because the leverage ratio of the second firm is closer to the default barrier, it will be likely that this increase will also bring the second firm into default. However, when firm's leverage ratio drifts to smaller values on average, in which firms' leverage ratio are away from the default barrier, so if one firm defaults, the leverage ratio of the other firm will rise (because of the positive correlation), but the leverage ratio of the second firm is distant from the default barrier, so that it will be less likely that this rise will bring it into default.

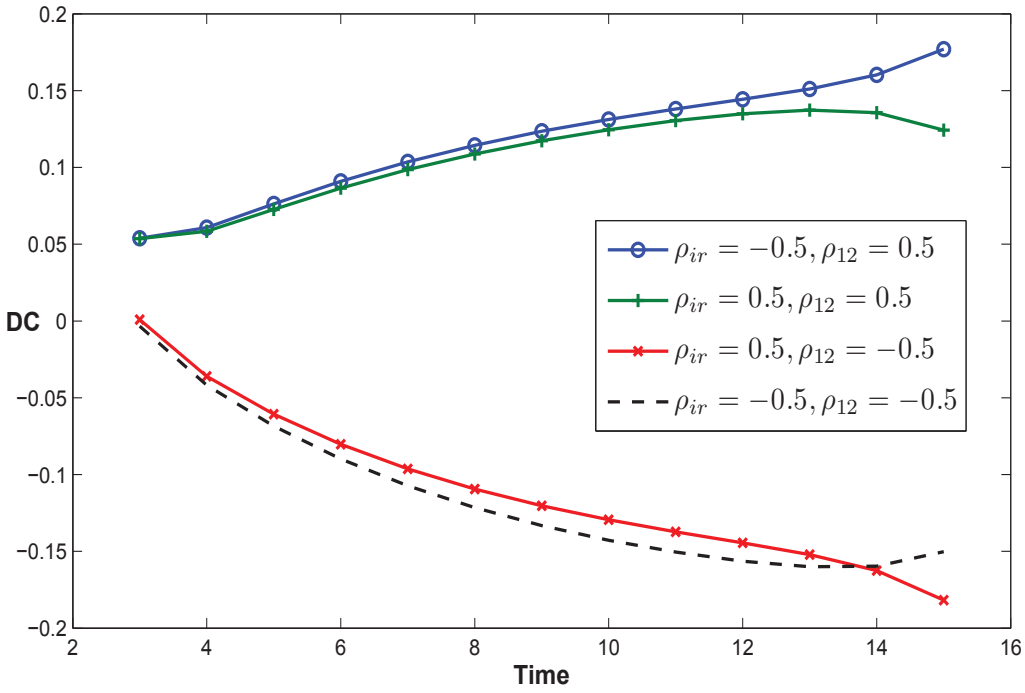

FIGURE 6.12. The impact of correlation ρ_{ir} between firms & interest rate for BBB-CCC paired firms on default correlations. Initial leverage for the CCC-rated firm is $L_1 = 73.2\%$, for the BBB-rated firm is $L_2 = 31.5\%$ and the volatilities are $\sigma_1 = 0.299$, $\sigma_2 = 0.213$. Other parameters used are $\widetilde{\mu}_1 = \widetilde{\mu}_2 = 0$, $\rho_{12} = -0.5, 0.5$, $\rho_{1r} = \rho_{2r} = -0.75, -0.1$ and 0.75, the maturity of risk-free bond price is $T = 15$, $\kappa_r = 1.0$ and $\sigma_r = 0.03162$.

6.2.5. The Impact of Leverage Ratio Levels.

In this subsection, we investigate the impact on joint survival probabilities and default correlations of changes in the leverage ratio levels . We use the volatility levels corresponding to BBB-rated firms. From Table 6.1 we take the leverage ratio levels $L_1 = L_2 = 31.5\%$ (values for BBB-rated firms) and 80% (values for CCC-rated firms). This shows the impact of leverage ratios when they are at very high levels. The correlation between the two firms ranges over $\rho_{12} = -0.5$ and 0.5. The drift terms and interest rate effects are again isolated by setting $\widetilde{\mu}_i = 0$ and $\rho_{ir} = 0$ $(i = 1, 2)$.

Figure 6.9 shows the impact of leverage ratio levels L_i on joint survival probabilities. The joint survival probability curves are generally decreasing over the time horizon for different values of σ_i. The smaller the leverage ratio levels, the higher the joint survival probabilities. Figure 6.9 also shows that the smaller are the leverage levels, the less significant is the correlation ρ_{12} on joint survival probability curves, which is similar to the effects observed in Figure 6.3, Figure 6.7 and Figure 6.5. This seems to show that when firms are healthy (which means less volatile, or lower

leverage ratios or lower drift levels or a combination of all of these), the effect of correlations between the two firms on joint survival probability is small.

Figure 6.10 illustrates the impact of leverage ratio levels L_i of a BBB-CCC paired firm on default correlations. We observe that the higher the leverage levels, the higher in absolute values are the default correlations, which is similar to the effect observed in Figure 6.4.

6.2.6. Impact of Correlation Between Firms & Interest Rates.

This subsection presents the interest rate effects on joint survival probabilities and default correlations. When the correlation to the interest ratio process ρ_{ir} is nonzero, the joint survival probability and the probability of individual defaults are related to the parameter κ_r that controls the speed of the mean reversion of interest rate process via the time-dependent coefficient $b(t)$, which is given in (3.81). For this case, we use the parameters $\kappa_r = 1.0$, $\sigma_r = 0.03162$ which is consistent with those used by Hui et al. (2007). We assume that they remain the same for all different ratings.

The values of correlation between firms and interest rates are $\rho_{1r} = \rho_{2r} = -0.75, -0.1$ and 0.75. The maturity of the risk-free bond is $T = 15$, $\widetilde{\kappa}_r = 1.0$ and $\sigma_r = 0.03162$. We use the BBB and CCC pairing of firms. The correlation between the two firms are $\rho_{12} = -0.5, 0.5$. The effect of drift terms is isolated by setting $\widetilde{\mu}_i = 0$ $(i = 1, 2)$.

Figure 6.11 displays the impact of the interest rate process on the joint survival probability. The joint survival probability increases as the correlation coefficients ρ_{ir} rises, irrespective of the sign of ρ_{12}. Since the leverage ratio is the debt to asset ratio, when it is positively correlated to the interest rate process, the asset value rises as the interest rate rises, this leads to a decline in the leverage ratio (because of its definition), so the joint survival probability increases . We observe that changes in correlation coefficient ρ_{ir} do not have a significant effect on the joint survival probability with the difference being 0.941% at four years and rising to 1.23% at 15 years. Figure 6.12 plots the default correlation with different levels of correlation coefficient ρ_{ir}, and as with the joint survival probabilities we observe that changes in ρ_{ir} makes little difference to the default correlations. We also observe that the default correlation declines as the correlation coefficient ρ_{ir} increases. This reflects the situation that the increase of joint survival probability due to the decline of leverage ratios, as already indicated in the discussion of the effect on the joint survival probability in Figure 6.11.

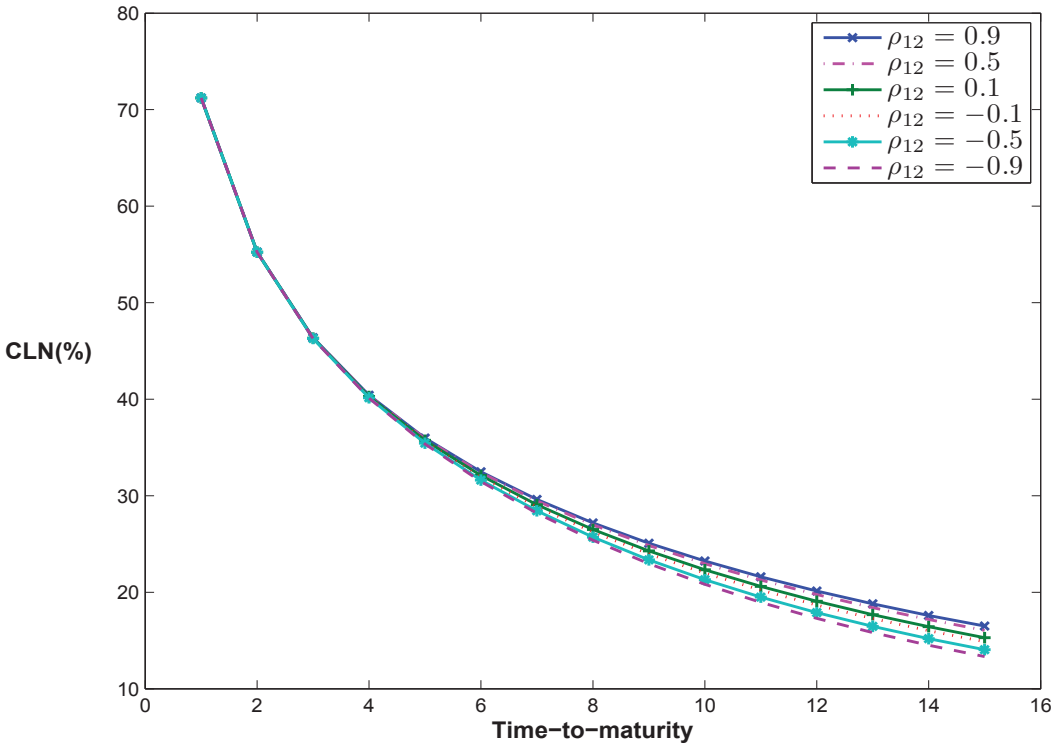

FIGURE 6.13. The price of credit linked notes for BBB-CCC paired firms. Initial leverage for the CCC-rated firm is L_1=73.2%, for the BBB-rated firm is L_2=31.5% and the volatilities are σ_1=0.299, σ_2 =0.213. Other parameters used are $r = 5\%$, $\kappa_r = 1$, $\widetilde{\theta}_r = 5\%$ and $\sigma_r^2 = 0.001$, $\widetilde{\mu}_1 = \widetilde{\mu}_2 = 0$, $\rho_{1r} = \rho_{2r} = 0$ and $\rho_{12} = -0.9, -0.5, -0.1, 0.5$ and 0.9.

6.3. The Price of Credit Linked Notes

The focus of this thesis is on default correlations and joint survival probabilities, while the other application of the two-firm model is to price the credit linked note. In this section, we illustrate the impact on the prices of credit linked notes with respect to variation in the values of correlation coefficients between two firms and with respect to different credit quality paired firms.

Recall from (3.75) that the price of a credit linked note is the product of the risk-free bond price $B(r,t)$ of Vasicek (1977) model and the risk ratio function $\widehat{P}(L_1, L_2, t)$. The calculation of the risk-free bond price $B(r,t)$ is based on equations (E.9)-(E.11) in Appendix E. For numerical calculation we use parameters similar to Hui et al. (2007), where $r = 5\%$, $\kappa_r = 1$, $\widetilde{\theta}_r = 5\%$ and $\sigma_r^2 = 0.001$. The valuation of the risk ratio function $\widehat{P}(L_1, L_2, t)$ is based on the analytical results in Chapter 4 or numerical algorithms in Chapter 5.

Figure 6.13 shows the impact on credit linked note prices of different values of the correlation coefficient ρ_{12} between BBB-CCC paired firms as a function of time-to-maturity. The parameters used to calculate $\widehat{P}(L_1, L_2, t)$ are the same as in Figure 6.1. We observe that the credit lined note

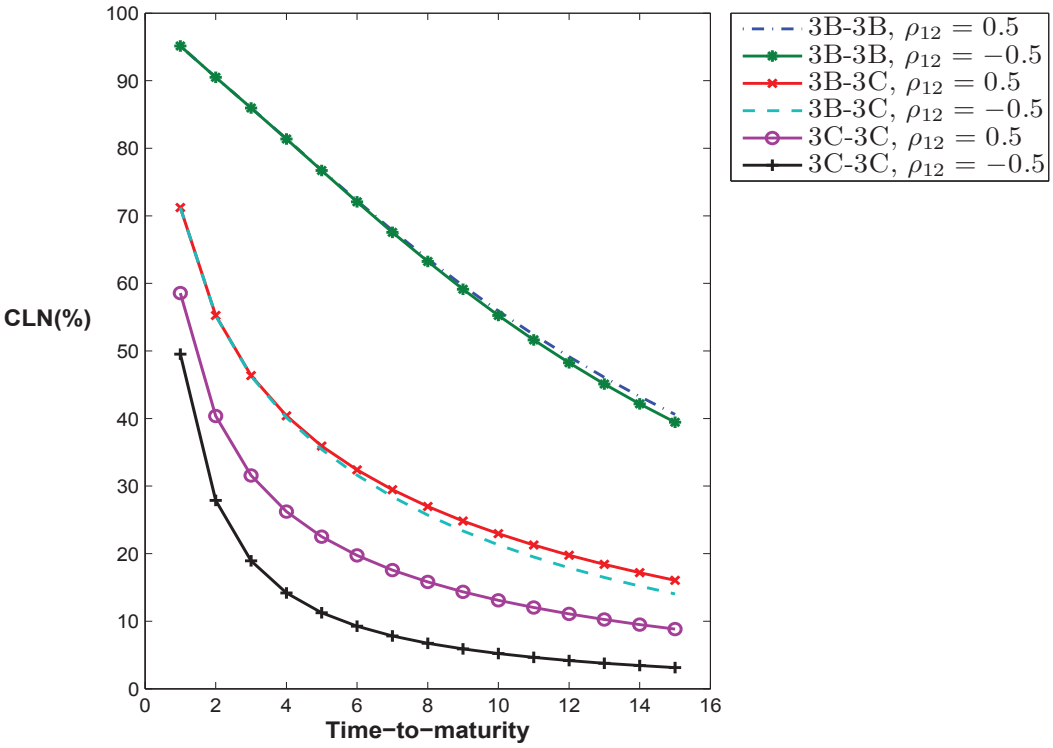

FIGURE 6.14. The price of credit linked notes for BBB-CCC paired firms. Initial leverage for the CCC-rated firm is L_1=73.2%, for the BBB-rated firm is L_2=31.5% and volatilities σ_1=0.299, σ_2 =0.213. Other parameters used are $r = 5\%$, $\kappa_r = 1$, $\widetilde{\theta}_r = 5\%$ and $\sigma_r^2 = 0.001$, $\widetilde{\mu}_1 = \widetilde{\mu}_2 = 0$, $\rho_{1r} = \rho_{2r} = 0$ and $\rho_{12} = -0.5$ and 0.5.

prices decrease with respect to time-to-maturity as the correlation coefficient ρ_{12} decreases. This may be due to the fact that when firms' leverage ratios move in the same direction the price of a credit linked note is higher than that for moves in the opposite direction. If firms' leverage ratios move in opposite directions, as one firm's leverage ratio moves closer to the default barrier (and is less likely to survive), the second firm moves away from the default barrier (and is more likely to survive), so the chance of both firms survival is small because they are always moving in opposite directions, therefore, the price of credit linked note is lower.

Figure 6.14 shows the impact on credit linked note prices for BBB-BBB, BBB-CCC and CCC-CCC paired firms over the time-to-maturity. The parameter used to evaluate $\widehat{P}(L_1, L_2, t)$ are the same as in Figure 6.3. We observe that the price of a credit linked note of BBB-BBB paired firms is the highest, while the price of CCC-CCC paired firms is the lowest among those paired firms. This makes sense since the price of credit linked note issued by good credit quality firms is higher than that issued by low credit quality firms.

We also observe that the impact of the correlation coefficient ρ_{12} or the credit quality of firms on the price of credit linked note is the same as the impact on joint survival probabilities (see Figure 6.1

GBM parameters	Impact on JSP	Impact on DC (in absolute value)
Credit quality ↑	⇑	⇓ (not symmetric for $\pm\rho_{12}$)
Correlation ρ_{12} ↑	⇑	⇑
Volatilities σ_i ↑	⇓	⇑
Average means $\widetilde{\mu}_i$ ↑	⇓	⇑
Initial leverage ratios L_i ↑	⇓	⇑
Correlation w/ interest rate risk ρ_{ir} ↑	⇑	⇓

TABLE 6.2. A summary of the impact on joint survival probabilities and default correlations for geometric Brownian motions.

and Figure 6.3). This is because the risk ratio function (3.89) and the joint survival probability function (3.90) both depend principally on the same transition probability density function. As the payoff condition of the credit linked note is the par value (see (3.69)), the risk ratio function as a function of time-to-maturity is equivalent the joint survival probability function. Thus, if we use the same risk-free bond price function, the impact of other parameters on credit linked note prices will be similar to the impact on joint survival probabilities as in Section 6.2.

6.4. Overview

In this chapter, we have discussed the choice of parameters, evaluated and compared the impact on the joint survival probabilities and default correlations of various scenarios when the leverage ratios dynamics are driven by geometric Brownian motions. The results are summarized in Table 6.2. We find that when the volatilities of firms' leverage ratios, the average mean levels, or the initial leverage ratios decrease respectively, the values of joint survival probabilities rise. On the other hand, the joint survival probabilities decline as the firms' leverage ratio correlation, or the correlation between firm's leverage ratio and interest rate decrease. We also find that when the firms' leverage ratio correlation, the volatilities of firms' leverage ratios, the average mean levels, or the initial leverage ratios increase, the absolute values of default correlation rises, but it declines as the values of correlation between firm's leverage ratio and interest rate increases.

We note that these findings are based on a study of the impact of the model parameters chosen. Whilst there is a rationale for these values as we have explained, it remains a task for future research to calibrate the types of model discussed here to market data. The effects summarized in Table 6.2 also need to be investigated empirically in future research. Of course such studies need to first examine which type of process for the leverage ratio dynamics is most suitable, since as we shall see in subsequent chapters the effects observed in Table 6.2 can be sensitive to this issue.

CHAPTER 7

Two-Firm Model with Mean-Reverting Processes

As discussed in Chapter 2, Collin-Dufresne & Goldstein (2001) point out that most structural models preclude the possibility that firms may alter their capital structure. They argue that in practice, firms could adjust their outstanding debts levels in response to the change in firm values, hence generating mean-reverting leverage ratios. To model this feature, Collin-Dufresne & Goldstein (2001) extend the Longstaff & Schwartz (1995) model by considering a deterministic mean-reverting default threshold, which can be linearly related to the outstanding debts. This setting captures the fact that firms tend to issue debt when their leverage ratio falls below some target, and replace maturing debt when their leverage ratio rises above this target. Hui et al. (2006) generalize the Collin-Dufresne & Goldstein (2001) model by incorporating a time-dependent target leverage ratio. This is done by introducing a stochastic mean-reverting default threshold that relates to the firm's liability. Hui et al. (2006) point out that the time-dependent target leverage ratio reflects the movements of a firm's initial target ratio towards a long-run target ratio over time.

This chapter extends the framework of the two-firm model to consider the case in which the dynamic leverage ratios are mean-reverting to constant target ratios (as was the case in Collin-Dufresne & Goldstein (2001)) and also to time-dependent target ratios (as was the case in Hui et al. (2006)), in order to study the impact of firms altering their capital structure on joint survival probabilities and default correlations. Section 7.1 presents the framework of the two-firm model with dynamic leverage ratios following mean-reverting processes, and extends the method of images approach in two-dimensions developed in Chapter 4 to handle this situation. However, as was shown in Section 4.1 the method of images approach in the two-dimensional case works only for certain values of the correlation coefficient ρ_{12}. Therefore, in the second part of this chapter, we extend the Monte Carlo scheme of Section 5.2 to develop a numerical scheme applicable for all values of the correlation ρ_{12} as well as to serve as a benchmark. Then we discuss the accuracy of the results obtained by these methods and compare them to the approximate analytical solution based on Huang (2003), in which the relative percentage error is very large based on the method of images using a single-stage approximation scheme, while the Monte Carlo results generally have relative percentage errors of less than 1%. In the last part of this chapter, we study the impact of mean-reverting processes on joint survival probabilities and default correlations.

7.1. The Two-Firm Framework in the Case of Mean-Reverting Leverage Ratios

In order to capture the effect of mean-reverting processes for the leverage ratios we need to modify assumption 1 in Chapter 3 to

Assumption 1′. *Let L_1 and L_2 denote respectively the leverage ratios of the note issuer and the reference obligor. The leverage ratio is defined as the ratio of a firm's liability to its market-value capitalization. Assume L_1 and L_2 follow mean-reverting processes with a time varying long run target ratio. The dynamics of L_1 and L_2 are described by*

$$dL_i \;=\; \kappa_i[\ln\theta_i(t) - \ln L_i]L_i dt + \sigma_i L_i dZ_i,\ (i=1,2), \tag{7.1}$$

where the parameters κ_i control the speed of mean reversion, the $\theta_i(t)$ are the mean reversion levels, the σ_i govern the volatility of the proportional change in leverage ratio for the two firms, and the Z_i are Wiener processes capturing the uncertainty in the leverage ratio dynamics under the historical measure $\mathbb{P}$. The Wiener increments dZ_1 and dZ_2 are correlated with

$$\mathbb{E}[dZ_1 dZ_2] = \rho_{12}dt, \tag{7.2}$$

where ρ_{12} denotes the correlation coefficient of the proportional leverage ratio level of the two firms.

The interpretation is similar to that in Collin-Dufresne & Goldstein (2001): when the log-leverage ratio of a firm $\ln L_i$ falls below the long term log-target ratio $\ln\theta_i$, the firm increases $\ln L_i$ by, for example, issuing debt. On contrast, when $\ln L_i$ is higher than $\ln\theta_i$, the firm may decrease $\ln L_i$ by replacing outstanding debt. As mentioned in Collin-Dufresne & Goldstein (2001), this setting captures the features of firm behaviour that they tend to issue debt when their leverage ratios fall below some target, and tend to replace maturing debt when their leverage ratio rises above that target.

Assumptions 2-4 remain the same as in Chapter 2.

To obtain the the partial differential equation for the credit linked note price $P(L_1, L_2, r, t)$, we apply the standard arbitrage pricing argument outlined in Appendix D, and under the Assumptions

$1'$, 2, 3 and 4, we find that the price of the credit linked note satisfies

$$\begin{aligned}
-\frac{\partial P}{\partial t} &= \frac{1}{2}\sigma_1^2 L_1^2 \frac{\partial^2 P}{\partial L_1^2} + \frac{1}{2}\sigma_r^2 \frac{\partial^2 P}{\partial r^2} + \frac{1}{2}\sigma_2^2 L_2^2 \frac{\partial^2 P}{\partial L_2^2} + \rho_{12}\sigma_1\sigma_2 L_1 L_2 \frac{\partial^2 P}{\partial L_1 \partial L_2} \\
&\quad + \rho_{1r}\sigma_1\sigma_r L_1 \frac{\partial^2 P}{\partial L_1 \partial r} + \rho_{2r}\sigma_2\sigma_r L_2 \frac{\partial^2 P}{\partial L_2 \partial r} \\
&\quad + [\kappa_1(\ln\theta_1(t) - \ln L_1) - \lambda_1\sigma_1] L_1 \frac{\partial P}{\partial L_1} + [\kappa_2(\ln\theta_2(t) - \ln L_2) - \lambda_2\sigma_2] L_2 \frac{\partial P}{\partial L_2} \\
&\quad + [\kappa_r(\theta_r - r) - \lambda_r\sigma_r] \frac{\partial P}{\partial r} - rP, \qquad (7.3)
\end{aligned}$$

for $t \in (0, T)$, $L_1 \in (0, \widehat{L}_1)$, $L_2 \in (0, \widehat{L}_2)$ and subject to the boundary conditions

$$P(L_1, L_2, r, T) = 1, \qquad (7.4)$$

$$P(\widehat{L}_1, L_2, r, t) = 0, \qquad (7.5)$$

$$P(L_1, \widehat{L}_2, r, t) = 0. \qquad (7.6)$$

Here $\widetilde{\theta}_i(t)$ and $\widetilde{\theta}_r$ incorporate the market prices of risk (λ_1, λ_2) (assumed constant here) associated with leverage ratios and interest rate processes respectively λ_r, according to

$$\widetilde{\theta}_i(t) = \theta_i(t) e^{-\lambda_i\sigma_i/\kappa_i}, \qquad (7.7)$$

$$\widetilde{\theta}_r = \theta_r - \frac{\lambda_r\sigma_r}{\kappa_r}, \qquad (7.8)$$

then (7.3) becomes

$$\begin{aligned}
-\frac{\partial P}{\partial t} &= \frac{1}{2}\sigma_1^2 L_1^2 \frac{\partial^2 P}{\partial L_1^2} + \frac{1}{2}\sigma_r^2 \frac{\partial^2 P}{\partial r^2} + \frac{1}{2}\sigma_2^2 L_2^2 \frac{\partial^2 P}{\partial L_2^2} + \rho_{12}\sigma_1\sigma_2 L_1 L_2 \frac{\partial^2 P}{\partial L_1 \partial L_2} \\
&\quad + \rho_{1r}\sigma_1\sigma_r L_1 \frac{\partial^2 P}{\partial L_1 \partial r} + \rho_{2r}\sigma_2\sigma_r L_2 \frac{\partial^2 P}{\partial L_2 \partial r} \\
&\quad + \kappa_1[\ln\widetilde{\theta}_1(t) - \ln L_1] L_1 \frac{\partial P}{\partial L_1} + \kappa_2[\ln\widetilde{\theta}_2(t) - \ln L_2] L_2 \frac{\partial P}{\partial L_2} \\
&\quad + \kappa_r[\widetilde{\theta}_r - r] \frac{\partial P}{\partial r} - rP, \qquad (7.9)
\end{aligned}$$

Using the separation of variables technique discussed in Section 3.3, the price of the credit linked note can be expressed as a product of the risk-free bond price $B(r, t)$ and the risk ratio function $\widehat{P}(L_1, L_2, t)$ so that

$$P(L_1, L_2, r, t) = B(r, t)\widehat{P}(L_1, L_2, t). \qquad (7.10)$$

Applying the same calculations as used in Appendix E, and simply replacing the terms $\widetilde{\mu}_i$ with $\kappa_i[\ln\widetilde{\theta}_i(t) - \ln L_i]$, it turns out that $\widehat{P}(L_1, L_2, t)$ satisfies the partial differential equation

$$\begin{aligned} -\frac{\partial\widehat{P}}{\partial t} &= \frac{1}{2}\sigma_1^2 L_1\frac{\partial^2\widehat{P}}{\partial L_1^2} + \rho_{12}\sigma_1\sigma_2 L_1 L_2\frac{\partial^2\widehat{P}}{\partial L_1\partial L_2} + \frac{1}{2}\sigma_2^2 L_2\frac{\partial^2\bar{P}}{\partial L_2^2} \\ &\quad + \Big[\kappa_1\big(\ln\widetilde{\theta}_1(t) - \ln L_1\big) + \rho_{1r}\sigma_1\sigma_r b(t)\Big] L_1\frac{\partial\widehat{P}}{\partial L_1} \\ &\quad + \Big[\kappa_2\big(\ln\widetilde{\theta}_2(t) + \ln L_2\big) + \rho_{2r}\sigma_2\sigma_r b(t)\Big] L_2\frac{\partial\widehat{P}}{\partial L_2}, \end{aligned} \tag{7.11}$$

subject to the boundary conditions

$$\widehat{P}(L_1, L_2, T) = 1, \tag{7.12}$$

$$\widehat{P}(\widehat{L}_1, L_2, t) = 0, \tag{7.13}$$

$$\widehat{P}(L_1, \widehat{L}_2, t) = 0. \tag{7.14}$$

Note that the function $b(t)$ is still given by (3.81).

Next, we make the change of variables to the volatility adjusted log-leverage ratios as defined in (3.83) and transform $\widehat{P}(\widehat{L}_1 e^{\sigma_1 X_1}, \widehat{L}_2 e^{\sigma_2 X_2}, t)$ to $\bar{P}(X_1, X_2, \tau)$ with time-to-maturity variable $\tau = T - t$. The partial differential equation (7.11) thus transforms to

$$\begin{aligned} \frac{\partial\bar{P}}{\partial\tau} &= \frac{1}{2}\frac{\partial^2\bar{P}}{\partial X_1^2} + \rho_{12}\frac{\partial^2\bar{P}}{\partial X_1\partial X_2} + \frac{1}{2}\frac{\partial^2\bar{P}}{\partial X_2^2} + \big(\bar{\gamma}_1(\tau) - \kappa_1 X_1\big)\frac{\partial\bar{P}}{\partial X_1} \\ &\quad + \big(\bar{\gamma}_2(\tau) - \kappa_2 X_2\big)\frac{\partial\bar{P}}{\partial X_2}, \end{aligned} \tag{7.15}$$

for $\tau \in (0, T)$, $X_1 \in (-\infty, 0)$, $X_2 \in (-\infty, 0)$ and subject to the boundary conditions

$$\bar{P}(X_1, X_2, 0) = 1, \tag{7.16}$$

$$\bar{P}(0, X_2, \tau) = 0, \tag{7.17}$$

$$\bar{P}(X_1, 0, \tau) = 0. \tag{7.18}$$

The drift coefficients $\bar{\gamma}_i(\tau)$ appearing in the partial differential equation (7.15) are defined as

$$\bar{\gamma}_i(\tau) = \Big[\kappa_i\big(\ln\widetilde{\theta}_i(T-\tau) + \ln\widehat{L}_i - \sigma_i^2/(2\kappa_i)\big) + \rho_{ir}\sigma_i\sigma_r b(T-\tau)\Big]/\sigma_i,\ (i = 1, 2). \tag{7.19}$$

7.2. Solution of the CLN Partial Differential Equation by the Method of Images

This section seeks to extend the method of images approach developed in Chapter 4 to the solution of the partial different equation (7.15), subject to the zero boundary conditions (7.17)-(7.17). We point out that through the definition of the $\bar{\gamma}_i(\tau)$ in (7.19) we are dealing with the case of time varying coefficients. Just as with the method of images for the time varying coefficients case in Section 4.3, we proceed to solve the problem for the case of mean reversion via the transformation to the two-dimensional heat equation.

We write the integral form of the solution to (7.15) as

$$\bar{P}(X_1, X_2, \tau) = \int_{-\infty}^{0} \int_{-\infty}^{0} \bar{f}(X_1, X_2, Y_1, Y_2; \tau) \bar{P}(Y_1, Y_2) dY_1 dY_2, \tag{7.20}$$

where $\bar{f}(X_1, X_2, Y_1, Y_2; \tau)$ is the transition probability density function for transition from the values $X_1(0) = Y_1$ and $X_1(0) = Y_2$ at time-to-maturity $\tau = 0$ below the barriers and to the value X_1 and X_2 at time-to-maturity τ within the region $X_1 \in (-\infty, 0)$ and $X_2 \in (-\infty, 0)$. The initial condition function $\bar{P}(X_1, X_2, 0) \equiv \bar{P}(Y_1, Y_2)$ is given in (7.16).

We note that the partial differential equation (7.15) has drift terms that depend on variables X_1 and X_2, and this can be eliminated by carrying out the transformation[1]

$$\bar{P}(X_1, X_2, \tau) \;=\; P^{\ddagger}(X_1 e^{-\kappa_1 \tau}, X_2 e^{-\kappa_2 \tau}, \tau), \tag{7.21}$$

where $P^{\ddagger}(X_1, X_2, \tau)$ satisfies the partial differential equation

$$\begin{aligned} \frac{\partial P^{\ddagger}}{\partial \tau} \;=\; & \frac{1}{2} e^{-2\kappa_1 \tau} \frac{\partial^2 P^{\ddagger}}{\partial X_1^2} + \rho_{12} e^{-(\kappa_1 + \kappa_2)\tau} \frac{\partial^2 P^{\ddagger}}{\partial X_1 \partial X_2} + \frac{1}{2} e^{-2\kappa_2 \tau} \frac{\partial^2 P^{\ddagger}}{\partial X_2^2} \\ & + \bar{\gamma}_1(\tau) e^{-\kappa_1 \tau} \frac{\partial P^{\ddagger}}{\partial X_1} + \bar{\gamma}_2(\tau) e^{-\kappa_2 \tau} \frac{\partial P^{\ddagger}}{\partial X_2}. \end{aligned} \tag{7.22}$$

[1] A proof can be found in Appendix J.

Substituting the relation (7.21) into the initial condition and boundary conditions (7.16)-(7.18) yields the initial condition and boundary conditions for $P^{\ddagger}$ which are[2]

$$P^{\ddagger}(Y_1, Y_2) = 1, \tag{7.23}$$

$$P^{\ddagger}(0, X_2 e^{-\kappa_2 \tau}, \tau) = 0, \tag{7.24}$$

$$P^{\ddagger}(X_1 e^{-\kappa_1 \tau}, 0, \tau) = 0. \tag{7.25}$$

Note that the partial differential equation (7.22) has time-dependent coefficients. In Section 3.2, we pointed out that the solution to the heat equation obtained by the method of images approach for solving the zero boundary condition cannot be applied directly in the case where drift terms are time-dependent. Therefore, we apply in the current situation the time varying barrier approach in a similar way to Section 3.2 and Section 4.3. However, here we find that the method of images approach is only applicable to solving the partial differential equation (7.22) when the speed of mean reversion parameters are identical[3]. Therefore we assume that

$$\kappa_1 = \kappa_2 \equiv \kappa, \tag{7.27}$$

so that the partial differential equation (7.22) becomes

$$\begin{aligned} \frac{\partial P^{\ddagger}}{\partial \tau} &= \frac{1}{2} e^{-2\kappa\tau} \frac{\partial^2 P^{\ddagger}}{\partial X_1^2} + \rho_{12} e^{-2\kappa\tau} \frac{\partial^2 P^{\ddagger}}{\partial X_1 \partial X_2} + \frac{1}{2} e^{-2\kappa\tau} \frac{\partial^2 P^{\ddagger}}{\partial X_2^2} \\ &\quad + \bar{\gamma}_1(\tau) e^{-\kappa\tau} \frac{\partial P^{\ddagger}}{\partial X_1} + \bar{\gamma}_2(\tau) e^{-\kappa\tau} \frac{\partial P^{\ddagger}}{\partial X_2}. \end{aligned} \tag{7.28}$$

---

[2]We note that when $\tau = 0$, the initial condition becomes

$$\bar{P}(Y_1, Y_2) = 1 = P^{\ddagger}(Y_1 e^{-\kappa_1 \cdot 0}, Y_2 e^{-\kappa_2 \cdot 0}) = P^{\ddagger}(Y_1, Y_2).$$

The boundary conditions

$$\bar{P}(0, X_2, \tau) = 0 = P^{\ddagger}(0 \cdot e^{-\kappa_1 \tau}, X_2 e^{-\kappa_2 \tau}, \tau) = P^{\ddagger}(0, X_2 e^{-\kappa_2 \tau}, \tau),$$
$$\bar{P}(X_1, 0, \tau) = 0 = P^{\ddagger}(X_1 e^{-\kappa_1 \tau}, 0 \cdot e^{-\kappa_2 \tau}, \tau) = P^{\ddagger}(X_1 e^{-\kappa_1 \tau}, 0, \tau).$$

[3]To show this, we apply the result of Lo & Hui (2002), who use the solution of a European call option depending on multi-assets with time varying coefficients, to obtain the transition probability density function for equation (7.22), which is

$$\begin{aligned} &\frac{e^{\tau(\kappa_1+\kappa_2)}}{2\pi\sqrt{(1-\rho_{12}^2)}} \exp\Big\{ -\frac{1}{2}\Big[\frac{e^{2\kappa_1\tau}}{1-\rho_{12}} (X_1 + d_1(\tau) - Y_1)^2 + \frac{e^{2\kappa_2\tau}}{1-\rho_{12}} (X_2 + d_2(\tau) - Y_2)^2 \\ &-2\rho_{12} \frac{e^{(\kappa_1+\kappa_2)\tau}}{1-\rho_{12}} (X_1 + d_1(\tau) - Y_1)(X_2 + d_2(\tau) - Y_2) \Big] \Big\}, \end{aligned} \tag{7.26}$$

for $d_i = \int_0^\tau \bar{\gamma}_i(v)$.
In order to apply the solution $\widetilde{g}$ obtained by the method of images in (4.25), it is necessary to reduce the above density function to the form of the density g given in (4.3). Straight forward calculations reveal that this can only be done by assuming $\kappa_1 = \kappa_2 = \kappa$.

As discussed in Section 3.2 and Section 4.3 when coefficients are time-dependent, the solution for the heat equation obtained by the method of images approach to handle the zero boundary condition cannot be applied directly. This is due to the fact that the zero boundary condition of the function in which we are interested, after being transformed to the heat equation, is no longer at zero, see for example (3.43). A way to solve this problem is to set the zero boundary condition at a time varying barrier, which depends on a free parameter β as in Section 3.2. The parameter β is chosen so as to minimize the deviation between the time varying barrier and the exact barrier. Therefore, the solution depends on β and will be an approximation to the exact solution. Here, we extend the approach outlined in Section 4.3 to obtain an approximate solution for the partial differential equation (7.28).

Denote by $P^{\ddagger}_{\boldsymbol{\beta}}$ the approximation to the exact solution $P^{\ddagger}$ of the partial differential equation (7.28). The quantity $P^{\ddagger}_{\boldsymbol{\beta}}$ also satisfies the same partial differential equation, that is

$$\begin{aligned}\frac{\partial P^{\ddagger}_{\boldsymbol{\beta}}}{\partial \tau} &= \frac{1}{2}e^{-2\kappa\tau}\frac{\partial^2 P^{\ddagger}_{\boldsymbol{\beta}}}{\partial X_1^2} + \rho_{12}e^{-2\kappa\tau}\frac{\partial^2 P^{\ddagger}_{\boldsymbol{\beta}}}{\partial X_1 \partial X_2} + \frac{1}{2}e^{-2\kappa\tau}\frac{\partial^2 P^{\ddagger}_{\boldsymbol{\beta}}}{\partial X_2^2} \\ &\quad + \bar{\gamma}_1(\tau)e^{-\kappa\tau}\frac{\partial P^{\ddagger}_{\boldsymbol{\beta}}}{\partial X_1} + \bar{\gamma}_2(\tau)e^{-\kappa\tau}\frac{\partial P^{\ddagger}_{\boldsymbol{\beta}}}{\partial X_2}. \end{aligned} \tag{7.29}$$

However the zero boundary conditions of the approximate solution $P^{\ddagger}_{\boldsymbol{\beta}}$ are not the same as for the exact solution $P^{\ddagger}$ at $X_1 = 0$ and $X_2 = 0$ (as shown in (7.24) and (7.25)), but rather

$$P^{\ddagger}_{\boldsymbol{\beta}}(X_1^*(\tau), X_2, \tau) = 0, \tag{7.30}$$

$$P^{\ddagger}_{\boldsymbol{\beta}}(X_1, X_2^*(\tau), \tau) = 0, \tag{7.31}$$

where $X_1^*(\tau)$ and $X_2^*(\tau)$ are time varying barriers close to the X_1-axis and X_2-axis respectively.

Now, X_1 and X_2 are restricted to the region $X_1 \in (-\infty, X_1^*(\tau))$ and $X_2 \in (-\infty, X_2^*(\tau))$. We apply the same procedures used in Section 4.3 in this case, and we find that the dynamic forms of the time varying barriers are

$$X_i^*(\tau) = -\int_0^\tau \bar{\gamma}_i(v)e^{-\kappa v}dv - \beta_i \int_0^\tau e^{-2\kappa v}dv, \ (i = 1, 2). \tag{7.32}$$

The coefficients $\bar{\gamma}_i(\tau)$ are given in (7.19), and β_1 and β_2 are the adjustable parameters to be chosen in some "optimal" sense to control the shape of the time varying barriers $X_1^*(\tau)$ and $X_2^*(\tau)$ so that they remain as close as possible to the exact barriers $X_1 = 0$ and $X_2 = 0$, respectively. Note that the initial condition of the approximate solution $P^{\ddagger}_{\boldsymbol{\beta}}$ is the same as for the exact solution $P^{\ddagger}$ in

(7.23), that is

$$P^{\ddagger}_{\boldsymbol{\beta}}(X_1, X_2, 0) = 1. \tag{7.33}$$

The solution to the partial differential equation (7.29) can be written as

$$P^{\ddagger}_{\boldsymbol{\beta}}(X_1, X_2, \tau) = \int_{-\infty}^{0}\int_{-\infty}^{0} f^{\ddagger}_{\boldsymbol{\beta}}(X_1, X_2, Y_1, Y_2; \tau) P^{\ddagger}_{\boldsymbol{\beta}}(Y_1, Y_2) dY_1 dY_2. \tag{7.34}$$

To obtain the form of the joint transition probability density function $f^{\ddagger}_{\beta}$, which in the density function of the stochastic process restricted to $(-\infty, X_1^*(\tau)) \times (-\infty, X_2^*(\tau))$, in terms to the bivariate density functions $\widetilde{g}$ in (4.25), we transform the partial differential equation (7.29) for $\bar{P}^{\ddagger}_{\boldsymbol{\beta}}$ to the heat equation by setting[4]

$$\begin{aligned} P^{\ddagger}_{\boldsymbol{\beta}}(X_1, X_2, \tau) &= e^{-X_1^*(\tau)\frac{\partial}{\partial X_1} - X_2^*(\tau)\frac{\partial}{\partial X_2}} \left[e^{\eta_1 X_1 + \eta_2 X_2 + \xi\zeta}\widetilde{u}(X_1, X_2, \zeta)\right], & (7.35)\\ &= e^{\eta_1[X_1 - X_1^*(\tau)] + \eta_2[X_2 - X_2^*(\tau)] + \xi\zeta}\widetilde{u}(X_1 - X_1^*(\tau), X_2 - X_2^*(\tau), \zeta), & (7.36) \end{aligned}$$

where

$$\zeta = \int_0^{\tau} e^{-2\kappa v} dv, \tag{7.37}$$

and $\widetilde{u}(X_1, X_2, \zeta)$ satisfies the heat equation (4.1) (with τ related by ζ and x_1, x_2 by X_1, X_2). The constants η_1, η_2 and ξ are derived in Appendix L and given in (4.52)-(4.54).

Substitution of the zero boundary conditions (7.30) and (7.31) into the relation (7.36) yields the boundary conditions for $\widetilde{u}$ as[5]

$$\widetilde{u}(0, X_2 - X_2^*(\tau), \zeta) = 0, \tag{7.38}$$

$$\widetilde{u}(X_1 - X_1^*(\tau), 0, \zeta) = 0. \tag{7.39}$$

We note that the zero boundary conditions (7.38)-(7.39) for $\widetilde{u}$ is same as the zero boundary conditions (4.4)-(4.5) for u. Therefore the solution for the density function $\widetilde{g}$ in (4.25) subject to the zero boundary conditions obtained by the method of images, can now be applied to obtain the approximate solution $P^{\ddagger}_{\boldsymbol{\beta}}$. Substituting the initial condition (7.33) with $X_1(0) = Y_1$ and $X_2(0) = Y_2$

[4] A derivation can be found in Appendix L.

[5] We note that

$$P^{\ddagger}_{\boldsymbol{\beta}}(X_1^*(\tau), X_2, \tau) = 0 = e^{\eta_1 \cdot 0 + \eta_2[X_2 - X_2^*(\tau)] + \xi\zeta}\widetilde{u}(0, X_2 - X_2^*(\tau), \zeta),$$
$$P^{\ddagger}_{\boldsymbol{\beta}}(X_1, X_2^*(\tau), \tau) = 0 = e^{\eta_1[X_1 - X_1^*(\tau)] + \eta_2 \cdot 0 + \xi\zeta}\widetilde{u}(X_1 - X_1^*(\tau), 0, \zeta).$$

into the relation (7.36) determines the initial condition of u, which is given by

$$P^{\ddagger}_{\boldsymbol{\beta}}(Y_1, Y_2) = 1 = e^{\eta_1 Y_1 + \eta_2 Y_2}\widetilde{u}(Y_1, Y_2), \tag{7.40}$$

so that

$$\widetilde{u}(Y_1, Y_2) = e^{-\eta_1 Y_1 - \eta_2 Y_2}. \tag{7.41}$$

Substituting the initial condition (7.41) and the relation (7.36) into (4.6), yields

$$\begin{aligned} &e^{-\eta_1[X_1 - X_1^*(\tau)] - \eta_2[X_2 - X_2^*(\tau)] - \xi\zeta} P^{\ddagger}_{\boldsymbol{\beta}}(X_1, X_2, \tau) \\ &\quad = \int_{-\infty}^{0}\int_{-\infty}^{0} \widetilde{g}(X_1 - X_1^*(\tau), X_2 - X_2^*(\tau), Y_1, Y_2; \zeta) e^{-\eta_1 Y_1 - \eta_2 Y_2} P^{\ddagger}_{\boldsymbol{\beta}}(Y_1, Y_2) dY_1 dY_2, \end{aligned} \tag{7.42}$$

where the density function $\widetilde{g}$ is obtained by the method of images illustrated in Section 4.1 and is given by (4.25). Equation (7.42) can be simplified to

$$\begin{aligned} P^{\ddagger}_{\boldsymbol{\beta}}(X_1, X_2, \tau) \;=\; & \int_{-\infty}^{0}\int_{-\infty}^{0} e^{\eta_1[X_1 - X_1^*(\tau) - Y_1] + \eta_2[X_2 - X_2^*(\tau) - Y_2] + \xi\zeta} \times \\ & \widetilde{g}(X_1 - X_1^*(\tau), X_2 - X_2^*(\tau), Y_1, Y_2; \zeta) P^{\ddagger}_{\boldsymbol{\beta}}(Y_1, Y_2) dY_1 dY_2. \end{aligned} \tag{7.43}$$

Therefore, the expression for the approximate solution for the $P^{\ddagger}_{\boldsymbol{\beta}}$ is obtained. A comparison of the two equations (7.34) and (7.43), yields the result that

$$\begin{aligned} f^{\ddagger}_{\beta}(X_1, X_2, Y_1, Y_2; \tau) \;=\; & e^{\eta_1[X_1 - X_1^*(\tau) - Y_1] + \eta_2[X_2 - X_2^*(\tau) - Y_2] + \xi\zeta} \times \\ & \widetilde{g}(X_1 - X_1^*(\tau), X_2 - X_2^*(\tau), Y_1, Y_2; \zeta). \end{aligned} \tag{7.44}$$

Next, we work back through the transformation (7.21) (applied to the $\bar{P}_{\boldsymbol{\beta}}$ function) to obtain the solution for the original problem, the risk ratio function $\bar{P}$. Since $P^{\ddagger}_{\boldsymbol{\beta}}$ is an approximate solution, so also is the expression obtained for $\bar{P}$. Thus, let $\bar{P}_{\boldsymbol{\beta}}$ denote the approximate solution to $\bar{P}$, and the approximate solution to (7.20) therefore can be written as

$$\bar{P}_{\boldsymbol{\beta}}(X_1, X_2, \tau) = \int_{-\infty}^{0}\int_{-\infty}^{0} \bar{f}_{\boldsymbol{\beta}}(X_1, X_2, Y_1, Y_2; \tau) \bar{P}_{\boldsymbol{\beta}}(Y_1, Y_2) dY_1 dY_2. \tag{7.45}$$

Substituting the relation (7.21) into the solution (7.43) with the assumption (7.27), yields the approximate solution $\bar{P}_{\boldsymbol{\beta}}$, namely

$$\begin{aligned} \bar{P}_{\boldsymbol{\beta}}(X_1, X_2, \tau) \;=\; & \int_{-\infty}^{0}\int_{-\infty}^{0} e^{\eta_1[X_1 e^{-\kappa\tau} - X_1^*(\tau) - Y_1] + \eta_2[X_2 e^{-\kappa\tau} - X_2^*(\tau) - Y_2] + \xi\zeta} \times \\ & \widetilde{g}(X_1 e^{-\kappa\tau} - X_1^*(\tau), X_2 e^{-\kappa\tau} - X_2^*(\tau), Y_1, Y_2; \zeta) \bar{P}_{\boldsymbol{\beta}}(Y_1, Y_2) dY_1 dY_2, \end{aligned} \tag{7.46}$$

where the initial condition for the approximate solution $\bar{P}_{\boldsymbol{\beta}}(Y_1, Y_2)$ is the same as for the exact solution $\bar{P}$ and equal to 1. By setting $\tau = 0$ in equation (7.21) the initial condition transforms as $\bar{P}_{\boldsymbol{\beta}}(Y_1, Y_2) = 1 = P^{\ddagger}_{\boldsymbol{\beta}}(Y_1, Y_2)$.

Substituting the solution for the density function $\widetilde{g}$ from (4.25) into (7.46), we obtained the approximate solution for the risk ratio function as

$$\begin{aligned}\bar{P}_{\boldsymbol{\beta}}(X_1, X_2, \tau) &= \int_{-\infty}^{0}\int_{-\infty}^{0} e^{\eta_1[X_1 e^{-\kappa\tau} - X_1^*(\tau) - Y_1] + \eta_2[X_2 e^{-\kappa\tau} - X_2^*(\tau) - Y_2] + \xi\zeta} \times \\ &\quad \Big[g(X_1 e^{-\kappa\tau} - X_1^*(\tau), X_2 e^{-\kappa\tau} - X_2^*(\tau), Y_1, Y_2; \zeta) \\ &\quad + \sum_{k=1}^{m} (-1)^k g^k(X_1 e^{-\kappa\tau} - X_1^*(\tau), X_2 e^{-\kappa\tau} - X_2^*(\tau), Y_1^k, Y_2^k; \zeta)\Big] \times \\ &\quad \bar{P}_{\boldsymbol{\beta}}(Y_1, Y_2) dY_1 dY_2. \end{aligned} \tag{7.47}$$

Comparing equations (7.45) and (7.47), we obtain for the transition density function appearing in (7.45) the expression

$$\begin{aligned}&\bar{f}_{\boldsymbol{\beta}}(X_1, X_2, Y_1, Y_2; \tau) \\ &\quad = e^{\eta_1[X_1 e^{-\kappa\tau} - X_1^*(\tau) - Y_1] + \eta_2[X_2 e^{-\kappa\tau} - X_2^*(\tau) - Y_2] + \xi\zeta} \times \\ &\qquad \Big[g(X_1 e^{-\kappa\tau} - X_1^*(\tau), X_2 e^{-\kappa\tau} - X_2^*(\tau), Y_1, Y_2; \zeta) \\ &\qquad + \sum_{k=1}^{m} (-1)^k g^k(X_1 e^{-\kappa\tau} - X_1^*(\tau), X_2 e^{-\kappa\tau} - X_2^*(\tau), Y_1^k, Y_2^k; \zeta)\Big]. \end{aligned} \tag{7.48}$$

Using a similar argument to that used in Subsection 3.1.2, the probability of any path with barriers at zero, initiating below the barriers $X_1 < 0$ and $X_2 < 0$ at time $t_0 = 0$ and ending up in the region $X_1 \in (-\infty, 0)$ and $X_2 \in (-\infty, 0)$ at the later time t in the period of time $\tau = t - t_0$, is approximated by

$$F_{\boldsymbol{\beta}}(X_1, X_2, t) = \int_{-\infty}^{0}\int_{-\infty}^{0} \bar{f}_{\boldsymbol{\beta}}(X_1, X_2, Y_1, Y_2; t) dY_1 dY_2. \tag{7.49}$$

The cumulative probability $F_{\boldsymbol{\beta}}(X_1, X_2, \tau)$ can be interpreted as the joint survival probability that the absorption at $X_1 = 0$ and $X_2 = 0$ has not yet occurred during the period of time τ.

Note that the approximate solutions $\bar{P}_{\boldsymbol{\beta}}$ and $F_{\boldsymbol{\beta}}$ obtained by the method of images approach are only valid for the values of ρ_{12} given in Table 4.1 and for $\kappa_1 = \kappa_2 = \kappa$.

7.3. Numerical Implementation for the Case of Mean-Reversion

In a similar way to Section 4.4, we can express the solution derived in Section 7.1 in terms of the bivariate normal distribution function $N_2(.)$.

Consider the approximate solution for the joint survival probability (7.49), after some algebraic manipulations, it can be simplified to

$$\begin{aligned} & F_{\boldsymbol{\beta}}(X_1, X_2, \tau) \\ &= \int_{-\infty}^{0}\int_{-\infty}^{0} g(X_1 e^{-\kappa\tau} + d_1(\tau), X_2 e^{-\kappa\tau} + d_2(\tau), Y_1, Y_2; \zeta) dY_1 dY_2 \\ &\quad + \sum_{k=1}^{m} (-1)^k \int_{-\infty}^{0}\int_{-\infty}^{0} \times \\ &\quad g^k(X_1 e^{-\kappa\tau} + d_1(\tau), X_2 e^{-\kappa\tau} + d_2(\tau), (a_1^k Y_1 + b_1^k Y_2), (a_2^k Y_1 + b_2^k Y_2); \zeta) \\ &\quad e^{\beta_a^k Y_1 + \beta_b^k Y_2} dY_1 dY_2, \end{aligned} \tag{7.50}$$

where

$$d_i(\tau) = \int_0^{\tau} \bar{\gamma}_i(v) e^{-\kappa v} dv. \tag{7.51}$$

The Y_1^k and Y_2^k are replaced by the relations given in (4.74) and (4.75), the a^k's and b^k's are given in (4.76)-(4.77), and β_a^k and β_b^k are defined in (4.83)-(4.84).

Following similar procedures and carrying out the change of variables shown in Appendix I, the first integral in (7.50) can be written in terms of the $N_2(.)$ as

$$\sqrt{\frac{(1-\rho_{12}^2)}{AB(1-\widetilde{\rho}^2)}}\ \exp\left(-\frac{\widetilde{h}}{2\zeta(1-\rho_{12}^2)}\right) \times N_2(\widetilde{a}, \widetilde{b}, \widetilde{\rho}). \tag{7.52}$$

where

$$\widetilde{\rho} = -\frac{E}{2\sqrt{AB}}, \tag{7.53}$$

$$\widetilde{a} = \sqrt{2(1-\widetilde{\rho}^2)}\,\widetilde{u}_1 = \sqrt{\frac{A}{\zeta}}\left(\frac{C}{2A} - \frac{Eh_2}{4Ah_1}\right)\sqrt{\frac{1-\widetilde{\rho}^2}{1-\rho_{12}^2}}, \tag{7.54}$$

$$\widetilde{b} = \sqrt{2(1-\widetilde{\rho}^2)}\,\widetilde{v}_1 = \frac{1}{\sqrt{\zeta}}\sqrt{1 + \frac{E^2}{4Ah_1}}\,\frac{h_2}{2\sqrt{h_1}}\sqrt{\frac{1-\widetilde{\rho}^2}{1-\rho_{12}^2}}, \tag{7.55}$$

and

$$h_1 = B - \frac{E^2}{4A},\ h_2 = D - \frac{CE}{2A},\ \widetilde{h} = H - \frac{C^2}{4A} - \frac{h_2^2}{4h_1}, \tag{7.56}$$

with

$$\begin{aligned} A &= 1,\ B = 1, \\ C &= 2(-\mathbb{X}_1 + \rho_{12}\mathbb{X}_2),\ D = 2(-\mathbb{X}_2 + \rho_{12}\mathbb{X}_1), \\ E &= -2\rho_{12},\ H = \mathbb{X}_1^2 + \mathbb{X}_2^2 - 2\rho_{12}\mathbb{X}_1\mathbb{X}_2. \end{aligned} \tag{7.57}$$

Here $\mathbb{X}_i = X_i e^{-\kappa\tau} + d_i(\tau)$ for $i = 1, 2$.

Similarly, the second integral (7.50) can be expressed in terms of $N_2(.)$ as

$$\sum_{n=1}^{m}(-1)^k \sqrt{\frac{(1-\rho_{12}^2)}{A_k B_k(1-\widetilde{\rho}_k^2)}}\ \exp\left(-\frac{\widetilde{h}_k}{2\zeta(1-\rho_{12}^2)}\right) \times N_2\big(\widetilde{a}_k, \widetilde{b}_k, \widetilde{\rho}_k\big). \tag{7.58}$$

The expressions for $\widetilde{\rho}_k$, $\widetilde{a}_k$, $\widetilde{b}_k$ and $\widetilde{h}_k$ are same as in (7.53)-(7.56) after replacing A_k, B_k, C_k, D_k and E_k with

$$\begin{aligned} A_k &= (a_1^k)^2 + (a_2^k)^2 - 2\rho_{12}a_1^k a_2^k\ , \\ B_k &= (b_1^k)^2 + (b_2^k)^2 - 2\rho_{12}b_1^k b_2^k\ , \\ C_k &= 2\mathbb{X}_1(\rho_{12}a_2^k - a_1^k) + 2\mathbb{X}_2(\rho_{12}a_1^k - a_2^k) - \zeta\beta_a^k\ , \\ D_k &= 2\mathbb{X}_1(\rho_{12}b_2^k - b_1^k) + 2\mathbb{X}_2(\rho_{12}b_1^k - b_2^k) - \zeta\beta_b^k\ , \\ E_k &= 2(a_1^k b_1^k + a_2^k b_2^k - \rho_{12}b_1^k a_2^k - \rho_{12}a_1^k b_2^k)\ . \end{aligned} \tag{7.59}$$

The approximate solution is in an analytical form, however, it only works for identical values of the mean-reverting speed parameters (see the assumption in (7.27)). We also stress that the approximate solution obtained by the method of images approach in only valid for the values of correlation coefficient ρ_{12} given in Table 4.1. Hence this solution can only be used as a benchmark and numerical methods are needed for the case of general values of correlation ρ_{12} as well as the case that $\kappa_1 \neq \kappa_2$[6]. The alternating direction implicit schemes developed in Section 5.1 can be extended to cover this problem. However, the main drawback is lack of knowledge of the stability conditions of the Douglas-Rachford scheme when the drift coefficients of the partial differential equation (7.15) depend on the spatial variables X_1, X_2. So, in order to study the impact on default

[6]The use of identical values of the speed of mean-reversion and the selected values of the correlation coefficient in this chapter is purely a technical requirement, so that the analytical solutions can be derived. It does not seem possible to give any economic interpretation to these requirements.

correlations with leverage ratios following mean-revering processes, the Monte Carlo scheme that was developed in Section 5.2 can be extended to cover in this case, to which we turn next.

7.4. A Monte Carlo Simulation Scheme

In this section we will develop a Monte Carlo scheme to simulate the joint survival probability function when the leverage ratios are mean-reverting as well as providing a numerical solution in all situations of interest it will also serve as a benchmark for the approximate solution obtained by the method of images. Recall the partial differential equation for the risk ratio function (7.11) derived in the previous section, applying the Feynman-Kac theorem, the stochastic differential equations corresponding to equation (7.11) are

$$dL_1 = \Big[\kappa_1\big(\ln\widetilde{\theta}_1(t) - \ln L_1\big) + \rho_{1r}\sigma_1\sigma_r b(t)\Big] L_1 dt + \sigma_1 L_1 d\widetilde{Z}_1, \tag{7.60}$$

$$dL_2 = \Big[\kappa_2\big(\ln\widetilde{\theta}_2(t) - \ln L_2\big) + \rho_{2r}\sigma_2\sigma_r b(t)\Big] L_2 dt + \sigma_2 L_2 d\widetilde{Z}_2, \tag{7.61}$$

where $\widetilde{Z}_1$ and $\widetilde{Z}_2$ are Wiener processes under the risk-neutral measure $\widetilde{\mathbb{P}}$. The Wiener increments $d\widetilde{Z}_1$ and $d\widetilde{Z}_2$ are correlated with $\widetilde{\mathbb{E}}[d\widetilde{Z}_1 d\widetilde{Z}_2] = \rho_{12}dt$.

We can also rewrite (7.60) and (7.61) in terms of uncorrelated Wiener processes W_1, W_2, and change the variables to the log-leverage ratios as defined in (3.82), then we have

$$dx_1 = \left[\kappa_1\big(\ln\widetilde{\theta}_1(t) - \ln\widehat{L}_1 - x_1\big) - \frac{1}{2}\sigma_1^2 + \rho_{1r}\sigma_1\sigma_r b(t)\right] dt + \sigma_1 dW_1, \tag{7.62}$$

$$dx_2 = \left[\kappa_2\big(\ln\widetilde{\theta}_2(t) - \ln\widehat{L}_2 - x_2\big) - \frac{1}{2}\sigma_2^2 + \rho_{2r}\sigma_2\sigma_r b(t)\right] dt + \sigma_2\big(\rho_{12}dW_1 + \sqrt{1-\rho_{12}^2}dW_2\big). \tag{7.63}$$

To simulate the system (7.62) and (7.63), we employ the Monte Carlo approach developed in Section 5.2, the only required change being to replace Step 2.2. with the following:-

Step 2.2*. In discrete time equations (7.62)-(7.63) become

$$\begin{aligned} x_1(t_j) &= x_1(t_{j-1}) + \Big[\kappa_1\big(\ln\widetilde{\theta}_1(t_{j-1}) - \ln\widehat{L}_1 - x_1(t_{j-1})\big) \\ &\quad -\frac{1}{2}\sigma_1^2 + \rho_{1r}\sigma_1\sigma_r b(t_{j-1})\Big]\Delta t + \sigma_1\sqrt{\Delta t}e_1, \end{aligned} \tag{7.64}$$

$$\begin{aligned} x_2(t_j) &= x_2(t_{j-1}) + \Big[\kappa_2\big(\ln\widetilde{\theta}_2(t_{j-1}) - \ln\widehat{L}_2 - x_2(t_{j-1})\big) \\ &\quad -\frac{1}{2}\sigma_2^2 + \rho_{2r}\sigma_2\sigma_r b(t_{j-1})\Big]\Delta t + \sigma_2\sqrt{\Delta t}\hat{e}_2, \end{aligned} \tag{7.65}$$

where $\hat{e}_2 = \rho_{12}e_1 + \sqrt{1-\rho_{12}^2}e_2$.

Time	Monte Carlo results n=36500 M=1x10^6	2-D MOI single-stage approx.	Relative % error
1	0.8281	0.8246	-0.4160
2	0.7357	0.7265	-1.2507
3	0.6885	0.6703	-2.6412
4	0.6587	0.6292	-4.4789
5	0.6375	0.5947	-6.7106
6	0.6209	0.5634	-9.2709
7	0.6077	0.5337	-12.1852
8	0.5965	0.5048	-15.3729
9	0.5869	0.4764	-18.8176
10	0.5783	0.4483	-22.4830
11	0.5708	0.4203	-26.3606
12	0.5641	0.3926	-30.4061
13	0.5579	0.3651	-34.5564
14	0.5520	0.3380	-38.7763
15	0.5465	0.3114	-43.0310

TABLE 7.1. Accuracy of the approximate solution (7.49) for the joint survival probabilities based on the numerical implementation developed in Section 7.3, which is a single-stage approximation (2-D MOI single-stage approx.) for the constant target ratios case, compared to the Monte Carlo results based on the scheme developed in Section 7.4. The constant target ratios take the values $\widetilde{\theta}_1 = \widetilde{\theta}_2 = 31.5\%$ and $\kappa = 0.1$. Other parameters used are $L_1 = 73.2\%$, $L_2 = 31.5\%$, $\sigma_1 = 0.299$, $\sigma_2 = 0.213$, $\widetilde{\mu}_1 = \widetilde{\mu}_2 = 0$, $\rho_{1r} = \rho_{2r} = 0$ and $\rho_{12} = 0$.

Using a total of M simulation paths, the joint survival probability is approximated by $\text{JSP}(t_j) = \sum_{m=1}^{M} \text{JSP}_m(t_j)/M$ with $t_j = j\Delta t$.

7.5. Accuracy

This section discusses the accuracy of the results obtained by the method of images in Section 7.1 and the Monte Carlo method in Section 7.4.

As discussed in Section 5.3, when the coefficients are time-dependent, the solution obtained by the method of images approach is not exact, but an approximate one obtained by using the time varying

Time	Monte Carlo results n=36500 M=1x10^6	2-D MOI single-stage approx.	Relative % error
1	0.7572	0.7561	-0.1404
2	0.6201	0.6174	-0.4402
3	0.5454	0.5406	-0.8857
4	0.4954	0.4876	-1.5898
5	0.4576	0.4463	-2.4725
6	0.4274	0.4121	-3.5737
7	0.4024	0.3827	-4.9061
8	0.3814	0.3568	-6.4281
9	0.3639	0.3338	-8.2615
10	0.3489	0.3131	-10.2497
11	0.3359	0.2943	-12.3995
12	0.3253	0.2771	-14.8189
13	0.3163	0.2613	-17.3934
14	0.3087	0.2467	-20.0836
15	0.3025	0.2332	-22.9255

TABLE 7.2. Accuracy of the approximate solution (7.49) for the joint survival probabilities based on the numerical implementation developed in Section 7.3, which is a single-stage approximation (2-D MOI single-stage approx.) for the time varying target ratios case, compared to the Monte Carlo results based on the scheme developed in Section 7.4. The time-dependent target ratios are based on equation (7.66) with $\widetilde{\theta}_i(0) = 73.2\%$ and $\widetilde{\theta}_i(15) = 31.5\%$. Other parameters used are $L_1 = 73.2\%$, $L_2 = 31.5\%$, $\sigma_1 = 0.299$, $\sigma_2 = 0.213$, $\widetilde{\mu}_1 = \widetilde{\mu}_2 = 0$, $\rho_{1r} = \rho_{2r} = 0$, $\rho_{12} = 0$ and $\kappa = 0.1$.

barrier approach (see Section 4.3). The drawback of the time varying barrier method is that the accuracy decreases as the time period is increased. Table 7.1 and Table 7.2 show that the relative percentage error compared to the Monte Carlo results is less than 1% for the first few years, but the relative percentage error increases rapidly with time from 1-2% at 4 and 5 years, to 23% at 15 years. This is due to the fact that the solution for the joint survival probability developed in Section 7.3 is based on the single-stage approximation. A way to deal with this problem is to develop the multi-stage approximation, which for the one-firm case has been discussed in Section 3.2. The idea is to reduce the deviation of the time varying barrier from the exact barrier by the multi-stage

approximation, so as to increases the accuracy of the method. Here, we are more interested in studying the impact of mean-reverting processes on default correlations, and this will do by use of the Monte Carlo simulation scheme. The analysis of Section 7.3 and the numerical results of this section have nevertheless indicated that the time varying barriers approach is a feasible one for developing benchmark solutions. However to bring it to the implementation stage it needs to be extended by the multistage approximation technique. This development is beyond the scope of this thesis but is a very fruitful avenue of future research.

7.6. The Impact of Mean-Reverting Processes for Leverage Ratios on JSP & DC

In this section, we discuss impact on joint survival probabilities and default correlations of firms having mean-reverting leverage ratios. For the one-firm mean-reverting leverage ratio structural models, Collin-Dufresne & Goldstein (2001) and Hui et al. (2006) are the most representative. These two models investigate the effect on credit spreads and default probabilities of a firm's leverage ratio following a mean-reverting process. Collin-Dufresne & Goldstein (2001) (CDG) consider the leverage ratio to be mean-reverting to a constant target ratio and they observe that this target ratio is close to the average level of BBB-rated firms. CDG show that credit spreads are larger for low credit quality firms, which is consistent with empirical findings. The major difference between the CDG model and that of Hui et al. (2006) is that the latter authors consider the leverage ratio to be mean-reverting to a time-dependent target ratio. They point out that the time-dependent target ratio reflects the movement of a firm's initial target ratio towards a long-term target ratio over time. Hui et al. (2006) show that their model results in default probabilities that are consistent with some empirical findings.

The major feature of both models is the mean-reversion of the leverage ratio to a constant target ratio and to a time-dependent target ratio. Therefore, in this section, we are interested in studying how these two features affect the joint survival probabilities and default correlations. We use CCC-CCC and CCC-BBB paired firms as an illustration. The constant values of $\widetilde{\theta}_i$ are set to 31.5% (which represents the average leverage ratio of BBB-rated firms), which imply that the target leverage ratios $[\ln \widetilde{\theta}_i(t) + \ln \widehat{L}_i - \sigma_i^2/(2\kappa_i)]$ are close to 36%, the long term leverage that was obtained in the empirical investigations of Collin-Dufresne & Goldstein (2001). For time-dependent $\widetilde{\theta}_i$, we follow the setting in Hui et al. (2006), who use the simple linear time-dependent function

$$\widetilde{\theta}_i(t) = \widetilde{\theta}_{i0}(1 - \eta t), \tag{7.66}$$

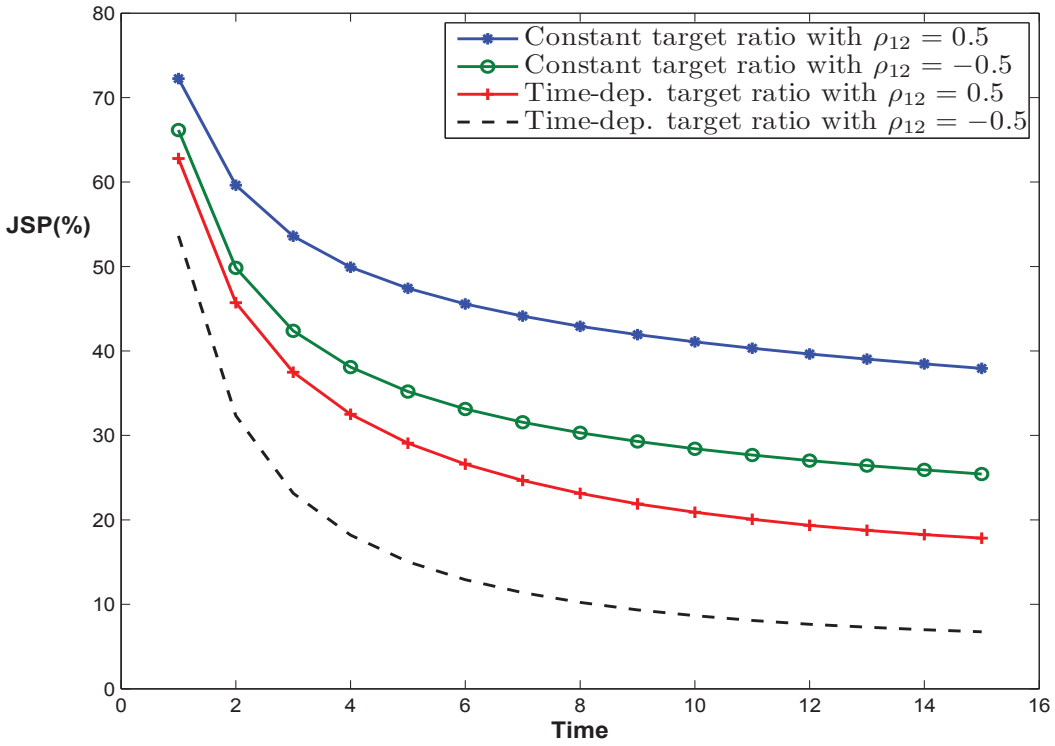

FIGURE 7.1. The impact of constant target ratios and time-dependent target ratios on joint survival probabilities for CCC-CCC paired firms. Initial leverage for the CCC-rated firm is $L_1 = L_2 = 73.2\%$ and the volatilities are $\sigma_1 = \sigma_2 = 0.299$. Other parameters used are $\rho_{1r} = \rho_{2r} = 0$ and $\rho_{12} = -0.5$ and $\rho_{12} = 0.5$. The constant target ratio is $\widetilde{\theta}_i = 31.5\%$ and the time-dependent target ratio is based on equation (7.66) with $\widetilde{\theta}_i(0) = 73.2\%$ and $\widetilde{\theta}_i(15) = 31.5\%$.

where $\widetilde{\theta}_{i0}$, η are constants and their values are chosen such that the initial value of the long term leverage is very high at a value for a CCC-rated firm, that is $\widetilde{\theta}_i(0) = 73.2\%$ and is close to the value of a BBB-rated firm towards the end of the time period, so that $\widetilde{\theta}_i(15) = 31.5\%$.

We continue to assume $\kappa_1 = \kappa_2 \equiv \kappa$, with the value $\kappa = 0.1$ that is used in Hui et al. (2006). Other parameters are based on those used in Subsection 6.1. The default barriers of the two-firms are set at $\widehat{L}_1 = \widehat{L}_2 = 1$ as previously. The leverage ratio levels and values of volatility used are given in Table 6.1. The time period considered is fifteen years as previously.

7.6.1. Joint Survival Probabilities.

Figures 7.1 and 7.2 plot the joint survival probability with constant and time-dependent target ratios for CCC-CCC and CCC-BBB paired firms, respectively. The use of constant target ratios represents the Collin-Dufresne & Goldstein (2001) model in the two-firm case, which generates joint survival probabilities higher than those obtained of using the time-dependent target ratio, a result which holds for both positive and negative correlation ρ_{12}. From Figure 7.2 the effect of the

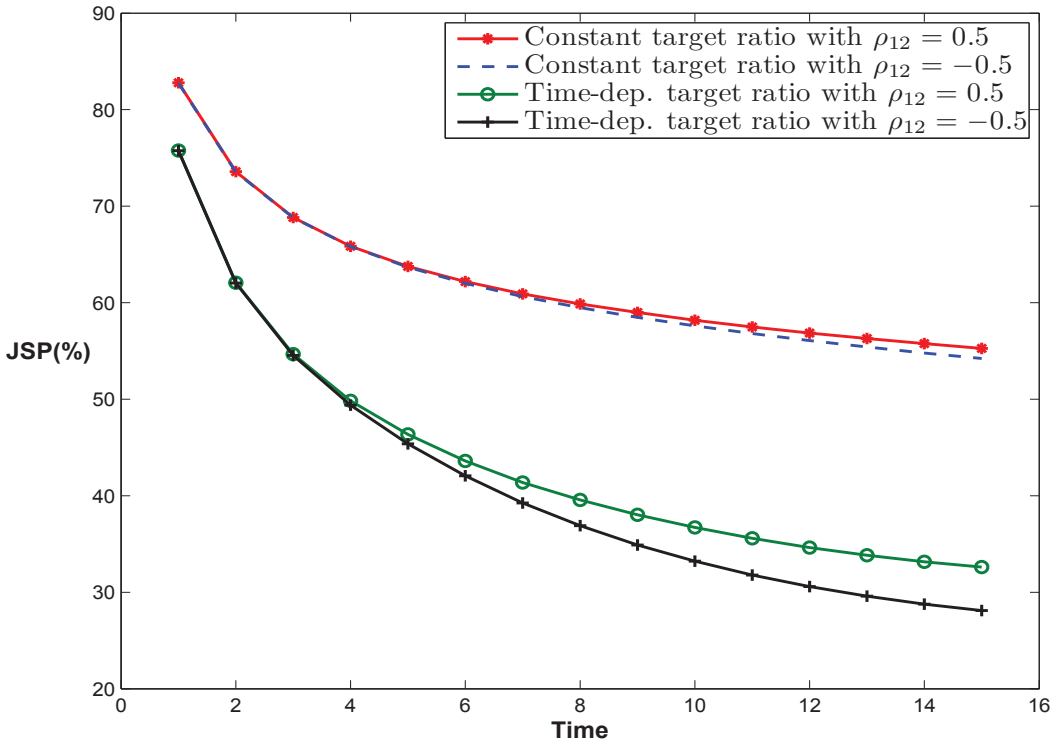

FIGURE 7.2. The impact of constant target ratios and time-dependent target ratios on joint survival probabilities for CCC-BBB paired firms. Initial leverage for the CCC-rated firm is L_1=73.2%, for the BBB-rated firm is L_2=31.5% and the volatilities are σ_1=0.299, σ_2 =0.213. Other parameters used are $\rho_{1r} = \rho_{2r} = 0$ and $\rho_{12} = -0.5$ and $\rho_{12} = 0.5$. The constant target ratio is $\widetilde{\theta}_i = 31.5\%$ and the time-dependent target ratio is based on equation (7.66) with $\widetilde{\theta}_i(0) = 73.2\%$ and $\widetilde{\theta}_i(15) = 31.5\%$.

correlation coefficient ρ_{12} is more pronounced for time varying target ratios and for lower credit quality paired firms (as can be seen when comparing Figure 7.1 to Figure 7.2).

7.6.2. Default Correlations.

Figures 7.3-7.4 graphs the defaults correlation with constant and time-dependent target ratios for CCC-CCC and CCC-BBB paired firms, respectively. Figure 7.3 shows that both models generate similar values of the default correlation in the case of CCC-CCC paired firms. When considering a pairing of a low rated firm with a higher rated firm, the use of constant target ratios generates smaller values of default correlations than the use of time-dependent target ratios, as indicated in Figure 7.4. We also observe that when firms are positively correlated ($\rho_{12} > 0$), both models generate similar default correlations, and when firms are negatively correlated ($\rho_{12} < 0$), the use of time-dependent target ratio generates larger values of default correlations (in absolute value).

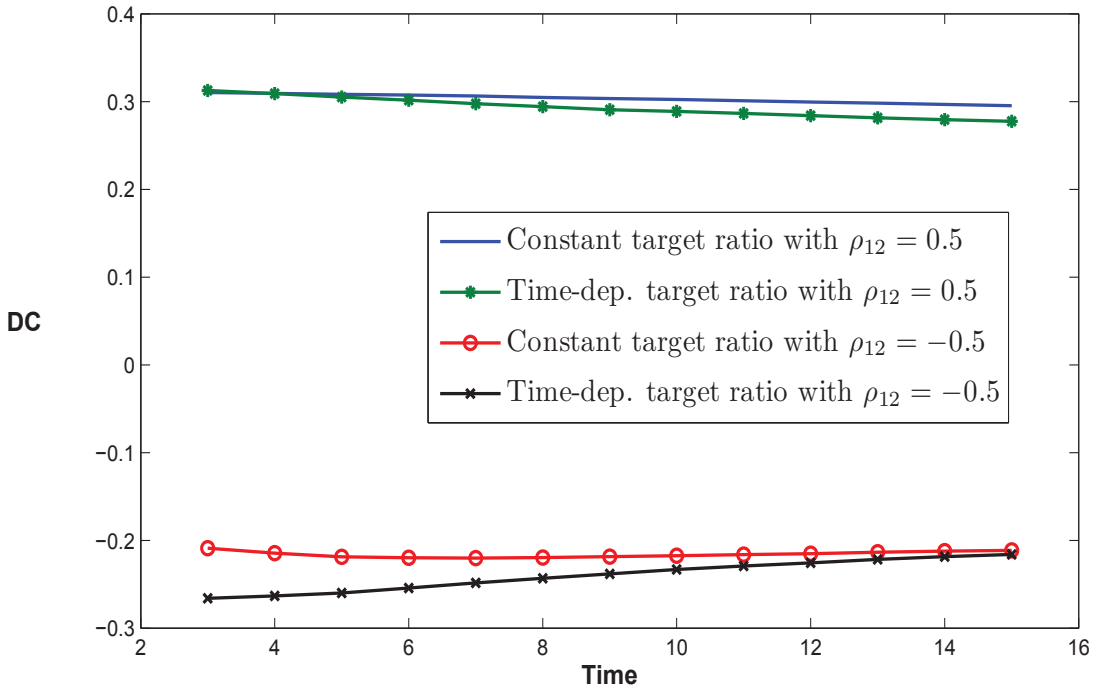

FIGURE 7.3. The impact of constant target ratios and time-dependent target ratios on default correlations for CCC-CCC paired firms. Initial leverage for the CCC-rated firm is $L_1 = L_2 = 73.2\%$ and the volatilities are $\sigma_1 = \sigma_2 = 0.299$. Other parameters used are $\rho_{1r} = \rho_{2r} = 0$ and $\rho_{12} = -0.5$ and $\rho_{12} = 0.5$. The constant target ratio is $\widetilde{\theta}_i = 31.5\%$ and the time-dependent target ratio is based on equation (7.66) with $\widetilde{\theta}_i(0) = 73.2\%$ and $\widetilde{\theta}_i(15) = 31.5\%$.

7.7. Overview

In this chapter, we have extended the framework of the two-firm model to incorporate mean-reverting leverage ratios, in order to capture the effect of firms altering their capital structures. We also extended the analytical solution developed in Section 4.1 by the method of images to cover this case. However, the solution obtained by the method of images is only valid for certain values of correlation coefficient ρ_{12} only, and here is further limited by the condition that speeds of mean-reversion must be equal. Therefore, the Monte Carlo scheme based on Section 5.2 is extended to cover the general values of ρ_{12} as well as unequal speeds of mean-reversion. The numerical results extend the models of Collin-Dufresne & Goldstein (2001) and Hui et al. (2006) to the two-firm case, in which the use of constant target ratios generate higher joint survival probability values and smaller default correlation values, and the use of time-dependent target ratio generates lower joint survival probabilities and larger default correlations. These findings are summarized in Table 7.3.

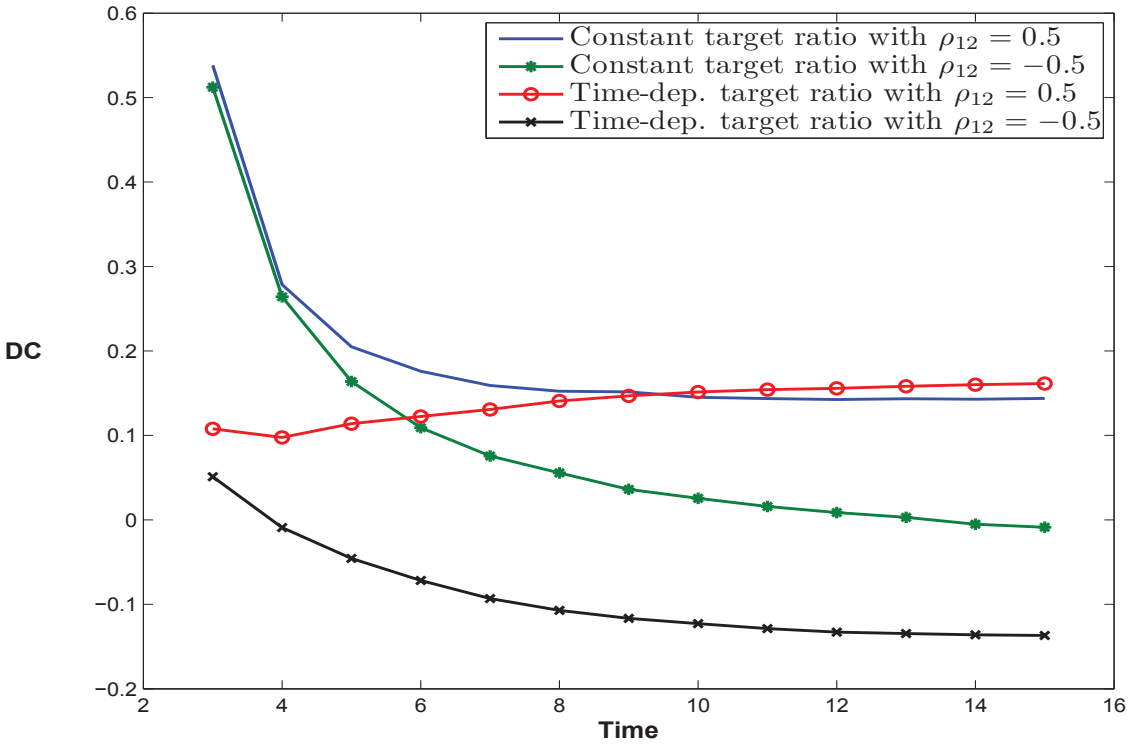

FIGURE 7.4. The impact of constant target ratios and time-dependent target ratios on default correlations for CCC-BBB paired firms. Initial leverage for the CCC-rated firm is L_1=73.2%, for the BBB-rated firm is L_2=31.5% and the volatilities are σ_1=0.299, σ_2 =0.213. Other parameters used are $\rho_{1r} = \rho_{2r} = 0$ and $\rho_{12} = -0.5$ and $\rho_{12} = 0.5$. The constant target ratio is $\widetilde{\theta}_i = 31.5\%$ and the time-dependent target ratio is based on equation (7.66) with $\widetilde{\theta}_i(0) = 73.2\%$ and $\widetilde{\theta}_i(15) = 31.5\%$.

Mean-reverting processes	Impact on JSP	Impact on DC (in absolute value)
Constant target ratio	$\Uparrow$	$\Downarrow$
Time varying target level	$\Downarrow$	$\Uparrow$

TABLE 7.3. A summary of the impact on joint survival probabilities and default correlations of mean-reverting processes for the leverage ratios.

CHAPTER 8

One-Firm Dynamic Leverage Ratio Model with Jumps

The uncertainty in the previous chapters was modelled by Wiener processes, the essential idea of which is that uncertain events evolve not too rapidly. However in many area of finance, especially in the area of credit risk, it is sudden, abrupt changes that are of interest, for example the sudden default of a firm or a sovereign borrower. A very useful way of capturing such sudden changes in financial markets is to add to the Wiener process component of uncertainty a jump process. Such a framework was first developed in finance by Merton (1976) who proposed a framework for valuing option prices when the underlying stock price follows a jump-diffusion process. This allows one to capture the 'abnormal' change in price due to the sudden arrival of important news concerning the stock.

In credit risk modelling, if one uses only continuous diffusion structural models, firms can never default by surprise. Zhou (1997) argues that in reality, a firm can default either by a gradual diffusion process, or by surprise due to unexpected external shocks. This idea combines the structural and reduced-form approaches, as shown in Zhou (2001*b*) who extended the framework for the pricing of corporate bonds by assuming the firm value variable follows a jump-diffusion process.

To capture the sudden external shocks, in this chapter, we extend the Hui et al. (2007) dynamic leverage ratio model by assuming that the dynamics of the leverage ratio follow a jump-diffusion process. We note that to the best of our knowledge there has been no work on the one-firm model with leverage ratio following a jump-diffusion process in literature. So this chapter might provide some insight into credit risk analysis when the firm's leverage ratio follows a jump-diffusion process.

Section 8.1 presents the framework of the one-firm dynamic leverage ratio model with jump risks. In Section 8.2, we discuss how to extend the Monte Carlo scheme to cover this case. Section 8.3 discuss the choice of parameters for evaluation of the individual default probabilities. Section 8.4 shows the impact on default probability of the parameters that characterise the jump component: in particular the jump size mean, the jump size volatility and the jump intensity. In Section 8.5, we will seek for the optimal values of average jump size by calibrating to S&P historical default data for different credit ratings. Section 8.6 will give an overview of the results of the chapter.

8.1. The Framework

We assume that the firm's leverage ratio follows a jump-diffusion process. Assumption 1 developed in chapter 3, in this case will become

Assumption 1 $''$***.*** *Let L denote the leverage ratio of the firm. The dynamics of L are given by the jump-diffusion process*

$$\frac{dL}{L} = (\mu_L - \lambda_q k_q)dt + \sigma_L dZ_L + (Y-1)dq\,, \tag{8.1}$$

where μ_L is the instantaneous expected drift rate of the leverage ratio per unit time , σ_L is the instantaneous volatility of the proportional change of the leverage ratio per unit time conditional on no jumps, Z_L is a standard Wiener process driving the continuous change of the leverage ratio under the historical measure $\mathbb{P}$, q is a Poisson counting process with intensity λ_q so that

$$dq = \begin{cases} 1 & \textit{with probability } \lambda_q dt\,, \\ 0 & \textit{with probability } (1-\lambda_q dt)\,. \end{cases} \tag{8.2}$$

$(Y-1)$[1] is the random variable percentage change in the leverage ratio level if the Poisson event occurs, where Y is log-normally distributed: $\ln Y \sim N(\mu_q - \sigma_q^2/2, \sigma_q^2)$ with the expected mean value $k_q \equiv \mathbb{E}[Y-1]$ for $\mathbb{E}$ is the expectation operator under the historical measure $\mathbb{P}$.

Given that the Poisson event occurs, the impact of the jump on the leverage ratio level is determined by drawing Y from the distribution $G(Y)$. If $L(t^-)$ is the leverage ratio level at time t^- just prior to the jump, then the leverage ratio level at time t^+ immediately after the jump is $L(t^+) = L(t^-)Y$. The successive draws from $G(Y)$ are independently and identically distributed.

Let $P(L,r,t)$ be the price of a corporate bond written on the underlying asset, this will depend on L, r and t. Under Assumptions 1$''$, 2, 3, 4 and adapting to the current situation Merton's (1976) argument for hedging jump risk, the bond price $P(L,r,t)$ satisfies the integro-partial differential equation (IPDE)

$$\begin{aligned} -\frac{\partial P(L,r,t)}{\partial t} &= \frac{1}{2}\sigma_L^2 L^2 \frac{\partial^2 P}{\partial L^2} + \frac{1}{2}\sigma_r^2 \frac{\partial^2 P}{\partial r^2} + \rho_{Lr}\sigma_L\sigma_r L \frac{\partial^2 P}{\partial L \partial r} \\ &\quad + (\widetilde{\mu}_L - \widetilde{\lambda}_q \widetilde{k}_q) L \frac{\partial P}{\partial L} + \kappa_r[\widetilde{\theta}_r - r]\frac{\partial P}{\partial r} - rP \\ &\quad + \widetilde{\lambda}_q \int_0^\infty [P(LY,r,t) - P(L,r,t)]\widetilde{G}(Y)dY, \end{aligned} \tag{8.3}$$

[1]Note that Y no longer has the same meaning as in previous chapters.

for $L \in (0, \widehat{L})$ and subject to boundary conditions

$$\begin{aligned} P(L, r, T) &= 1, \\ P(\widehat{L}, r, t) &= 0. \end{aligned} \tag{8.4}$$

The parameters $\widetilde{\mu}_L$, $\widetilde{\theta}_r$ incorporate the market prices of risk associated with the pure diffusion uncertainly driving the leverage ratio λ_L (assumed constant here) and interest rate process λ_r (assumed constant here) respectively as

$$\begin{aligned} \widetilde{\mu}_L &= \mu_L - \lambda_L \sigma_L, \\ \widetilde{\theta}_r &= \theta_r - \frac{\lambda_r \sigma_r}{\kappa_r}. \end{aligned} \tag{8.5}$$

Following the discussion in Cheang & Chiarella (2007), the Poisson process under the risk-neutral measure $\widetilde{\mathbb{P}}$ has a new intensity rate $\widetilde{\lambda}_q$ and a new distribution $\widetilde{G}(Y)$ for the jump-sizes. Using $\widetilde{\mu}_q$ to denote the jump size mean under the risk-neutral measure, the distribution $\widetilde{G}(Y)$ is given by[2]

$$\widetilde{G}(Y) = \frac{1}{Y \sigma_q \sqrt{2\pi}} \exp\Big\{ - \frac{[\ln Y - (\widetilde{\mu}_q - \sigma_q^2/2)]^2}{2\sigma_q^2} \Big\}, \tag{8.6}$$

so that the expected jump-increment under the risk-neutral measure is

$$\widetilde{k}_q = \widetilde{\mathbb{E}}[Y - 1] = \int_0^\infty (Y - 1) \widetilde{G}(Y) dY, \tag{8.7}$$

and $\widetilde{k}_q = e^{\widetilde{\mu}_q} - 1$.

Using the same technique of separation of variables as was used in Chapter 3, the bond price can be expressed as a product of the risk-free bond price $B(r, t)$ and a discounting factor function $\bar{P}(L, t)$, so that

$$P(L, r, t) = B(r, t) \bar{P}(L, t). \tag{8.8}$$

[2]Cheang & Chiarella (2007) introduce a Radon-Nikodým derivative process that induces the change of measure from the market measure to the risk-neutral measure for the jump-arrival process. They derive the relationships for the jump intensity and the distribution of the jump-sizes (represented by the moment of generating function) between the risk-neutral measure and the market measure. The relation shows that if the distribution of jump size in the market measure comes from an exponential family, then the distribution of jump size under the risk-neutral measure also comes from the same exponential family but with different parameters.

The quantity $\bar{P}(L,t)$ as discussed in Chapter 3 it can be viewed as a risk ratio function and by substitution of (8.8) into (8.3) it is found to satisfy the integro-partial differential equation

$$\begin{aligned} -\frac{\partial \bar{P}(L,t)}{\partial t} &= \frac{1}{2}\sigma_L^2 L^2 \frac{\partial^2 \bar{P}}{\partial L^2} + (\widetilde{\mu}_L + \rho_{Lr}\sigma_L\sigma_r b(t) - \widetilde{\lambda}_q \widetilde{k}_q) L \frac{\partial \bar{P}}{\partial L} \\ &\quad + \widetilde{\lambda}_q \int_0^\infty [\bar{P}(LY,t) - \bar{P}(L,t)]\widetilde{G}(Y)dY, \end{aligned} \tag{8.9}$$

subject to boundary conditions

$$\begin{aligned} \bar{P}(L,T) &= 1, \\ \bar{P}(\widehat{L},t) &= 0, \end{aligned} \tag{8.10}$$

with $b(t)$ is given in (3.81).

8.2. Monte Carlo Simulations

It is difficult to solve the first-passage-time problem of the integro-partial differential equation (8.9) in closed-form. However, a general approach to solving it numerically is the Monte Carlo method.

By the Feynman-Kac formula for the jump-diffusion processes (Gikhman & Skorokhod (1972)), the stochastic differential equation linked to the IPDE (8.9) is

$$\frac{dL}{L} = \left[\widetilde{\mu}_L + \rho_{Lr}\sigma_L\sigma_r b(t) - \widetilde{\lambda}_q \widetilde{k}_q\right]dt + \sigma_L d\widetilde{Z}_L + (Y-1)dq, \tag{8.11}$$

where $\widetilde{Z}_L$ is a Wiener process under a risk-neutral measure $\widetilde{\mathbb{P}}$. Note that the jump size Y now is drawn from the distribution of $\widetilde{G}(Y)$ given in (8.6) and the Poisson process q now has intensity $\widetilde{\lambda}_q$.

To evaluate the probability of default PD ($= 1 - F$), we follow the Monte Carlo approach in Section 5.2, and replace Step 2 and Step 3 by

Step 2$'$. Do the MC simulations $M(m = 1, 2, ..., M)$ times.

- 2.1.$'$ For the mth simulation, at the jth time step, generate an independent normal random number e from the $N(0,1)$ distribution;
- 2.2.$'$ Let $x = \ln(L/\widehat{L})$, then (8.11) becomes

$$x(t_j) = x(t_{j-1}) + \left[\widetilde{\mu}_L + \rho_{Lr}\sigma_L\sigma_r b(t_{j-1}) - \frac{1}{2}\sigma_L^2 - \widetilde{\lambda}_q \widetilde{k}_q\right]\Delta t + \sigma_L\sqrt{\Delta t}e + H, \tag{8.12}$$

  where H is the jump component.

We use the general method suggested in Glasserman (2004) to simulate H from t_{j-1} to t_j consisting of the following steps:

2.3.′ Generate the arrival of the jump event ω in the time interval $(t_j - t_{j-1})$:

$\omega \sim \mathbf{P}\big(\widetilde{\lambda}_q(t_j - t_{j-1})\big)$;

* if $\omega = 0$, set $H = 0$, that is no jump occurs in this time interval and go to Step 2.2′;
* if $\omega \neq 0$, generate $\ln Y$ from its distribution, namely $\ln Y \sim N(\widetilde{\mu}_q - \sigma_q^2/2, \sigma_q^2)$, and set $H = \ln Y$, then go to Step 2.2′.

Here $\mathbf{P}\big(\widetilde{\lambda}_q(t_j - t_{j-1})\big)$ is a Poisson process and is simulated by the inverse transform method and will be discussed in more detail in the next section.

Step 3′. Check the boundary condition: if $x(t_j) \geq 0$, then $\text{PD}_m(t_j)$=1, and go to the next simulation m+1. Otherwise $\text{PD}_m(t_j)$=0, and go to the next time step j+1. Set $\text{PD}(t_j) = \sum_{m=1}^{M} \text{PD}_m(t_j)/M$, which is the approximate value of the probability of default.

8.2.1. Generating Poisson Samples.

If $\{\omega(t), t \geq 0\}$ is a Poisson process, then the number of arrivals in any time interval of length Δt is a Poisson random variable with parameter $\widetilde{\lambda}_q \Delta t$ (where $\widetilde{\lambda}_q$ is a positive real number). That is

$$\mathbf{P}(\omega(t + \Delta t) - \omega(t) = k) = e^{-\phi}\frac{\phi^k}{k!},\ \phi = \widetilde{\lambda}_q \Delta t\ ;\ k = 0, 1, 2, ...$$

A simple method to generate Poisson samples is to generate exponential random variables $X_i = -\log(U_i)/\phi$ from independent uniform U_i's, and take ω to be the largest integer for which $X_1 + ... + X_\omega \leq 1$. Alternatively take ω to be the largest integer for which $U_1 \times \cdots \times U_n \geq e^{-\phi}$. The following steps and table illustrate this method (see Figure 8.1):

1. set $a = e^{-\phi}$, $c = 1$ and $i = 0$;
2. then loop while $(c >= a)\{$ generate $U_{i+1} \sim U(0, 1)$, $c = cU_{i+1}$ and $i = i + 1\}$;
3. return $\omega = i$.

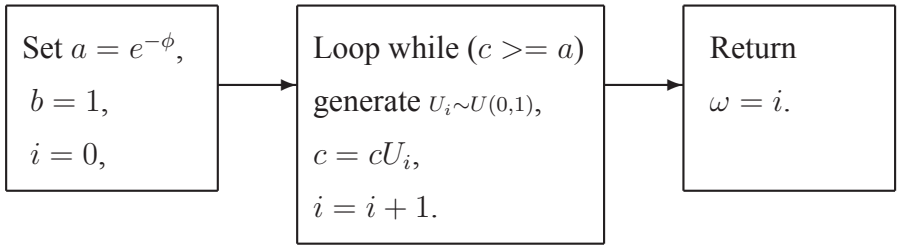

FIGURE 8.1. A simple method to generate Poisson samples.

However, this method is rather slow. As ϕ increases, $e^{-\phi}$ decreases, so the algorithm needs to keep looping for an ever increasing time to achieve the condition ($c < a$) and so exit the while loop. This can be improved by the inverse transform method, the idea of which is to search for the smallest ω at which $F(\omega) \leq U$. Here $F(\omega)$ denotes the cumulative distribution function, that is $F(\omega) = \mathbf{P}(0)+\mathbf{P}(1)+...+\mathbf{P}(\omega)$, and $\mathbf{P}(k+1) = \mathbf{P}(k)\phi/(k+1)$. The main steps of the algorithm are as follows (see Figure 8.2):

1. set $F = p = e^{-\theta}$ and $i = 0$;
2. generate $U \sim U(0, 1)$;
3. while loop $(U > F)$ $\{ i = i + 1, p = p\theta/i$ and $F = F + p\}$;
4. return $\omega = i$.

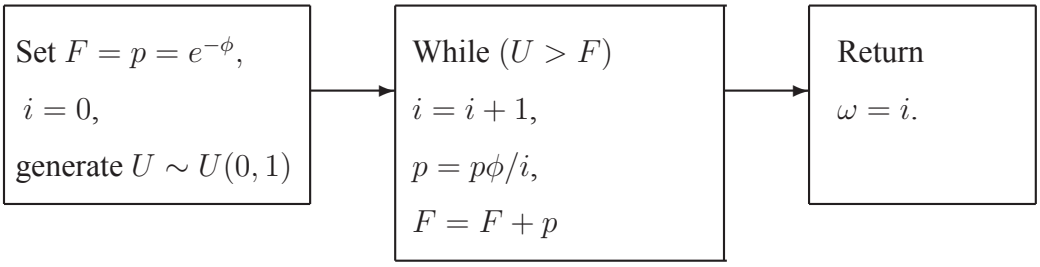

FIGURE 8.2. The inverse transform method algorithm to generate Poisson samples.

Note that the number of jump arrivals ω in the time interval Δt generated by the above methods can be larger than one. However, the definition (8.2) assumes no more than one jump can occur in the period of time Δt. To fulfill the assumption while using these methods, a relatively small Δt should be used. The idea is that if the time interval Δt is sufficiently small, the probability of two jumps occurring is negligible because $(\widetilde{\lambda}_q \Delta t)^2$ is much lower than $(\widetilde{\lambda}_q \Delta t)$. To illustrate suppose, for example that $\Delta t = 1$ year and $\widetilde{\lambda}_q = 0.1$ per year, then the probability of the occurrence of two jumps in one year is given by $\mathbf{P}(\omega = k) = e^{-\widetilde{\lambda}_q \Delta t}(\widetilde{\lambda}_q \Delta t)^k/k! = 0.45\%$ (for $k = 2$, $\Delta t = 1$ and $\widetilde{\lambda}_q = 1$). However, if $\Delta t = 1/365$, then the probability of two jumps in one year is $\mathbf{P}(\omega = 2) = 3.75 \times 10^{-6}$ %, which is negligible.

8.3. Choice of Parameters

The choice of parameters for the pure diffusion component, is based on those described in Section 6.1. The default barrier of the firm is set at $\widehat{L} = 1$. The leverage ratio levels L and values of volatility σ_L of individual firms are given in Table 6.1. To isolate the effects of the drift term of the

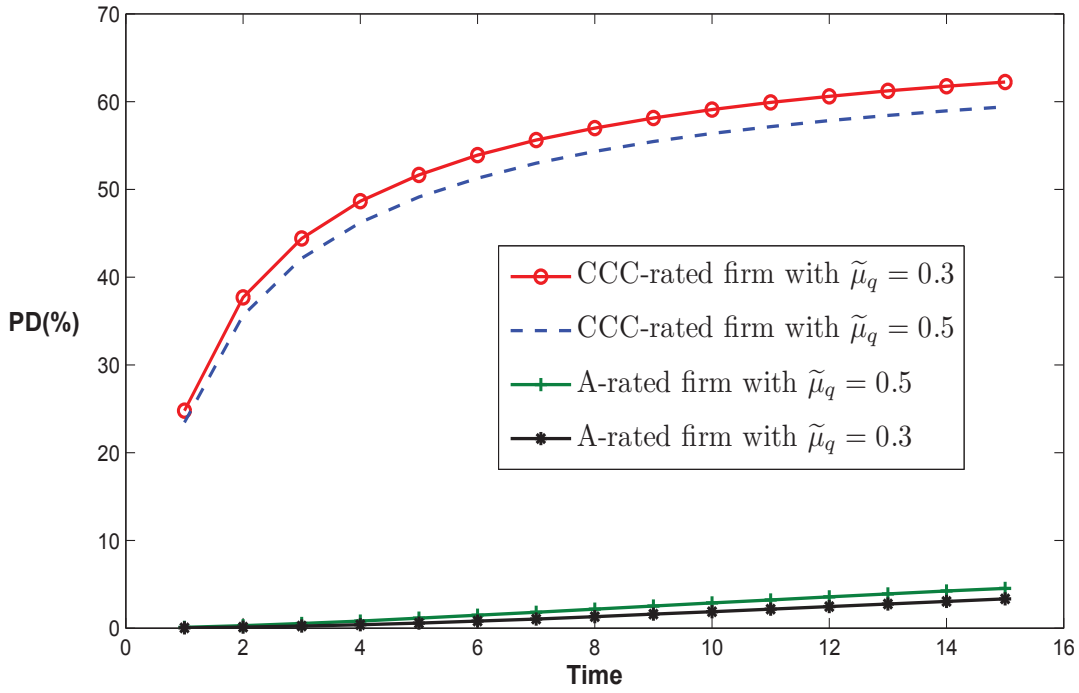

FIGURE 8.3. The impact of the jump size mean on the default probability for CCC and A-rated firms. Initial leverage for the CCC-rated firm is $L = 73.2\%$ and the volatility is $\sigma_L = 0.299$ and for the A-rated firm it is $L = 17.2\%$ and the volatility is $\sigma_L = 0.184$. Other parameters used for both firms are $\widetilde{\mu}_L = 0$, $\rho_{Lr} = 0$. The values of jump size mean takes $\widetilde{\mu}_q = 0.3$ and $\widetilde{\mu}_q = 0.5$, $\widetilde{\lambda}_q = 0.1$ and $\sigma_q^2 = 0.25$.

diffusion component and correlation with the interest rate process, we set $\widetilde{\mu}_L$=0 and ρ_{Lr}=0. The time horizon used is fifteen years which is the same as in previous chapters.

The choice of jump intensity and jump size volatility is based on Zhang & Melnik (2007), who extend the Zhou (2001*b*) model to the multi-firm case, where firms' asset values follow jump-diffusion processes. Zhang & Melnik (2007) assume that the arrival of the jump event is the same for each firm. This corresponds to assuming that the jump event is caused by some economy wide macroeconomic factor that effects all firms at the same time, regardless of their rating. However the impact of the jump event when it occurs, will be different for firms of different credit rating. Following their setting, we assume that the jump intensity is the same for the different credit rated firms and it is equal to 0.1, that is $\widetilde{\lambda}_q = 0.1$. Zhang & Melnik (2007) calibrate their model to market data and obtained the optimal values of jump size volatility of 0.5 for an A-rated firm. Here, we assume that the jump size volatility of the leverage ratio is the same as the jump size volatility of the firm value, and so we take $\sigma_q = 0.5$ for each firm. Therefore, we have left one parameter, the jump size mean that remains free and we choose it to calibrate to the S&P historical data in Section 8.5.

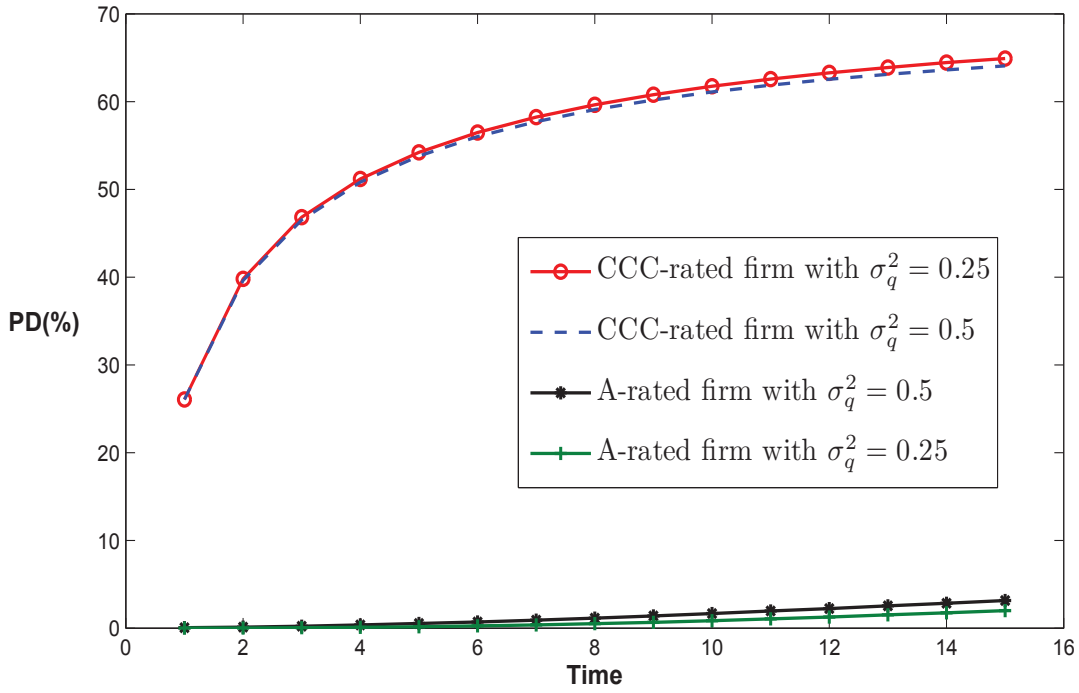

FIGURE 8.4. The impact of jump size volatility on the default probability for CCC and A-rated firms. Initial leverage for the CCC-rated firm is $L = 73.2\%$ and the volatility is $\sigma_L = 0.299$ and for the A-rated firm is $L = 17.2\%$ and the volatility is $\sigma_L = 0.184$. Other parameters used for both firms are $\widetilde{\mu}_L = 0$, $\rho_{Lr} = 0$. The jump size volatility takes the value$\sigma_q^2 = 0.25$ and $\sigma_q^2 = 0.5$, and we set $\widetilde{\mu}_q = 0$ and $\widetilde{\lambda}_q = 0.1$.

The numerical results presented in the following subsection are based on the Monte Carlo scheme developed in the previous section based on the dynamics (8.11), which is under a risk-neutral measure. The number of time steps n per year is 36,500, and the number of paths M used is $M = 500,000$. We do not know the exact solution for the jump-diffusion model here, so to the accuracy of the Monte Carlo results we use the confidence limits generated. Given the Monte Carlo simulated results for the probability of default $\text{PD}(t)$ with M paths, the standard deviation (SD) measures the amount of error in $\text{PD}(t)$ when it is used to estimate the exact value of PD_{exact}, and it is given by

$$\text{SD} = \sqrt{\frac{\sum_{m=1}^{M} \text{PD}_m^2(t) - \left(\sum_{m=1}^{M} \text{PD}_m(t)\right)^2/M}{M-1}}. \tag{8.13}$$

From Snedecor & Cochran (1991) (see Chapter 4), with knowledge of the standard deviation (SD), the 95% confidence interval for exact value of PD_{exact} can be expressed as the pair of inequalities

$$\text{PD}(t) - 1.96\varepsilon \leq \text{PD}_{\text{exact}} \leq \text{PD}(t) + 1.96\varepsilon, \tag{8.14}$$

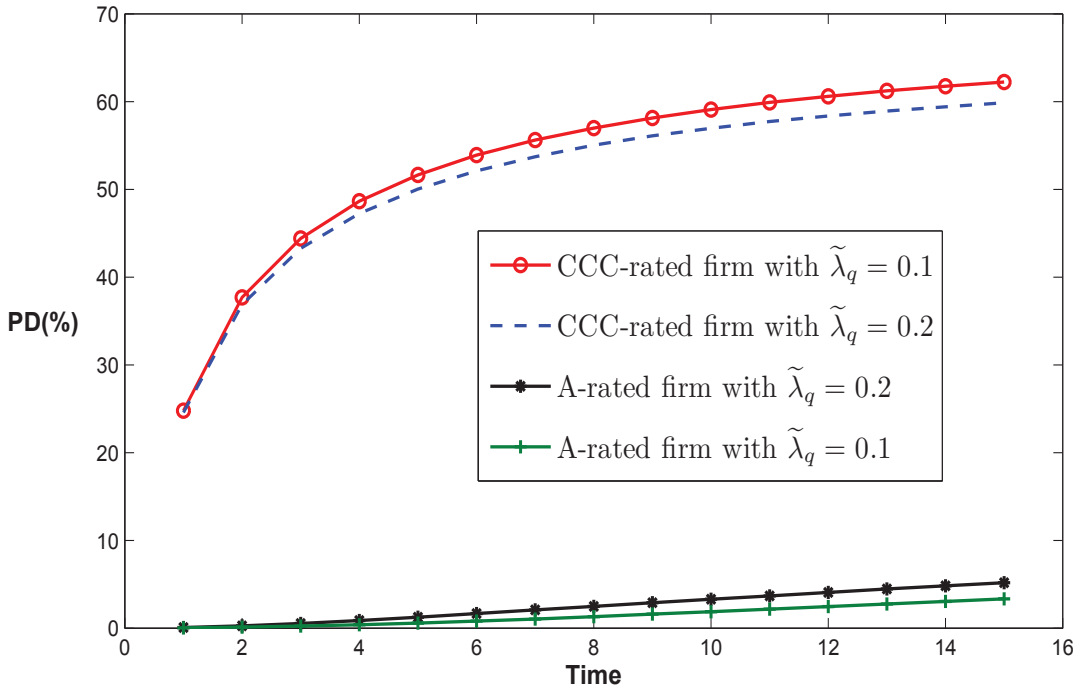

FIGURE 8.5. The impact of jump intensity on the default probability for CCC and A-rated firms. Initial leverage for the CCC-rated firm it is $L = 73.2\%$ and the volatility is $\sigma_L = 0.299$ and for the A-rated firm it is $L = 17.2\%$ and the volatility is $\sigma_L = 0.184$. Other parameters used for both firms are $\widetilde{\mu}_L = 0$, $\rho_{Lr} = 0$. The of jump size intensity takes the values $\widetilde{\lambda}_q = 0.1$ and $\widetilde{\lambda}_q = 0.2$, and we set $\sigma_q^2 = 0.25$ and $\widetilde{\mu}_q = 0.3$.

where standard error ε is given by

$$\varepsilon = \frac{\text{SD}}{\sqrt{M}}. \tag{8.15}$$

The 95% confidence interval for PD_{exact} means that there is a 95% chance for the Monte Carlo result of $\text{PD}(t)$ to lie between $\text{PD}_{\text{exact}} - 1.96\varepsilon$ and $\text{PD}_{\text{exact}} + 1.96\varepsilon$.

Using $M = 500,000$ paths for the simulation of the default probabilities, the maximum standard deviation and standard error over time for the Monte Carlo simulated default probabilities of a CCC-rated firm (for example) is SD=0.4998 and ε=0.0007, respectively. Therefore, with 95% confidence $\text{PD}(t)$ will lie between $\text{PD}_{\text{exact}} - 0.00137$ and $\text{PD}_{\text{exact}} + 0.00137$.

8.4. The Impact of Jump Risks on Default Probabilities

In this section, we study the impact of jump risks on individual default probabilities for CCC and AA-rated firms. To illustrate the effect of average jump size on the default probability, we vary the jump size mean value from $\widetilde{\mu}_q = 0.3$ to $\widetilde{\mu}_q = 0.5$.

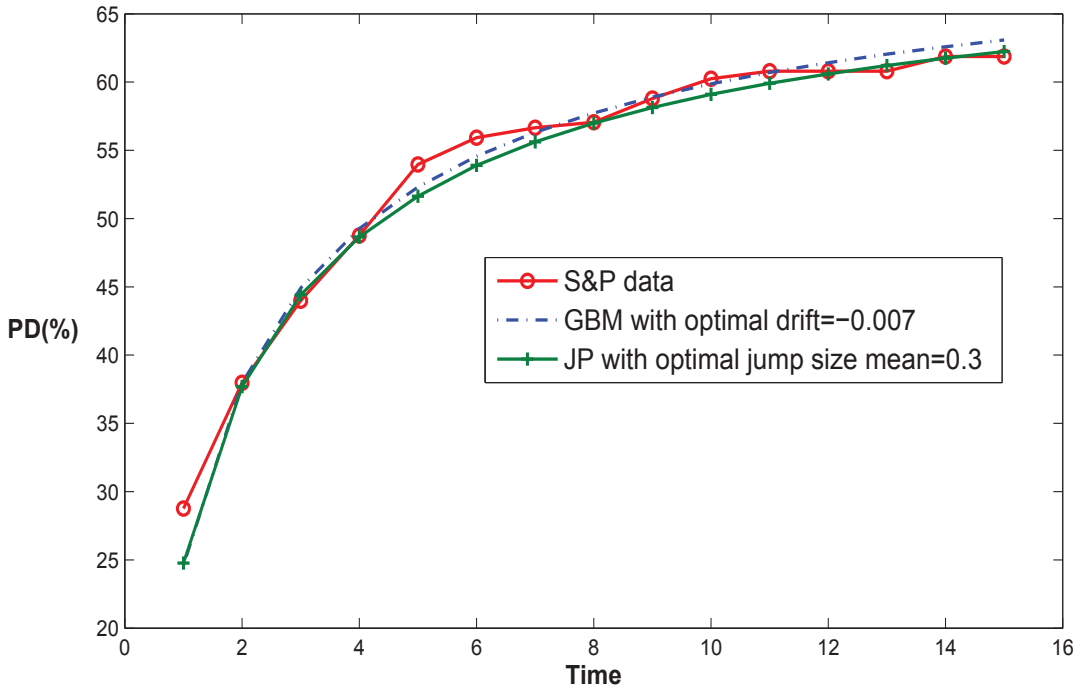

FIGURE 8.6. Comparing the best fit to the observed S&P default probabilities with the jump-diffusion model and with the pure diffusion model for a CCC-rated firm. The initial leverage for the CCC-rated firm is $L = 73.2\%$ and the volatility is $\sigma_L = 0.299$. Other parameters used for the jump-diffusion model (JP) are $\widetilde{\mu}_L = 0$, $\rho_{Lr} = 0$, $\widetilde{\mu}_q = 0.3$, $\sigma_q^2 = 0.25$, $\widetilde{\lambda}_q = 0.1$. For the pure diffusion model (GBM), the drift is $\widetilde{\mu}_L = -0.007$.

Figure 8.3 shows the default probability for A and CCC rated firms over a time horizon of fifteen years. We note that when the average jump size increases, the default probability for the CCC-rated firm declines, while the default probability for the A-rated firm rises. This may be due to the high initial leverage level of low quality firms, so the possibility of jumping down to a lower leverage level is higher than jumping up to a higher leverage level, therefore the default probability declines over time. A contrasting effect is at work for the good quality firms, because of the low initial leverage level, the probability of jumping up to a higher leverage level is more than that of jumping down to a lower leverage level, so that the default probability rises over time.

In order to study the effect of jump size volatility and of jump intensity, we vary the value of jump size variance from $\sigma_q^2 = 0.25$ to $\sigma_q^2 = 0.5$, and the jump intensity from $\widetilde{\lambda}_q = 0.1$ to $\widetilde{\lambda}_q = 0.2$, which corresponds respectively to one jump per ten years and one jump per five years.

Figure 8.4 plots the default probabilities for the CCC-rated firm and A-rated firm as a function of time for different values of the jump size volatility and Figure 8.5 plots the default probabilities for these two firms for different values of the jump intensity. We observe that the default probability for the CCC-rated firm declines, while the default probability for the A-rated firm rises, as in

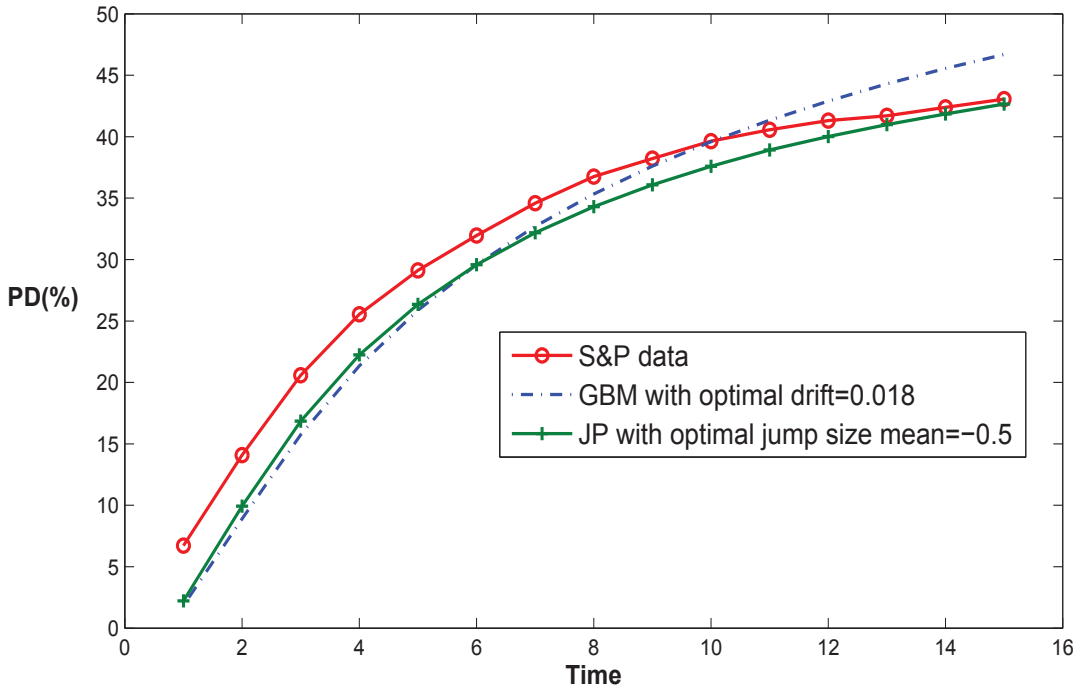

FIGURE 8.7. Comparing the best fit to the observed S&P default probabilities with the jump-diffusion model and with the pure diffusion model for a B-rated firm. The initial leverage for the B-rated firm is $L = 53.8\%$ and the volatility is $\sigma_L = 0.270$. Other parameters used for the jump-diffusion model (JP) are $\widetilde{\mu}_L = 0$, $\rho_{Lr} = 0$, $\widetilde{\mu}_q = -0.5$, $\sigma_q^2 = 0.25$, $\widetilde{\lambda}_q = 0.1$. For the pure diffusion model (GBM), the drift is $\widetilde{\mu}_L = 0.018$.

Figure 8.3, with the increase in the average jump size. The same explanation as was given to explain the results in Figure 8.3 applies here, because of the high initial leverage ratio low credit quality firms have a higher probability of jumping down to a lower leverage level, while the low initial leverage ratio of good credit quality firms means that they have higher probability of jumping up to a higher leverage level.

8.5. Calibration of the Average Jump Size to the Historical Data

In this section, we calibrate the model to the S&P historical data. We set the jump intensity at $\widetilde{\lambda}_q = 0.1$ and jump size variance at $\sigma_q^2 = 0.25$ (as discussed in Section 8.3) and assume that they are the same for different credit rated firms. We leave the average jump size free to adjust and seek its optimal value so as to best fit the model to the S&P historical default rates. We vary the values of the average jump size $\widetilde{\mu}_q$ to fit the model calculated default probabilities (PD) to the S&P historical default rates (SP) by finding the minimum root mean square derivation RMSD over a

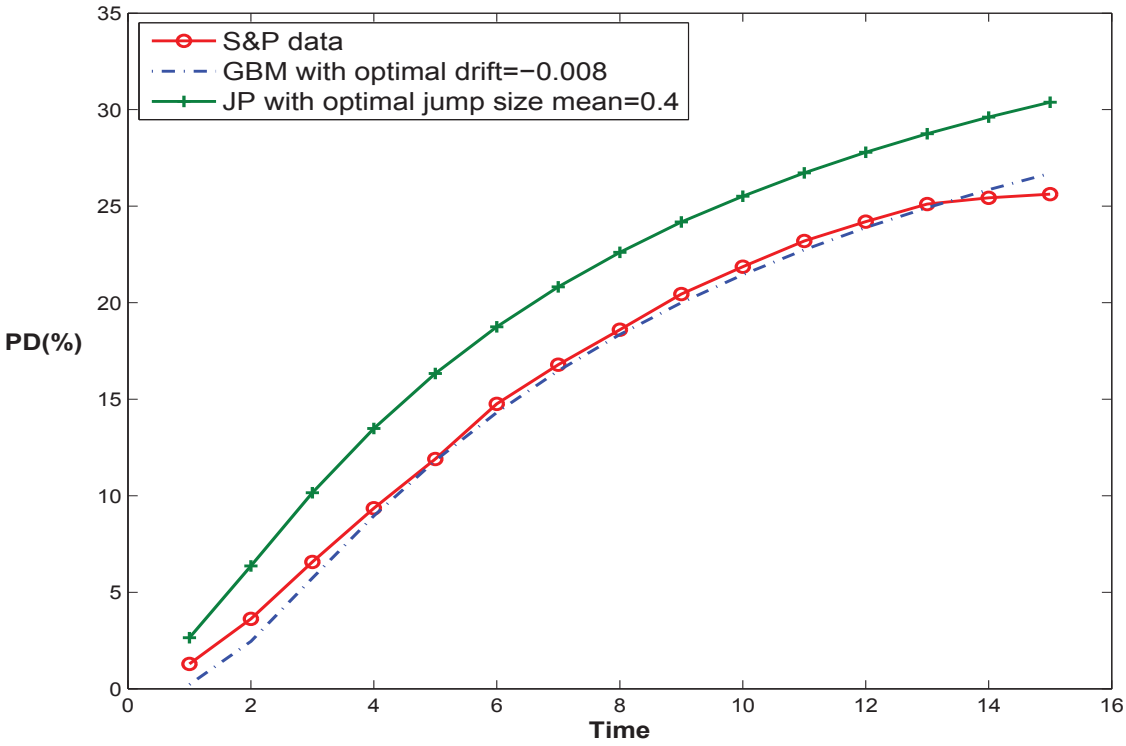

FIGURE 8.8. Comparing the best fit to the observed S&P default probabilities with the jump-diffusion model and with the pure diffusion model for a BB-rated firm. The initial leverage for the BB-rated firm is $L = 49.5\%$ and the volatility is $\sigma_L = 0.241$. Other parameters used for the jump-diffusion model (JP) are $\widetilde{\mu}_L = 0$, $\rho_{Lr} = 0$, $\widetilde{\mu}_q = 4$, $\sigma_q^2 = 0.25$, $\widetilde{\lambda}_q = 0.1$. For the pure diffusion model (GBM), the drift is $\widetilde{\mu}_L = -0.008$.

time horizon of $t_N = 15$ years[3], that is :

$$\text{RMSD} = \sqrt{\frac{\sum_{t=1}^{t_N} \big(\text{PD}(t) - \text{SP}(t)\big)^2}{t_N}}. \tag{8.16}$$

We denote by $\widetilde{\mu}_q^*$ the value of the best fit and of course this value will be different for each rating class. Table 8.1 gives the values of $\widetilde{\mu}_L^*$ for each rating class. In order to compare the performance of dynamic leverage model with jump risks to the model without jump (that is the Hui et al. (2007) model where leverage ratio follows the geometric Brownian motion), we also calibrate the Hui et al. (2007) model to the historical data, by seeking the optimal values of the drift rate $\widetilde{\mu}_L$ of the leverage ratio when it follows a geometric Brownian motion, to fit the model to the S&P historical default rates for each rating class and their values (namely $\widetilde{\mu}_L^*$) are given in Table 8.1.

[3]We take the time horizon of fifteen years as S&P historical data is available for up to fifteen years.

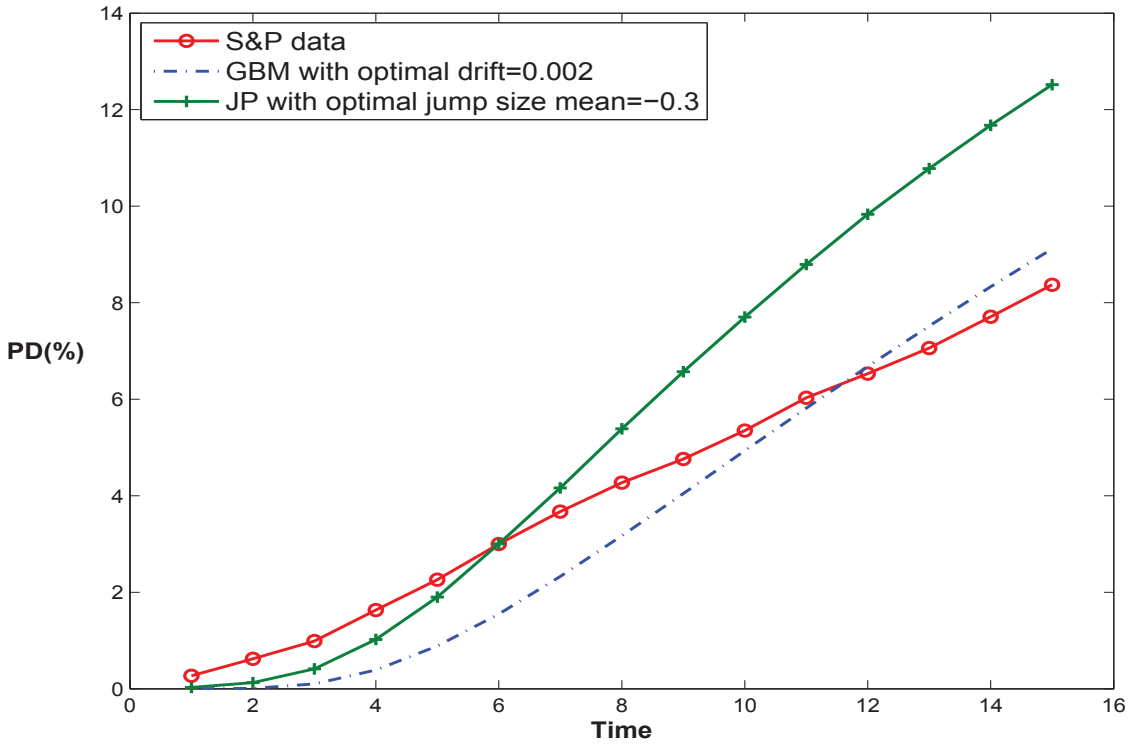

FIGURE 8.9. Comparing the best fit to the observed S&P default probabilities with the jump-diffusion model and with the pure diffusion model for a BBB-rated firm. The initial leverage for the BBB-rated firm is $L = 31.5\%$ and the volatility is $\sigma_L = 0.213$. Other parameters used for the jump-diffusion model (JP) are $\widetilde{\mu}_L = 0$, $\rho_{Lr} = 0$, $\widetilde{\mu}_q = -0.3$, $\sigma_q^2 = 0.25$, $\widetilde{\lambda}_q = 0.1$. For the pure diffusion model (GBM), the drift is $\widetilde{\mu}_L = 0.002$.

	AAA	AA	A	BBB	BB	B	CCC
$\widetilde{\mu}_q^*$	1.1	0.6	0.3	-0.3	0.4	-0.5	0.3
$\widetilde{\mu}_L^*$	0.16	0.08	0.039	0.002	-0.008	0.018	-0.007

TABLE 8.1. Calibrating to S&P data. The first row gives the optimal values of the jump component for different credit ratings. The second row gives the optimal drift of a diffusion model for different credit ratings.

Figure 8.6 plots the default probability of a CCC-rated firm with the leverage ratio following the geometric Brownian Motion (GBM) with optimal drift ($\widetilde{\mu}_L^*$) and under the jump-diffusion process (JP) ($\widetilde{\mu}_q^*$) with optimal jump size, and compares these to the S&P historical data. We observe that

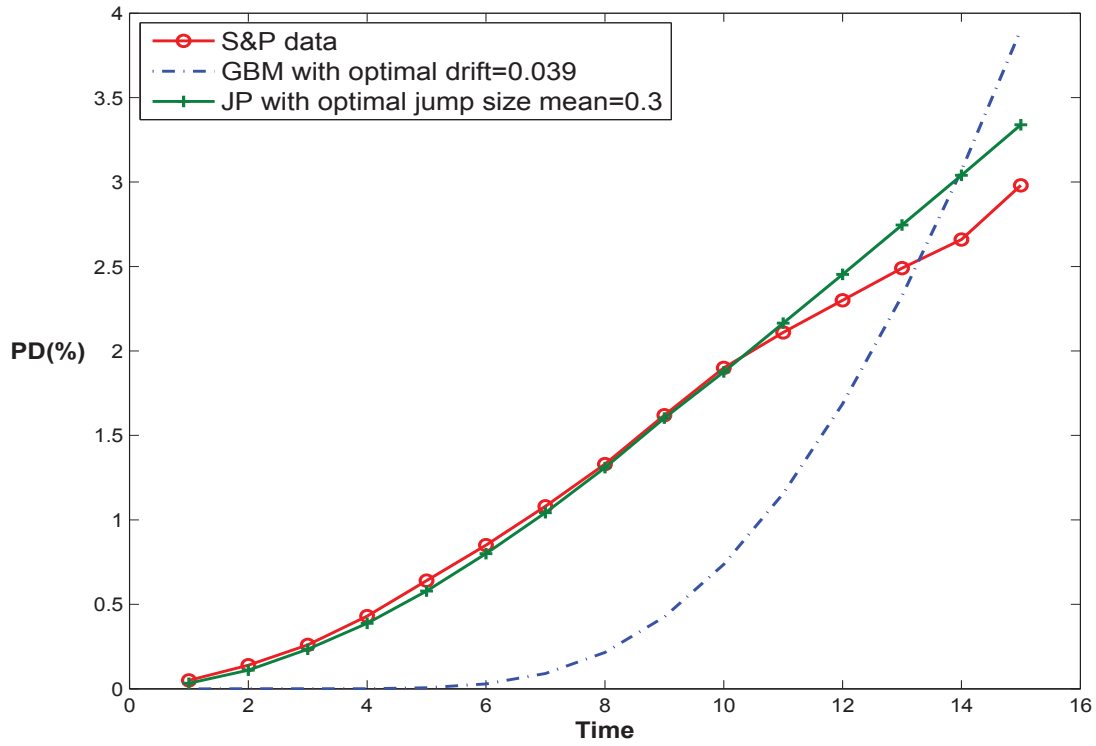

FIGURE 8.10. Comparing the best fit to the observed S&P default probabilities with the jump-diffusion model and with the pure diffusion model for an A-rated firm. The initial leverage for the A-rated firm is $L = 17.2\%$ and the volatility is $\sigma_L = 0.184$. Other parameters used for the jump-diffusion model (JP) are $\widetilde{\mu}_L = 0$, $\rho_{Lr} = 0$, $\widetilde{\mu}_q = 0.3$, $\sigma_q^2 = 0.25$, $\widetilde{\lambda}_q = 0.1$. For the pure diffusion model (GBM), the drift is $\widetilde{\mu}_L = 0.039$.

both models can generally track quite well the S&P historical data. The results are similar for B-rated firms as displayed in Figure 8.7. For the BB-rated firms, the model under the geometric Brownian motion generates default probabilities very close to the S&P data, the model under the jump-diffusion process generates default probabilities slightly higher than the S&P data, but it tacks the general trend quite well (see Figure 8.8). For the BBB-rated firm, we observe that neither model is able to give a good approximation to the S& P historical data, as exhibited in Figure 8.9.

For investment grade firms, for example, A-rated and AA-rated firms, the model under the jump-diffusion process gives a very close approximation to the historical data (see Figure 8.10 and Figure 8.11), where for these ratings the model under geometric Brownian motion is not able to track the historical data at all. Similar results are found for AAA-rated firms, as shown in Figure 8.12, where we see that the jump-diffusion model generally tracks the historical data, though not so well at longer times, but this may due to the some problems with the data.

Figure 8.6 and Figure 8.7 show that if the leverage ratio follows geometric Brownian motion (as in Hui et al. (2007)) or jump-diffusion process (as here), the model can generally approximate the historical default rates quite well for low credit quality firms, for example, CCC, B and BB-rated

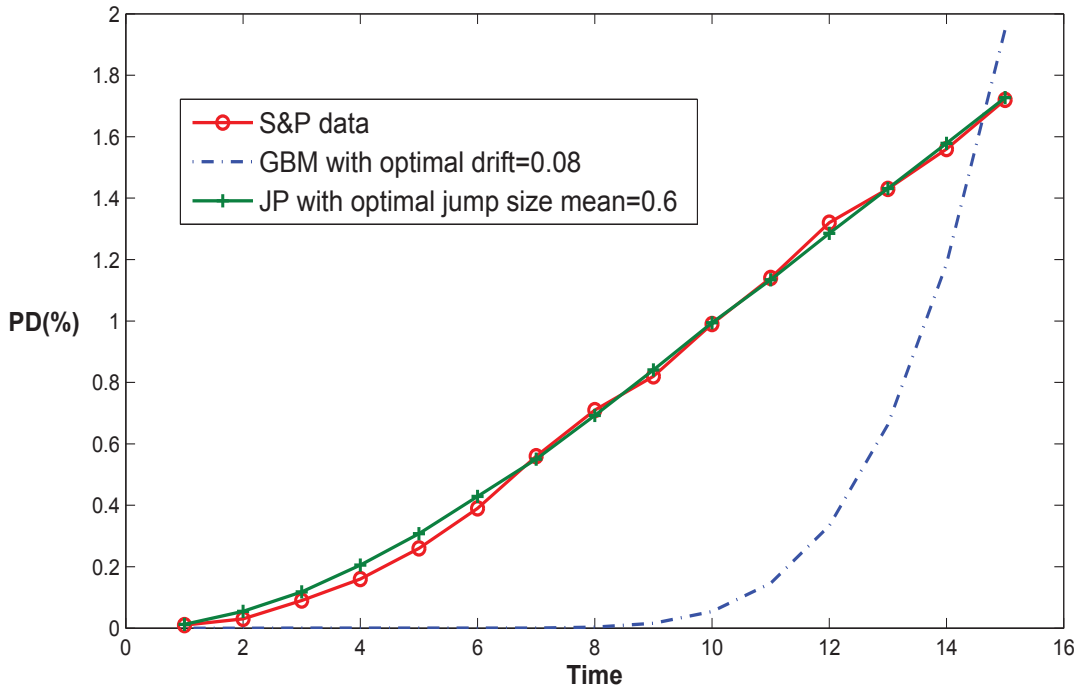

FIGURE 8.11. Comparing the best fit to the observed S&P default probabilities with the jump-diffusion model and with the pure diffusion model for a AA-rated firm. The initial leverage for the AA-rated firm is $L = 9.5\%$ and the volatility is $\sigma_L = 0.156$. Other parameters used for the jump-diffusion model (JP) are $\widetilde{\mu}_L = 0$, $\rho_{Lr} = 0$, $\widetilde{\mu}_q = 0.6$, $\sigma_q^2 = 0.25$, $\widetilde{\lambda}_q = 0.1$. For the pure diffusion model (GBM), the drift is $\widetilde{\mu}_L = 0.08$.

firms. However, when the credit quality of firms increases, only the model with leverage ratio following a jump-diffusion process is able to give a good fit to the historical data (see for example, Figures 8.10-8.12). These results seem to reflect the fact that for non-investment grade firms, there is no significant difference between default being driven by gradual diffusion or sudden external shocks, however, for investment grade firms, defaults seem to be mainly due to the external shocks. Compare the optimal values of jump size mean for A, AA and AAA-rated firms, which increases from 0.3 for the A-rated firm to 1.1 for the AAA-rated firm, this is a reflection of the fact that for the better credit quality firm, such as AAA-rated firm, defaults are driven by a higher value of jump size mean. Hence our argument that for better credit quality firms, default is driven by strong external shocks. For lower quality firms they are closer to the default barrier so diffusion may be sufficient to cause default.

8.6. Overview

This chapter has extended the work of Hui et al. (2007) model (which the dynamic leverage ratio follows geometric Brownian motion) to incorporate jump risks. The Monte Carlo scheme has

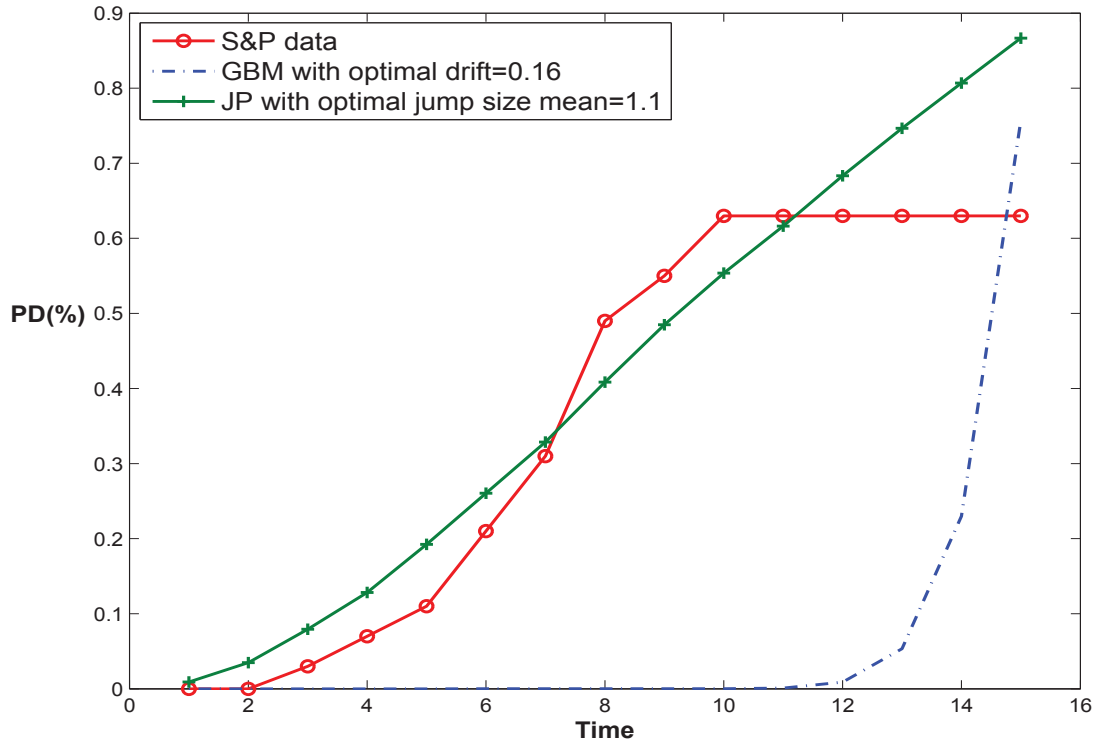

FIGURE 8.12. Comparing the best fit to the observed S&P default probabilities with the jump-diffusion model and with the pure diffusion model for a AAA-rated firm. The initial leverage for the AAA-rated firm is $L = 3.1\%$ and the volatility is $\sigma_L = 0.127$. Other parameters used for the jump-diffusion model (JP) are $\widetilde{\mu}_L = 0$, $\rho_{Lr} = 0$, $\widetilde{\mu}_q = 1.1$, $\sigma_q^2 = 0.25$, $\widetilde{\lambda}_q = 0.1$. For the pure diffusion model (GBM), the drift is $\widetilde{\mu}_L = 0.16$.

been extended to evaluate the default probability, the behaviour of which in the presence of jump risks are studied. By searching for the optimal value of jump size mean, the model is calibrated to the Standard & Poor's (2001) reported historical data. We also have compared our fits using jump-diffusion model to those obtained using the Hui et al. (2007) model as a comparison[4]. The results seem to reflect the fact that for non-investment grade firms, default of firms is driven by either gradual diffusion or jumps, while for investment grade firms, the default is mainly driven by jumps. It will be of interest to see how this effect works out when we come to consider the effect of jump-diffusion dynamics of the leverage ratios on joint survival probability or default correlation among two firms, a topic to which we will turn in the next chapter.

[4]Alternative specifications such as using asymmetric volatilities for firms' leverage ratios could probably achieve similar empirical outcomes. However, in this thesis our aim has been to extend the framework of Zhou (2001*b*), and for this reason we have chosen to work with jump-diffusion processes.

CHAPTER 9

The Two-Firm Model with Jumps

In this chapter, we extend the two-firm model developed in chapter 3 to incorporate the jump structure introduced in to the one-firm model in the previous chapter. The Assumption 1 in chapter 3 and Assumption $1''$ in chapter 8, in this case become

Assumption 1'''. *Let L_1 and L_2 denote the leverage ratios of the note issuer and the reference obligor, respectively. The leverage ratio is defined as the ratio of a firm's liability to its market-value capitalization. The dynamics of L_1 and L_2 are described by*

$$\frac{dL_i}{L_i} = (\mu_i - \lambda_{qi} k_{qi})dt + \sigma_i dZ_i + (Y_i - 1)dq \ , (i = 1, 2) \tag{9.1}$$

where the μ_i are the instantaneous expected drift rates, the σ_i are the instantaneous variances conditional on no jumps, Z_1 and Z_2 are Wiener processes capturing the uncertainty in the leverage ratio dynamics under the historical measure $\mathbb{P}$. The Wiener increments dZ_1 and dZ_2 are assumed to be correlated with $\mathbb{E}[dZ_1 dZ_2] = \rho_{12}dt$. The jump sizes Y_1 and Y_2 are assumed to be independent, however they both occur at the same time, q is the Poisson counting process defined in (8.2) *with the intensity λ_q, here we assume that the jump event affects both firms so the same intensity of the jump arrivals λ_q applies to both.*

The quantity $(Y_i - 1)$ is a random variable that is the percentage change in the leverage ratio level of firm i if the Poisson event occurs, where Y_i is log-normally distributed: $\ln Y_i \sim N(\mu_{qi} - \sigma_{qi}^2/2, \sigma_{qi}^2)$ with the expected mean value:

$$k_{qi} = \mathbb{E}\big[Y_i - 1\big] = \int_0^\infty (Y_i - 1)G(Y_i)dY_i. \tag{9.2}$$

We assume that $G(Y_1)$ and $G(Y_2)$ are independent.

Given that the Poisson event occurs, the impact of the jump on the leverage ratio level of firm i is determined by drawing Y_i from the distribution $G(Y_i)$. If $L_i(t^-)$ is the leverage ratio level at time t^- just prior to the jump, then the leverage ratio level at time t^+ immediately after the

jump is $L_i(t^+) = L_i(t^-)Y$. The successive draws from $G(Y_i)$ are independently and identically distributed.

Let $P(L_1, L_2, r, t)$ be the price of a credit linked note written on the underlying asset L_1, L_2 and r. Under Assumptions $1'''$, 2, 3, 4 and applying a similar approach to that described in Chapter 8, the integro-partial differential equation (IPDE) for $P(L_1, L_2, r, t)$ becomes

$$\begin{aligned}
-\frac{\partial P}{\partial t} &= \frac{1}{2}\sigma_1^2 L_1^2 \frac{\partial^2 P}{\partial L_1^2} + \frac{1}{2}\sigma_2^2 L_2^2 \frac{\partial^2 P}{\partial L_2^2} + \rho_{12}\sigma_1\sigma_2 L_1 L_2 \frac{\partial^2 P}{\partial L_1 \partial L_2} + \rho_{1r}\sigma_1\sigma_r L_1 \frac{\partial^2 P}{\partial L_1 \partial r} \\
&\quad + \rho_{2r}\sigma_2\sigma_r L_2 \frac{\partial^2 P}{\partial L_2 \partial r} + \frac{1}{2}\sigma_r^2 \frac{\partial^2 P}{\partial r^2} + (\widetilde{\mu}_1 - \widetilde{\lambda}_q \widetilde{k}_{q1}) L_1 \frac{\partial P}{\partial L_1} \\
&\quad + (\widetilde{\mu}_2 - \widetilde{\lambda}_q \widetilde{k}_{q2}) L_2 \frac{\partial P}{\partial L_2} + \kappa_r[\widetilde{\theta}_r - r]\frac{\partial P}{\partial r} - rP + \widetilde{\lambda}_q \int_0^\infty \int_0^\infty \Big[P(L_1 Y_1, L_2 Y_2, r, t) \\
&\quad - P(L_1, L_2, r, t)\Big] \widetilde{G}(Y_1)\widetilde{G}(Y_2) dY_1 dY_2, \qquad (9.3)
\end{aligned}$$

for $t \in (0, T)$, $L_i \in (0, \widehat{L}_i)$ and subject to the boundary conditions:

$$P(L_1, L_2, r, T) = 1, \qquad (9.4)$$

$$P(\widehat{L}_1, L_2, r, t) = 0, \qquad (9.5)$$

$$P(L_1, \widehat{L}_2, r, t) = 0. \qquad (9.6)$$

In (9.3) $\widetilde{\mu}_i$ and $\widetilde{\theta}_r$ incorporate the market prices of risk associated with diffusion processes λ_1, λ_2 (assumed constant here) and interest rate processes λ_r (assumed constant here) and extends to the two-firm situation the definitions in (8.5). The quantity $\widetilde{\lambda}_q$ is the jump intensity under the risk-neutral measure $\widetilde{\mathbb{P}}$. The market risk of jump risk is defined in a similar fashion to equation (8.7), that is

$$\widetilde{k}_{qi} = \widetilde{\mathbb{E}}[Y_i - 1] = \int_0^\infty (Y_i - 1)\widetilde{G}(Y_i) dY_i, \ (i = 1, 2), \qquad (9.7)$$

where $\widetilde{\mathbb{E}}$ is the expectation operator under risk-neutral measure $\widetilde{\mathbb{P}}$ and $\widetilde{G}(Y_i)$ is given in (8.6).

As in Chapter 8 we apply the separation of variables technique and again find that the price of credit linked note can be expressed as the product of a risk-free bond price $B(r, t)$ and a function $\bar{P}(L_1, L_2, t)$, so that

$$P(L_1, L_2, r, t) = B(r, t)\bar{P}(L_1, L_2, t). \qquad (9.8)$$

Substituting (9.8) into (9.3) we find that the integro-partial differential equation for $\bar{P}(L_1, L_2, t)$ is given by

$$\begin{aligned} -\frac{\partial \bar{P}}{\partial t} &= \frac{1}{2}\sigma_1^2 L_1^2 \frac{\partial^2 \bar{P}}{\partial L_1^2} + \left[\widetilde{\mu}_1 + \rho_{1r}\sigma_1\sigma_r b(t) - \widetilde{\lambda}_q \widetilde{k}_{q1}\right] L_1 \frac{\partial \bar{P}}{\partial L_1} \\ &\quad \frac{1}{2}\sigma_2^2 L_2^2 \frac{\partial^2 \bar{P}}{\partial L_2^2} + \left[\widetilde{\mu}_2 + \rho_{2r}\sigma_2\sigma_r b(t) - \widetilde{\lambda}_q \widetilde{k}_{q2}\right] L_2 \frac{\partial \bar{P}}{\partial L_2} \\ &\quad + \rho_{12}\sigma_1\sigma_2 L_1 L_2 \frac{\partial^2 \bar{P}}{\partial L_1 \partial L_2} + \widetilde{\lambda}_q \int_0^\infty \int_0^\infty \Big[\bar{P}(L_1 Y_1, L_2 Y_2, t) \\ &\quad - \bar{P}(L_1 Y_1, L_2 Y_2, t)\Big] \widetilde{G}(Y_1)\widetilde{G}(Y_2) dY_1 dY_2, \end{aligned} \tag{9.9}$$

for $t \in (0, T)$, $L_i \in (0, \widehat{L}_i)$ subject to the boundary conditions:

$$\bar{P}(L_1, L_2, T) = 1, \tag{9.10}$$

$$\bar{P}(\widehat{L}_1, L_2, t) = 0, \tag{9.11}$$

$$\bar{P}(L_1, \widehat{L}_2, t) = 0. \tag{9.12}$$

Here $b(t)$ is given in (3.81).

9.1. A Monte Carlo Simulation Scheme to Calculate JSP under Jump-Diffusion Dynamics

In this section, we follow the same steps as in Chapter 8 and develop a Monte Carlo scheme to simulate the joint survival probability when incorporating jumps. By the Feynman-Kac formula for jump-diffusion processes (see Gikhman & Skorokhod (1972)), the stochastic differential equations associated with (9.9) are

$$\frac{dL_1}{L_1} = \left[\widetilde{\mu}_1 + \rho_{1r}\sigma_1\sigma_r b(t) - \widetilde{\lambda}_{q1}\widetilde{k}_{q1}\right] dt + \sigma_1 d\widetilde{Z}_1 + (Y_1 - 1) dq\ , \tag{9.13}$$

$$\frac{dL_2}{L_2} = \left[\widetilde{\mu}_2 + \rho_{2r}\sigma_2\sigma_r b(t) - \widetilde{\lambda}_{q2}\widetilde{k}_{q2}\right] dt + \sigma_2 d\widetilde{Z}_2 + (Y_2 - 1) dq\ , \tag{9.14}$$

where $\widetilde{Z}_1$ and $\widetilde{Z}_2$ are Wiener processes under risk-neutral measure $\widetilde{\mathbb{P}}$, and the Wiener increments $d\widetilde{Z}_1$ and $d\widetilde{Z}_2$ are correlated with $\widetilde{\mathbb{E}}[d\widetilde{Z}_1 d\widetilde{Z}_2] = \rho_{12} dt$ with $\widetilde{\mathbb{E}}$ being the expectation operation under the $\widetilde{\mathbb{P}}$ measure. Note that the jump sizes Y_i now, as in Chapter 8, are drawn from the distribution of $\widetilde{G}(Y_i)$

$$\widetilde{G}(Y_i) = \frac{1}{Y\sigma_{qi}\sqrt{2\pi}} \exp\Big\{ - \frac{[\ln Y_i - (\widetilde{\mu}_{qi} - \sigma_{qi}^2/2)]^2}{2\sigma_{qi}^2}\Big\},\ (i = 1, 2), \tag{9.15}$$

and $\widetilde{k}_{qi} = e^{\widetilde{\mu}_{qi}} - 1$.

The Poisson counting process q now has the new intensity $\widetilde{\lambda}_q$.

We can also rewrite (9.13) in terms of uncorrelated Wiener processes W_1, W_2 as

$$\frac{dL_1}{L_1} = \big[\widetilde{\mu}_1 + \rho_{1r}\sigma_1\sigma_r b(t) - \widetilde{\lambda}_{q1}\widetilde{k}_{q1}\big]dt + \sigma_1 dW_1 + (Y_1 - 1)dq, \tag{9.16}$$

$$\frac{dL_2}{L_2} = \big[\widetilde{\mu}_2 + \rho_{2r}\sigma_2\sigma_r b(t) - \widetilde{\lambda}_{q2}\widetilde{k}_{q2}\big]dt + \sigma_2\big(\rho_{12}dW_1 + \sqrt{1-\rho_{12}^2}dW_2\big) + (Y_2 - 1)dq. \tag{9.17}$$

Recall the Monte Carlo approach developed in Section 8.2, to evaluate the joint survival probability, in order to extend this to the two firm case we replace Step 2$'$ and Step 3$'$ by:-

Step 2$''$. Do the MC simulations $M(m = 1, 2, ..., M)$ times.

2.1$''$. For the mth simulation, at the jth time step, generate independent normal random numbers e_1 and e_2 from the $N(0, 1)$ distribution ;

2.2$''$. Let $x_i = \ln(L_i/L_{i0})$, then (9.16) and (9.17) become

$$x_1(t_j) = x_1(t_{j-1}) + \big[\widetilde{\gamma}_1(t_{j-1}) - \frac{1}{2}\sigma_1^2 - \widetilde{\lambda}_q\widetilde{k}_{q1}\big]\Delta t + \sigma_1\sqrt{\Delta t}e_1 + H_1, \tag{9.18}$$

$$x_2(t_j) = x_2(t_{j-1}) + \big[\widetilde{\gamma}_2(t_{j-1}) - \frac{1}{2}\sigma_2^2 - \widetilde{\lambda}_q\widetilde{k}_{q2}\big]\Delta t + \sigma_2\sqrt{\Delta t}z_2 + H_2, \tag{9.19}$$

where $z_2 = \rho_{12}e_1 + \sqrt{1-\rho_{12}^2}e_2$ and the H_1 and H_2 are the jump components.

We generate the arrival of the jump event ω in the similar way as in the previous chapter which consists of the following steps:

2.3.$''$ Generate the arrival of the jump event ω in the time interval $(t_j - t_{j-1})$:
$\omega \sim \mathbf{P}\big(\widetilde{\lambda}_q(t_j - t_{j-1})\big)$;

* if $\omega = 0$, set $H_1 = H_2 = 0$, that is no jump occurs in this time interval and go to Step 2.2.$''$;
* if $\omega \neq 0$, generate $\ln Y_1$ and $\ln Y_2$ from their distributions, respectively, namely $\ln Y_i \sim N(\widetilde{\mu}_{qi} - \sigma_{qi}^2/2, \sigma_{qi}^2)$ for $(i = 1, 2)$, and set $H_1 = \ln Y_1$, $H_2 = \ln Y_2$, then go to Step 2.2.$''$.

Step 3$''$. Check the boundary conditions: if $x_1(t_j) \geq 0$ or $x_2(t_j) \geq 0$, then JSP$_m(t_j)$=0, and go to the next simulation m+1. Otherwise JSP$_m(t_j)$=1, and go to the next time step j+1.

Compute JSP$(t_j) = \sum_{m=1}^{M}$JSP$_m(t_j)/M$, which is the approximate value of the joint survival probability.

The Poisson samples used in Step 2.3.$''$ can be generated by the algorithm outlined in Subsection 8.2.1.

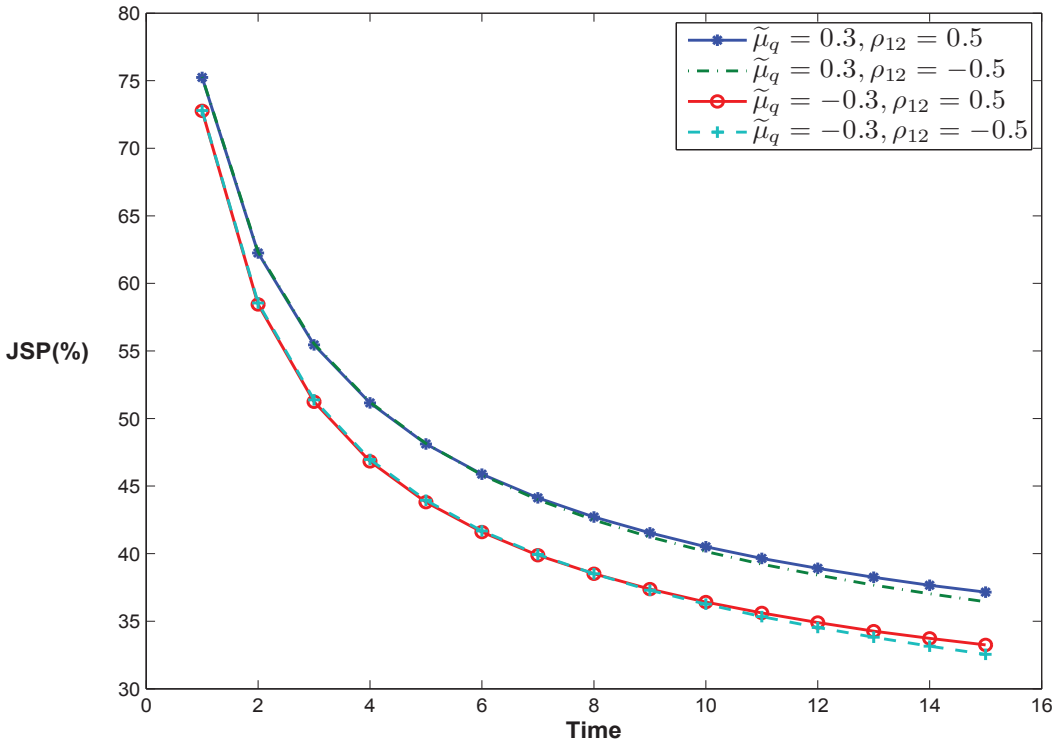

FIGURE 9.1. The impact of average jump sizes on the joint survival probabilities for CCC-A paired firms. The initial leverage for the CCC-rated firm is L_1=73.2%, and for the A-rated firm is L_2=17.2%, and the volatilities are σ_1=0.299, σ_2 =0.184. Other parameters used are $\widetilde{\mu}_i = 0$, $\rho_{ir} = 0$, $\rho_{12} = 0.5$ and $\rho_{12} = -0.5$. The jump size means take the values $\widetilde{\mu}_{q1} = \widetilde{\mu}_{q2} = \widetilde{\mu}_q = 0.3$ and -0.3, and $\widetilde{\lambda}_q = 0.1$ and $\sigma_{qi}^2 = 0.25$.

9.2. Choice of Parameters

The choice of parameters is similar to that used in Subsection 6.1. The default barriers of the two-firms are set at $\widehat{L}_1 = \widehat{L}_2 = 1$. The leverage ratio levels L_i and values of volatility σ_i of individual firms are again taken from Table 6.1. To isolate the effects of the drift term of the diffusion component and correlation with the interest rate process, we set $\widetilde{\mu}_i$=0 and ρ_{ir}=0. The correlation coefficient between the increment of firms' leverage ratios is set at $\rho_{12} = 0.5$ and $\rho_{12} = -0.5$ as previously used in Chapters 6 and 7, because they represent intermediate values.

The parameters used for the jump component are based on Section 8.3, where again the choices of jump intensity $\widetilde{\lambda}_q = 0.1$ and jump size volatility $\sigma_{qi}^2 = 0.25$ are based on Zhang & Melnik (2007).

The numerical results presented below are based on the Monte Carlo scheme developed in the previous section based on the system (9.16)-(9.17). The number of paths M used is 1,000,000 and the number of time steps per day is set at 100 which means the time step size is $\Delta t = 1/36,500$. As discussed in Section 8.3, there is no known exact solution to the integro-partial differential equation (9.9), so we need to rely on the Monte Carlo scheme and to check its accuracy we use

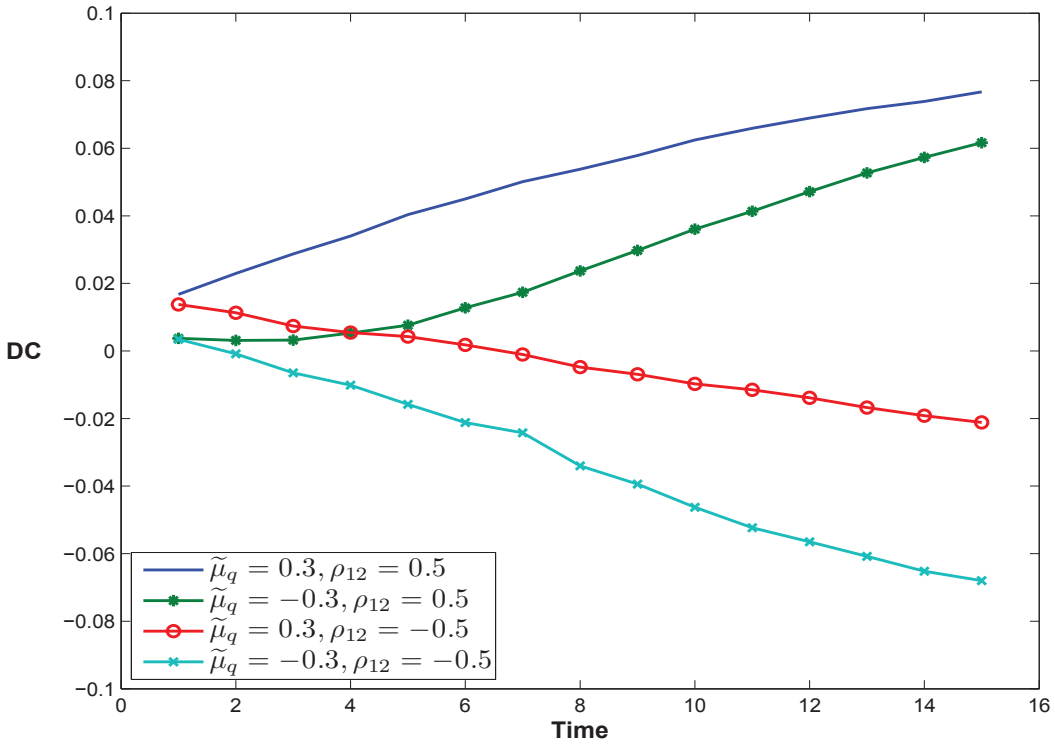

FIGURE 9.2. The impact of average jump sizes on the default correlations for CCC-A paired firms. The initial leverage for the CCC-rated firm is L_1=73.2%, and for the A-rated firm is L_2=17.2%, and the volatilities are σ_1=0.299, σ_2 =0.184. Other parameters used are $\widetilde{\mu}_i = 0$, $\rho_{ir} = 0$, $\rho_{12} = 0.5$ and $\rho_{12} = -0.5$. The jump size means take the values $\widetilde{\mu}_{q1} = \widetilde{\mu}_{q2} = \widetilde{\mu}_q = 0.3$ and -0.3, and $\widetilde{\lambda}_q = 0.1$ and $\sigma_{qi}^2 = 0.25$.

the confidence limits as discussed in Chapter 8. For Monte Carlo simulation results for the joint survival probabilities JSP(t) with M paths, the standard deviation (SD)

$$\text{SD} = \sqrt{\frac{\sum_{m=1}^{M} \text{JSP}_m^2(t) - \left(\sum_{m=1}^{M} \text{JSP}_m(t)\right)^2/M}{M-1}}. \tag{9.20}$$

The maximum standard deviation (SD) and standard error ε (defined in equation (8.15)) over time for the Monte Carlo simulated default probabilities of CCC-A paired firms (for example) is SD=0.4999 and ε=0.0005, respectively. Therefore, with 95% confidence the Monte Carlo result of JSP(t) will lie between $\text{JSP}_{\text{exact}} - 0.00098$ and $\text{JSP}_{\text{exact}} + 0.00098$.

9.3. The Impact of Jump Risk on the Two-Firm model

In this section, we show the impact of jump risk on joint survival probabilities and default correlations for CCC-A paired firms.

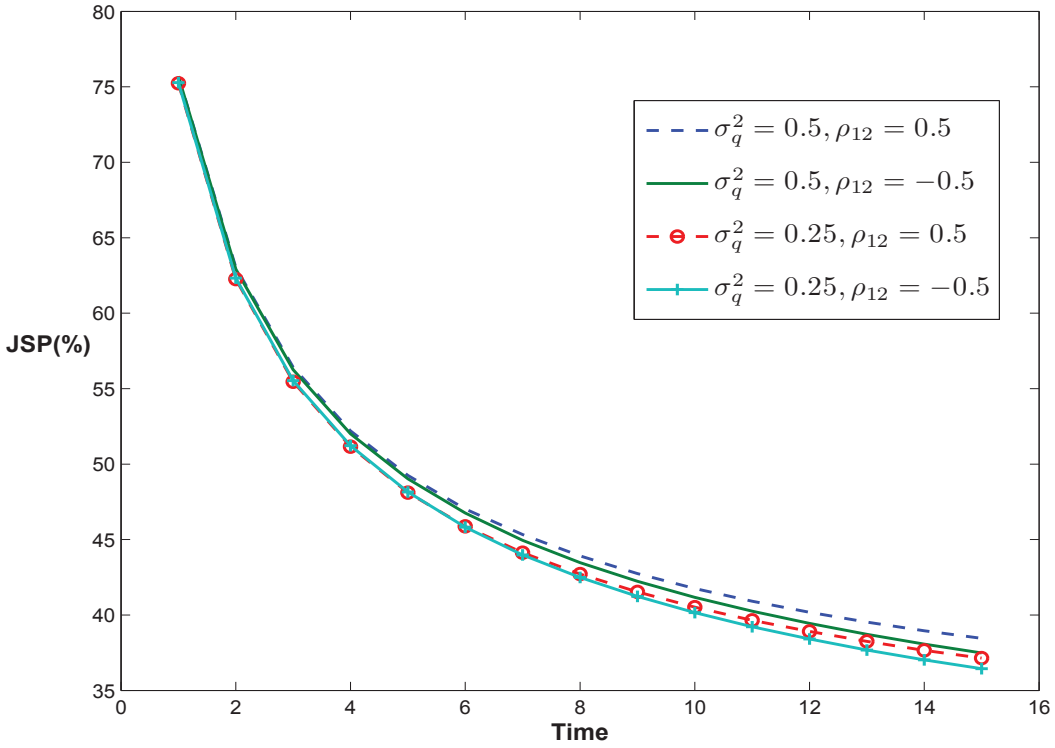

FIGURE 9.3. The impact of the jump size volatility on the joint survival probabilities for CCC-A paired firms. The initial leverage for the CCC-rated firm is L_1=73.2%, and for the A-rated firm is L_2=17.2%, and the volatilities are σ_1=0.299, σ_2 =0.184. Other parameters used are $\widetilde{\mu}_i = 0$, $\rho_{ir} = 0$, $\rho_{12} = 0.5$ and $\rho_{12} = -0.5$. The values of the jump size volatilities are $\sigma_{q1}^2 = \sigma_{q2}^2 = \sigma_q^2 = 0.25$ and 0.5, and $\widetilde{\mu}_{qi} = 0.3$ and $\widetilde{\lambda}_q = 0.1$.

9.3.1. Impact of the Jump Size Mean.

This subsection studies the impact of jump size volatilities on joint survival probabilities and default correlations. We take the values of jump size means $\widetilde{\mu}_{qi} = 0.3$ and $\widetilde{\mu}_q = 0.5$.

Figure 9.1 shows the joint survival probabilities rises as the jump size mean increases. Recalling the discussion on the impact of jump risks on individual default probabilities in Subsection 8.4, default probabilities of the A-rated firm would be expected to increase as the jump effect increases, which means that the individual survival probability of the A-rated firm decreases, however the individual survival probabilities of the CCC-rated firm correspondingly increase. These results seem to reflect the fact that the CCC-rated firm plays a more important role then the A-rated firm when they are paired. The increasing effect in individual survival probability of the CCC-rated firm outweighs the decreasing effect in survival probability of the A-rated firm.

Figure 9.2 graphs the default correlation for different values of the average jump size and the correlation coefficient. The default correlation rises as the average jump size increases for positively correlated firms. This is due to the fact that, when the jump event occurs, the leverage ratios jump

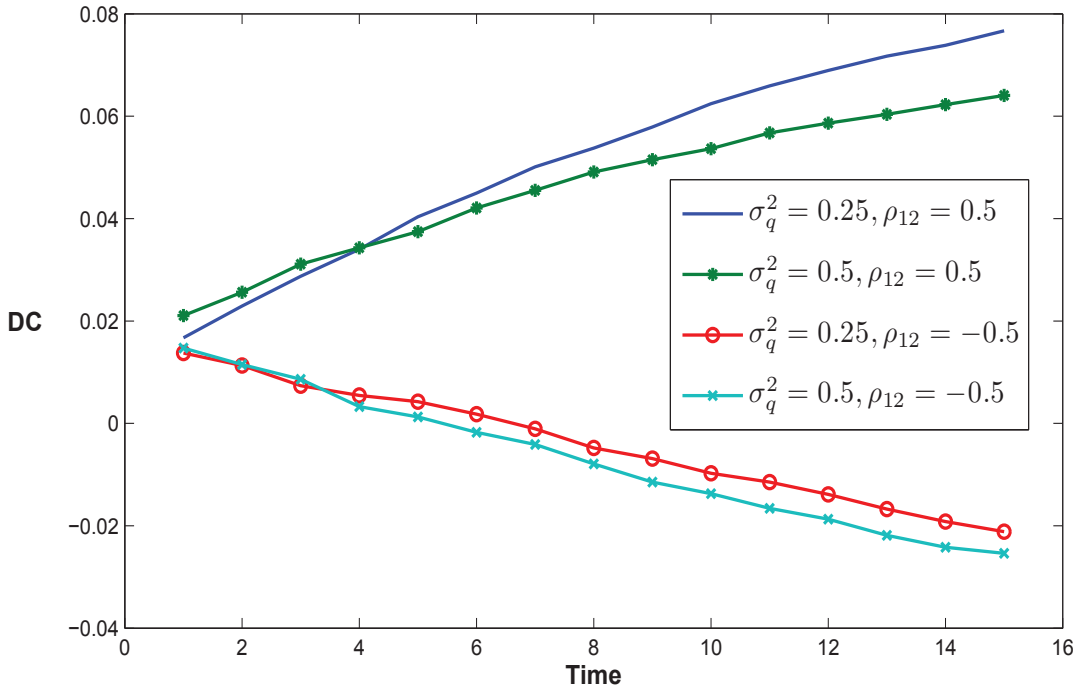

FIGURE 9.4. The impact of the jump size volatility on the default correlations for CCC-A paired firms. The initial leverage for the CCC-rated firm is L_1=73.2%, and for the A-rated firm is L_2=17.2%, and the volatilities are σ_1=0.299, σ_2 =0.184. Other parameters used are $\widetilde{\mu}_i = 0$, $\rho_{ir} = 0$, $\rho_{12} = 0.5$ and $\rho_{12} = -0.5$. The values of the jump size volatilities are $\sigma_{q1}^2 = \sigma_{q2}^2 = \sigma_q^2 = 0.25$ and 0.5, and $\widetilde{\mu}_{qi} = 0.3$ and $\widetilde{\lambda}_q = 0.1$.

to higher values on average with a larger jump size mean, and so move closer to the default barrier. Therefore, if one firm has defaulted, this is a signal that the leverage ratio of the other firm moves in the same direction (because of $\rho_{12} > 0$) towards the default barrier, since the leverage ratio of the other firm is already close to the default barrier with a larger jump size mean, thus the default of one firm will be a signal that the other firm is likely to default.

In contrast, when firms are negatively correlated ($\rho_{12} < 0$), the default correlation (in absolute value) increases as the average jump size decreases. The argument is similar to the case of $\rho_{12} > 0$. When the jump event occurs, the leverage ratios jump to lower values on average with a small jump size mean, and away from the default barrier. Therefore, if one firm has defaulted, then leverage ratio of the other firm moves in the opposite direction (because of $\rho_{12} < 0$) away from the default barrier, since the leverage ratio of this firm is already far from the default barrier due to the small jump size mean. Thus combining these two effects, the default of one firm will make it less likely on average that the other firm will default.

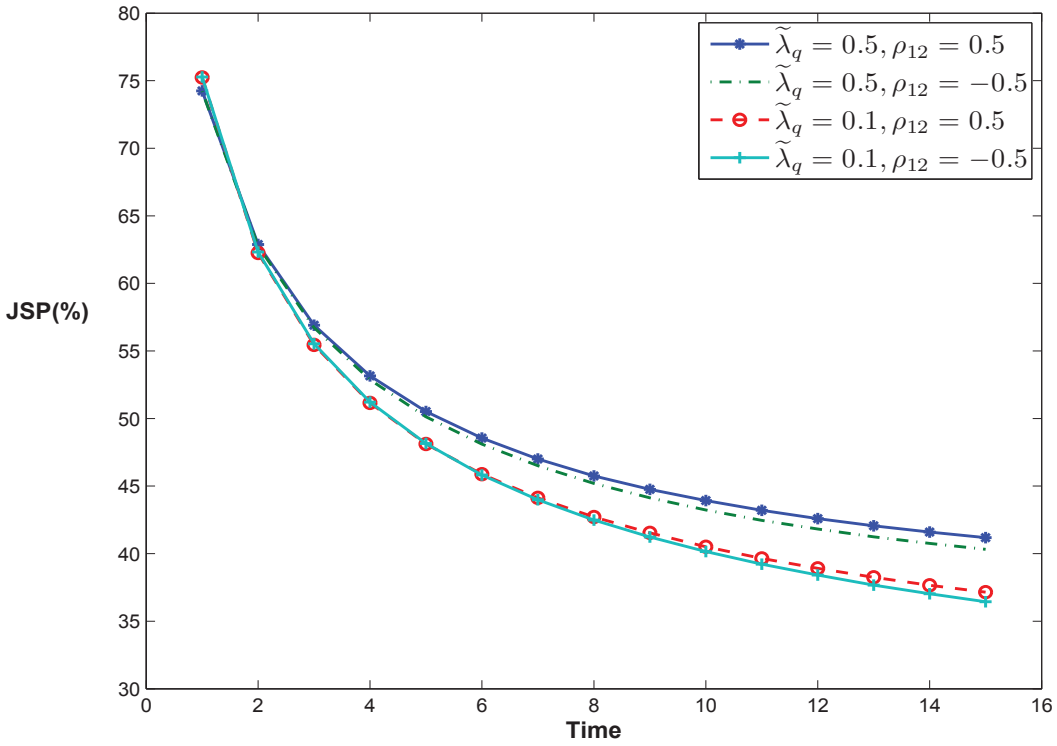

FIGURE 9.5. The impact of the jump intensity on the joint survival probabilities for CCC-A paired firms. The initial leverage for the CCC-rated firm is L_1=73.2%, and for the A-rated firm is L_2=17.2%, and the volatilities are σ_1=0.299, σ_2 =0.184. Other parameters used are $\widetilde{\mu}_i = 0$, $\rho_{ir} = 0$, $\rho_{12} = 0.5$ and $\rho_{12} = -0.5$. The jump intensity takes the values $\widetilde{\lambda}_q = 0.1$ and 0.5, and $\sigma_{qi}^2 = 0.25$ and $\widetilde{\mu}_{qi} = 0.3$.

9.3.2. Impact of the Jump Size Volatility.

This subsection studies the impact of jump size volatilities on joint survival probabilities and default correlations. We double the size of the variances of the jump size process from $\sigma_{qi}^2 = 0.25$ to $\sigma_{qi}^2 = 0.5$.

Figure 9.3 shows that the joint survival probabilities for CCC-A paired firms barely change as the jump size volatilities increase. This is similar to the results of the impact of the jump size mean, but the impact of jump size variance is not very significant, which may be due to the small change in values of the jump size volatility σ_{qi} ($\sqrt{0.25} = 0.5$ to $\sqrt{0.5} \approx 0.7$).

Figure 9.4 shows impact of the doubling of variances on default correlation. The default correlation declines as the jump size variance increase for positively correlated firms ($\rho_{12} > 0$), and default correlation (in absolute value) increases as the jump size variance increases for negatively correlated firms ($\rho_{12} < 0$). The argument is similar to that relating to the impact of average jump sizes in Subsection 9.3.1. When the jump event occurs, the leverage ratios may jump to higher (lower) values on average with a larger (smaller) jump size volatility, and closer to (from) the default barrier. Therefore, if one firm defaults, the leverage ratio of the other firm moves in the same

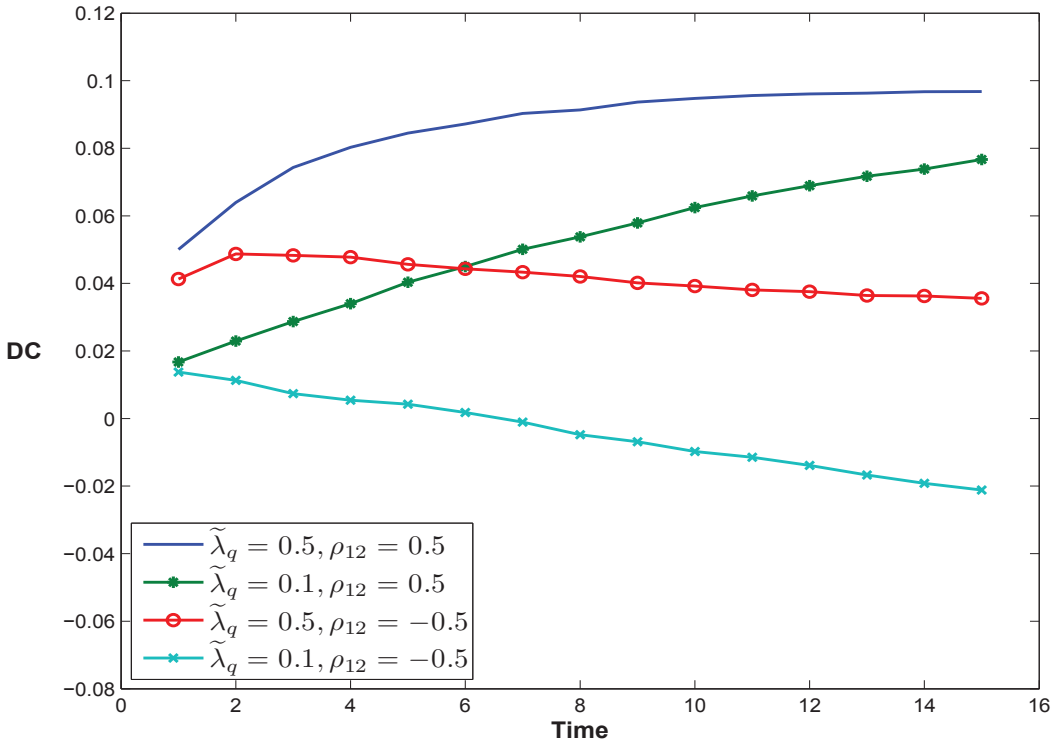

FIGURE 9.6. The impact of the jump intensity on the default correlations for CCC-A paired firms. The initial leverage for the CCC-rated firm is L_1=73.2%, and for the A-rated firm is L_2=17.2%, and the volatilities are σ_1=0.299, σ_2 =0.184. Other parameters used are $\widetilde{\mu}_i = 0$, $\rho_{ir} = 0$, $\rho_{12} = 0.5$ and $\rho_{12} = -0.5$. The jump intensity takes the values $\widetilde{\lambda}_q = 0.1$ and 0.5, and $\sigma_{qi}^2 = 0.25$ and $\widetilde{\mu}_{qi} = 0.3$.

(opposite) direction because of $\rho_{12} > 0$ ($\rho_{12} < 0$) towards (away from) the default barrier. Since the leverage ratio of the other firm is already close to (distant from) the default barrier with a larger (smaller) jump size volatility , thus the default of one firm will more likely (unlikely) so signal the possible default of the other firm.

9.3.3. Impact of the Jump Intensity.

Next we study the impact of jump intensity on joint survival probabilities and default correlations. We increase the jump intensity five-fold from $\widetilde{\lambda}_q = 0.1$ to $\widetilde{\lambda}_q = 0.5$, which correspond to going from one jump per ten years to one jump per two years.

Figure 9.5 shows that the joint survival probability decreases for both positively and negatively correlated firms as the jump intensity increases. The result is similar to that of the impact of jump size means and a similar argument applies here that when jump intensity increases, the increasing effect in individual survival probability of the CCC-rated firm outweighs the decreasing effect in survival probability of the A-rated firm, therefore the joint survival probability increases with the jump intensity.

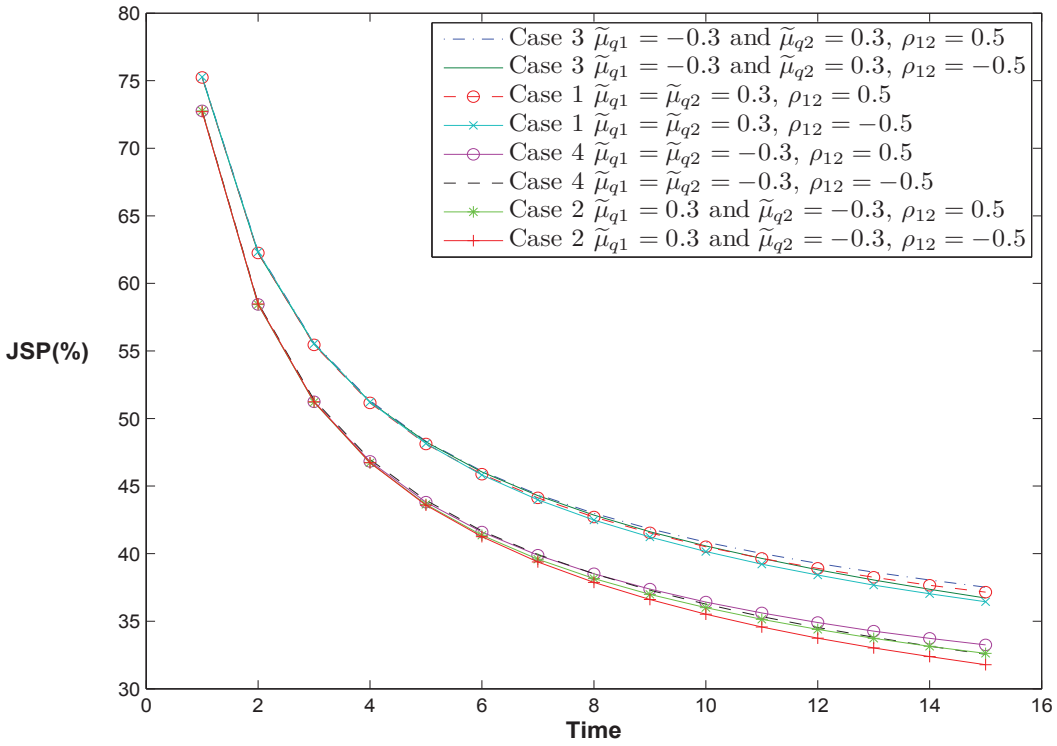

FIGURE 9.7. The impact of the sign of the average jump sizes on the joint survival probabilities for CCC-A paired firms. The initial leverage for the CCC-rated firm is L_1=73.2%, and for the A-rated firm is L_2=17.2%, and the volatilities are σ_1=0.299, σ_2 =0.184. Other parameters used are $\widetilde{\mu}_i = 0$, $\rho_{ir} = 0$, $\rho_{12} = 0.5$ and $\rho_{12} = -0.5$, $\widetilde{\lambda}_q = 0.1$ and $\sigma_{qi}^2 = 0.25$. Case 1: $\widetilde{\mu}_{q1} = \widetilde{\mu}_{q2} = 0.3$; Case 2: $\widetilde{\mu}_{q1} = 0.3$ and $\widetilde{\mu}_{q2} = -0.3$; Case 3: $\widetilde{\mu}_{q1} = -0.3$ and $\widetilde{\mu}_{q2} = 0.3$ and Case 4: $\widetilde{\mu}_{q1} = \widetilde{\mu}_{q2} = -0.3$.

Figure 9.6 plots the corresponding default correlation for the given change of jump intensity. The default correlation rises as the jump intensity increases for positively correlated firm, while when firms are negatively correlated, a higher jump intensity shifts the default correlation to positive values. This may be due to the fact that, when the frequency of the arrival of the jump event increases, the frequency of the leverage ratios jumping to higher values is increased, and this drives the leverage ratios closer to the default barrier. Therefore, if one firm has defaulted, the leverage ratio of the other firm moves in the opposite direction (because of $\rho_{12} < 0$) away from the default barrier. The leverage ratio of this firm is already very close to the default barrier (because the high frequency of jump arrivals), thus the default of one firm will be more likely to signal the possibility of the default of the other firm.

9.3.4. Impact of the Sign of the Average Jump Size.

This subsection studies the impact of the sign of the average jump sizes on joint survival probabilities and default probabilities for CCC-A paired firms. We consider four cases. First we assume that both firms have positive average jump sizes (say Case 1), the case when that both firms jump

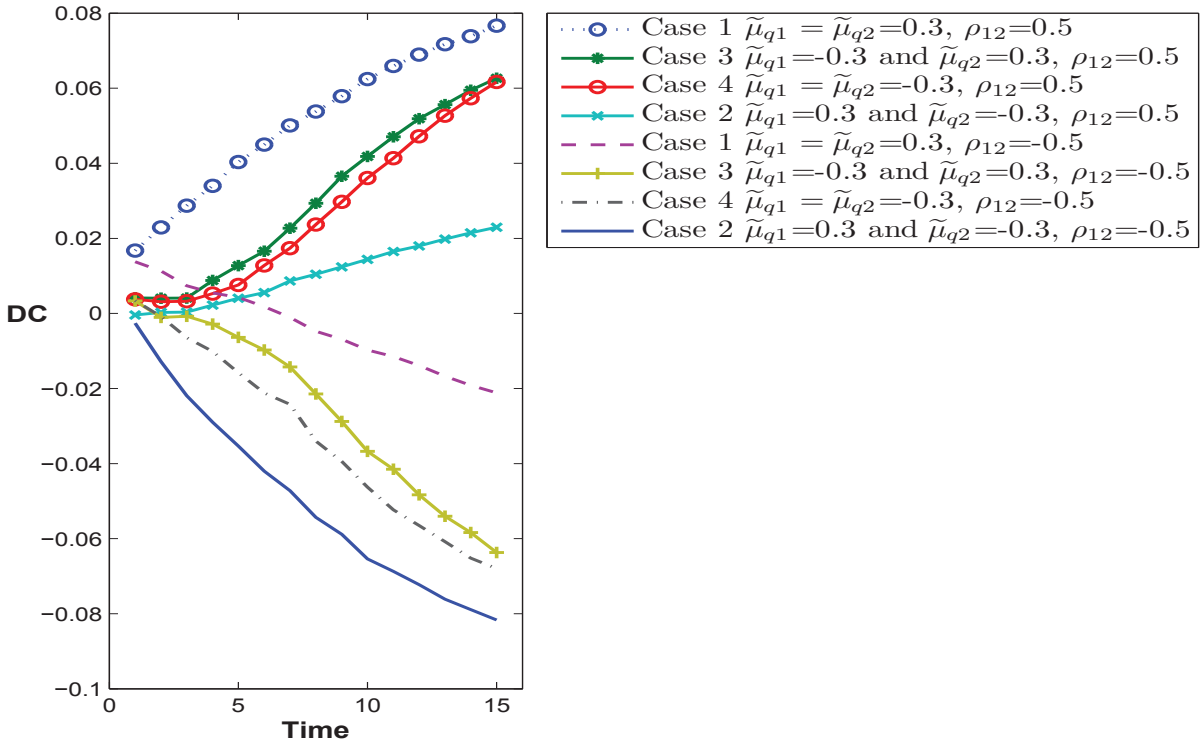

FIGURE 9.8. The impact of the sign of the average jump sizes on the default correlations for CCC-A paired firms. The initial leverage for the CCC-rated firm is L_1=73.2%, and for the A-rated firm is L_2=17.2%, and the volatilities are σ_1=0.299, σ_2 =0.184. Other parameters used are $\widetilde{\mu}_i = 0$, $\rho_{ir} = 0$, $\rho_{12} = 0.5$ and $\rho_{12} = -0.5$, $\widetilde{\lambda}_q = 0.1$ and $\sigma_{qi}^2 = 0.25$. Case 1: $\widetilde{\mu}_{q1} = \widetilde{\mu}_{q2} = 0.3$; Case 2: $\widetilde{\mu}_{q1} = 0.3$ and $\widetilde{\mu}_{q2} = -0.3$; Case 3: $\widetilde{\mu}_{q1} = -0.3$ and $\widetilde{\mu}_{q2} = 0.3$ and Case 4: $\widetilde{\mu}_{q1} = \widetilde{\mu}_{q2} = -0.3$.

up to positive values on average. In the second case both firms jump down to negative values on average. In the other two cases one firm jumps up to a positive value on average while the the other firm jump down to a negative value on average (Case 3), and one firm jump down to a negative value on average, while the the other firm jump up to a positive value on average (Case 4). The scenarios are illustrated as follows:

* Case 1: $\widetilde{\mu}_{q1} > 0$; $\widetilde{\mu}_{q2} > 0$ (both firms jump up to positive values on average);
* Case 2:$\widetilde{\mu}^*_{q1} < 0$; $\widetilde{\mu}^*_{q2} > 0$ (one firm jumps down to a negative value on average, while the other firm jumps up to a positive value on average);
* Case 3: $\widetilde{\mu}^*_{q1} > 0$; $\widetilde{\mu}^*_{q2} < 0$ (one firm jump up to a positive value on average while the other firm jump down to a negative value on average);
* Case 4: $\widetilde{\mu}_{q1} < 0$; $\widetilde{\mu}_{q2} < 0$ (both jump down to negative values on average);

Figure 9.7 shows that the joint survival probabilities for Case 3 is highest and Case 2 is lowest. Since in Case 3, the CCC-rated firm (one firm) jumps with a positive average jump size and the A-rated firm (the other firm) jumps with a negative average jump size, as discussed previously

the low quality firm will experience an increase in survival probability as the jump effect increases while for good quality firm's survival probability increases as the jump effect decreases. Therefore Case 3 combines these two increasing effects and hence the joint survival probabilities are highest. Case 2 is a reverse of the effect in Case 3. In contrast, the joint survival probabilities for Case 1 are higher than for Case 4, indicating that the CCC-rated firm weighs more heavily than the A-rated firm in their pairing relationship.

Figure 9.8 illustrates the corresponding default correlations for the different signs of the average jump sizes. The default correlation for Case 1 is the highest and Case 2 is lowest, for positively correlated firms, however, it is the other way around for negatively correlated firms, with default correlation for Case 2 being the highest (in absolute values) and Case 1 being the smallest. The argument is similar to the one for the impact of the jump size mean in Subsection 9.3.1. When the jump event occurs, both firms' leverage ratios jump to higher values on average with a larger jump size mean, and their leverage ratios are thus closer to the default barrier. Therefore, if either firm has defaulted, this is a signal about the other firm and on average its leverage ratio moves in the same direction (because of $\rho_{12} > 0$) towards the default barrier, since the leverage ratio of the second firm is already close to the default barrier, thus the default of this firm will become more likely. Therefore, default correlation for Case 1 is the highest for positively correlated firms. For Case2, the CCC-rated firm jumps down on average with a small value of the jump size mean, this moves its leverage ratio away from the default barrier. The A-rated firm jumps up on average with a positive average jump size, since the initial leverage ratio of A-rated firm is already far from default barrier, the other firm is even less likely to be driven to default. The argument is just reversed for the case when firms are negatively correlated.

9.4. Overview

This chapter has extended the two-firm model to incorporate jump risks. The Monte Carlo scheme developed in Chapter 8 has been extended to evaluate the joint survival probability. The impact of the jump components on joint survival probabilities and default correlations have been studied and the results (as well as the default probabilities in Chapter 8) are summarized in Table 9.1.

The default probability of the CCC-rated firm decreases as the jump effect increases, while the default probability of the A-rated firm increases as the jump effect increases. The joint survival probability of CCC-A paired firms declines as the jump effect increases.

When firms' leverage ratios are positively correlated ($\rho_{12} > 0$), the default correlation increases with the jump size mean or jump intensity, however, default correlation decreases as the jump

Jump-diffusion processes	Impact on PD		Impact on JSP	Impact on DC	
	CCC	A		$+\rho_{12}$	$-\rho_{12}$
jump size volatilities ↑	⇓	⇑	⇓	⇓	⇑
jump intensity ↑	⇓	⇑	⇓	⇑	⇓
jump size means ↑	⇓	⇑	⇓	⇑	⇓

TABLE 9.1. A summary of the impact on individual defaults, joint survival probabilities and default correlations for jump-diffusion processes.

size volatility increases. These effects are just reversed when the leverage ratios are negatively correlated ($\rho_{12} < 0$).

CHAPTER 10

Comparison of the Two-Firm Model for Different Processes

This thesis developed the two-firm model based on the three different processes of firms' leverage ratios. In the previous chapters, we have studied separately for these three types of processes, how their model parameters affect joint survival probabilities, individual default probabilities and default correlations. This chapter brings these three types of processes together and compares the individual default probabilities, joint survival probabilities and default correlations, so as to provide some insights for credit risk analysis and risk management. These processes represent the different features of firms that are considered in this thesis: the leverage processes either following simple continuous diffusion processes (captured by geometric Brownian motions), or having features that alter their capital structures (by use of mean-reverting processes), or facing default risk both from gradual processes as well as sudden unforeseen external shocks (modelled with jump-diffusion processes).

10.1. The Impact of Different Dynamic Leverage Ratio Processes on Default Probabilities

In this section, we bring the recent development of the one-firm leverage ratio models of default together and compare with the model with jump risk and see how these models perform when comparing their default probabilities to the S&P historical data, since there is no similar study in previous literature.

When firm's leverage ratio follows a geometric Brownian motion process (GBM), we have the extension of the Hui et al. (2007) model; when the leverage ratio follows a mean-reverting process to a constant target ratio (MR constant), we have the extension of the Collin-Dufresne & Goldstein (2001) model; if the leverage ratio follows a mean-reverting process to a time-dependent target ratio (MR time-dep.), we have the extension of the Hui et al. (2006) model); when the leverage ratio follows the jump-diffusion process (JP), we have the model proposed in Chapter 8 that extends the Hui et al. (2007) model.

Figure 10.1 shows that for a CCC-rated firm the geometric Brownian motion and jump-diffusion models can both generate default probabilities close to the historical data, while the model mean-reverting to a constant target ratio underestimates the S&P data, and the results for mean-reverting

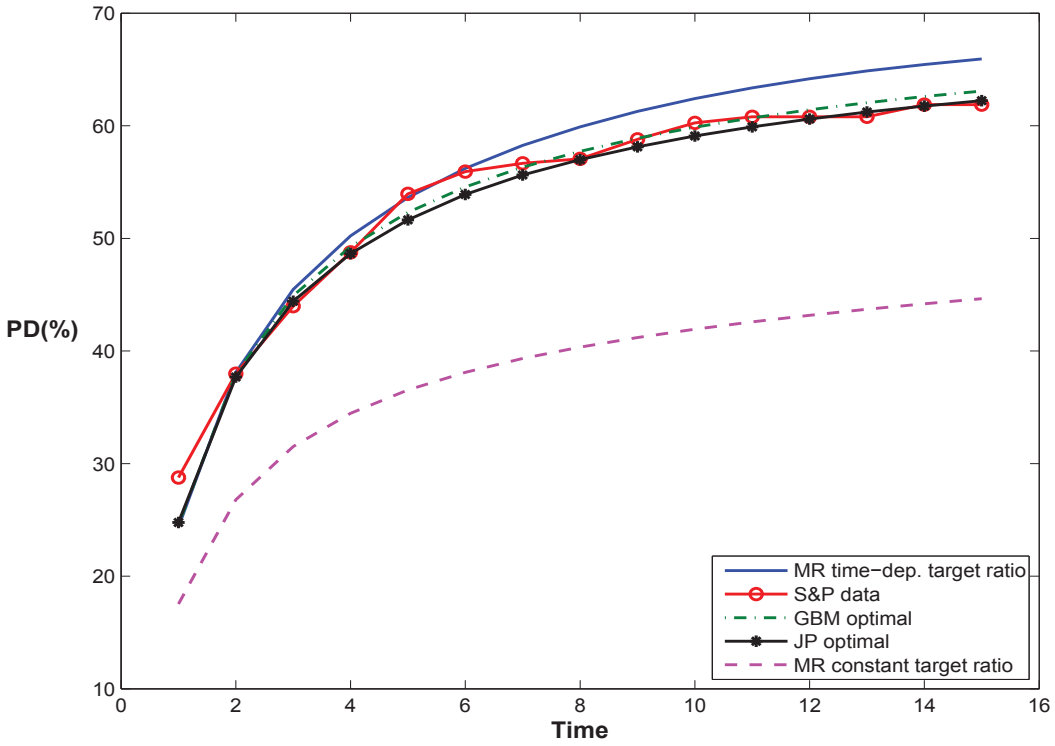

FIGURE 10.1. Comparison with S&P data for a CCC-rated firm of the default probabilities when the firm's leverage ratio follows the three processes the jump-diffusion process (JP), the geometric Brownian motion (GBM) process, the mean-reverting process to a constant target level (MR constant) and to a time-dependent target level (MR time-dep.). Initial leverage for the CCC-rated firm is $L = 73.2\%$ and the volatility is $\sigma_L = 0.299$. Other parameters used for the jump-diffusion model are $\widetilde{\mu}_L = 0$, $\rho_{Lr} = 0$, $\widetilde{\mu}_q = 0.3$, $\sigma_q^2 = 0.25$, $\widetilde{\lambda}_q = 0.1$. For the pure diffusion model, the drift is $\widetilde{\mu}_L = -0.007$. For mean-reverting models, the constant target level used is $\widetilde{\theta} = 31.5\%$ and the time-dependent target ratio is based on equation (7.66) with $\widetilde{\theta}(0) = 73.2\%$ and $\widetilde{\theta}(15) = 31.5\%$.

Fit to S&P data	GBM optimal	MR constant	MR time-dep.	JP optimal
CCC-rated firms	Fits well	Underestimate	Overestimate	Fits well
BBB-rated firms	No model fits well			
AA-rated firms	Underestimate	Underestimate	Underestimate	Fits well

TABLE 10.1. A summary of the comparison of different processes on individual default probabilities fit to S&P historical data for the one firm model.

to a time-dependent target ratio are an overestimate. However, Figure 10.2 shows that for a BBB-rated firm, no single model provides a good approximation to the historical data. For a AA-rated firm, Figure 10.3 shows that only the jump-diffusion model generates default probabilities close to the historical data, while all other models provide underestimates. Table 10.1 gives an overall summary and comparison of the results for the one firm model. The results indicate that if the leverage ratio of low credit quality firms follows a mean-reverting process, the firm's default

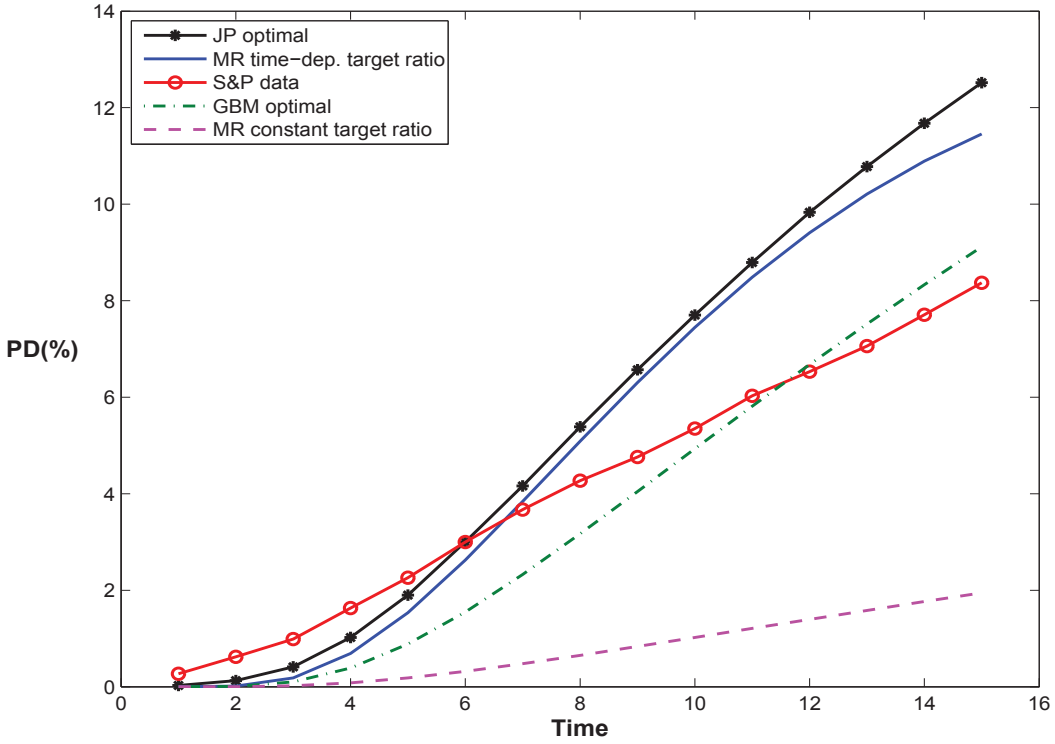

FIGURE 10.2. Comparison with S&P data for a BBB-rated firm of the default probabilities when the firm's leverage ratio follows the three processes the jump-diffusion process (JP), the geometric Brownian motion (GBM) process, the mean-reverting process to a constant target level (MR constant) and to a time-dependent target level (MR time-dep.). Initial leverage for the BBB-rated firm is $L = 31.5\%$ and the volatility is $\sigma_L = 0.213$. Other parameters used for the jump-diffusion model are $\widetilde{\mu}_L = 0$, $\rho_{Lr} = 0$, $\widetilde{\mu}_q = -0.3$, $\sigma_q^2 = 0.25$, $\widetilde{\lambda}_q = 0.1$. For the pure diffusion model, the drift is $\widetilde{\mu}_L = 0.002$. For mean-reverting models, the constant target level used is $\widetilde{\theta} = 31.5\%$ and the time-dependent target ratio is based on equation (7.66) with $\widetilde{\theta}(0) = 73.2\%$ and $\widetilde{\theta}(15) = 31.5\%$.

probability will be calculated to be lower, while the default of good credit quality firms is mainly due to sudden external shocks.

10.2. The Impact of Different Dynamic Leverage Ratio Processes on Joint Survival Probabilities

In this section, we compare the joint survival probabilities of the two-firm model when the firms' leverage ratios follow the three types of processes under consideration.

Figure 10.4 gives a comparison of the joint survival probabilities between the three types of processes with positive correlation $\rho_{12} = 0.5$ for CCC-BBB paired firms. The joint survival probability of the two-firm model when leverage ratios follow mean-reverting processes to a constant target ratio is the highest, while the other processes generate similar values of the joint survival probability and much lower (by about 20% at 15 years) than the highest. This seems to suggest

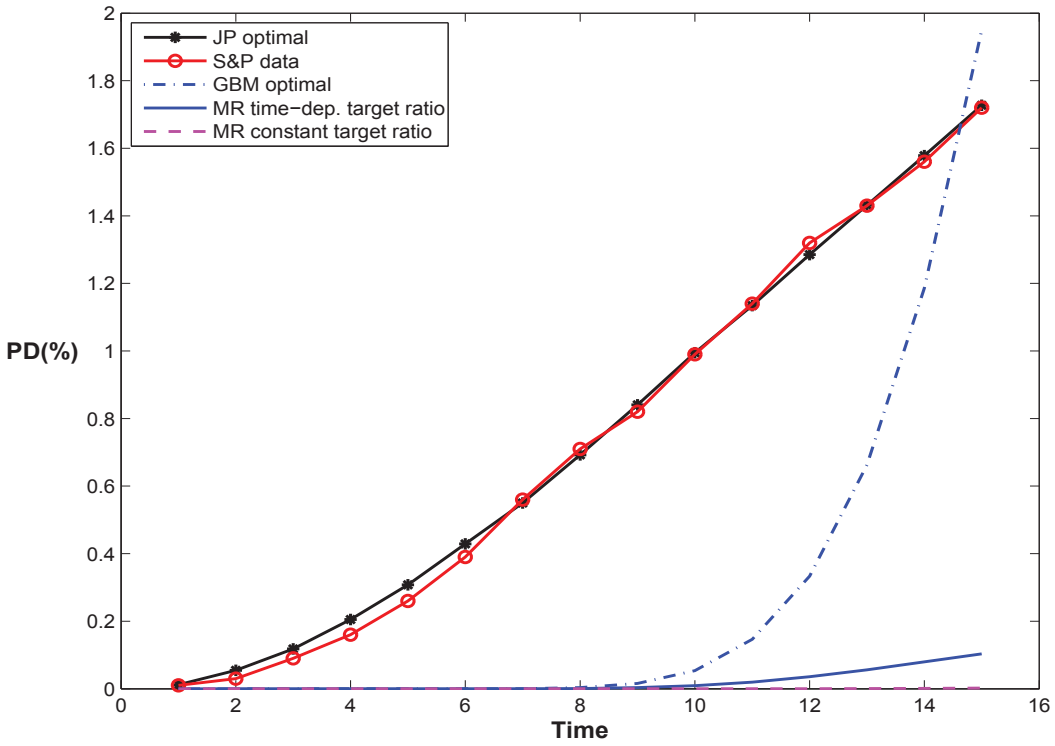

FIGURE 10.3. Comparison with S&P data for a AA-rated firm of the default probabilities when the firm's leverage ratio follows the three processes the jump-diffusion process (JP), the geometric Brownian motion (GBM) process, the mean-reverting process to a constant target level (MR constant) and to a time-dependent target level (MR time-dep.). Initial leverage for the AA-rated firm is $L = 9.5\%$ and the volatility is $\sigma_L = 0.156$. Other parameters used for the jump-diffusion model are $\widetilde{\mu}_L = 0$, $\rho_{Lr} = 0$, $\widetilde{\mu}_q = 0.6$, $\sigma_q^2 = 0.25$, $\widetilde{\lambda}_q = 0.1$. For the pure diffusion model, the drift is $\widetilde{\mu}_L = 0.08$. For mean-reverting models, the constant target level used is $\widetilde{\theta} = 31.5\%$ and the time-dependent target ratio is based on equation (7.66) with $\widetilde{\theta}(0) = 73.2\%$ and $\widetilde{\theta}(15) = 31.5\%$.

that when the firms' leverage ratios follow mean-reverting processes to a constant target ratio, their joint survival probabilities are higher.

10.3. The Impact of Different Dynamic Leverage Ratio Processes on Default Correlations

In this section, we compare the default correlations of the two-firm model when the firms' leverage ratios follow these three types of processes.

Figure 10.5 compares the default correlations between the two-firm model when the leverage ratios follow the three types of processes for CCC-BBB paired firms. We observe that for positively correlated firms ($\rho_{12} > 0$), the two-firm model based on different types of processes generate similar values of default correlation. When firms are negatively correlated ($\rho_{12} < 0$), with leverage ratios follow mean-reverting processes to constant target ratios, the model generates very small values (close to zero) of default correlation (in absolute value), while the model based on the other

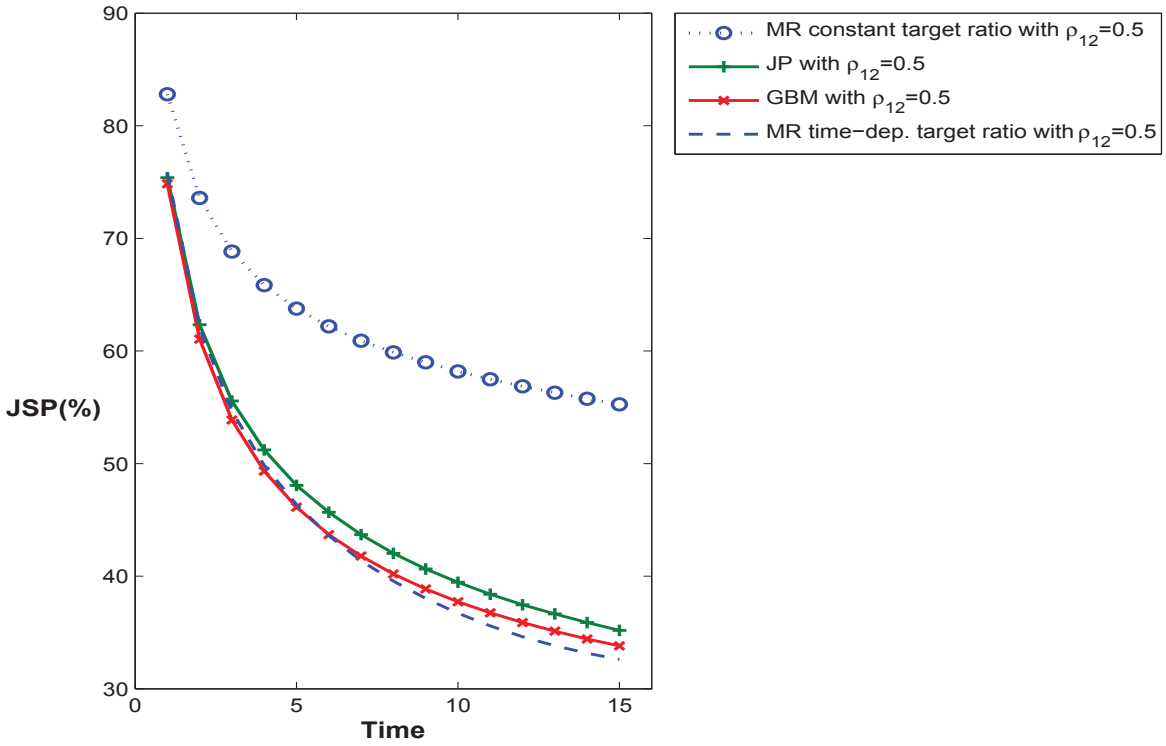

FIGURE 10.4. The comparison of joint survival probabilities for CCC-BBB paired firms when their leverage ratios follow the jump-diffusion process (JP), the geometric Brownian motion (GBM) process, the mean-reverting process to a constant target level (MR constant) and to a time-dependent target level (MR time-dep.). Initial leverage for thr CCC-rated firm is L_1=73.2%, for the BBB-rated firm is L_2=31.5% and volatilities are σ_1=0.299, σ_2 =0.213. Other parameters used for the jump-diffusion model are $\widetilde{\mu}_i = 0$, $\rho_{ir} = 0$, $\widetilde{\mu}_{q1} = 0.3$, $\widetilde{\mu}_{q2} = -0.3$ $\sigma_{qi}^2 = 0.25$, $\widetilde{\lambda}_q = 0.1$. For the pure diffusion model, the drifts used are $\widetilde{\mu}_1 = -0.007$ and $\widetilde{\mu}_1 = 0.002$. For mean-reverting models, the constant target level used is $\widetilde{\theta}_i = 31.5\%$ and the time-dependent target ratio is based on equation (7.66) with $\widetilde{\theta}_i(0) = 73.2\%$ and $\widetilde{\theta}_i(15) = 31.5\%$.

processes, gives similar values for default correlation. Note that the default correlation of the model based on mean-reverting to constant target ratios rises up at very small time, this is due to the division of very small value of individual default probabilities discussed in Chapter 6.

The result seems to indicate that if firms' leverage ratios are positively correlated, the default correlation seems less affected by which types of dynamics of firm's leverage ratio follows. However, it does become an issue if firms' leverage ratios are negatively correlated.

10.4. Overview

In this chapter, we have brought together and compared the performance of the model in terms of individual default probabilities, joint survival probabilities and default correlations, when firms' leverage ratios follow geometric Brownian motions, mean-reverting processes, or jump-diffusion

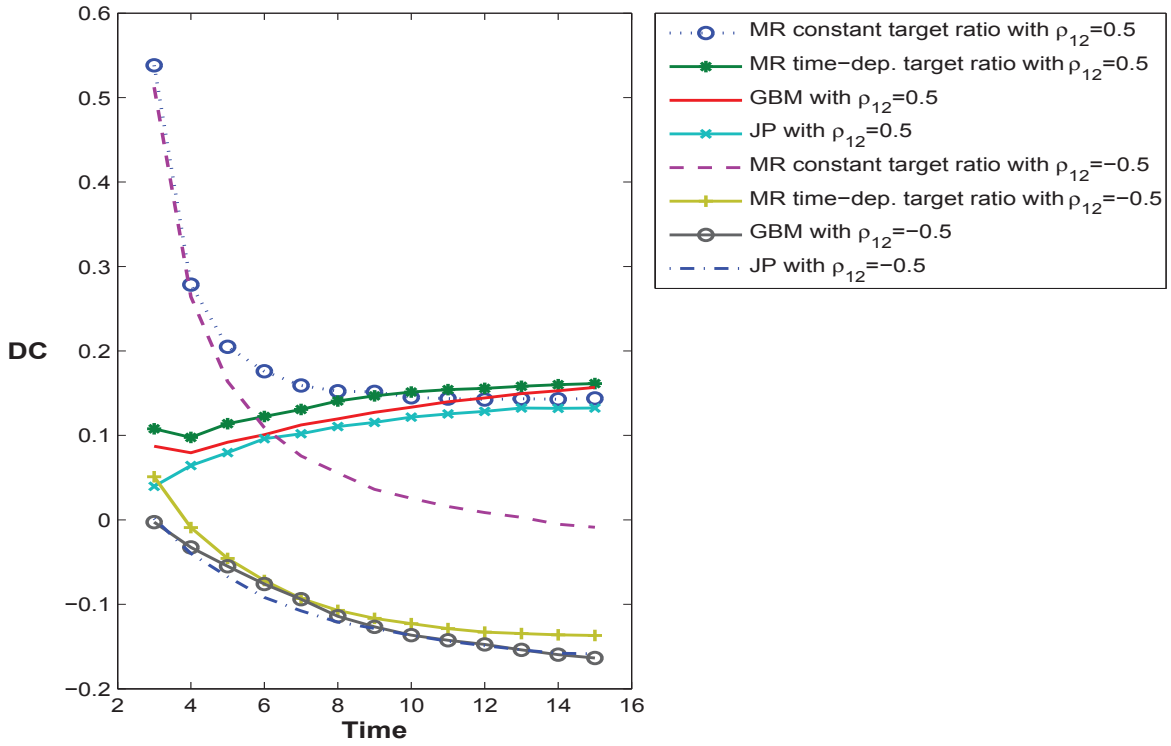

FIGURE 10.5. The comparison of default correlations for CCC-BBB paired firms when their leverage ratios follow the jump-diffusion process (JP), the geometric Brownian motion (GBM) process, the mean-reverting process to a constant target level (MR constant) and to a time-dependent target level (MR time-dep.). Initial leverage for the CCC-rated firm is L_1=73.2%, for the BBB-rated firm is L_2=31.5% and volatilities are σ_1=0.299, σ_2 =0.213. Other parameters used for the jump-diffusion model are $\widetilde{\mu}_i = 0$, $\rho_{ir} = 0$, $\widetilde{\mu}_{q1} = 0.3$, $\widetilde{\mu}_{q2} = -0.3$ $\sigma_{qi}^2 = 0.25$, $\widetilde{\lambda}_q = 0.1$. For the pure diffusion model, the drifts used are $\widetilde{\mu}_1 = -0.007$ and $\widetilde{\mu}_1 = 0.002$. For mean-reverting models, the constant target level used is $\widetilde{\theta}_i = 31.5\%$ and the time-dependent target ratio is based on equation (7.66) with $\widetilde{\theta}_i(0) = 73.2\%$ and $\widetilde{\theta}_i(15) = 31.5\%$.

processes, so as to provide some insights for credit risk analysis and risk management into the use of these different processes.

One may make a number of observations on the results. First, if the leverage ratio of low credit quality firms follows a mean-reverting process, the firm's default probability will be calculated to be lower. Second, the default of good credit quality firms is mainly due to sudden external shocks. Third, if the firms'leverage ratios follow mean-reverting processes to a constant target ratio, their joint survival probabilities are higher. Fourth, if firms' leverage ratios are positively correlated, the default correlation seems to be less affected by the type of dynamics the firm's leverage ratio follows. However, it becomes an issue if the firms' leverage ratios are negatively correlated. In future empirical research, it would be interesting to study which process best models the real market environment.

CHAPTER 11

Conclusions

In this chapter we summarize the main finding of the Thesis, draw some conclusions, and raise suggestions for the future research topics.

11.1. Summary

The principal aim of this thesis has been to extend the dynamic leverage ratio model for Hui et al. (2007) to the two-firm case so as to study its implications of default correlations and joint survival probabilities. In Chapter 2 we surveyed the relevant background literature. In Chapter 3 we reviewed the one-firm dynamic leverage ratio model of Hui et al. (2007) for corporate bond pricing. In their model by use of the separation of variables method, the corporate bond price can be interpreted as the product of a riskless bond price and a discounting factor. The risk-free bond price has a known closed-form solution, therefore the main focus is on solving for the discounting factor. We reviewed the method of images approach for obtaining a closed-form solution in terms of cumulative normal distribution functions and then the time varying barrier method proposed by Lo et al. (2003) to deal with the case in which parameters are time varying. In the second part of Chapter 3, we developed the framework for the dynamic leverage ratio model in the two-firm situation for pricing financial derivatives involving default risks among two firms using the credit linked note as the motivating example. We showed that the problem can be reduced to that of solving the partial differential equation for the risk ratio function. We also discussed the application of the results to the evaluation of default correlations.

In Chapter 4, we extended the method of images approach to the two-dimensional heat equation case and obtained the analytical solution subject to zero boundary conditions. This result was then applied to solve the partial differential equation for the risk ratio with constant coefficients. However, for coefficients in the time-dependent case, we extended the time varying barrier approach to obtain an approximate solution. In the second part of Chapter 4, we developed solutions in terms of the cumulative bivariate normal distribution functions. We saw that the limitation of the method of images approach applied in the two-dimensional situation is that it works only for certain values of the correlation coefficient between the dynamic leverage ratios of firms.

In order to obtain solutions for general values of the correlation coefficient, we consider numerical methods in Chapter 5. First we developed the alternating direction implicit numerical scheme based on Douglas & Rachford (1956) (the Douglas-Rachford scheme). The challenge here was to deal with the cross-derivative term and time-dependent drift terms. In order to develop an efficient numerical solution, we focussed on alternating direction implicit schemes that are unconditionally stable, that is stable without any restrictions on the time step. In Chapter 5, we also developed a Monte Carlo scheme to serve as a benchmark. We then discussed the accuracy and the convergence of the two methods and compared them to the solution developed by using the method of images with an extreme value of the correlation coefficient for which this method is applicable. We found that the relative percentage errors are generally less than 1% for the alternating direction implicit results based on using the number of time steps of 100 per year and number of spatial points of $3,830$, and for the Monte Carlo methods based on using the number of time steps of $36,500$ per year and the number of simulations between $500,000$ and $1,000,000$. When coefficients are time-dependent, we use the Monte Carlo results as a benchmark, and compared the accuracy of the alternating direction implicit method and the approximate solution based on the method of images. The relative percentage error for the approximate method is generally less than 1%. The relative percentage error for the alternating direction implicit method is less than 1% except at fifteen years where the error is around 1.3%.

In Chapter 6, we presented some numerical results for joint survival probabilities and default correlations of the two-firm model when the leverage ratios are driven by Brownian motion. We also studied the impact of different parameters on the joint survival probabilities and default correlations. Our main finding were that the joint survival probabilities rise if there is (i) a decrease in the leverage ratio volatility, the average mean levels, the initial leverage ratios, or (ii) an increase in the correlation coefficient between leverage ratios processes, or in the correlation coefficient between leverage ratio and interest rate processes. We also found that the default correlation (in absolute value) rises if there is (i) an increase in the firms' leverage ratios correlation, or their volatilities, or average mean levels, or initial leverage ratios, or (ii) a decrease in the correlation between firm's leverage ratio and interest rate.

In order to study the impact on default correlations of firms altering their capital structure, in Chapter 7 we extended the framework of the two-firm model to consider the case in which the dynamic leverage ratios are mean-reverting to constant target ratios and time-dependent target ratios. We extended the method of images approach to apply in this situation. Because of the limitation that the method of images approach works only for certain values of the correlation coefficient between leverage ratio processes, we also developed a Monte Carlo scheme to solve

the problem for all values of the correlation coefficient between leverage ratio processes so as to serve as a benchmark. We discussed the accuracy of the results for which we find that the relative percentage error compared to the Monte Carlo results are very large. A way to solve this problem is to develop the multi-stage approximation for the two-firm case. This task is beyond the scope of the present thesis and we leave it to future research. As our focus here is on the study of the impact of mean-reverting processes on default correlations, we do the calculations using the Monte Carlo simulation approach. In the last part of Chapter 7, we studied the impact of mean-reverting processes on joint survival probabilities and default correlations, in which the use of constant target ratios generate higher joint survival probability values and smaller default correlation values, and the use of time-dependent target ratios generates lower joint survival probabilities and larger default correlations.

Chapter 8 contains our next extension that draws on the discussion of Zhou (1997), who argues that in reality a firm can default either by a gradual diffusion process, or by a surprise due to unexpected external shocks. Zhou (2001*b*) combines these measures of risk by assuming that the firm asset value follows a jump-diffusion process. In order to capture the effect of external shocks on default correlations, we extend the model of Hui et al. (2007) to the case in which the dynamic leverage ratio follows a jump-diffusion process. We consider the one-firm model with jump risk, and extend the Monte Carlo scheme to cover this case. The impact of jump components: the jump size mean, the jump size volatility and the jump intensity, on single firm default probabilities for different credit rated firms are studied. We also find the optimal values of average jump size by calibrating to the S&P historical default data for different credit ratings. The results seems to indicate that for low rated firms, default is driven by either gradual diffusion or jumps, while for high rated firms, the default is mainly driven by jumps.

In Chapter 9, we extended the one-firm model with jump risk to the two-firm case, and studied the impact of jump risk on joint survival probabilities and default correlations. Our main findings were that the joint survival probability for a low and good credit quality paired firms declines as the jump effect increases. If firms' leverage ratios are positively correlated, the default correlation increases as the jump size volatility decreases, or as either the jump size mean or jump intensity increase. When firms' leverage ratios are negatively correlated, the jump effect on default correlation is just the other way around.

In Chapter 10, we brought together and compared the performance of the model in terms of individual default probabilities, joint survival probabilities and default correlations, when the leverage

ratios of firms follow simple geometric Brownian motions, mean-reverting processes and jump-diffusion processes, so as to provide some insights for credit risk analysis and risk management. The results seem to suggest that if the leverage ratios of low credit quality firms follow a mean-reverting process, the firm's default probability will be lower. On the other hand, the results show that defaults of good credit quality firms are mainly due to the sudden external shocks. The results also seem to suggest a higher joint survival probability if firms'leverage ratios follow mean-reverting processes to a constant target ratio. The result indicate that the default correlation seems less affected by which types of dynamics the firm's leverage ratio follows if firms' leverage ratios are positively correlated, however, if firms's leverage ratios are negatively correlated, this becomes an issue.

11.2. Topics for Future Research

The Thesis has confronted the mathematical challenges associated with the solution of first passage time problems in a two-dimensional situation, the further development of which will provide some major directions for future research. For example, the method of images approach in the two-dimensional case only works for certain values of the correlation coefficient between firms' leverage ratio. An interesting problem for future research would be to try to develop some approximate ways of completing the loop for arbitrary values of the correlation coefficient. Moreover, the accuracy of the solution based on the method of images approach for the model with mean-reverting processes is very low, therefore an improvement in the accuracy of the solution by developing the multi-stage approximation scheme is another important issue for future research.

We note that it is difficult to obtain the analytical solution (even approximated ones) for the first passage time problem of jump-diffusion processes. Such problems are usually solved by using Monte Carlo simulation. However, Monte Carlo simulation requires long computational times, especially in the two-dimensional case, therefore the development of an efficient and accurate numerical scheme, for example the method of lines approach (see for example Chiarella et al. (2009)), is a fruitful main topic for future research.

Another approach to solving the first passage time problem is the two-dimensional generalization of the Fortet (1943) equation that was used by Collin-Dufresne & Goldstein (2001), who solved the first passage time density under the risk-neutral measure in their one dimensional model by discretizing the generalized Fortet equation. The extension of this approach to the two-firm model would be an important topic for future research. The recent work of Bernard et al. (2008) offers one possible approach.

We note that the findings in this thesis are mostly based on the study of the impact of model parameters the values of which have been from various pervious studies and so are plausible. The values of the parameters need to be obtained by some robust econometric estimation methodology from market data, this will certainly be a key topic for future research. Finally, the results of this thesis could be used as a benchmark for assessing different copula functions used in valuing default correlations, which would be another topic for future research.

APPENDIX A

Applying the Separation of Variables to the PDE for the Corporate Bond Price

This appendix applies the separation of variables technique to simplify the partial differential equation for corporate bond price of the one-firm model. Suppose the differential equation (3.4) can be written in terms of two separate functions as

$$P(L,r,t) = f(r,t)\widehat{P}(L,t), \tag{A.1}$$

where function $f(r,t)$ depends only on r and t, and $\widehat{P}(L,t)$ is a function of L and t only.

To determine differential equations of $f(r,t)$ and $\widehat{P}(L,t)$, we note that

$$\frac{\partial P}{\partial t} = \widehat{P}\frac{\partial f}{\partial t} + f\frac{\partial \widehat{P}}{\partial t}, \tag{A.2}$$

$$\frac{\partial P}{\partial L} = f\frac{\partial \widehat{P}}{\partial L}, \quad \frac{\partial^2 P}{\partial L^2} = f\frac{\partial^2 \widehat{P}}{\partial L^2}, \tag{A.3}$$

$$\frac{\partial^2 P}{\partial r \partial L} = \frac{\partial f}{\partial r}\frac{\partial \widehat{P}}{\partial L}, \quad \frac{\partial P}{\partial r} = \widehat{P}\frac{\partial f}{\partial r}, \quad \frac{\partial^2 P}{\partial r^2} = \widehat{P}\frac{\partial^2 f}{\partial r^2}. \tag{A.4}$$

Substituting equations (A.1)-(A.4) into (3.4), we obtain the partial differential equation

$$\begin{aligned} -\widehat{P}\frac{\partial f}{\partial t} - f\frac{\partial \widehat{P}}{\partial t} &= f\frac{1}{2}\sigma_L^2(t)L\frac{\partial^2 \widehat{P}}{\partial L} + \widehat{P}\frac{1}{2}\sigma_r^2(t)\frac{\partial^2 f}{\partial r^2} \\ &\quad + \frac{\partial f}{\partial r}\rho_{Lr}(t)\sigma_L(t)\sigma_r(t)L\frac{\partial \widehat{P}}{\partial L} + f\widetilde{\mu}_L(t)L\frac{\partial \widehat{P}}{\partial L} \\ &\quad + \widehat{P}\kappa_r(t)\left[\widetilde{\theta}_r(t) - r\right]\frac{\partial f}{\partial r} - rf\widehat{P}. \end{aligned} \tag{A.5}$$

We group f and $\widehat{P}$ terms respectively, so that (A.5) becomes

$$\begin{aligned} &\frac{1}{f}\left(\frac{\partial f}{\partial t} + \frac{1}{2}\sigma_r^2(t)\frac{\partial^2 f}{\partial r^2} + \kappa_r(t)\left[\widetilde{\theta}_r(t) - r\right]\frac{\partial f}{\partial r} - rf\right) \\ &= \frac{1}{\widehat{P}}\left(-\frac{\partial \widehat{P}}{\partial t} - \frac{1}{2}\sigma_L^2(t)L^2\frac{\partial^2 \widehat{P}}{\partial L^2} - \frac{1}{f}\frac{\partial f}{\partial r}\rho_{Lr}(t)\sigma_L(t)\sigma_r(t)L\frac{\partial \widehat{P}}{\partial L} - \widetilde{\mu}_L(t)L\frac{\partial \widehat{P}}{\partial L}\right). \end{aligned} \tag{A.6}$$

Since the LHS of (A.6) depends only on r and t and the RHS only on L and t, the only way that both sides can be equal for all possible values of r, L and t is that both sides equal to a constant. We note that the partial differential equation in the bracket of LHS of (A.6) is the partial differential

equation of the risk-free bond price $B(r,t)$ of the Hull & White (1990) model, which satisfies

$$\frac{\partial B}{\partial t}+\frac{1}{2}\sigma_r^2(t)\frac{\partial^2 B}{\partial r^2}+\kappa_r(t)(\widetilde{\theta}_r(t)-r)\frac{\partial B}{\partial r}-rB=0. \tag{A.7}$$

Hence, both sides of (A.6) equal zero, and (A.1) becomes

$$P(L,r,t)=B(r,t)\widehat{P}(L,t). \tag{A.8}$$

The solution of the risk-free bond price $B(r,t)$ is[1]

$$B(r,t)=e^{-a(t)+b(t)r}, \tag{A.9}$$

where

$$b(t) = -\int_t^T e^{\mathcal{K}(t)-\mathcal{K}(v)}dv, \tag{A.10}$$

$$a(t) = \int_t^T b(v)\kappa_r(v)\widetilde{\theta}_r(v)dv-\frac{1}{2}\int_t^T \sigma_r^2(v)b^2(v)dv, \tag{A.11}$$

for $\mathcal{K}(t)=\int_0^t \kappa_r(u)du$.

Moreover, the solution (A.9) yields that the first derivative of $B(r,t)$ with respect to r satisfies

$$\frac{1}{B}\frac{\partial B}{\partial r} = b(t). \tag{A.12}$$

Substituting from equations (A.7) and (A.12) into (A.5), we obtain the differential equation of $\widehat{P}(L,t)$ as

$$-\frac{\partial \widehat{P}}{\partial t} = \frac{1}{2}\sigma_L^2(t)L^2\frac{\partial^2 \widehat{P}}{\partial L^2}+\left[\widetilde{\mu}_L(t)+\rho_{Lr}(t)\sigma_L(t)\sigma_r(t)b(t)\right]L\frac{\partial \widehat{P}}{\partial L}, \tag{A.13}$$

in the region of $0\leq t\leq T$.

Since the final time condition for the risk-free bond price is $B(r,T)=1$, substituting this and equation (3.9) into boundary conditions (3.5)-(3.6), gives boundary conditions for $\widehat{P}$, namely

$$\widehat{P}(L,T) = 1, \tag{A.14}$$

$$\widehat{P}(\widehat{L},t) = 0. \tag{A.15}$$

[1]See for example, Wilmott et al. (1995) (Section 17.6) or Hull (2000) (Section 21.9).

APPENDIX B

Transformation to the Heat Equation with Time Independent Coefficients

This appendix gives the details of the transformation in (3.31).

Proposition B.1. *The solution to the partial differential equation (3.30) may be written*

$$\bar{P}(x,\tau) = e^{\eta x+\xi\tau}u(x,\zeta), \tag{B.1}$$

where η, ξ and ζ are constants given by

$$\eta = -\frac{\gamma}{\sigma_L}, \tag{B.2}$$

$$\xi = -\frac{1}{2}(\frac{\gamma}{\sigma_L})^2, \tag{B.3}$$

$$\zeta = \sigma_L\tau. \tag{B.4}$$

and $u(x,\zeta)$ satisfies the partial differential equation

$$\frac{\partial u}{\partial \zeta} = \frac{1}{2}\frac{\partial^2 u}{\partial X^2}. \tag{B.5}$$

Proof: We Calculate

$$\begin{aligned}
\frac{\partial \bar{P}}{\partial \tau} &= e^{\eta x+\xi\tau}\left[\xi u + \frac{\partial u}{\partial \tau}\right], \\
\frac{\partial \bar{P}}{\partial x} &= e^{\eta x+\xi\tau}\left[\eta u + \frac{\partial u}{\partial x}\right], \\
\frac{\partial^2 \bar{P}}{\partial x^2} &= e^{\eta x+\xi\tau}\left[\eta^2 u + 2\eta\frac{\partial u}{\partial x} + \frac{\partial^2 u}{\partial x^2}\right].
\end{aligned} \tag{B.6}$$

Substituting from equations (B.6) into equation (3.15), the partial differential equation reduces to

$$\begin{aligned}
\frac{\partial u}{\partial \tau} &= \frac{1}{2}\sigma_L^2\left[\eta^2 u + 2\eta\frac{\partial u}{\partial x} + \frac{\partial^2 u}{\partial x^2}\right] + \gamma\left[\eta u + \frac{\partial u}{\partial x}\right], \\
&= \frac{1}{2}\sigma_L^2\frac{\partial^2 u}{\partial x^2} + (\sigma_L^2\eta + \gamma)\frac{\partial u}{\partial x} + (-\xi + \frac{1}{2}\sigma_L^2\eta^2 + \gamma\eta)u.
\end{aligned} \tag{B.7}$$

The $\frac{\partial u}{\partial x}$ and u terms can be eliminated by choosing

$$\sigma_L^2\eta + \gamma = 0 \quad \Rightarrow \quad \eta = -\frac{\gamma}{\sigma_L^2}, \tag{B.8}$$

$$-\xi + \frac{1}{2}\sigma_L^2\eta^2 + \gamma\eta = 0 \quad \Rightarrow \quad \xi = -\frac{1}{2}\frac{\gamma^2}{\sigma_L^2}, \tag{B.9}$$

the (B.7) becomes

$$\frac{\partial u}{\partial \tau} = \frac{1}{2}\sigma_L^2 \frac{\partial^2 u}{\partial x^2}. \tag{B.10}$$

Since $u(x,\zeta)$ depends on ζ, we can express $\frac{\partial u}{\partial \tau} = \frac{\partial \zeta}{\partial \tau}\frac{\partial u}{\partial \zeta}$, then (B.10) becomes

$$[\sigma_L^2]^{-1}\frac{\partial \zeta}{\partial \tau}\frac{\partial u}{\partial \zeta} = \frac{1}{2}\frac{\partial^2 u}{\partial x^2}, \tag{B.11}$$

In order to eliminate the term $[\sigma_L^2]^{-1}$, we choose ζ to satisfy

$$[\sigma_L^2]^{-1}\frac{\partial \zeta}{\partial \tau} = 1, \tag{B.12}$$

from which

$$\zeta = \sigma_L^2 \tau. \tag{B.13}$$

So that (B.11) reduces to the heat equation (B.5).

■

APPENDIX C

Transformation to the Heat Equation with Time Dependent Parameters

This appendix illustrate the transformation of the equation (3.39).

Consider

$$e^{c(\tau)\frac{\partial}{\partial x}} f(x,\tau), \tag{C.1}$$

where $c(\tau)$ is a time-dependent function. $e^{\frac{\partial}{\partial x}}$ is an operator (the exponential operator), it operates on a function to produce the other function according to the rule (3.38).

In order to transform the partial differential equation (3.38) using (3.39), we need to take the first derivative of (C.1) with respect to τ, namely to calculate

$$\frac{\partial}{\partial \tau}\big[e^{c(\tau)\frac{\partial}{\partial x}} f(x,\tau)\big]. \tag{C.2}$$

This is done by applying the Baker-Campbell-Hausdorff formula. The Baker-Campbell-Hausdorff formula is widely used in quantum mechanics to obtain a solution with combined exponentials of operators when these operators do not commute. The Baker-Campbell-Hausdorff formula is defined as (see for example, Hassani (1998), Chapter 2.2)

$$e^{\mathbf{A}}\mathbf{B}e^{-\mathbf{A}} \equiv \mathbf{B} + [\mathbf{A},\mathbf{B}] + \frac{1}{2!}[\mathbf{A},[\mathbf{A},\mathbf{B}]] + \cdots, \tag{C.3}$$

where $\mathbf{A}$ and $\mathbf{B}$ are operators. The expression $[\mathbf{A},\mathbf{B}]$ is called the commutator of two operators, and is defined as $[\mathbf{A},\mathbf{B}] \equiv \mathbf{AB} - \mathbf{BA}$.

To carry out the operation in (C.2), we consider the following proposition.

Proposition C.1. *The expression* (C.2) *may be written*

$$e^{c(\tau)\frac{\partial}{\partial x}}\Big[\frac{\partial f(x,\tau)}{\partial \tau} + \frac{\partial c(\tau)}{\partial \tau}\frac{\partial f(x,\tau)}{\partial x}\Big]. \tag{C.4}$$

Proof: First, we multiply (C.2) by the term

$$e^{c(\tau)\frac{\partial}{\partial x}} e^{-c(\tau)\frac{\partial}{\partial x}} \equiv 1, \tag{C.5}$$

to obtain

$$\begin{aligned} &\big(e^{c(\tau)\frac{\partial}{\partial x}} e^{-c(\tau)\frac{\partial}{\partial x}}\big)\frac{\partial}{\partial \tau}\big[e^{c(\tau)\frac{\partial}{\partial x}} f(x,\tau)\big] \\ = \;& e^{c(\tau)\frac{\partial}{\partial x}}\Big(e^{-c(\tau)\frac{\partial}{\partial x}}\frac{\partial}{\partial \tau}e^{c(\tau)\frac{\partial}{\partial x}}\Big) f(x,\tau). \end{aligned} \tag{C.6}$$

Considering the term in the bracket and applying the Baker-Campbell-Hausdorff formula (C.3) (setting $A \equiv -c(\tau)\frac{\partial}{\partial x}$ and $B \equiv \frac{\partial}{\partial \tau}$), we have

$$\begin{aligned}
&\Big(e^{-c(\tau)\frac{\partial}{\partial x}}\frac{\partial}{\partial \tau}e^{c(\tau)\frac{\partial}{\partial x}}\Big) \\
&= \frac{\partial}{\partial \tau} + [-c(\tau)\frac{\partial}{\partial x}, \frac{\partial}{\partial \tau}] + \frac{1}{2!}[-c(\tau)\frac{\partial}{\partial x}, [-c(\tau)\frac{\partial}{\partial x}, \frac{\partial}{\partial \tau}]] + \cdots, \\
&= \frac{\partial}{\partial \tau} + \Big(-c(\tau)\frac{\partial}{\partial x}\cdot\frac{\partial}{\partial \tau} - \frac{\partial}{\partial \tau}\cdot(-c(\tau)\frac{\partial}{\partial x})\Big) + 0, \\
&= \frac{\partial}{\partial \tau} + \frac{\partial c(\tau)}{\partial \tau}\frac{\partial}{\partial x}. \qquad \text{(C.7)}
\end{aligned}$$

Note that the higher order terms vanish, as is quite straight forward to see, for example, by calculating the second term

$$\begin{aligned}
\frac{1}{2!}[-c(\tau)\frac{\partial}{\partial x}, [-c(\tau)\frac{\partial}{\partial x}, \frac{\partial}{\partial \tau}]] &= \frac{1}{2!}[-c(\tau)\frac{\partial}{\partial x}, \frac{\partial c(\tau)}{\partial \tau}\frac{\partial}{\partial x}] \\
&= -c(\tau)\frac{\partial}{\partial x}\cdot\frac{\partial c(\tau)}{\partial \tau}\frac{\partial}{\partial x} - \frac{\partial c(\tau)}{\partial \tau}\frac{\partial}{\partial x}\cdot(-c(\tau)\frac{\partial}{\partial x}) \\
&= -c(\tau)\frac{\partial c(\tau)}{\partial \tau}\frac{\partial^2}{\partial x^2} + c(\tau)\frac{\partial c(\tau)}{\partial \tau}\frac{\partial^2}{\partial x^2} = 0. \qquad \text{(C.8)}
\end{aligned}$$

Substituting (C.7) into (C.6), we obtain

$$\begin{aligned}
&e^{c(\tau)\frac{\partial}{\partial x}}\Big(\frac{\partial}{\partial \tau} + \frac{\partial c(\tau)}{\partial \tau}\frac{\partial}{\partial x}\Big)f(x,\tau) \\
&= e^{c(\tau)\frac{\partial}{\partial x}}\Big[\frac{\partial f(x,\tau)}{\partial \tau} + \frac{\partial c(\tau)}{\partial \tau}\frac{\partial f(x,\tau)}{\partial x}\Big]. \qquad \text{(C.9)}
\end{aligned}$$

■

We also take the first and second derivatives of (C.1) with respect to x in the following propositions.

Proposition C.2. *The following result holds:-*

$$\frac{\partial}{\partial x}\big[e^{c(\tau)\frac{\partial}{\partial x}}f(x,\tau)\big] = e^{c(\tau)\frac{\partial}{\partial x}}\Big[\frac{\partial f(x,\tau)}{\partial x}\Big]. \qquad \text{(C.10)}$$

Proof: We calculate

$$\frac{\partial}{\partial x}\big[e^{c(\tau)\frac{\partial}{\partial x}}f(x,\tau)\big], \qquad \text{(C.11)}$$

in a similar way to Proposition C.1. We multiply by the term

$$e^{c(\tau)\frac{\partial}{\partial x}}e^{-c(\tau)\frac{\partial}{\partial x}} \equiv 1, \qquad \text{(C.12)}$$

to obtain

$$\begin{aligned}
&\big(e^{c(\tau)\frac{\partial}{\partial x}}e^{-c(\tau)\frac{\partial}{\partial x}}\big)\frac{\partial}{\partial x}\big[e^{c(\tau)\frac{\partial}{\partial x}}f(x,\tau)\big] \\
&= e^{c(\tau)\frac{\partial}{\partial x}}\Big(e^{-c(\tau)\frac{\partial}{\partial x}}\frac{\partial}{\partial x}e^{c(\tau)\frac{\partial}{\partial x}}\Big)f(x,\tau). \qquad \text{(C.13)}
\end{aligned}$$

Again apply the Baker-Campbell-Hausdorff formula to the term in the brackets to botain

$$\begin{aligned}
&\Big(e^{-c(\tau)\frac{\partial}{\partial x}}\frac{\partial}{\partial x}e^{c(\tau)\frac{\partial}{\partial x}}\Big)\\
&= \frac{\partial}{\partial x}+[-c(\tau)\frac{\partial}{\partial x},\frac{\partial}{\partial x}]+\frac{1}{2!}[-c(\tau)\frac{\partial}{\partial x},[-c(\tau)\frac{\partial}{\partial x},\frac{\partial}{\partial x}]]+\cdots,\\
&= \frac{\partial}{\partial x}+\Big(-c(\tau)\frac{\partial}{\partial x}\cdot\frac{\partial}{\partial x}-\frac{\partial}{\partial x}\cdot(-c(\tau)\frac{\partial}{\partial x})\Big)+\cdots,\\
&= \frac{\partial}{\partial x}+0. \qquad \text{(C.14)}
\end{aligned}$$

Again all higher order terms are zero.

Substituting (C.14) into (C.13), we obtain

$$e^{c(\tau)\frac{\partial}{\partial x}}\Big[\frac{\partial f(x,\tau)}{\partial x}\Big]. \qquad \text{(C.15)}$$

■

Proposition C.3. *The following result holds:-*

$$\frac{\partial^2}{\partial x^2}\big[e^{c(\tau)\frac{\partial}{\partial x}}f(x,\tau)\big]=e^{c(\tau)\frac{\partial}{\partial x}}\Big[\frac{\partial^2 f(x,\tau)}{\partial x^2}\Big]. \qquad \text{(C.16)}$$

Proof: We calculate

$$\frac{\partial^2}{\partial x^2}\big[e^{c(\tau)\frac{\partial}{\partial x}}f(x,\tau)\big], \qquad \text{(C.17)}$$

in a similar way to Proposition C.1. We multiply by the term

$$e^{c(\tau)\frac{\partial}{\partial x}}e^{-c(\tau)\frac{\partial}{\partial x}}\equiv 1, \qquad \text{(C.18)}$$

to obtain

$$\begin{aligned}
&\big(e^{c(\tau)\frac{\partial}{\partial x}}e^{-c(\tau)\frac{\partial}{\partial x}}\big)\frac{\partial^2}{\partial x^2}\big[e^{c(\tau)\frac{\partial}{\partial x}}f(x,\tau)\big]\\
&= e^{c(\tau)\frac{\partial}{\partial x}}\Big(e^{-c(\tau)\frac{\partial}{\partial x}}\frac{\partial^2}{\partial x^2}e^{c(\tau)\frac{\partial}{\partial x}}\Big)f(x,\tau). \qquad \text{(C.19)}
\end{aligned}$$

Apply the Baker-Campbell-Hausdorff formula to the term in the bracket to obtain

$$\begin{aligned}
&\Big(e^{-c(\tau)\frac{\partial}{\partial x}}\frac{\partial^2}{\partial x^2}e^{c(\tau)\frac{\partial}{\partial x}}\Big)\\
&= \frac{\partial^2}{\partial x^2}+[-c(\tau)\frac{\partial}{\partial x},\frac{\partial^2}{\partial x^2}]+\frac{1}{2!}[-c(\tau)\frac{\partial}{\partial x},[-c(\tau)\frac{\partial}{\partial x},\frac{\partial^2}{\partial x^2}]]+\cdots,\\
&= \frac{\partial^2}{\partial x^2}+\Big(-c(\tau)\frac{\partial}{\partial x}\cdot\frac{\partial^2}{\partial x^2}-\frac{\partial^2}{\partial x^2}\cdot(-c(\tau)\frac{\partial}{\partial x})\Big)+\cdots,\\
&= \frac{\partial^2}{\partial x^2}+0. \qquad \text{(C.20)}
\end{aligned}$$

Again all higher order terms are zero.

Substituting (C.20) into (C.19), we obtain the term

$$e^{c(\tau)\frac{\partial}{\partial x}}\Big[\frac{\partial^2 f(x,\tau)}{\partial x^2}\Big], \tag{C.21}$$

and hence the result of the proposition is proven.

■

Next, we obtain the functional form of the partial differential equation (3.15) after taking the transformation, namely by setting

$$\bar{P}(x,\tau) \;=\; e^{\int_0^\tau \gamma(v)dv\frac{\partial}{\partial x}}\widetilde{P}(x,\tau). \tag{C.22}$$

We consider the following proposition.

Proposition C.4. *The quantity $\widetilde{P}(x,\tau)$ appearing in the representation* (C.22) *satisfies the partial differential equation*

$$\frac{\partial \widetilde{P}}{\partial \tau} \;=\; \frac{1}{2}\sigma_L^2(\tau)\frac{\partial^2 \widetilde{P}}{\partial x^2}. \tag{C.23}$$

Proof: The partial differential equation $\widetilde{P}(x,\tau)$ is obtained by calculating

$$\frac{\partial \bar{P}}{\partial \tau} \;=\; \frac{\partial}{\partial \tau}[e^{\int_0^\tau \gamma(v)dv\frac{\partial}{\partial x}}\widetilde{P}], \tag{C.24}$$

$$\frac{\partial \bar{P}}{\partial x} \;=\; \frac{\partial}{\partial x}[e^{\int_0^\tau \gamma(v)dv\frac{\partial}{\partial x}}\widetilde{P}], \tag{C.25}$$

$$\frac{\partial^2 \bar{P}}{\partial x^2} \;=\; \frac{\partial^2}{\partial x^2}[e^{\int_0^\tau \gamma(v)dv\frac{\partial}{\partial x}}\widetilde{P}]. \tag{C.26}$$

By the relations in Proposition C.1, Proposition C.2 and Proposition C.3, we obtain

$$\frac{\partial \bar{P}}{\partial \tau} \;=\; e^{\int_0^\tau \gamma(v)dv\frac{\partial}{\partial x}}\Big(\frac{\partial \widetilde{P}}{\partial \tau}+\frac{\partial[e^{\int_0^\tau \gamma(v)dv}]}{\partial \tau}\frac{\partial \widetilde{P}}{\partial x}\Big)=\Big(\frac{\partial \widetilde{P}}{\partial \tau}+\gamma(\tau)\frac{\partial \widetilde{P}}{\partial x}\Big), \tag{C.27}$$

$$\frac{\partial \bar{P}}{\partial x} \;=\; e^{\int_0^\tau \gamma(v)dv\frac{\partial}{\partial x}}\frac{\partial \widetilde{P}}{\partial x}, \tag{C.28}$$

$$\frac{\partial^2 \bar{P}}{\partial x^2} \;=\; e^{\int_0^\tau \gamma(v)dv\frac{\partial}{\partial x}}\frac{\partial^2 \widetilde{P}}{\partial x^2}. \tag{C.29}$$

Substituting (C.29) into the partial differential equation (3.15), we obtain

$$\frac{\partial \widetilde{P}}{\partial \tau}+\gamma(\tau)\frac{\partial \widetilde{P}}{\partial x} \;=\; \frac{1}{2}\sigma_L^2(\tau)\frac{\partial^2 \widetilde{P}}{\partial x^2}+\gamma(\tau)\frac{\partial \widetilde{P}}{\partial x}. \tag{C.30}$$

We see readily that the $\partial\widetilde{P}/\partial x$ term drops out so that

$$\frac{\partial \widetilde{P}}{\partial \tau} \;=\; \frac{1}{2}\sigma_L^2(\tau)\frac{\partial^2 \widetilde{P}}{\partial x^2}. \tag{C.31}$$

■

Note that, equation (C.31) has a time dependent coefficient. This can be reduced by transforming the time to maturity variable. Consider the following proposition.

Proposition C.5. *Define the new time-to-maturity variable ζ as*

$$\zeta = \int_0^\tau \sigma_L^2(v)dv. \tag{C.32}$$

and set $\widetilde{u}(x,\zeta) = \widetilde{P}(x,\tau)$, then $\widetilde{u}(x,\zeta)$ satisfies

$$\frac{\partial \widetilde{u}}{\partial \zeta} = \frac{1}{2}\frac{\partial^2 \widetilde{u}}{\partial x^2}. \tag{C.33}$$

Proof: Consider equation (C.31), and multiply both sides by the term $[\sigma_L^2(\tau)]^{-1}$, so that

$$\left[\sigma_L^2(\tau)\right]^{-1}\frac{\partial \widetilde{P}}{\partial \tau} = \frac{1}{2}\frac{\partial^2 \widetilde{P}}{\partial x^2}. \tag{C.34}$$

Using the chain rule we transform to a new time-to-maturity variable ζ defined in (C.32), so that (C.34) in terms of $\widetilde{u}$, becomes

$$\left[\sigma_L^2(\tau)\right]^{-1}\frac{\partial}{\partial \zeta}\left[\widetilde{u}\right]\frac{\partial \zeta}{\partial \tau} = \frac{1}{2}\frac{\partial^2 \widetilde{u}}{\partial x^2}. \tag{C.35}$$

In order to eliminate the $[\sigma_L^2(\tau)]^{-1}$ term, we choose ζ to satisfy

$$\left[\sigma_L^2(\tau)\right]^{-1} \times \frac{\partial \zeta}{\partial \tau} = 1, \tag{C.36}$$

from which

$$\zeta = \int_0^\tau \sigma_L^2(v)dv. \tag{C.37}$$

■

Proposition C.6. *The evolution operator $e^{c(\tau)\frac{\partial}{\partial x}}$ satisfies the relation*

$$e^{c(\tau)\frac{\partial}{\partial x}} f(x) = f(x + c(\tau)). \tag{C.38}$$

Proof: Using Taylor series expansion, $f(x + c(\tau))$ can be expressed as

$$\begin{aligned} f(x+c(\tau)) &= f(x) + f'(x)(c(\tau)) + \frac{1}{2!}f''(x)(c(\tau))^2 + \cdots, \\ &= \sum_{n=0}^{\infty}\frac{1}{n!}(c(\tau))^n\frac{\partial^n f(x)}{\partial x^n}, \\ &= \left[\sum_{n=0}^{\infty}\frac{c(\tau)^n}{n!}\frac{\partial^n}{\partial x^n}\right] f(x), \\ &= e^{c(\tau)\frac{\partial}{\partial x}} f(x), \end{aligned} \tag{C.39}$$

where to obtain the last line we have used the definition (3.38). ■

APPENDIX D

Derivation of Differential Equation Satisfied by a Credit-Linked Note

In this appendix, we derive the partial differential equation for the credit linked note price. Since the leverage ratios L_1, L_2 are not themselves traded equations so we employ the "trick" of setting up a portfolio that contains four credit linked notes with different maturities in order to hedge away the risks of the non-traded assets L_1, L_2 and r, see Wilmott et al. (1995) (Chapter 17.5) for the basic idea of this approach and Chiarella (2009) (Chapter 10.4) for a more genal discussion.

We consider three non-traded state variables following the stochastic differential equations

$$dx_j = m_j x_j dt + s_j x_j dZ_j, \ (j = 1, 2, 3). \tag{D.1}$$

We write the correlation structure as

$$\mathbb{E}[dZ_j dZ_k] = \rho_{jk} dt. \tag{D.2}$$

We identify L_1, L_2 with x_1, x_2 and r with $\ln x_3$.

In order to hedge away these three non-traded risks we need to introduce $l = 4$ traded credit linked notes of maturities T_1, T_2, T_3 and T_4. We use $f^l(x_1, x_2, x_3, t)$ for $l = 1, 2, 3, 4$ to denote these credit linked notes which are assumed to be dependent on x_1, x_2, x_3 and t. Applying Ito's lemma, the dynamics of each credit linked note is given by

$$df^l = \mu^l f^l dt + \sum_{j=1}^{3} \sigma_j^l f^l dZ_j, \tag{D.3}$$

where

$$\mu^l f^l = \frac{\partial f^l}{\partial t} + \sum_{j=1}^{3} m_j x_j \frac{\partial f^l}{\partial x_j} + \frac{1}{2} \sum_{j,k=1}^{3} \rho_{jk} s_j s_k x_j x_k \frac{\partial^2 f^l}{\partial x_j \partial x_k}, \tag{D.4}$$

$$\sigma_j^l f^l = s_j x_j \frac{\partial f^l}{\partial x_j}. \tag{D.5}$$

We form a hedging portfolio consisting of Q^l unit of the traded credit linked notes f^l for $l = 1, 2, 3, 4$. The value of this portfolio at time t is given by

$$V = \sum_{l=1}^{4} Q^l f^l, \tag{D.6}$$

and the instantaneous change in V may be written

$$dV = \sum_{l=1}^{4} Q^l df^l, \tag{D.7}$$

$$= \sum_{l=1}^{4} Q^l [\mu^l f^l dt + \sum_{j=1}^{3} \sigma_j^l f^l dZ_j], \tag{D.8}$$

$$= \sum_{l=1}^{4} Q^l \mu^l f^l dt + \sum_{l=1}^{4} Q^l \sum_{j=1}^{3} \sigma_j^l f^l dZ_j. \tag{D.9}$$

In order to render the portfolio riskless the Q^l have to be chosen to that

$$\sum_{l=1}^{4} Q^l \sum_{j=1}^{3} \sigma_j^l f^l dZ_j = 0, \tag{D.10}$$

which can be rewritten as

$$\sum_{j=1}^{3} \left[\sum_{l=1}^{4} Q^l \sigma_j^l f^l \right] dZ_j = 0. \tag{D.11}$$

For each dZ_j term to vanish, the quantity in the bracket in (D.11) must equal zero, that is

$$\sum_{l=1}^{4} Q^l \sigma_j^l f^l = 0, \tag{D.12}$$

for $1 \leq j \leq 3$. In this case, the return from the portfolio in equation (D.9) is then riskless and given by

$$dV = \sum_{l=1}^{4} Q^l \mu^l f^l dt. \tag{D.13}$$

If there are no arbitrage opportunities, the riskless hedging portfolio can only earn the risk-free of interest, so that (D.13) becomes

$$dV = r \sum_{l=1}^{4} Q^l df^l dt. \tag{D.14}$$

Substituting (D.14) into (D.13), we have

$$\sum_{l=1}^{4} Q^l \mu^l f^l dt = r \sum_{l=1}^{4} Q^l df^l dt, \tag{D.15}$$

then

$$\sum_{l=1}^{4} Q^l [\mu^l - r] f^l = 0. \tag{D.16}$$

Following the argument Hull (2000) (Chapter 19), equations (D.12) and (D.16) can be regarded as 4 homogeneous linear equations in the Q^l's, which are non-zero otherwise there would be no

hedging portfolio. By the results from linear algebra, equations (D.12) and (D.16) can be consistent only if

$$\mu^l - r = \sum_{j=1}^{3} \lambda_j \sigma_j^l. \tag{D.17}$$

for some parameters λ_j $(j = 1, 2, 3)$ that are dependent only on the state variables and time. Following the argument in Wilmott et al. (1995), the parameters λ_j are the market prices of risk associated to the underlying non-traded variables.

Since the maturities T_l are arbitrary the relation (D.17) must hold for a credit linked note of any maturity, that is we can write

$$\mu - r = \sum_{j=1}^{3} \lambda_j \sigma_j. \tag{D.18}$$

Substituting the expressions for σ_j and μ defined in equations (D.4)-(D.5), equation (D.18) reduces to the partial differential equation

$$\frac{\partial f}{\partial t} + \sum_{j=1}^{3} [m_j - \lambda_j s_j] x_j \frac{\partial f}{\partial x_j} + \frac{1}{2} \sum_{j}^{3} \sum_{k}^{3} \rho_{jk} s_j s_k x_j x_k \frac{\partial f}{\partial x_j \partial x_k} - rf = 0. \tag{D.19}$$

Replacing $(x_1, x_2, \ln x_3)$ by (L_1, L_2, r), the partial differential equation (D.19) becomes the partial differential equation (3.68) for the credit linked note $P(L_1, L_2, r)$ with the drift coefficients m_1, m_2 and $m_3 - s_3^2/2$ identified with μ_1, μ_2 and $\kappa_r(\theta_r - r)$ and the volatility coefficients s_1, s_2 and s_3 identified with σ_1, σ_2 and σ_r.

APPENDIX E

Applying the Separation of Variables to the PDE for the CLN

This appendix applies the separation of variables technique to simplify the partial differential equation for the price of the credit linked note. Suppose the differential equation (3.74) can be written in terms of two separate functions as

$$P(L_1, L_2, r, t) = f(r, t)\widehat{P}(L_1, L_2, t), \tag{E.1}$$

where function $f(r,t)$ depends only on r and t, and $\widehat{P}(L_1, L_2, t)$ is a function of L_1, L_2 and t only. To determine differential equations of $f(r,t)$ and $\widehat{P}(L_1, L_2, t)$, we note that

$$\frac{\partial P}{\partial t} = \widehat{P}\frac{\partial f}{\partial t} + f\frac{\partial \widehat{P}}{\partial t}, \tag{E.2}$$

$$\frac{\partial^2 P}{\partial L_1 \partial L_2} = f\frac{\partial^2 \widehat{P}}{\partial L_1 \partial L_2}, \ \frac{\partial P}{\partial L_i} = f\frac{\partial \widehat{P}}{\partial L_i}, \ \frac{\partial^2 P}{\partial L_i^2} = f\frac{\partial^2 \widehat{P}}{\partial L_i^2}, \tag{E.3}$$

$$\frac{\partial^2 P}{\partial r \partial L_i} = \frac{\partial f}{\partial r}\frac{\partial \widehat{P}}{\partial L_i}, \quad \frac{\partial P}{\partial r} = \widehat{P}\frac{\partial f}{\partial r}, \ \frac{\partial^2 P}{\partial r^2} = \widehat{P}\frac{\partial^2 f}{\partial r^2}, \tag{E.4}$$

for $i = 1, 2$.

Substituting equations (E.1)-(E.4) into (3.74), we obtain the partial differential equation

$$\begin{aligned} -\widehat{P}\frac{\partial f}{\partial t} - f\frac{\partial \widehat{P}}{\partial t} = {} & f\frac{1}{2}\sigma_1^2 L_1^2 \frac{\partial^2 \widehat{P}}{\partial L_1^2} + f\frac{1}{2}\sigma_2^2 L_2^2 \frac{\partial^2 \widehat{P}}{\partial L_2^2} + \widehat{P}\frac{1}{2}\sigma_r^2 \frac{\partial^2 f}{\partial r^2} \\ & + f\rho_{12}\sigma_1\sigma_2 L_1 L_2 \frac{\partial^2 \widehat{P}}{\partial L_1 \partial L_2} + \frac{\partial f}{\partial r}\rho_{1r}\sigma_1\sigma_r L_1 \frac{\partial \widehat{P}}{\partial L_1} \\ & + \frac{\partial f}{\partial r}\rho_{2r}\sigma_2\sigma_r L_2 \frac{\partial \widehat{P}}{\partial L_2} + f\widetilde{\mu}_1 L_1 \frac{\partial \widehat{P}}{\partial L_1} + f\widetilde{\mu}_2 L_2 \frac{\partial \widehat{P}}{\partial L_2} \\ & + \widehat{P}\kappa_r\left[\widetilde{\theta}_r - r\right]\frac{\partial f}{\partial r} - rf\widehat{P}. \end{aligned} \tag{E.5}$$

We group f and $\widehat{P}$ terms respectively, so that (E.5) becomes

$$\begin{aligned}
&\frac{1}{f}\left(\frac{\partial f}{\partial t}+\frac{1}{2}\sigma_r^2\frac{\partial^2 f}{\partial r^2}+\kappa_r\left[\widetilde{\theta}_r-r\right]\frac{\partial f}{\partial r}-rf\right)\\
&= \frac{1}{\widehat{P}}\left(-\frac{\partial \widehat{P}}{\partial t}-\frac{1}{2}\sigma_1^2L_1^2\frac{\partial^2\widehat{P}}{\partial L_1^2}-\frac{1}{2}\sigma_2^2L_2^2\frac{\partial^2\widehat{P}}{\partial L_2^2}-\rho_{12}\sigma_1\sigma_2L_1L_2\frac{\partial^2\widehat{P}}{\partial L_1\partial L_2}\right.\\
&\quad -\frac{1}{f}\frac{\partial f}{\partial r}\rho_{1r}\sigma_1\sigma_rL_1\frac{\partial\widehat{P}}{\partial L_1}-\frac{1}{f}\frac{\partial f}{\partial r}\rho_{2r}\sigma_2\sigma_rL_2\frac{\partial\widehat{P}}{\partial L_2}\\
&\quad \left.-\widetilde{\mu}_1L_1\frac{\partial\widehat{P}}{\partial L_1}-\widetilde{\mu}_2L_2\frac{\partial\widehat{P}}{\partial L_2}\right). \qquad \text{(E.6)}
\end{aligned}$$

Since the LHS of (E.6) depends only on r and t and the RHS only on L_1, L_2 and t, the only way that both sides can be equal for all possible values of r, L_1, L_2 and t is that both sides equal to a constant. We note that the partial differential equation in the bracket of LHS of (E.6) is the partial differential equation of the risk-free bond price $B(r,t)$ of the Vasicek (1977) model, which satisfies

$$\frac{\partial B}{\partial t}+\frac{1}{2}\sigma_r^2\frac{\partial^2 B}{\partial r^2}+\kappa_r(\widetilde{\theta}_r-r)\frac{\partial B}{\partial r}-rB=0. \qquad \text{(E.7)}$$

Hence, both sides of (E.6) equal zero, and (E.1) becomes

$$P(L_1,L_2,r,t)=B(r,t)\widehat{P}(L_1,L_2,t). \qquad \text{(E.8)}$$

The solution of the risk-free bond price $B(r,t)$ of the Vasicek (1977) model is[1]

$$B(r,t)=e^{a(t)+b(t)r}, \qquad \text{(E.9)}$$

where

$$b(t) = \frac{e^{-\kappa_r(T-t)}-1}{\kappa_r}, \qquad \text{(E.10)}$$

$$a(t) = \frac{(-b(t)-T+t)(\kappa_r^2\widetilde{\theta}_r-\sigma_r^2/2)}{\kappa_r^2}-\frac{\sigma_r^2b(t)^2}{4\kappa_r}. \qquad \text{(E.11)}$$

Moreover, the solution (E.9) yields that the first derivative of $B(r,t)$ with respect to r satisfies

$$\frac{1}{B}\frac{\partial B}{\partial r} = b(t). \qquad \text{(E.12)}$$

[1]For example, Wilmott et al. (1995), Section 17.5.

Substituting from equations (E.7) and (E.12) into (E.5), we obtain the differential equation of $\widehat{P}(L_1, L_2, t)$ as

$$\begin{aligned} -\frac{\partial \widehat{P}}{\partial t} &= \frac{1}{2}\sigma_1^2 L_1^2 \frac{\partial^2 \widehat{P}}{\partial L_1^2} + \rho_{12}\sigma_1\sigma_2 L_1 L_2 \frac{\partial^2 \widehat{P}}{\partial L_1 \partial L_2} + \frac{1}{2}\sigma_2^2 L_2^2 \frac{\partial^2 \widehat{P}}{\partial L_2^2} \\ &\quad + [\widetilde{\mu}_1 + \rho_{1r}\sigma_1\sigma_r b(t)]\, L_1 \frac{\partial \widehat{P}}{\partial L_1} \\ &\quad + [\widetilde{\mu}_2 + \rho_{2r}\sigma_2\sigma_r b(t)]\, L_2 \frac{\partial \widehat{P}}{\partial L_2}, \end{aligned} \tag{E.13}$$

in the region of $0 \leq t \leq T$.

Since the final time condition for the risk-free bond price is $B(r, T) = 1$, substituting this and equation (E.8) into boundary conditions (3.69)-(3.71), gives boundary conditions for $\widehat{P}$, namely

$$\widehat{P}(L_1, L_2, T) = 1, \tag{E.14}$$

$$\widehat{P}(\widehat{L}_1, L_2, t) = 0, \tag{E.15}$$

$$\widehat{P}(L_1, \widehat{L}_2, t) = 0. \tag{E.16}$$

APPENDIX F

The Number of Images and the Correlation Coefficient ρ_{12}

The method of images applied in Chapter 4 for the two absorbing barriers case is only valid for certain values of the correlation coefficient between two firms' leverage ratios. This appendix demonstrates the relationship between the total number of images required to form a "closed-loop" and the corresponding value of the correlation coefficient ρ_{12}.

In order to obtain the number of images that form the closed-loop, it is convenient to transform the volatility adjusted correlated log-leverage ratio variables x_1 and x_2 to the uncorrelated variables z_1, z_2 by setting

$$z_2 = x_2, \tag{F.1}$$

$$z_1 = \frac{1}{\sqrt{1-\rho_{12}^2}}(x_1 - \rho_{12}x_2). \tag{F.2}$$

In order to eliminate the mixed derivative term from the heat equation (4.1), we make the transformation

$$u(x_1, x_2, \tau) = \widetilde{u}(z_1(x_1, x_2), z_2(x_2), \tau), \tag{F.3}$$

using the change of variables defined in equations (F.1)-(F.2).

Since

$$\frac{\partial z_2}{\partial x_1} = 0 \quad ; \quad \frac{\partial z_2}{\partial x_2} = 1$$
$$\frac{\partial z_1}{\partial x_1} = \alpha \quad ; \quad \frac{\partial z_1}{\partial x_2} = -\alpha\rho,$$

with $\alpha = 1/\sqrt{1-\rho^2}$, we have

$$\begin{aligned}
\frac{\partial u}{\partial x_1} &= \alpha\frac{\partial}{\partial z_1}\widetilde{P} \\
\frac{\partial^2 u}{\partial x_1^2} &= \alpha^2\frac{\partial^2}{\partial z_1^2}\widetilde{u} \\
\frac{\partial u}{\partial x_2} &= \left[\frac{\partial}{\partial z_2} - \alpha\rho\frac{\partial}{\partial z_1}\right]\widetilde{u} \\
\frac{\partial^2 u}{\partial x_2^2} &= \left[\frac{\partial^2}{\partial z_2^2} - 2\alpha\rho\frac{\partial^2}{\partial z_1\partial z_2} + (\alpha\rho)^2\frac{\partial^2}{\partial z_1^2}\right]\widetilde{u} \\
\frac{\partial^2 u}{\partial x_1\partial x_2} &= \left[\alpha\frac{\partial^2}{\partial z_1\partial z_2} - \alpha^2\rho\frac{\partial^2}{\partial z_1^2}\right]\widetilde{u}.
\end{aligned} \tag{F.4}$$

Substituting (F.4) into (4.1), yields

$$\begin{aligned}\frac{\partial \widetilde{u}}{\partial \tau} =& \frac{1}{2}\left[\alpha^2\frac{\partial^2}{\partial z_1^2}\right]\widetilde{u} + \frac{1}{2}\left[\frac{\partial^2}{\partial z_2^2} - 2\alpha\rho\frac{\partial^2}{\partial z_1 \partial z_2} + (\alpha\rho)^2\frac{\partial^2}{\partial z_1^2}\right]\widetilde{u} + \rho\left[\alpha\frac{\partial^2}{\partial z_1 \partial z_2} - \alpha^2\rho\frac{\partial^2}{\partial z_1^2}\right]\widetilde{u} \\ =& \frac{1}{2}\alpha^2\frac{\partial^2 \widetilde{u}}{\partial z_1^2} + \frac{1}{2}\frac{\partial^2 \widetilde{u}}{\partial z_2^2} - \alpha\rho\frac{\partial^2 \widetilde{u}}{\partial z_1 \partial z_2} + \frac{1}{2}(\alpha\rho)^2\frac{\partial^2 \widetilde{u}}{\partial z_1^2} + \rho\alpha\frac{\partial^2 \widetilde{u}}{\partial z_1 \partial z_2} - (\rho\alpha)^2\frac{\partial^2 \widetilde{u}}{\partial z_1^2} \\ =& \left[\frac{1}{2}\alpha^2 + \frac{1}{2}(\alpha\rho)^2 - (\rho\alpha)^2\right]\frac{\partial^2 \widetilde{u}}{\partial z_1^2} + \frac{1}{2}\frac{\partial^2 \widetilde{u}}{\partial z_2^2},\end{aligned}$$

rearranging the term in the bracket on the right hand side $\left[\frac{1}{2}\alpha^2 + \frac{1}{2}(\alpha\rho)^2 - (\rho\alpha)^2\right]$ we find that it equals $\frac{1}{2}$, therefore we obtain

$$\frac{\partial \widetilde{u}}{\partial \tau} = \frac{1}{2}\frac{\partial^2 \widetilde{u}}{\partial z_1^2} + \frac{1}{2}\frac{\partial^2 \widetilde{u}}{\partial z_2^2}. \tag{F.5}$$

The absorbing barriers $x_1 = 0$ and $x_2 = 0$ determine the barriers of the uncorrelated variables, which become

$$z_2 = 0, \tag{F.6}$$

$$z_1 = -\frac{\rho_{12}}{\sqrt{1-\rho_{12}^2}}z_2. \tag{F.7}$$

The transformation of the barriers is also illustrated in Figure F.1, and we note that the barrier for z_1 depends on z_2 as well.

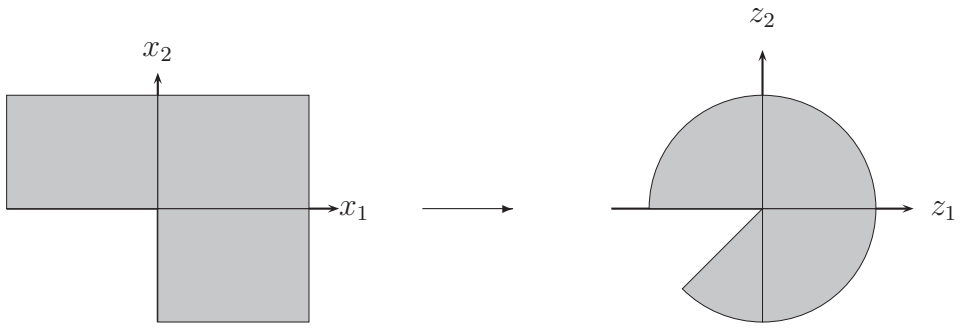

FIGURE F.1. The transformation of the barriers.

Since x_1 and x_2 are defined in the region $x_1, x_2 \in (-\infty, 0) \times (-\infty, 0)$ (represented by the non-shaded region in the left hand panel in Figure F.2), then for z_1, z_2 the regions of definition are $z_2 \in (-\frac{\sqrt{1-\rho_{12}^2}}{\rho_{12}}z_1, 0)$ and $z_1 \in (-\infty, -\frac{\rho_{12}}{\sqrt{1-\rho_{12}^2}}z_2)$, and there is an angle ϕ' (represented by the angle ϕ' in the right hand panel in Figure F.2) between the two planes of the barrier $z_2 = 0$ and $z_1 = -\frac{\rho_{12}}{\sqrt{1-\rho_{12}^2}}z_2$.

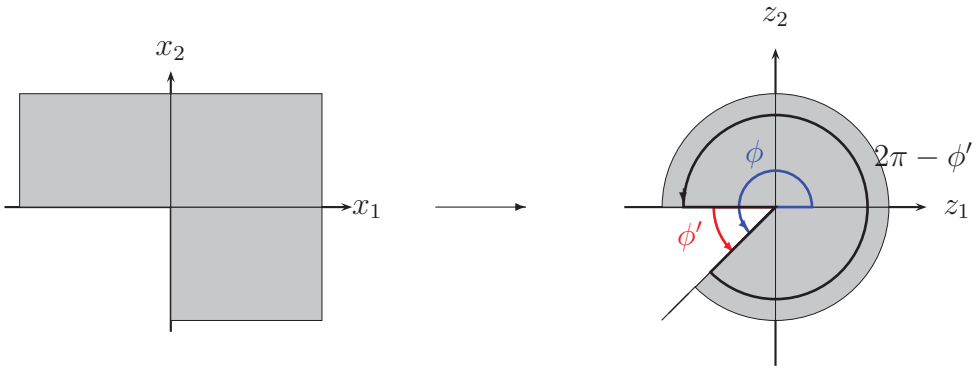

FIGURE F.2. The non-shaded area in the left hand panel represents the restricted region in x_1, x_2 co-ordinates. After the transformation, the wedge shaped non-shaded region forming the angle ϕ' in the right hand panel represents the restricted region in z_1, z_2 co-ordinates.

In the ensuing discussion it is important to distinguish between the polar angle ϕ (measured clockwise from the positive z_1 axis) and the angle ϕ' (measured clockwise from the negative z_1 axis), as shown in the right panel of Figure F.2, and which are related by $\phi' = \phi - \pi$.

Next, we relate the angle ϕ' to the correlation coefficient ρ_{12}. By simple trigonometry for a point (z_1, z_2) in the line $z_1 = -\frac{\rho_{12}}{\sqrt{1-\rho_{12}^2}} z_2$, we have

$$z_1 = R\cos\phi, \tag{F.8}$$

where R is the radius defined as $R = \sqrt{z_1^2 + z_2^2}$.

Equation (F.8) may be written as

$$z_1 = \sqrt{z_1^2 + z_2^2}\cos\phi, \tag{F.9}$$

which by use of the relation (F.7) becomes

$$z_1^2 = \left(z_1^2 + \frac{1-\rho_{12}^2}{\rho_{12}^2} z_1^2\right)\cos^2\phi, \tag{F.10}$$

from which we obtain

$$\rho_{12} = \pm\cos\phi. \tag{F.11}$$

From (F.11), we note that the condition $-1 < \rho_{12} < 1$ determines region of ϕ which is $\pi < \phi < 2\pi$, hence the values of ϕ' satisfy $0 < \phi' < \pi$ (since $\phi' = \phi - \pi$). If $\rho_{12} < 0$ then $0 < \phi' < \frac{\pi}{2}$, if $\rho_{12} = 0$ then $\phi' = \frac{\pi}{2}$ and if $\rho_{12} > 0$ then $\frac{\pi}{2} < \phi' < \pi$ as illustrated in Figure F.3:

Note that we can only form the closed loop of images for values of the angle ϕ' that divide the angle $(2\pi - \phi')$ into an exact integer number. Denote by m the number of images, then in order to

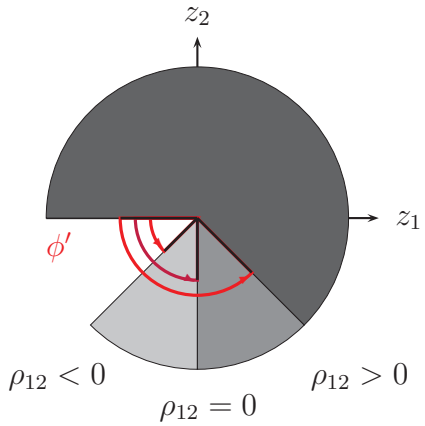

FIGURE F.3. The relationship between the correlation coefficient ρ_{12} and the angle ϕ'.

form the closed-loop, the integer m must be related to the angle ϕ' by

$$m = \frac{2\pi - \phi'}{\phi'}. \tag{F.12}$$

We stress that m must be a positive integer, also the values of m that satisfy this relation are the odd integers starting from 3. These values of m via equation (F.12), will then determine the values of ρ_{12} for which the method of images can be applied.

For example, given $\phi' = \frac{\pi}{2}$ (at which $\rho_{12} = 0$), we require $m = 3$ images to form the closed-loop (see Figure F.4), that is if we successively reflect a point in the physical region in the mirrors at the lines radiating from the origin at polar angles $\phi = \frac{3\pi}{2}$, $\phi = 0$, $\phi = \frac{\pi}{2}$ and $\phi = \pi$ we will arrive back at the original point.

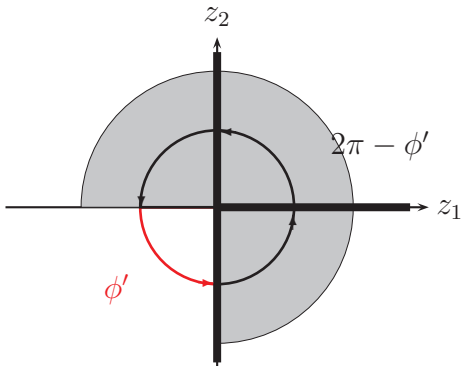

FIGURE F.4. To form the closed-loop for the angle $\phi' = \frac{\pi}{2}$, three images are required.

Next consider $\phi' = \frac{\pi}{3}$ (at which $\rho_{12} = -0.5$) illustrated in Figure F.5. The lines bounding the image region (shaded in Figure F.5) lie between the polar angles $\phi = \pi$ and $\phi = \frac{4\pi}{3}$ in the

clockwise direction. So the angle separating the two defining lines is $\frac{5\pi}{3}$ $(= 2\pi - \phi')$, which can be divided precisely into five regions separated by lines at an angle of $\pi/3$ apart, as shown in Figure F.5. These lines are five mirrors in which the point in the physical region is successively reflected to give the five image points. A further reflection in the line $\phi = \pi$ would take us back to the original point, thus completing the loop. Figure F.6 illustrates the situation for $\phi' = \frac{\pi}{4}$ (at which $\rho_{12} = -0.707$) for which seven mirrors, resulting in seven images, are required to form a closed loop.

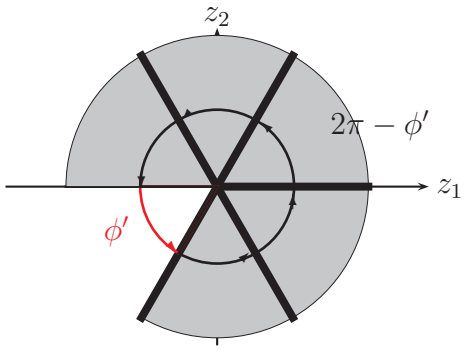

FIGURE F.5. To form a closed loop for the angle $\phi' = \frac{\pi}{3}$, five images are required.

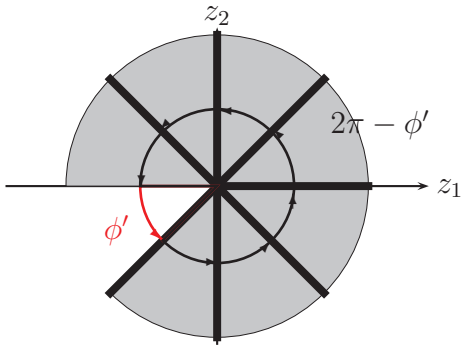

FIGURE F.6. To form a closed loop for the angle $\phi' = \frac{\pi}{4}$, seven images are required.

We can now see that the general relationship between the value of ρ_{12} and the member of images m needed to form a closed-loop is obtained by substituting (F.12) into (F.11), using the relation $\phi' = \phi - \pi$, to yield

$$\rho_{12} = -\cos(\frac{2\pi}{(m+1)}), \tag{F.13}$$

for $m = 3, 5, 7, \ldots$. The corresponding values of ρ_{12} are summarized in Table 4.1.

APPENDIX G

Transformation of the PDE (4.30) to the 2-D Heat Equation in the Case of Constant Coefficients

Proposition G.1. *The solution to the partial differential equation* (4.30) *may be written*

$$\bar{P}(X_1, X_2, \tau) = e^{\eta_1 X_1 + \eta_2 X_2 + \xi\tau} u(X_1, X_2, \tau), \tag{G.1}$$

where η_1, η_2 and ξ are constants given by

$$\eta_1 = \frac{\gamma_2\rho_{12} - \gamma_1}{1 - \rho_{12}^2}, \tag{G.2}$$

$$\eta_2 = \frac{\gamma_1\rho_{12} - \gamma_2}{1 - \rho_{12}^2}, \tag{G.3}$$

$$\xi = -\frac{\frac{1}{2}\gamma_1^2 - \rho_{12}\gamma_1\gamma_2 + \frac{1}{2}\gamma_1^2}{1 - \rho_{12}^2}, \tag{G.4}$$

and $u(X_1, X_2, \tau)$ satisfies the partial differential equation

$$\frac{\partial u}{\partial \tau} = \frac{1}{2}\frac{\partial^2 u}{\partial X_1^2} + \rho_{12}\frac{\partial^2 u}{\partial X_1 \partial X_2} + \frac{1}{2}\frac{\partial^2 u}{\partial X_2^2}. \tag{G.5}$$

Proof: We define $\bar{P}$ such that $\bar{P}(X_1, X_2, \tau) = e^{\eta_1 X_1 + \eta_2 X_2}\widetilde{P}(X_1, X_2, \tau)$, where the η_1 and η_2 are to be chosen in a "convenient" way. We calculate

$$\begin{aligned}
\frac{\partial \bar{P}}{\partial \tau} &= e^{\eta_1 X_1 + \eta_2 X_2}\frac{\partial \widetilde{P}}{\partial \tau}, \\
\frac{\partial \bar{P}}{\partial X_i} &= e^{\eta_1 X_1 + \eta_2 X_2}\left[\eta_i \widetilde{P} + \frac{\partial \widetilde{P}}{\partial X_i}\right], \ (i = 1, 2) \\
\frac{\partial^2 \bar{P}}{\partial X_i^2} &= e^{\eta_1 X_1 + \eta_2 X_2}\left[\eta_i^2 \widetilde{P} + 2\eta_i\frac{\partial \widetilde{P}}{\partial X_i} + \frac{\partial^2 \widetilde{P}}{\partial X_i^2}\right], \ (i = 1, 2) \\
\frac{\partial^2 \bar{P}}{\partial X_1 \partial X_2} &= e^{\eta_1 X_1 + \eta_2 X_2}\left[\eta_1\eta_2 \widetilde{P} + \eta_2\frac{\partial \widetilde{P}}{\partial X_1} + \eta_1\frac{\partial \widetilde{P}}{\partial X_2} + \frac{\partial^2 \widetilde{P}}{\partial X_1 \partial X_2}\right].
\end{aligned} \tag{G.6}$$

Then equation (4.30) becomes

$$\begin{aligned}\frac{\partial \widetilde{P}}{\partial \tau} &= \frac{1}{2}\left[\eta_1^2\widetilde{P} + 2\eta_1\frac{\partial \widetilde{P}}{\partial X_1} + \frac{\partial^2 \widetilde{P}}{\partial X_1^2}\right] + \frac{1}{2}\left[\eta_2^2\widetilde{P} + 2\eta_2\frac{\partial \widetilde{P}}{\partial X_2} + \frac{\partial^2 \widetilde{P}}{\partial X_2^2}\right] \\ &\quad + \rho_{12}\left[\eta_1\eta_2\widetilde{P} + \eta_2\frac{\partial \widetilde{P}}{\partial X_1} + \eta_1\frac{\partial \widetilde{P}}{\partial X_2} + \frac{\partial^2 \widetilde{P}}{\partial X_1 \partial X_2}\right] \\ &\quad + \gamma_1\left[\eta_1\widetilde{P} + \frac{\partial \widetilde{P}}{\partial X_1}\right] + \gamma_2\left[\eta_2\widetilde{P} + \frac{\partial \widetilde{P}}{\partial X_2}\right]. \end{aligned} \tag{G.7}$$

Rearranging this last equation we obtain

$$\begin{aligned}\frac{\partial \widetilde{P}}{\partial \tau} &= \frac{1}{2}\frac{\partial^2 \widetilde{P}}{\partial X_1^2} + \rho_{12}\frac{\partial^2 \widetilde{P}}{\partial X_1 \partial X_2} + \frac{1}{2}\frac{\partial^2 \widetilde{P}}{\partial X_2^2} \\ &\quad + \left[\eta_1 + \rho_{12}\eta_2 + \gamma_1\right]\frac{\partial \widetilde{P}}{\partial X_1} + \left[\eta_2 + \rho_{12}\eta_1 + \gamma_2\right]\frac{\partial \widetilde{P}}{\partial X_2} \\ &\quad + \left[\frac{1}{2}\eta_1^2 + \frac{1}{2}\eta_2^2 + \rho_{12}\eta_1\eta_2 + \gamma_1\eta_1 + \gamma_2\eta_2\right]\widetilde{P}. \end{aligned} \tag{G.8}$$

We may eliminate the $\partial \widetilde{P}/\partial X_1$ terms and $\partial \widetilde{P}/\partial X_2$ by choosing

$$\begin{aligned}\eta_1 + \rho_{12}\eta_2 + \gamma_1 &= 0, \\ \eta_2 + \rho_{12}\eta_1 + \gamma_2 &= 0, \end{aligned} \tag{G.9}$$

the simultaneous solution of which yields

$$\begin{aligned}\eta_1 &= \frac{\gamma_2\rho_{12} - \gamma_1}{1 - \rho_{12}^2}, \\ \eta_2 &= \frac{\gamma_1\rho_{12} - \gamma_2}{1 - \rho_{12}^2}. \end{aligned} \tag{G.10}$$

With these choices of η_1 and η_2 equation (G.8) reduce to

$$\frac{\partial \widetilde{P}}{\partial \tau} = \frac{1}{2}\frac{\partial^2 \widetilde{P}}{\partial X_1^2} + \rho_{12}\frac{\partial^2 \widetilde{P}}{\partial X_1 \partial X_2} + \frac{1}{2}\frac{\partial^2 \widetilde{P}}{\partial X_2^2} + \xi\widetilde{P}, \tag{G.11}$$

where, by use of equation (G.10)

$$\xi = -\frac{\left(\frac{1}{2}\gamma_1^2 - \rho_{12}\gamma_1\gamma_2 + \frac{1}{2}\gamma_2^2\right)}{1 - \rho_{12}^2}. \tag{G.12}$$

Next, we define u such that

$$\widetilde{P}(X_1, X_2, \tau) = e^{\xi\tau}u(X_1, X_2, \tau), \tag{G.13}$$

and calculate

$$\begin{aligned}
\frac{\partial \widetilde{P}}{\partial \tau} &= e^{\xi\tau}\left[\xi u + \frac{\partial u}{\partial \tau}\right], \\
\frac{\partial \widetilde{P}}{\partial X_i} &= e^{\xi\tau}\frac{\partial u}{\partial X_i},\ (i=1,2) \\
\frac{\partial^2 \widetilde{P}}{\partial X_i^2} &= e^{\xi\tau}\frac{\partial^2 u}{\partial X_i^2},\ (i=1,2) \\
\frac{\partial^2 \widetilde{P}}{\partial X_1 \partial X_2} &= e^{\xi s}\frac{\partial^2 u}{\partial X_1 \partial X_2}.
\end{aligned} \tag{G.14}$$

It then follows that $u(X_1, X_2, \tau)$ satisfies

$$\frac{\partial u}{\partial \tau} = \frac{1}{2}\frac{\partial^2 u}{\partial X_1^2} + \rho_{12}\frac{\partial^2 u}{\partial X_1 \partial X_2} + \frac{1}{2}\frac{\partial^2 u}{\partial X_2^2}. \tag{G.15}$$

■

APPENDIX H

The Derivation of the PDE (4.44) in the Case of Time Varying Barriers

In this appendix we show how to the transform equation (4.44) to equation (4.50). We remind the reader of the operator $e^{c(\tau)\frac{\partial}{\partial x}}$ defined in equation (3.38) and the techniques used in Appendix C.

Proposition H.1. *The partial differential equation* (4.44) *can be transformed by setting*

$$\bar{P}_{\boldsymbol{\beta}}(X_1, X_2, \tau) \;=\; e^{-X_1^*(\tau)\frac{\partial}{\partial X_1} - X_2^*(\tau)\frac{\partial}{\partial X_2}}\,\widetilde{P}(X_1, X_2, \tau), \tag{H.1}$$

where the $X_i^*(\tau)$ *is given by*

$$X_i^*(\tau) = -\int_0^\tau \gamma_i(v)dv - \beta_i\tau,\ (i = 1, 2), \tag{H.2}$$

and $\widetilde{P}(X_1, X_2, \tau)$ *satisfies the partial differential*

$$\frac{\partial \widetilde{P}}{\partial \tau} \;=\; \frac{1}{2}\frac{\partial^2 \widetilde{P}}{\partial X_1^2} + \rho_{12}\frac{\partial^2 \widetilde{P}}{\partial X_1 \partial X_2} + \frac{1}{2}\frac{\partial^2 \widetilde{P}}{\partial X_2^2} - \beta_1\frac{\partial \widetilde{P}}{\partial X_1} - \beta_2\frac{\partial \widetilde{P}}{\partial X_2}. \tag{H.3}$$

Proof: Apply the Baker-Campbell-Hausdorff formula in Appendix C, and after some algebraic manipulations, we obtain

$$\begin{aligned}
\frac{\partial \bar{P}_{\boldsymbol{\beta}}}{\partial \tau} &= e^{-X_1^*(\tau)\frac{\partial}{\partial X_1} - X_2^*(\tau)\frac{\partial}{\partial X_2}}\left[\frac{\partial \widetilde{P}}{\partial \tau} - \frac{\partial X_1^*(\tau)}{\partial \tau}\frac{\partial \widetilde{P}}{\partial X_1} - \frac{\partial X_2^*(\tau)}{\partial \tau}\frac{\partial \widetilde{P}}{\partial X_2}\right],\\
\frac{\partial \bar{P}_{\boldsymbol{\beta}}}{\partial X_i} &= e^{-X_1^*(\tau)\frac{\partial}{\partial X_1} - X_2^*(\tau)\frac{\partial}{\partial X_2}}\frac{\partial \widetilde{P}}{\partial X_i},\ (i = 1, 2),\\
\frac{\partial^2 \bar{P}_{\boldsymbol{\beta}}}{\partial X_i^2} &= e^{-X_1^*(\tau)\frac{\partial}{\partial X_1} - X_2^*(\tau)\frac{\partial}{\partial X_2}}\frac{\partial^2 \widetilde{P}}{\partial X_i^2},\ (i = 1, 2),\\
\frac{\partial^2 \bar{P}_{\boldsymbol{\beta}}}{\partial X_1 \partial X_2} &= e^{-X_1^*(\tau)\frac{\partial}{\partial X_1} - X_2^*(\tau)\frac{\partial}{\partial X_2}}\frac{\partial^2 \widetilde{P}}{\partial X_1 \partial X_2}.
\end{aligned} \tag{H.4}$$

Then equation (4.44) becomes

$$\begin{aligned}
\frac{\partial \widetilde{P}}{\partial \tau} - \frac{\partial X_1^*(\tau)}{\partial \tau}\frac{\partial \widetilde{P}}{\partial X_1} - \frac{\partial X_2^*(\tau)}{\partial \tau}\frac{\partial \widetilde{P}}{\partial X_2} \;=\; & \frac{1}{2}\frac{\partial^2 \widetilde{P}}{\partial X_1^2} + \rho_{12}\frac{\partial^2 \widetilde{P}}{\partial X_1 \partial X_2} + \frac{1}{2}\frac{\partial^2 \widetilde{P}}{\partial X_2^2}\\
& + \gamma_1(\tau)\frac{\partial \widetilde{P}}{\partial X_1} + \gamma_2(\tau)\frac{\partial \widetilde{P}}{\partial X_2}.
\end{aligned} \tag{H.5}$$

Define $X_1^*(\tau)$ and $X_2^*(\tau)$ by setting

$$-\frac{\partial X_1^*(\tau)}{\partial \tau} = \gamma_1(\tau) + \beta_1, \tag{H.6}$$

$$-\frac{\partial X_2^*(\tau)}{\partial \tau} = \gamma_2(\tau) + \beta_2, \tag{H.7}$$

so that

$$X_1^*(\tau) = -\int_0^\tau \gamma_1(v)dv - \beta_1\tau, \tag{H.8}$$

$$X_2^*(\tau) = -\int_0^\tau \gamma_2(v)dv - \beta_2\tau, \tag{H.9}$$

then, the partial differential equation (H.5) becomes

$$\begin{aligned} &\frac{\partial \widetilde{P}}{\partial \tau} + \gamma_1(\tau)\frac{\partial \widetilde{P}}{\partial X_1} + \beta_1\frac{\partial \widetilde{P}}{\partial X_1} + \gamma_2(\tau)\frac{\partial \widetilde{P}}{\partial X_2} + \beta_2\frac{\partial \widetilde{P}}{\partial X_2} \\ = &\frac{1}{2}\frac{\partial^2 \widetilde{P}}{\partial X_1^2} + \rho_{12}\frac{\partial^2 \widetilde{P}}{\partial X_1 \partial X_2} + \frac{1}{2}\frac{\partial^2 \widetilde{P}}{\partial X_2^2} + \gamma_1(\tau)\frac{\partial \widetilde{P}}{\partial X_1} + \gamma_2(\tau)\frac{\partial \widetilde{P}}{\partial X_2}, \end{aligned} \tag{H.10}$$

which then turns out to be equation (H.3).

We note that the partial differential equation (H.3) can be further reduced to the two-dimensional heat equation u. We apply the transformation illustrated in Appendix G, simply replacing $\bar{P}$ by $\widetilde{P}$, and replacing the coefficients γ_i by $-\beta_i$ (for $i = 1, 2$), we obtain

$$\widetilde{P}(X_1, X_2, \tau) = e^{\eta_1 X_1 + \eta_2 X_2 + \xi\tau} u(X_1, X_2, \tau), \tag{H.11}$$

where η_1, η_2 and ξ are constants given by

$$\eta_1 = \frac{-\beta_2\rho_{12} + \beta_1}{1 - \rho_{12}^2}, \tag{H.12}$$

$$\eta_2 = \frac{-\beta_1\rho_{12} + \beta_2}{1 - \rho_{12}^2}, \tag{H.13}$$

$$\xi = -\frac{\frac{1}{2}\beta_1^2 - \rho_{12}\beta_1\beta_2 + \frac{1}{2}\beta_1^2}{1 - \rho_{12}^2}. \tag{H.14}$$

■

The following proposition gives the proof of equation (4.51).

Proposition H.2. *The expression*

$$e^{c_1(\tau)\frac{\partial}{\partial x_1} + c_2(\tau)\frac{\partial}{\partial x_2}} f(x_1, x_2), \tag{H.15}$$

may be written as

$$f(x_1 + c_1(\tau), x_2 + c_2(\tau)). \tag{H.16}$$

Proof: Using Taylor series expansion, $f(x_1 + c_1(\tau), x_2 + c_2(\tau))$

$$\begin{aligned} f(x_1 + c_1(\tau), x_2 + c_2(\tau)) &= \sum_{n=0}^{\infty}\sum_{m=0}^{\infty} \frac{1}{n!m!}\frac{\partial^n}{\partial x_1^n}\frac{\partial^m}{\partial x_2^m}[f(x_1, x_2)]c_1(\tau)^n c_2(\tau)^m, \\ &= \left[\sum_{n=0}^{\infty} \frac{c_1(\tau)^n}{n!}\frac{\partial^n}{\partial x_1^n}\right]\left[\sum_{m=0}^{\infty} \frac{c_2(\tau)^m}{m!}\frac{\partial^m}{\partial x_2^m}\right] f(x_1, x_2), \\ &= e^{c_1(\tau)\frac{\partial}{\partial x_1}} e^{c_2(\tau)\frac{\partial}{\partial x_2}} f(x_1, x_2). \end{aligned} \tag{H.17}$$

The last equality follows from repeated application of the definition (3.38).

■

APPENDIX I

Expressing the JSP in terms of the Bivariate Normal Distribution

This appendix develops a scheme for the simplification of the expression for the joint survival probability to the cumulative bivariate normal distribution function $N_2(.)$ given in Section 4.4. This scheme involves five steps:

Step I. Consider the integral in the form

$$\int_{-\infty}^{0}\int_{-\infty}^{0}\frac{1}{2\pi s\sqrt{1-\rho_{12}^2}}\exp\left(-\frac{\phi(y_1,y_2)}{2s(1-\rho_{12}^2)}\right)dy_1dy_2, \tag{I.1}$$

where

$$\phi(y_1,y_2) \;=\; Ay_1^2+By_2^2+Cy_1+Dy_2+Ey_1y_2+H, \tag{I.2}$$

and $A,\ B,\ C,\ D,\ E$ and H are constants (defined by equation (4.68)).

Step II. Group the terms y_1 and y_2 by completing the square, then

$$\phi(y_1,y_2)=Ay_1^2+y_1(C+Ey_2)+By_2^2+Dy_2+H. \tag{I.3}$$

By completing square, this last expression can be written as

$$\phi(y_1,y_2)=A\left(\frac{C}{2A}+\frac{E}{2A}y_2+y_1\right)^2+h_1\left(\frac{h_2}{2h_1}+y_2\right)^2+\widetilde{h}, \tag{I.4}$$

where h_1, h_2 and $\widetilde{h}$ are expressed in (4.73).

Step III. First we make the change of variable in the second term in equation (I.4) by setting

$$v^2 \;=\; h_1\left(\frac{h_2}{2h_1}+y_2\right)^2, \tag{I.5}$$

which implies that

$$v \;=\; \sqrt{h_1}\left(\frac{h_2}{2h_1}+y_2\right), \tag{I.6}$$

so that

$$dv=\sqrt{h_1}dy_2, \tag{I.7}$$

and the limits transform as

$$y_2 \;\rightarrow\; -\infty \text{ as } v\rightarrow-\infty, \tag{I.8}$$

$$y_2 \;=\; 0 \text{ when } v=\frac{h_2}{2\sqrt{h_1}}. \tag{I.9}$$

Substituting from (I.6) (that is $y_2 = \frac{v}{\sqrt{h_1}} - \frac{h_2}{2h_1}$) into equation (I.4), and setting $\phi(y_1, \frac{v}{\sqrt{h_1}} - \frac{h_2}{2h_1})$ to $\widehat{\phi}(y_1, v)$, yields

$$\widehat{\phi}(y_1, v) = A\left[(\frac{C}{2A} - \frac{Eh_2}{4Ah_1} + y_1) + \frac{Eh_2}{4Ah_1}v\right]^2 + v^2 + \widetilde{h}. \tag{I.10}$$

Next, we make the change of variable to y_1 in the above equation by setting

$$u = \frac{C}{2A} - \frac{Eh_2}{4Ah_1} + y_1, \tag{I.11}$$

so that

$$du = dy_1, \tag{I.12}$$

and take the limits

$$y_1 \rightarrow -\infty \text{ as } u \rightarrow -\infty, \tag{I.13}$$

$$y_1 = 0 \text{ when } u = \frac{C}{2A} - \frac{Eh_2}{4Ah_1}. \tag{I.14}$$

Substituting from (I.11) into equation (I.10), and setting $\widehat{\phi}(\frac{C}{2A} - \frac{Eh_2}{4Ah_1}, v)$ to $\widetilde{\phi}(u, v)$, yields

$$\widetilde{\phi}(u, v) = Au^2 + \frac{E}{\sqrt{h_1}}uv + (1 + \frac{E^2}{4Ah_1})v^2 + \widetilde{h}. \tag{I.15}$$

Next, we make a further change of variables by setting

$$\widetilde{u} = \sqrt{\frac{A}{2s(1-\rho_{12}^2)}}\, u, \tag{I.16}$$

so that,

$$d\widetilde{u} = \sqrt{\frac{A}{2s(1-\rho_{12}^2)}}\, du, \tag{I.17}$$

and the limits transform as

$$u \rightarrow -\infty \text{ as } \widetilde{u} \rightarrow -\infty, \tag{I.18}$$

$$u = \frac{C}{2A} - \frac{Eh_2}{4Ah_1} \text{ when } \widetilde{u}_1 = \sqrt{\frac{A}{2s(1-\rho_{12}^2)}}\left(\frac{C}{2A} - \frac{Eh_2}{4Ah_1}\right). \tag{I.19}$$

We also make change of variable with respect to v by setting

$$\widetilde{v} = \sqrt{\frac{1 + \frac{E^2}{4Ah_1}}{2s(1-\rho_{12}^2)}}\, v, \tag{I.20}$$

so that

$$d\widetilde{v} = \frac{\sqrt{1 + \frac{E^2}{4Ah_1}}}{\sqrt{2s(1-\rho_{12}^2)}}\, dv, \tag{I.21}$$

and transform the limits

$$v \;\rightarrow\; -\infty \text{ as } \widetilde{v} \rightarrow -\infty, \tag{I.22}$$

$$v \;=\; \frac{h_2}{2\sqrt{h_1}} \text{ when } \widetilde{v}_1 = \frac{\sqrt{1+\frac{E^2}{4Ah_1}}\cdot\frac{h_2}{2\sqrt{h_1}}}{\sqrt{2s(1-\rho_{12}^2)}}. \tag{I.23}$$

Substituting from (I.16) and (I.20) into equation (I.15), yield

$$\phi(\widetilde{u},\widetilde{v}) \;=\; \widetilde{u}^2 + \frac{E}{\sqrt{AB}}\,\widetilde{u}\widetilde{v} + \widetilde{v}^2 + \widetilde{h}. \tag{I.24}$$

Substituting this into equation (I.1), we obtain the integral term

$$\frac{1}{\sqrt{AB}}\,\exp\left(-\frac{\widetilde{h}}{2s(1-\rho_{12}^2)}\right) \times\frac{\sqrt{1-\rho_{12}^2}}{\pi}\int_{-\infty}^{\widetilde{u}_1}\int_{-\infty}^{\widetilde{v}_1}\exp\left\{-\left(\widetilde{u}^2+\frac{E}{\sqrt{AB}}\,\widetilde{u}\widetilde{v}+\widetilde{v}^2\right)\right\}d\widetilde{u}d\widetilde{v}, \tag{I.25}$$

where $\widetilde{u}_1$ and $\widetilde{v}_1$ are the limits that are given in equations (I.19) and (I.23).

Step IV. We let

$$\widetilde{\rho} \;=\; -\frac{E}{2\sqrt{AB}}, \tag{I.26}$$

$$\widetilde{a} \;=\; \sqrt{2(1-\widetilde{\rho}^2)}\,\widetilde{u}_1 = \sqrt{\frac{A}{s}}\left(\frac{C}{2A}-\frac{Eh_2}{4Ah_1}\right)\sqrt{\frac{1-\widetilde{\rho}^2}{1-\rho_{12}^2}}, \tag{I.27}$$

$$\widetilde{b} \;=\; \sqrt{2(1-\widetilde{\rho}^2)}\,\widetilde{v}_1 = \frac{1}{\sqrt{s}}\sqrt{1+\frac{E^2}{4Ah_1}}\,\frac{h_2}{2\sqrt{h_1}}\,\sqrt{\frac{1-\widetilde{\rho}^2}{1-\rho_{12}^2}}, \tag{I.28}$$

then Eq (I.25) can be written as

$$\sqrt{\frac{(1-\rho_{12}^2)}{AB(1-\widetilde{\rho}^2)}}\,\exp\left(\frac{-\widetilde{h}}{2s(1-\rho_{12}^2)}\right)\times\frac{\sqrt{1-\widetilde{\rho}^2}}{\pi}\int_{-\infty}^{\frac{\widetilde{a}}{\sqrt{2(1-\widetilde{\rho}^2)}}}\int_{-\infty}^{\frac{\widetilde{b}}{\sqrt{2(1-\widetilde{\rho}^2)}}} \times\exp\left\{-\left(\widetilde{u}^2-2\widetilde{\rho}\,\widetilde{u}\widetilde{v}+\widetilde{v}^2\right)\right\}d\widetilde{u}d\widetilde{v}. \tag{I.29}$$

Step V. Note that the bivariate normal distribution function has the form

$$N_2(a,b,\rho) \;=\; \frac{1}{2\pi\sqrt{1-\rho^2}}\int_{-\infty}^{a}\int_{-\infty}^{b}\exp\left(-\frac{u^2-2\rho uv+v^2}{2(1-\rho^2)}\right)dudv,$$

and can also be expressed as

$$N_2(a,b,\rho) \;=\; \frac{\sqrt{1-\rho^2}}{\pi}\int_{-\infty}^{\frac{a}{\sqrt{2(1-\rho^2)}}}\int_{-\infty}^{\frac{b}{\sqrt{2(1-\rho^2)}}}\exp\left\{-(x^2-2\rho xy+y^2)\right\}dxdy, \tag{I.30}$$

by making the change of variables

$$x = u/\sqrt{2s(1-\rho^2)}, \tag{I.31}$$

and

$$y = v/\sqrt{2s(1-\rho^2)}. \tag{I.32}$$

By comparing equation (I.29) to equation (I.30), we see that the integral (I.1) can be expressed in terms of the $N_2(.)$ function as

$$\begin{aligned} &\int_{-\infty}^{0}\int_{-\infty}^{0} \frac{1}{2\pi s\sqrt{1-\rho_{12}^2}} \exp\left(-\frac{\phi(y_1,y_2)}{2s(1-\rho_{12}^2)}\right) dy_1 dy_2, \\ &= \sqrt{\frac{(1-\rho_{12}^2)}{AB(1-\widetilde{\rho}^2)}} \exp\left(\frac{-\widetilde{h}}{2s(1-\rho_{12}^2)}\right) \times N_2(\widetilde{a},\widetilde{b},\widetilde{\rho}). \end{aligned} \tag{I.33}$$

APPENDIX J

The Operator $e^{x\frac{\partial}{\partial x}}$

This appendix gives a proof of equation (7.21).

First we define

$$\begin{aligned} e^{x\frac{\partial}{\partial x}} f(x) &= 1 + x\frac{\partial}{\partial x} f(x) + \frac{1}{2!}(x\frac{\partial}{\partial x})^2 f''(x) + \cdots, \\ &= \sum_{n=0}^{\infty} \frac{1}{n!}(x\frac{\partial}{\partial x})^n f(x), \end{aligned} \tag{J.1}$$

where we use the notation

$$(x\frac{\partial}{\partial x})^n f(x) = (x\frac{\partial}{\partial x})(x\frac{\partial}{\partial x})\cdots(x\frac{\partial}{\partial x}) f(x). \tag{J.2}$$

Proposition J.1. *The expression $e^{ax\frac{\partial}{\partial x}} f(x)$ may be written*

$$e^{ax\frac{\partial}{\partial x}} f(x) = f(xe^a). \tag{J.3}$$

Proof: Using Taylor series expansion, $e^{ax\frac{\partial}{\partial x}} f(x)$ can be expressed as

$$\begin{aligned} e^{ax\frac{\partial}{\partial x}} f(x) &= \left[\sum_{n=0}^{\infty} \frac{1}{n!}\big(ax\frac{\partial}{\partial x}\big)^n\right] f(x), \\ &= \left[1 + ax\frac{\partial}{\partial x} + \frac{1}{2!}(ax\frac{\partial}{\partial x})^2 + \frac{1}{3!}(ax\frac{\partial}{\partial x})^3 + \cdots\right] f(x), \\ &= f(x) + ax\frac{\partial}{\partial x} f(x) + \frac{1}{2!}(ax\frac{\partial}{\partial x})^2 f(x) + \frac{1}{3!}(ax\frac{\partial}{\partial x})^3 f(x) + \cdots, \\ &= f(x) + ax\frac{\partial}{\partial x} f(x) + \frac{1}{2!}a^2 x f'(x) + \frac{1}{2!}a^2 x^2 f''(x) \\ &\quad + \frac{1}{3!}a^3 x f'(x) + \frac{1}{3!}3a^3 x^2 f''(x) + \frac{1}{3!}a^3 x^3 f'''(x) + \cdots, \\ &= f(x) + x f'(x)[a + \frac{1}{2!}a^2 + \frac{1}{3!}a^3 + \cdots] + x^2 f''(x)[\frac{1}{2!}a^2 + \frac{1}{3!}a^3 + \cdots] \\ &\quad + x^3 f'''(x)[\frac{1}{3!}a^3 + \cdots] + \cdots \end{aligned} \tag{J.4}$$

Notice that

$$\begin{aligned} xf'(x)[a+\frac{1}{2!}a^2+\frac{1}{3!}a^3+\cdots] &= (e^a-1)xf'(x), \\ x^2f''(x)[\frac{1}{2!}a^2+\frac{1}{3!}a^3+\cdots] &= \frac{(e^a-1)^2}{2!}x^2f''(x), \\ x^3f'''(x)[\frac{1}{3!}a^3+\cdots] &= \frac{(e^a-1)^3}{3!}x^3f'''(x), \\ \vdots &= \vdots \end{aligned} \tag{J.5}$$

Therefore, (J.4) can be expressed as

$$\begin{aligned} & f(x)+(e^a-1)xf'(x)+\frac{(e^a-1)^2}{2!}x^2f''(x)+\frac{(e^a-1)^3}{3!}x^3f'''(x)+\cdots \\ = \; & f(x)+(xe^a-x)f'(x)+\frac{(xe^a-x)^2}{2!}f''(x)+\frac{(xe^a-x)^3}{3!}f'''(x)+\cdots \\ = \; & f(xe^a). \end{aligned} \tag{J.6}$$

■

For the two variable case, the proof is similar to the one variable case.

Proposition J.2. *The expression* $e^{a_1x_1\frac{\partial}{\partial x_1}+a_2x_2\frac{\partial}{\partial x_2}}f(x_1,x_2)$ *may be written*

$$e^{a_1x_1\frac{\partial}{\partial x_1}+a_2x_2\frac{\partial}{\partial x_2}}f(x_1,x_2)=f(x_1e^{a_1},x_2e^{a_2}). \tag{J.7}$$

Proof: Using Taylor series expansion, $e^{a_1x_1\frac{\partial}{\partial x_1}+a_2x_2\frac{\partial}{\partial x_2}}f(x_1,x_2)$ can be expressed as

$$\begin{aligned} e^{a_1x_1\frac{\partial}{\partial x_1}+a_2x_2\frac{\partial}{\partial x_2}}f(x_1,x_2) &= \sum_{n=0}^{\infty}\sum_{m=0}^{\infty}\frac{1}{n!m!}\big(a_1x_1\frac{\partial}{\partial x_1}\big)^n\big(a_2x_2\frac{\partial}{\partial x_2}\big)^m f(x_1,x_2), \\ &= \left[\sum_{n=0}^{\infty}\frac{1}{n!}\big(a_1x_1\frac{\partial}{\partial x_1}\big)^n\right]\left[\sum_{m=0}^{\infty}\frac{1}{m!}\big(a_2x_2\frac{\partial}{\partial x_2}\big)^m\right]f(x_1,x_2), \\ &= \left[1+a_1x_1\frac{\partial}{\partial x_1}+\frac{1}{2!}(a_1x_1\frac{\partial}{\partial x_1})^2+\frac{1}{3!}(a_1x_1\frac{\partial}{\partial x_1})^3+\cdots\right] \\ &\quad\times\left[1+a_2x_2\frac{\partial}{\partial x_2}+\frac{1}{2!}(a_2x_2\frac{\partial}{\partial x_2})^2+\frac{1}{3!}(a_2x_2\frac{\partial}{\partial x_2})^3+\cdots\right] \\ &\quad\times f(x_1,x_2). \end{aligned} \tag{J.8}$$

By applying the results of Proposition J.1 to the brackets in (J.8), then the right hand side of (J.8) becomes

$$\begin{aligned}
& f(x_1,x_2)+(x_1e^{a_1}-x_1)f'_{x_1}(x_1,x_2)+(x_2e^{a_2}-x_2)f'_{x_2}(x_1,x_2)\\
& +\frac{1}{2!}\big[(x_1e^{a_1}-x_1)^2f''_{x_1}(x_1,x_2)+2(x_1e^{a_1}-x_1)(x_2e^{a_2}-x_2)f''_{x_1x_2}(x_1,x_2)\\
& +(x_2e^{a_2}-x_2)^2f''_{x_2}(x_1,x_2)\big]+\cdots\\
= & \sum_{n=0}^{\infty}\sum_{m=0}^{\infty}\frac{1}{n!m!}\frac{\partial^n}{\partial x_1^n}\frac{\partial^m}{\partial x_2^m}f(x_1,x_2)(x_1e^{a_1}-x_1)^n(x_2e^{a_2}-x_2)^m,\\
= & f(x_1e^{a_1},x_2e^{a_2}). \qquad \text{(J.9)}
\end{aligned}$$

■

APPENDIX K

The Transformation of the PDE for the CLN in the Mean-Reverting Case

This appendix gives a brief idea of the transformation of the partial differential equation (7.15) to equation (7.22).

Proposition K.1. *The solution to equation (7.15) may be written*

$$\begin{aligned} P^{\dagger}(X_1, X_2, \tau) &= e^{-\kappa_1 \tau X_1 \frac{\partial}{\partial X_1} - \kappa_2 \tau X_2 \frac{\partial}{\partial X_2}} P^{\ddagger}(X_1, X_2, \tau), & \text{(K.1)} \\ &= P^{\ddagger}(X_1 e^{-\kappa_1 \tau}, X_2 e^{-\kappa_2 \tau}, \tau). & \text{(K.2)} \end{aligned}$$

where $P^{\ddagger}(X_1, X_2, \tau)$ satisfies the partial differential equation

$$\begin{aligned} \frac{\partial P^{\ddagger}}{\partial \tau} &= \frac{1}{2} e^{-2\kappa_1 \tau} \frac{\partial^2 P^{\ddagger}}{\partial X_1^2} + \rho_{12} e^{-\kappa_1 \tau - \kappa_2 \tau} \frac{\partial^2 P^{\ddagger}}{\partial X_1 \partial X_2} + \frac{1}{2} e^{-2\kappa_2 \tau} \frac{\partial^2 P^{\ddagger}}{\partial X_2^2} \\ &\quad + \bar{\gamma}_1(\tau) e^{-\kappa_1 \tau} \frac{\partial P^{\ddagger}}{\partial X_1} + \bar{\gamma}_2(\tau) e^{-\kappa_2 \tau} \frac{\partial P^{\ddagger}}{\partial X_2}. \end{aligned} \quad \text{(K.3)}$$

Proof: Using the same approach back in Appendix C, we apply the Baker-Campbell-Hausdorff formula to find the relationships of the functions of operator, when taking the first or (and) second derivatives to the right hand side of equation (K.1) with respect to τ, X_1 and X_2, respectively.

After some algebraic manipulations as illustrated for example, Proposition C.1, Proposition C.2 or Proposition C.3, we obtain

$$\begin{aligned} \frac{\partial P^{\dagger}}{\partial \tau} &= e^{-\kappa_1 \tau X_1 \frac{\partial}{\partial X_1} - \kappa_2 \tau X_2 \frac{\partial}{\partial X_2}} \left[\frac{\partial P^{\ddagger}}{\partial \tau} - \frac{\partial(\kappa_1 \tau)}{\partial \tau} X_1 \frac{\partial P^{\ddagger}}{\partial X_1} - \frac{\partial(\kappa_2 \tau)}{\partial \tau} X_2 \frac{\partial P^{\ddagger}}{\partial X_2} \right], \\ &= e^{-\kappa_1 \tau X_1 \frac{\partial}{\partial X_1} - \kappa_2 \tau X_2 \frac{\partial}{\partial X_2}} \left[\frac{\partial P^{\ddagger}}{\partial \tau} - \kappa_1 X_1 \frac{\partial P^{\ddagger}}{\partial X_1} - \kappa_2 X_2 \frac{\partial P^{\ddagger}}{\partial X_2} \right], \\ \frac{\partial P^{\dagger}}{\partial X_1} &= e^{-\kappa_1 \tau X_1 \frac{\partial}{\partial X_1} - \kappa_2 \tau X_2 \frac{\partial}{\partial X_2}} \left[e^{-\kappa_1 \tau} \frac{\partial P^{\ddagger}}{\partial X_1} \right], \\ \frac{\partial P^{\dagger}}{\partial X_2} &= e^{-\kappa_1 \tau X_1 \frac{\partial}{\partial X_1} - \kappa_2 \tau X_2 \frac{\partial}{\partial X_2}} \left[e^{-\kappa_2 \tau} \frac{\partial P^{\ddagger}}{\partial X_2} \right], \\ \frac{\partial^2 P^{\dagger}}{\partial X_1^2} &= e^{-\kappa_1 \tau X_1 \frac{\partial}{\partial X_1} - \kappa_2 \tau X_2 \frac{\partial}{\partial X_2}} \left[e^{-2\kappa_1 \tau} \frac{\partial^2 P^{\ddagger}}{\partial X_1^2} \right], \\ \frac{\partial^2 P^{\dagger}}{\partial X_2^2} &= e^{-\kappa_1 \tau X_1 \frac{\partial}{\partial X_1} - \kappa_2 \tau X_2 \frac{\partial}{\partial X_2}} \left[e^{-2\kappa_2 \tau} \frac{\partial^2 P^{\ddagger}}{\partial X_2^2} \right], \end{aligned} \quad \text{(K.4)}$$

moreover,

$$\begin{aligned} X_1\frac{\partial P^\dagger}{\partial X_1} &= e^{-\kappa_1\tau X_1\frac{\partial}{\partial X_1}-\kappa_2\tau X_2\frac{\partial}{\partial X_2}}\left[X_1\frac{\partial P^\ddagger}{\partial X_1}\right], \\ X_2\frac{\partial P^\dagger}{\partial X_2} &= e^{-\kappa_1\tau X_1\frac{\partial}{\partial X_1}-\kappa_2\tau X_2\frac{\partial}{\partial X_2}}\left[X_2\frac{\partial P^\ddagger}{\partial X_2}\right], \\ \frac{\partial^2 P^\ddagger}{\partial X_1\partial X_2} &= e^{-\kappa_1\tau X_1\frac{\partial}{\partial X_1}-\kappa_2\tau X_2\frac{\partial}{\partial X_2}}\left[e^{-\kappa_1\tau-\kappa_2\tau}\frac{\partial^2 P^\ddagger}{\partial X_1\partial X_2}\right]. \end{aligned} \tag{K.5}$$

Substituting from the equation (K.5) into (7.15), we obatin

$$\begin{aligned} &\frac{\partial P^\ddagger}{\partial\tau}-\kappa_1 X_1\frac{\partial P^\ddagger}{\partial X_1}-\kappa_2 X_2\frac{\partial P^\ddagger}{\partial X_2} \\ &= \frac{1}{2}e^{-2\kappa_1\tau}\frac{\partial^2 P^\ddagger}{\partial X_1^2}+\rho_{12}e^{-\kappa_1\tau-\kappa_2\tau}\frac{\partial^2 P^\ddagger}{\partial X_1\partial X_2}+\frac{1}{2}e^{-2\kappa_2\tau}\frac{\partial^2 P^\ddagger}{\partial X_2^2}+\bar\gamma_1(\tau)e^{-\kappa_1\tau}\frac{\partial P^\ddagger}{\partial X_1} \\ &\quad +\bar\gamma_2(\tau)e^{-\kappa_2\tau}\frac{\partial P^\ddagger}{\partial X_2}-\kappa_1 X_1\frac{\partial P^\ddagger}{\partial X_1}-\kappa_2 X_2\frac{\partial P^\ddagger}{\partial X_2}, \end{aligned} \tag{K.6}$$

which is equation (K.3).

■

APPENDIX L

Derivation of the PDE with Time Varying Barriers in the Mean-Reverting Case

This appendix gives details of the transformation of the partial differential equation (7.29) to the heat equation (4.1) by use of the transformation on given in equation (7.35).

Proposition L.1. *The partial differential equation* (7.29) *can be transformed to*

$$P^{\ddagger}_{\boldsymbol{\beta}}(X_1, X_2, \tau) \;=\; e^{-X_1^*(\tau)\frac{\partial}{\partial X_1} - X_2^*(\tau)\frac{\partial}{\partial X_2}} \widetilde{P}(X_1, X_2, \tau), \tag{L.1}$$

where $X_i^*(\tau)$ *is given by*

$$X_i^*(\tau) = -\int_0^\tau \bar{\gamma}_i(v) e^{-\kappa v} dv - \beta_i \int_0^\tau e^{-2\kappa v} dv, \; (i = 1, 2), \tag{L.2}$$

and $\widetilde{P}(X_1, X_2, \tau)$ *satisfies the partial differential equation*

$$\frac{\partial \widetilde{P}}{\partial \tau} = \frac{1}{2} e^{-2\kappa\tau} \frac{\partial^2 \widetilde{P}}{\partial X_1^2} + \rho_{12} e^{-2\kappa\tau} \frac{\partial^2 \widetilde{P}}{\partial X_1 \partial X_2} + \frac{1}{2} e^{-2\kappa\tau} \frac{\partial^2 \widetilde{P}}{\partial X_2^2} - \beta_1 e^{-2\kappa\tau} \frac{\partial \widetilde{P}}{\partial X_1} - \beta_2 e^{-2\kappa\tau} \frac{\partial \widetilde{P}}{\partial X_2}. \tag{L.3}$$

Proof: We apply the Baker-Campbell-Hausdorff formula in Appendix C, and after some algebraic manipulations, we obtain

$$\begin{aligned}
\frac{\partial P^{\ddagger}_{\boldsymbol{\beta}}}{\partial \tau} &= e^{-X_1^*(\tau)\frac{\partial}{\partial X_1} - X_2^*(\tau)\frac{\partial}{\partial X_2}} \left[\frac{\partial \widetilde{P}}{\partial \tau} - \frac{\partial X_1^*(\tau)}{\partial \tau} \frac{\partial \widetilde{P}}{\partial X_1} - \frac{\partial X_2^*(\tau)}{\partial \tau} \frac{\partial \widetilde{P}}{\partial X_2} \right], \\
\frac{\partial P^{\ddagger}_{\boldsymbol{\beta}}}{\partial X_i} &= e^{-X_1^*(\tau)\frac{\partial}{\partial X_1} - X_2^*(\tau)\frac{\partial}{\partial X_2}} \frac{\partial \widetilde{P}}{\partial X_i}, \; (i = 1, 2), \\
\frac{\partial^2 P^{\ddagger}_{\boldsymbol{\beta}}}{\partial X_i^2} &= e^{-X_1^*(\tau)\frac{\partial}{\partial X_1} - X_2^*(\tau)\frac{\partial}{\partial X_2}} \frac{\partial^2 \widetilde{P}}{\partial X_i^2}, \; (i = 1, 2), \\
\frac{\partial^2 P^{\ddagger}_{\boldsymbol{\beta}}}{\partial X_1 \partial X_2} &= e^{-X_1^*(\tau)\frac{\partial}{\partial X_1} - X_2^*(\tau)\frac{\partial}{\partial X_2}} \frac{\partial^2 \widetilde{P}}{\partial X_1 \partial X_2}.
\end{aligned} \tag{L.4}$$

Then equation (7.29) becomes

$$\begin{aligned}
\frac{\partial \widetilde{P}}{\partial \tau} - \frac{\partial X_1^*(\tau)}{\partial \tau} \frac{\partial \widetilde{P}}{\partial X_1} - \frac{\partial X_2^*(\tau)}{\partial \tau} \frac{\partial \widetilde{P}}{\partial X_2} &= \frac{1}{2} e^{-2\kappa\tau} \frac{\partial^2 \widetilde{P}}{\partial X_1^2} + \rho_{12} e^{-2\kappa\tau} \frac{\partial^2 \widetilde{P}}{\partial X_1 \partial X_2} + \frac{1}{2} e^{-2\kappa\tau} \frac{\partial^2 \widetilde{P}}{\partial X_2^2} \\
&\quad + \bar{\gamma}_1(\tau) e^{-\kappa\tau} \frac{\partial \widetilde{P}}{\partial X_1} + \bar{\gamma}_2(\tau) e^{-2\kappa\tau} \frac{\partial \widetilde{P}}{\partial X_2}.
\end{aligned} \tag{L.5}$$

Define $X_1^*(\tau)$ and $X_2^*(\tau)$ by setting

$$-\frac{\partial X_1^*(\tau)}{\partial \tau} = \bar{\gamma}_1(\tau)e^{-\kappa\tau} + \beta_1 e^{-2\kappa\tau}, \tag{L.6}$$

$$-\frac{\partial X_2^*(\tau)}{\partial \tau} = \bar{\gamma}_2(\tau)e^{-\kappa\tau} + \beta_2 e^{-2\kappa\tau}, \tag{L.7}$$

so that

$$X_1^*(\tau) = -\int_0^\tau \bar{\gamma}_1(v)e^{-\kappa v}dv - \beta_1\int_0^\tau e^{-2\kappa v}dv, \tag{L.8}$$

$$X_2^*(\tau) = = -\int_0^\tau \bar{\gamma}_2(v)e^{-\kappa v}dv - \beta_2\int_0^\tau e^{-2\kappa v}dv. \tag{L.9}$$

Then, taking the first derivative of $X_1^*(\tau)$ and $X_2^*(\tau)$ which respect to the variable τ, and substituting into partial differential equation (L.5) yields

$$\begin{aligned}&\frac{\partial \widetilde{P}}{\partial \tau} + \bar{\gamma}_1(\tau)e^{-\kappa\tau}\frac{\partial \widetilde{P}}{\partial X_1} + \beta_1 e^{-2\kappa\tau}\frac{\partial \widetilde{P}}{\partial X_1} + \bar{\gamma}_2(\tau)e^{-\kappa\tau}\frac{\partial \widetilde{P}}{\partial X_2} + \beta_2 e^{-2\kappa\tau}\frac{\partial \widetilde{P}}{\partial X_2}\\ &= \frac{1}{2}e^{-2\kappa\tau}\frac{\partial^2 \widetilde{P}}{\partial X_1^2} + \rho_{12}e^{-2\kappa\tau}\frac{\partial^2 \widetilde{P}}{\partial X_1 \partial X_2} + \frac{1}{2}e^{-2\kappa\tau}\frac{\partial^2 \widetilde{P}}{\partial X_2^2} + \bar{\gamma}_1(\tau)e^{-\kappa\tau}\frac{\partial \widetilde{P}}{\partial X_1} + \bar{\gamma}_2(\tau)e^{-\kappa\tau}\frac{\partial \widetilde{P}}{\partial X_2}\end{aligned} \tag{L.10}$$

which then turns out to be equation (L.3).

■

We note that the time dependent coefficients in equation (L.3) can be eliminated by transforming the time variable. This can be done by the following proposition.

Proposition L.2. *Define the new time-to-maturity variable ζ as*

$$\zeta = \int_0^\tau e^{-2\kappa v}dv. \tag{L.11}$$

and set $\acute{P}(X_1, X_2, \zeta) = \widetilde{P}(X_1, X_2, \tau)$, then $\acute{P}(X_1, X_2, \zeta)$ satisfies the partial differential equation

$$\frac{\partial \acute{P}}{\partial \zeta} = \frac{1}{2}\frac{\partial^2 \acute{P}}{\partial X_1^2} + \rho_{12}\frac{\partial^2 \acute{P}}{\partial X_1 \partial X_2} + \frac{1}{2}\frac{\partial^2 \acute{P}}{\partial X_2^2} - \beta_1\frac{\partial \acute{P}}{\partial X_1} - \beta_2\frac{\partial \acute{P}}{\partial X_2}. \tag{L.12}$$

Proof: Consider equation (L.3), and multiply both sides by the term $e^{2\kappa\tau}$, so that

$$e^{2\kappa\tau}\frac{\partial \widetilde{P}}{\partial \tau} = \frac{1}{2}\frac{\partial^2 \widetilde{P}}{\partial X_1^2} + \rho_{12}\frac{\partial^2 \widetilde{P}}{\partial X_1 \partial X_2} + \frac{1}{2}\frac{\partial^2 \widetilde{P}}{\partial X_2^2} - \beta_1\frac{\partial \widetilde{P}}{\partial X_1} - \beta_2\frac{\partial \widetilde{P}}{\partial X_2}. \tag{L.13}$$

Using the chain rule we transform to a new time-to-maturity variable ζ, so that (L.13) in terms of $\acute{P}$, becomes

$$e^{2\kappa\tau}\frac{\partial}{\partial\zeta}\big[\acute{P}\big]\frac{\partial\zeta}{\partial\tau} = \frac{1}{2}\frac{\partial^2\acute{P}}{\partial X_1^2} + \rho_{12}\frac{\partial^2\acute{P}}{\partial X_1\partial X_2} + \frac{1}{2}\frac{\partial^2\acute{P}}{\partial X_2^2} - \beta_1\frac{\partial\acute{P}}{\partial X_1} - \beta_2\frac{\partial\acute{P}}{\partial X_2}. \tag{L.14}$$

In order to eliminate the $e^{2\kappa\tau}$ term, we choose ζ to satify

$$e^{2\kappa\tau}\times\frac{\partial\zeta}{\partial\tau} = 1, \tag{L.15}$$

from which

$$\zeta \;=\; \int_0^\tau e^{-2\kappa v}dv. \tag{L.16}$$

We note that the partial differential equation (L.12) is similar to the partial differential equation (4.30), which can be reduced to the two-dimensional heat equation (4.1) via the transformation illustrated in Appendix G, by simply replacing $\bar{P}$ by $\acute{P}$, u by $\widetilde{u}$, and replacing the coefficients γ_i by $-\beta_i$ (for $i = 1, 2$), thus obtaining

$$\acute{P}(X_1, X_2, \zeta) \;=\; e^{\eta_1 X_1+\eta_2 X_2+\xi\zeta}\widetilde{u}(X_1, X_2, \zeta), \tag{L.17}$$

where η_1, η_2 and ξ are constants given by the expressions in (4.52)-(4.54).

Therefore, equation (7.35) is obtained by making use the Proposition L.1, Proposition L.2 and Appendix G.

■

Bibliography

Agca, S. & Chance, D. M. (2003), 'Speed and accuracy comparison of bivariate normal distribution approximations for option pricing', *Journal of Computational Finance* **6**(4), 61–96.

Albanese, C. & Campolieti, G. (2006), *Advanced Derivatives Pricing and Risk Management: Theory, Tools and Hands-on Programming Applications*, Elsevier Academic Press.

Bernard, C., LeCourtois, O. & Quittard-Pinon, F. (2008), 'Pricing derivatives with barriers in a stochastic interest rate environment', *Journal of Economic Dynamics & Control* **32**, 2903–2938.

Black, F. & Cox, J. (1976), 'Valuing corporate securities: Some effects of bond indenture provisions', *Journal of Finance* **35**, 351–367.

Briys, E. & de Varenne, F. (1997), 'Valuing risky fixed rate debt: An extension', *Journal of Financial and Quantitative Analysis* **32**(2), 239–248.

Cathcart, L. & El-Jahel, L. (2002), 'Defaultable bonds and default correlation', *Working Paper* . Imperial College, London.

Cheang, G. & Chiarella, C. (2007), 'An extension of Merton's jump-diffusion model', *Proceedings of the Fourth IASTED International Conference, Financial Engineering and Applications* (ISBN CD: 978-0-88986-681-2, September 24-26, 2007), 13–18.

Chiarella, C. (2009), *An Introduction to Derivative Security Pricing: Techniques, Methods and Applications*, Springer-Verlag. Forthcoming.

Chiarella, C., Kang, B., Meyer, G. H. & Ziogas, A. (2009), 'The evaluation of American option prices under stochastic volatility and jump-diffusion dynamics using the method of lines', *International Journal of Theoretical and Applied Finance* . Forthcoming.

Clewlow, L. & Strickland, C. (1998), *Implementing Derivative Models*, Wiley Series in Financial Engineering.

Collin-Dufresne, P. & Goldstein, R. S. (2001), 'Do credit spreads reflect stationary leverage ratios?', *Journal of Finance* **56**, 1929–1957.

Delianedis, G. & Geske, R. (1999), 'Credit risk and risk neutral default probabilities: Information about migrations and defaults?', *Working Paper* . University of California at Los Angeles.

Demo, P., Sveshnikov, A. M. & Kozisek, Z. (2000), 'Comment on " Propagator of the Fokker-Planck equation with a linear force – Lie-algebraic approach" by C.F. Lo', *Europhysics Letters* **50**(2), 278–279.

Douglas, J. (1961), *A survey of numerical methods for parabolic differential equations*, Advances in Computers 2, 1-55, Academic Press.

Douglas, J. & Rachford, H. H. (1956), 'On the numerical solution of heat conduction problems in two and three space variables', *Transactions of the American Mathematical Society* **82**, 421–439.

Drezner, Z. (1978), 'Computation of the bivariate normal integral', *Mathematics of Computation* **32**(141), 277–279.

Fortet, R. (1943), 'Les fónctions aleatoires du type de Markoff associées à certaines équations lineáires aux dérivées partielles du type parabolique', *Journal de Mathématiques Pures et Appliquées* **22**, 177 – 243.

Gikhman, I. I. & Skorokhod, A. V. (1972), *Stochastic differential equations*, Springer-Verlag.

Glasserman, P. (2004), *Monte Carlo methods in financial engineering*, New York: Springer.

Hassani, S. (1998), *Mathematical Physics: A Mordern Introduction to Its Fundations*, Springer.

Huang, J-Z. & Huang, M. (2003), 'How much of the corporate-treasury yield spread is due to credit risk?', *Working Paper* . Penn State University.

Huang, J-Z. & Zhou, H. (2008), 'Specification analysis of structural credit risk models', *Working Paper* . Penn State University.

Huang, M. X. (2003), 'A three-factor structure model of risky bonds and its applications'. M.Phil Thesis, The Chinese University of Hong Kong.

Hui, C. H., Lo, C. F. & Huang, M. X. (2006), 'Are corporates' target leverage ratios time-dependent?', *International Review of Financial Analysis* **15**, 220 – 236.

Hui, C. H., Lo, C. F., Huang, M. X. & Lee, H. C. (2007), 'Predictions of default probabilities by models with dynamic leverage ratios', *Working Paper* . Available at SSRN: http://ssrn.com/abstract=1113726.

Hui, C. H., Wong, T. C., Lo, C. F. & Huang, M. X. (2005), 'Benchmarking model of default probabilities of listed companies', *Journal of Fixed Income* **15**(2), 76–86.

Hull, J. C. (2000), *Options, Futures, & Other Derivatives*, 4th Ed., Pretice-Hall, Inc.

Hull, J., Pedrescu, M. & White, A. (2006), 'The valuation of correlation-dependent credit derivatives using a structural model', *, Working Paper* . University of Toronto.

Hull, J. & White, A. (1990), 'Pricing interest-rate-derivative securities', *Review of Financial Studies* **3**(4), 573–592.

in't Hout, K. J. & Welfert, B. D. (2007), 'Stability of ADI schemes applied to convection-diffusion equations with mixed derivative terms', *Applied Numerical Mathematics* **57**(1), 19–35.

John, F. (1978), *Partial Differential Equations*, 3rd Edn, New York: Springer.

Li, D. (2000), 'On default correlation: A copula approach', *Journal of Fixed Income* **9**, 43–54.

Lo, C. F. (1997), 'Propagator of the Fokker-Planck equation with a linear force – Lie-algebraic approach', *Europhysics Letters* **39**(3), 263–267.

Lo, C. F. & Hui, C. H. (2001), 'Valuation of financial derivatives with time-dependent parameters - Lie algebraic approach', *Quantative Finance* **1**, 73–78.

Lo, C. F. & Hui, C. H. (2002), 'Pricing multi-asset financial derivatives with time-dependent parameters - Lie algebraic approach', *International Journal of Mathematics and Mathematical Sciences* **32**(7), 401–410.

Lo, C. F., Lee, H. C. & Hui, C. H. (2003), 'A simple approach for pricing Black-Scholes barrier options with time-dependent parameters', *Quantitative Finance* **3**, 98–107.

Longstaff, F. A. & Schwartz, E. S. (1995), 'A simple approach to valuing risky fixed and floating rate debt', *Journal of Finance* **50**(3), 789–819.

Merton, R. (1974), 'On the pricing of corporate debt: The risk structure of interest rates', *Journal of Finance* **29**, 449–470.

Merton, R. C. (1976), 'Option pricing when underlying stock returns are discontinuous', *Journal of Financial Economics* **3**, 125–144.

Snedecor, G. W. & Cochran, W. G. (1991), *Statistical methods*, Blackwell Publishing. 8th Edition.

Standard & Poor's (2001), 'Adjust key U.S. industrial financial ratios'.

Strikwerda, J. C. (1989), *Finite difference schemes and partial differential equations*, Wadsworth & Brooks/Cole, Mathematics Series, Pacific Grove, California, USA.

Suzuki, M. (1989), 'New unified formulation of transient phenomena near the instability point on the basis of the fokker-planck equation', *Physica* **117**(A), 103–108.

Vasicek, O. A. (1977), 'An equilibrium characterisation of term structure', *Journal of Financial Economics* **5**, 177 – 188.

Wilmott, P., Howison, S. & Dewynne, J. (1995), *The Mathematics of Financial Derivatives: A Student Introduction*, Cambridge University Press.

Zhang, D. & Melnik, R. (2007), 'Monte-carlo simulations of the first passage time for multivariate jump-diffusion processes in financial applications', *Working Paper* (Version: February 2007). Wilfrid Laurier University, Canada.

Zhou, C. (1997), 'A jump-diffusion approach to modeling credit risk and valuing defaultable securities', *Working Paper* . Federal Reserve Board, Washington.

Zhou, C. (2001*a*), 'An analysis of default correlations and multiple defaults', *The Review of Financial Studies* **14**, 555 – 576.

Zhou, C. (2001*b*), 'The term structure of credit spreads with jump risk', *Journal of Banking and Finance* **25**, 2015 – 2040.